Aggregated Impact of Smart Grid Technologies on the Quality of Power Supply

Ndawula, Mike Brian

Award date:
2021

Awarding institution:
University of Bath

Aggregated Impact of Smart Grid Technologies on the Quality of Power Supply

Mike Brian Ndawula

A thesis submitted for the degree of Doctor of Philosophy

University of Bath

Department of Electronic and Electrical Engineering

January 2021

Declaration

I hereby declare that the material contained in this thesis is the result of my own work except where explicitly stated otherwise. No portion of the work has been submitted in support of an application for any other degree or professional qualification of this or any other university or institution of learning.

Signed: . . . . . .

Date: . . . . . .

Abstract

To strike the balance between carbon emissions reduction, economic growth and energy supply security, non-conventional distributed energy resources such as solar photovoltaic are expected to dominate electricity generation in the future envisaged "smart grid". However, the spatio-temporal variation of these smart grid technologies (SGTs) creates challenges for power system operation as there is limited knowledge regarding their impact on network reliability. Moreover, given their dependence on ambient conditions, there is a substantial risk of increased operational costs through the inefficient operation of backup conventional generation to maintain system reliability. This might defer the decarbonisation progress of several countries.

This thesis presents probabilistic time-sequential simulation techniques based on Monte Carlo methods to comprehensively assess the impact of SGTs on the reliability of power supply given the uncertainty of demand and the complexity of large networks. Accordingly, three major innovations are proposed to address these critical challenges a) the stochastic behaviour of SGTs is integrated into a reliability assessment methodology that is enhanced by the inclusion of the time-series variation of demand, electricity generation from SGTs, and the failure of network components; b) a rigorous characterisation of varying customer groups is developed by presenting the reliability performance for different load sectors (rural, suburban and urban) showing also the range of variability in terms of SGT influence; c) inspired by the model order reduction and state pruning techniques in control engineering, a novel network aggregation methodology is proposed to derive simplified grid representations that contain the most important system dynamics while minimising the error of the considered reliability metrics and being significantly faster to simulate.

The findings demonstrate that the coordinated deployment of SGTs such as demand-side response and energy storage will provide the most improvement to network reliability. The developed impact assessment methodology, which reduces network complexity through a reliability-based aggregation, will ensure that the impacts of SGTs can be analysed significantly faster while preserving accuracy. This will promote the practical use of reliability assessment for network planning and maintenance procedures that will result not only in satisfactory levels of supply continuity but also in the efficient operation of the power networks. Also, the resultant minimum targets set by national regulators to protect customers from supply outages will recognise varying customer groups and provide varying subsidies to promote uptake of relevant SGTs for the benefit of especially the worst served customers who often prefer continuous supply to the currently available outage compensation schemes.

Acknowledgements

I give most thanks to God for thus far he has led me through the twists and turns of this PhD path. I have had a relatively large supervisory team and I am grateful to have learnt lots from each member. First, my sincere appreciation goes out to my first supervisor, Assoc Prof Ignacio Hernando Gil, for his nonstop motivation, positivity, patience, honesty, and friendship. Second, I would like to thank Dr Antonio De Paola who willingly continued to guide my research and inspire me to innovate. Third, I thank Dr Ran Li with whom we joyously extended the research boundaries and Dr Chenghong Gu who has guided me to the finish line with constant encouragement. I also thank Prof Furong Li for her consistent support and finally, Dr Sasa Djokic (Edinburgh) for his constant motivation, inspiration, and wisdom in our collaborations.

I would like to acknowledge the financial support provided by the University through the research studentship that has funded this PhD. I also thank key departmental staff, Dr Adrian Evans, Ann Linfield, Karen Woods, Alana Fiorelli and Louise Lynes, for their contributions to my wellbeing. I am grateful to all the unit convenors and the technical staff who greatly supported me in lab demonstration for undergrad courses. Special mention goes to Dr Tareq Assaf, Dr Matt Cole, David Chapman, Dr Rob Wortham, Dr Philip Shields, Dr Roger Ngwompo, Dr Francis Robinson, Dr Paulo Rocha, Dr Ali Mohammadi, Dr Benjamin Metcalfe, Fatima Mustafa, and Sanjay Jussun. I deeply thank all my Widening Participation colleagues, Hilary Brummitt, Joy Cranham, Heather Lee-Wright, Luis Rodriguez, Nigel Goldsmith, Anne-Catherine Mechler, Sophie Kirtley, Kate Awdry, Katherine Davis, Sue Dimond, Stephanie Gan, Dr Andrew Ross, Dr Claire Bedrock, among others, with whom we have created beautiful memories. I thank my football mates, Mark, Roger, Tom, Jacob, Andrew, James, Ollie, Riccy, Ben, Tosin, Joel, Yasser and Petros, and my friends, Foteini, Jacqueline, Pooja, Sarra, Jahnavi, Taghried, Rebekah, Belinda, Armani, Khumbo, Elmira, Lanqing, Maximilian, Joshua, Kristian, Pengfei, Tim, Sotiris and Moanis.

Most importantly, I thank my family for their unending support. Even from thousands of miles away, they have remained my best friends in what has been a challenging journey. I thank my father for his invaluable financial and emotional support, and for having such great vision. I thank my mother, my number one, for always being there for me, financially, emotionally, when things did not make sense, and when I just needed a friend. I thank my sisters, Conifa and Maria, for ALWAYS lighting up my world and giving me real purpose, Martha, Lilian, Josephine, Natasha, Angel, Gabriel, Vanessa, Bernice, Bradley, Brandon, Isaac, grandma Rose, grandma Josephine, and the rest of my extended family (and friends) whose support means the world. Finally, thanks to God, again, and I can't wait for our next adventure.

Contents

List of Figures

List of Tables

Acronyms

1-ph	Single-Phase
3-ph	Three-Phase
ABC	Aerial Bundled Conductor
ac	Alternating Current
ACCI	Average Customer Curtailment Index
AEM	Alternative Existing Method
AGG	Aggregate
Al	Aluminium
API	Application Program Interface
ASIDI	Average System Interruption Duration Index
ASIFI	Average System Interruption Frequency Index
BSP	Bulk Supply Point
BT	Balanced Truncation
CAIDI	Customer Average Interruption Duration Index
CAIFI	Customer Average Interruption Frequency Index
CDF	Cumulative Distribution Function
CEER	Council of European Energy Regulators
CI	Customer Interruptions
CML	Customer Minutes Lost
CoS	Continuity of Supply
CoV	Coefficient of Variation
CSA	Cross-Sectional Area
CTMC	Continuous Time Markov Chain
Cu	Copper
CVaR	Conditional Value at Risk
dc	Direct Current
DER	Distributed Energy Resource
DG	Distributed Generation
DNO	Distribution Network Operator
DSO	Distribution System Operator
DSR	Demand Side Response
EMS	Energy Management System
ENA	Energy Networks Association
ENS	Energy Not Supplied

EPR	Ethylene Propylene Rubber
EPSRC	Engineering and Physical Sciences Research Council
ES	Energy Storage
EU	European Union
GB	Great Britain
GD	Group Demand
GS	Guaranteed Standards
GSP	Grid Supply Point
HILP	High Impact Low Probability
HPC	High Performance Computing
HSV	Hankel Singular Value
HV	High Voltage
IEEE	Institute of Electrical and Electronic Engineers
IIS	Interruption Incentive Scheme
LI	Long Interruption
LOLE	Loss of Load Expectation
LOLP	Loss of Load Probability
LP	Load Point
LV	Low Voltage
km	kilometre
kVA	kilovolt Ampere
kW	kilowatt
MAIFI	Momentary Average Interruption Frequency Index
$MAIFI_E$	Momentary Average Interruption Event Frequency Index
MCS	Monte Carlo Simulation
MESS	Matrix Equation Sparse Solver
MG	Micro-Generation
MOR	Model Order Reduction
MTTF	Mean Time to Fail
MTTR	Mean Time to Repair
MV	Medium Voltage
MVA	Megavolt Amperes
MW	Megawatt
NECP	National Energy and Climate Plan
NMCS	Non-sequential Monte Carlo Simulation
NR	Network Reconfiguration

NRA	National Regulatory Authority
OFGEM	Office of Gas and Electricity Markets
OHL	Overhead Line
OLTC	On Load Tap-Changing
OPF	Optimal Power Flow
OR	Order Reduction
PC	Power Component
PCC	Point of Common Coupling
PCU	Power Conditioning Unit
PDF	Probability Density Function
PNS	Power Not Supplied
PS	Power Supplied
PSS®E	Power System Simulator for Engineering
PQ	Power Quality
PV	Photovoltaic
PVC	Polyvinyl Chloride
QoS	Quality of Supply
RBTS	Roy Billinton Test System
RES	Renewable Energy Sources
RoRE	Return on Regulatory Equity
RU	Rural
RW	Relative Weight
SAIDI	System Average Interruption Duration Index
SAIFI	System Average Interruption Frequency Index
SC	Shunt Capacitor
SDS	State Duration Sampling
SE	State Enumeration
SGT	Smart Grid Technology
SI	Short Interruption
SMCS	Sequential Monte Carlo Simulation
SP	State Pruning
SP-MOR	Application of SP before MOR
SSD	State Space Diagram
STS	State Transition Sampling
SU	Suburban
SV	Singular Value

SVD	Singular Value Decomposition
SQS	Security and Quality of Supply
TCB	Tele-controlled Circuit Breaker
TNR	Traditional Network Reduction
TTF	Time to Fail
TTR	Time to Repair
WPD	Western Power Distribution
WSC	Worst Served Customer
WTP	Willingness to Pay
XLPE	Cross-linked Polyethylene
UC	Underground Cable
UR	Urban
UK	United Kingdom
U-MOR	Usual Implementation of MOR
UKPN	UK Power Networks
USA	United States of America
VaR	Value at Risk

Symbols

α	scale parameter
β	shape parameter
η_{ch}	ES charging efficiency
η_{dis}	ES discharging efficiency
$\hat{H}(s)$	transfer function of the reduced system
$\hat{y}(\cdot)$	output of the reduced system
λ	component failure rate
$\|\cdot\|_\infty$	H_∞-norm of a rational transfer function
μ	component repair rate
σ	HSV of a system
A	system matrix or state transition matrix
aff	affected
Av	availability
B	control/input matrix
C	output matrix
$cust$	customer
$H(s)$	transfer function of the original system
int	interrupted

N	number of samples
n	state space dimension of the original system
P	controllability Gramian
P_{ch}	electrical power input
P_{dis}	electrical power output
Q	observability Gramian
R	Random number
r	state space dimension of the reduced system
T	transformation matrix
U	unavailability
$u(\cdot)$	input
$x(t)$	state vector
y	year
$y(\cdot)$	output of the original system

To my family

Chapter 1

Introduction

There is international interest in the development of electrical energy systems that deliver on the ambition of climate neutrality. Given the high share of greenhouse emissions from the energy sector i.e. over 75% in the European Union (EU) [1], most countries have set out targets to increase the share of renewable energy across different economic sectors. Accordingly, the revised Renewable Energy Directive (2018) requires that at least 32% of the energy demands within the EU are met by renewable energy sources (RES) by 2030 [2]. Similar targets were set in the United Kingdom (UK) where the National Energy and Climate Plan (NECP) reported that RES accounted for around 28% of UK's electricity generation in 2017 with Scotland registering a remarkable 69% [3]. This is on the back of the UK's legal commitment, through the recently amended Climate Change Act 2008, to reduce greenhouse gas emissions to net-zero by 2050 [4].

These ambitious targets contextualise why RES are continuously being utilised to meet energy demands through the adoption of more decentralised means of energy distribution using the concept of distributed generation (DG). DG is defined as relatively small-scale generation when compared to traditional centralised generation. It is installed in the distribution system at low (11 kV) to medium (33 kV) voltage levels, through the connection at substations to distribution feeders and at customer load level. In cases where this energy production is done on yet even smaller scales (e.g. 415 V), with respect to DG, such as for residential dwellings, small businesses, and communities, it is called microgeneration (MG). Although DG units typically vary in fuel type, size, and efficiency, they are often categorised based on the type of energy source used – conventional and nonconventional sources. Conventional-type DG includes fuel cells, combustion and microturbines while the nonconventional-type DG is based on RES such as wind, hydro, geothermal, photovoltaic (PV) and biomass [5]. To illustrate the scale of the

nonconventional-type DG capacity, the electricity system operator in the UK, National Grid, publishes regular reports on future energy scenarios for projected capacity. It is estimated that to meet the 2050 net-zero emissions target, over 75% of the electricity generation will invariably be from wind and solar, with the other RES accounting for another 16%. In particular, PV capacity growth is illustrated in Figure 1.1 showing also the four future energy scenarios i.e. consumer transformation, system transformation, leading the way and steady progression. "Leading the way" is expected to have very high residential and commercial PV installations, lead to the fastest credible decarbonisation and require the highest level of societal change [6].

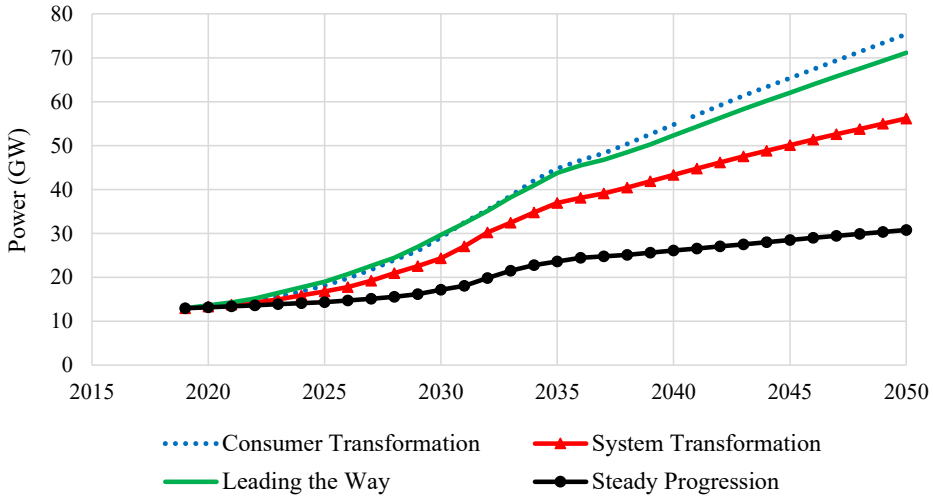

Figure 1.1: Projected PV capacity by future energy scenario in the UK [6].

Although RES present advantages such as reduced emissions, their uptake has invariably led to changes in the fundamental planning and operation of power systems requiring a paradigm shift to decentralised energy management. Firstly, this new paradigm is expected to result in palpable environmental and economic benefits through providing not only residential low-voltage (LV) customers but also commercial and industrial medium-voltage (MV) customers, with the capability for reducing their overall electricity consumption and energy bills. In addition, customers in future distribution systems, using smart metres, enhanced storage devices, and advanced communication infrastructure, are expected to exercise more active control of their electricity usage patterns (dynamic adjustment) in response to the state of the network. Therefore, they may participate in ancillary services markets through the provision of frequency response and short-term operating reserves [7]. To ensure efficient system operation, especially in deregulated power markets, this change in the traditional energy consumption patterns requires effective control and coordination. This constitutes one of the key motivations behind the "smart grid" concept.

1.1 The Integration of Smart Grid Technologies into Distribution Networks

The modernisation of electricity transmission and distribution systems into a "smart grid" is geared towards maintaining a reliable and secure energy infrastructure capable of meeting future demand growth. This smart grid is a flexible electricity network which provides different enhanced system functionalities such as enhancement of control and communications between network assets, balancing of power flows, enhanced fault protection, dynamic optimisation of grid operations and resources, provision to customers of timely information and control options, etc [8]. Among others, the smart grid considers the following technologies, DG, demand-side response (DSR), energy storage (ES), collectively termed as distributed energy resources (DERs) whose intelligent deployment constitutes their use as the so-called smart grid technologies (SGTs)[1]. The correct management of SGTs is expected to improve the quality of electricity supply by ensuring maximum asset utilisation, higher energy efficiency, lower energy bills, better environmental impact, and higher sustainability, among others. This also has the added advantage of allowing for the deferment of investments for network area reinforcement [9].

While the benefits of SGTs are undoubtedly significant, their reliance on intermittent RES means that there remains an overarching uncertainty regarding their stochastic behaviour. Many of these technologies also have a low capacity value which is defined as a measure of a generator's contribution in terms of electricity output to the system peak. This means that while they may replace the energy generated by the conventional plant, they may do so in a disproportionate way that requires retention of some conventional generation capacity to ensure that system reliability is not compromised. Operating the conventional plant with lower load factors and at reduced frequency can increase overall system costs [10]. Accordingly, the integration of SGTs into distribution networks requires updates to available methods of assessment to accurately quantify their various impacts on the operation of already existing systems. These include the contribution to generation capacity margin, quality of supply (QoS) to end customers and the resultant financial markets for example peer-to-peer energy trading and ancillary services markets. QoS is a general term encompassing power quality, quality of technical services and power system reliability. It is important to appreciate that reliability has become a comprehensive approach for evaluating not only system planning but also operation studies. It refers to the performance assessment of all or part of a system supplying electricity customers as it is closely linked with continuity of supply (CoS).

[1] Due to the specific use of DERs in smart applications, this thesis uses the acronyms, SGT and DER, interchangeably.

1.1.1 Changes to Traditional Reliability Analysis Methods

Traditional reliability analysis methods only require the fault and repair rates of network components and the network loading level. However, the current proliferation of SGTs integrated at the distribution network level requires the development of novel reliability assessment methodologies. These must account for the stochastic variation of SGTs while also providing accurate modelling of their interaction with pre-existing systems. Moreover, they must be capable of higher data input and computational capacity as the distribution networks increase both in size (network components) and in system complexity. The effect of increasing system complexity is of notable concern because SGTs introduce bidirectional power flow and uncontrolled customer-defined power generation patterns through local MG. This changes the impact of system operation on certain network components whose deterioration has previously been correlated with system loading. For example, in traditional power systems, transformer lifetimes are usually shortened if they are frequently overloaded.

Additionally, SGTs may require changes in pre-existing protection schemes as this can have significant effects in terms of the frequency of both momentary and sustained interruptions. For instance, sustained interruptions may occur when circuit breakers lockout due to multiple tripping caused by transient faults from faulty PV installations. Also, local DG installations may contribute to reverse power flow and this must be adequately catered for by protection settings. Accordingly, this research seeks to fill these research gaps by providing not only more accurate models of relevant SGTs (PV, DSR and ES) but also quantifying their impacts on reliability performance by developing and updating relevant reliability assessment methodologies. This research substantially adds to the literature in terms of providing SGT models as well as proven methods to include them in reliability analyses.

1.1.2 Regulator Requirements for Customer Supply Interruptions

The continued uptake of SGTs will invariably affect the level of supply continuity experienced by consumers who usually desire high levels of reliability but at reasonable cost. Energy regulators in several countries are tasked to ensure that distribution network operators (DNOs) make every effort to deliver energy to consumers as reliably and cost-effectively as possible. The regulators acknowledge that whilst supply interruptions may be inevitable, their duration and frequency can be limited, especially for consumer satisfaction. Traditionally, these regulators set targets for performance indicators for example, the Office of Gas and Electricity Markets (OFGEM) in the UK sets targets based on customer minutes lost (CML) and customer interruptions (CI) for which there are penalty/reward schemes [11, 12]. However, in the growing context of more bidirectional power flows due to the mass uptake of SGTs, these targets

will no doubt require to recognise the current system conditions for which networks are already accommodating large amounts of RES-generation [13].

Naturally, DNOs are eager to improve and maintain high network performance in the interest of their financial and technical goals. DNOs typically ensure that these performance targets are achieved by carrying out accelerated reactive maintenance (fixing faulty equipment by improved crew reaction times) and less prevalently, preventive maintenance by performing regular equipment inspection to replace those in poor condition. Also, using automation, the DNOs can redirect supplies and reduce the duration of supply interruptions. This is often alongside reinforcing their networks to enable them to cope with increasing and changing customer demands and patterns for example due to the use of the previously introduced SGTs as well as electric vehicles, heat pumps, etc. [14]. The proliferation of these SGTs also requires DNOs to take on system operator functions for example using real-time data and active network management to make network interventions. This is referred to as the transition from DNO to distribution system operator (DSO) [15]. Accordingly, this research investigates and quantifies the risk of customer interruptions in distribution networks endowed with SGTs as well as assessing the risk of failure to meet the regulator-imposed requirements for poor levels of CoS. On top of the implications for the regulators and DNOs (future DSOs), these results also communicate important information for CoS performance that are pivotal to assessing customer willingness-to-pay.

1.1.3 The role of Reliability Data as a Planning Tool

It is widely acknowledged that carrying out more planned hours of preventive maintenance often leads to fewer hours of unplanned (reactive) maintenance. However, it is also true that operational costs may be increased by carrying out too much preventive maintenance and in some cases, even leading to unnecessary system outages. By developing maintenance procedures based on predictive analysis through reliability studies, it is possible to determine the right amount of maintenance required to achieve a set performance level. This has partly been investigated in [16] which focuses on identifying critical network components for these improved maintenance schemes and in [17] where maintenance alternatives for asset management are compared. The reliability analyses presented in this thesis bolster those investigations by providing both average values of system performance as well as the associated probability distributions. Resultant indices communicate the level of system risk and the probability of failure to meet certain targets given the varying load demand and the SGT integration at different network points. The reduction of the system risk then motivates the development of predictive maintenance procedures informed by rigorous reliability analyses.

Currently, most DNOs collect asset reliability data mainly for asset management (planned maintenance) but do not use this data for reliability assessments [18]. This is primarily due to the computational complexity of carrying out detailed reliability assessments which is further increased by the addition of SGTs. DNOs also often cannot justify the cost associated with carrying out predictive reliability studies and tend to use reliability statistics after a reporting period rather than in the planning phase [19]. However, the DNOs have new motivations to look further into the function of reliability as a planning tool. This is due to the recent developments in computational capacity and the accelerated connection of RES to the grid (motivated by operational costs, climate neutrality and regulatory frameworks). Therefore, this research seeks to provide novel techniques for reliability assessment that allow for network reduction (to lower system size and complexity) as this is paramount to use of reliability assessment techniques in the industry. Also, by providing fast and accurate modelling of SGTs that accounts for their stochastic behaviour, this research can make a unique case for application in an industry context while also suggesting deployment techniques that maximise the associated benefits.

1.2 Research Objectives and Scope

The aim of this research is to assess the aggregated impact of SGTs namely PV, DSR and ES, on the reliability of power supply and propose recommendations for their deployment as smart interventions that maximise the benefits offered in electricity distribution networks.

This research addresses four main objectives:

- Development of accurate models describing the relevant SGTs namely PV, DSR and ES, and capturing their temporal variations to enable the accurate quantification of their impact on the reliability performance of electricity distribution networks at low and medium voltage levels.
- Assessment of the impact of SGTs on network reliability performance to enable the development of deployment measures that maximise their benefits to CoS which is measured using standard system and customer-oriented reliability indices, calculated through probabilistic methods.
- Differentiation between load sectors (rural, suburban, urban) in reliability assessment through the quantification of the frequency and duration of network faults, as well as energy not supplied. This includes an accurate assessment of the range of effectiveness of SGTs for varying customer groups.

- Formulation of new and efficient methods for optimal aggregation of distribution networks to enable the advancement of simulation techniques such as Markov, Monte-Carlo and risk modelling. Through the representation of detailed networks, these simplified models will allow for more accurate quantification of the impacts of integrated SGTs using relevant CoS metrics.

This research is driven by the outcomes of a research project "Integrated assessment of the quality of supply in future electricity networks", EP/G052530/1, funded by the Engineering and Physical Sciences Research Council (EPSRC) in the UK [20]. The main outcomes of this project included updated network component models, identification of configurations and topologies of generic LV and MV networks, development of the relevant load models for different types of demand profiles (e.g. rural, urban), the base methodology for the CoS performance assessment, and some minimal analyses using SGTs. However, there was no provision of comprehensive analyses covering the most relevant models and assessment methods involving SGTs. For example, neither the temporal variation of PV nor the state-of-charge variation of ES was explicitly modelled. Accordingly, through the first three objectives, this PhD research aims at filling that research gap and extending the knowledge of SGT modelling in reliability analyses in addition to updating the relevant network distribution models at both LV and MV to capture the most commonly used configurations, protection devices and operational schemes.

The fourth research objective is interlinked with the first three as it requires improvement to the existing techniques of network aggregation that will result in simplified models that can suitably represent the complexity of distribution networks without a significant loss of inherent variability/accuracy. For DNOs, this can have three major applications. Firstly, fast assessment of the reliability-based contribution from SGTs serves as an input to planning decisions for network operation especially considering DNO-led pilot schemes that promote the use of DERs to determine their practical effectiveness. Secondly, reliability assessments can be performed to predict future system performance and hence carry out reliability-based maintenance as opposed to the usually implemented reactive maintenance which is done because reliability is computed at the end of a reporting period using statistical analyses. Lastly, quicker reliability assessments allow for the evaluation of customer outage costs which are a function of outage time and associated agreements (contracts) with different customer groups. These outage costs, which can be calculated from the energy not supplied, are a key motivator for targeting investment costs in network areas with poor reliability.

1.3 Research Contributions

The original contributions to knowledge and elements of novelty from this PhD research are provided as follows and clustered according to the main research objectives.

Objective 1 Development of accurate SGT models:

- *Development of accurate PV models for reliability assessment*
  Due to the variability of solar irradiation, the output of PV models is usually limited to average values in reliability analyses. This lowers the complexity of analyses and allows for good first-order approximations of PV impacts. However, it neglects the inherent stochastic variation of PV and may overestimate the CoS benefits. Therefore, this work develops PV models that provide a more rigorous quantification of their benefits by modelling the stochastic variation of PV as well as the associated energy loss during power production due to unpredictable cloud movements. Furthermore, these PV models are integrated into a reliability assessment methodology that relies on probabilistic modelling for the calculation of relative reliability indices which are useful for lowering the uncertainty associated with utilised input data. This probabilistic methodology, which is enhanced by including the time-variation of demand and network component fault rates, ensures the accurate quantification of the reliability-based benefits offered by PV deployed in realistic MV networks.

- *Improved modelling of ES and DSR*
  Usually, the benefits offered by ES in terms of CoS improvement are obtained by considering ES devices with ideal outputs (no failure and constant state of charge). Although such analyses quantify benefits that are indicative of improved system performance, they may be improved by providing more accurate ES models. Accordingly, this research executes an innovative application of an intelligent energy management system (tested in a smart grid laboratory) to control ES operation and model the realistic variation of ES state of charge levels dependent on varying system conditions i.e. solar irradiation, load demand, and electricity tariff during grid supply. Inclusion of this more sophisticated ES model provides more confidence in the reliability results and substantially differentiates it from available similar reliability analyses. Additionally, while most DSR models are implemented for demand reduction during peak periods (peak shaving) or shifting demand to lower-demand periods, this research utilises a theoretical interruption model to propose the use of DSR during periods of highest fault probability. This novel application of DSR provides the highest reliability benefits compared with comparable techniques. Lastly, the results demonstrate that the combination of DSR and ES is the most effective measure to improve CoS.

Objective 2 Assessment of the impact of SGTs on reliability performance:

- *Comprehensive quantification of the CoS performance improvements offered by SGTs*
  There remains an under-appreciation of the benefits offered by probabilistic approaches in reliability assessments. Despite gaining more popularity in recent years, the dissemination of reliability statistics still takes the form of average values which may be obtained using deterministic approaches. This research provides a comprehensive set of average values and probability distributions of the system and customer-oriented reliability indices that measure the frequency and duration of supply interruptions and the associated energy not supplied to affected and non-affected consumers. Also, risk assessment indices that consider the high impact low probability events are presented in some cases to provide further analysis of the long tails of the probability distributions. The inclusion of the SGTs (PV, DSR and ES) makes the results directly applicable/useful to the planning and operation processes of DNOs. Moreover, probability distributions of the indices communicate the probability with which targets, which are set by regulatory authorities, may be exceeded thereby quantifying the associated financial risk.

Objective 3 Load sector classification in reliability assessment:

- *Differentiation between load sectors in reliability assessment*
  Although it is widely acknowledged that the location of demand and its density affects network reliability performance, the scale of distribution networks often requires customer aggregation into large clusters to reduce the complexity of reliability analyses. However, this research emphasises the capability of customer-oriented indices to provide more accurate SGT benefits, especially for worst served customers. Accordingly, customer groups are disaggregated by modelling and assessing MV networks serving different load sectors (rural, suburban, urban). This allows for an accurate demonstration of the range of variability and effectiveness of SGTs for different customer groups in different networks. This information is invaluable to DNOs whose investment decisions are invariably informed, in part, by reliability indicators. Not to mention, the results are useful for quantifying the impact of undergrounding on reliability performance given the different types of network components, topologies and spatial distributions of demand.

Objective 4 Optimal aggregation of distribution networks:

- *A novel technique for network aggregation using model order reduction*
  Distribution network models are often aggregated to reduce the computational time required for reliability analyses. These aggregate models often represent entire LV networks as single components connected to lumped load and neglect the variability of constituent network components as well as the spatial distribution of the demand served.

Therefore, this research develops a novel approach to the aggregation of network models for reliability assessment purposes using model order reduction (MOR). The proposed MOR-for-reliability method is used to analytically derive simplified grid representations that contain the most important system dynamics while simultaneously minimising the error of the considered grid reliability metrics and being substantially faster to simulate.

- *Accurate impact assessment of SGTs using reduced-order models*
  The addition of SGTs to distribution networks increases the complexity and size of network models. Given the prevalent use of aggregation in reliability analyses, it is necessary to accurately account for SGT impact in larger-scale reliability analyses. Accordingly, the proposed MOR-for-reliability technique is enhanced using state pruning methods to improve the aggregation accuracy especially for LV networks which are normally operated radially. Moreover, time-varying demand profiles are included as well as a more accurate representation of relevant SGTs to demonstrate the enhanced capability of the proposed method in rigorously quantifying their impact on network reliability.

1.4 Publications

Journal Publications

1. **M. B. Ndawula**, S. Djokic, and I. Hernando-Gil, "Reliability Enhancement in Power Networks under Uncertainty from Distributed Energy Resources," Energies, vol. 12, no. 3, p. 531, Feb. 2019. Energies 2019, 12, 531.

2. **M. B. Ndawula**, I. Hernando-Gil, R. Li, C. Gu and A. De Paola, "Model Order Reduction for Reliability Assessment of Flexible Power Networks," International Journal of Electrical Power & Energy Systems, vol. 127, p. 106623, May 2021.

Conference Publications

1. **M. B. Ndawula**, I. Hernando-Gil and S. Djokic, "Impact of the Stochastic Behaviour of Distributed Energy Resources on MV/LV Network Reliability," 2018 IEEE International Conference on Environment and Electrical Engineering and 2018 IEEE Industrial and Commercial Power Systems Europe (EEEIC / I&CPS Europe), Palermo, 2018, pp. 1-6, doi: 10.1109/EEEIC.2018.8494463.

2. **M. B. Ndawula**, P. Zhao and I. Hernando-Gil, "Smart Application of Energy Management Systems for Distribution Network Reliability Enhancement," 2018 IEEE International Conference on Environment and Electrical Engineering and 2018 IEEE Industrial

and Commercial Power Systems Europe (EEEIC / I&CPS Europe), Palermo, 2018, pp. 1-5, doi: 10.1109/EEEIC.2018.8494478.

3. **M. B. Ndawula**, A. D. Paola and I. Hernando-Gil, "Evaluation of Customer-oriented Power Supply Risk with Distributed PV-Storage Energy Systems," 2019 IEEE Milan PowerTech, Milan, Italy, 2019, pp. 1-6, doi: 10.1109/PTC.2019.8810753.

4. **M. B. Ndawula**, A. D. Paola and I. Hernando-Gil, "Disaggregation of Reported Reliability Performance Metrics in Power Distribution Networks," 2019 International Conference on Smart Energy Systems and Technologies (SEST), Porto, Portugal, 2019, pp. 1-6, doi: 10.1109/SEST.2019.8849130.

5. M. L. Ellery, **M. B. Ndawula** and I. Hernando-Gil, "Reliability Enhancement of LV Rural Networks using Smart Grid Technologies," 2019 International Conference on Smart Energy Systems and Technologies (SEST), Porto, Portugal, 2019, pp. 1-5, doi: 10.1109/SEST.2019.8849045.

6. I. Hernando-Gil, Z. Zhang, **M. B. Ndawula** and S. Djokic, "DG Locational Incremental Contribution to Grid Supply Level," 2020 IEEE International Conference on Environment and Electrical Engineering and 2020 IEEE Industrial and Commercial Power Systems Europe (EEEIC / I&CPS Europe), Madrid, Spain, 2020, pp. 1-6, doi: 10.1109/EEEIC/ICPSEurope49358.2020.9160745.

7. D. Fang, M. Zou, G. Harrison, S. Z. Djokic, I. Hernando-Gil, **M. B. Ndawula**, J. Gunda and X. Xu, "Deterministic and Probabilistic Assessment of Distribution Network Hosting Capacity for Wind-Based Renewable Generation," 2020 International Conference on Probabilistic Methods Applied to Power Systems (PMAPS), Liege, Belgium, 2020, pp. 1-6, doi: 10.1109/PMAPS47429.2020.9183525.

Poster Presentations

1. **M. B. Ndawula** and I. Hernando-Gil, "Impact of the Stochastic Behaviour of Renewable Resources on Power System Reliability[2]," STEM for Britain 2018 national poster competition for early career researchers, Westminster, UK, March 2018.

[2]This work was among the 45 shortlisted candidates for the 'STEM for Britain' national poster competition organised by the House of Commons Parliamentary and Scientific Committee. Poster content was adopted for intelligible and interested laypeople as opposed to members of a learned society.

2. **M. B. Ndawula** and I. Hernando-Gil, "Impact of the Stochastic Behaviour of Renewable Resources on Power System Reliability[3]," EPSRC HubNet Risk Day, Manchester, UK, March 2018.

3. **M. B. Ndawula**, A. D. Paola and I. Hernando-Gil, "Evaluation of Customer-Oriented Power Supply Risk with Distributed PV-Storage Energy Systems," EPSRC Supergen Energy Networks Hub Risk Day, Cambridge, UK, March 2019.

1.5 Thesis Structure

The rest of this thesis is structured as follows:

Chapter 2 presents the literature review related to the assessment of the continuity of electricity supply in power networks. Initially, the context is established using relevant interruption data from various European countries, highlighting also the different instruments used for regulation of CoS levels. It also includes an overview of the most widely used system performance metrics followed by an analysis of the impact of the considered SGTs (PV, DSR and ES) on network functionality and reliability. Finally, the chapter discusses the need to aggregate networks to provide more accurate SGT-impact assessments followed by the contributions of this PhD research to the state of the art in reliability assessment methodologies, SGT modelling and power network reduction methodologies.

Chapter 3 provides an integrated approach for assessing the impact of SGTs on the reliability performance of typical MV distribution networks. Analyses include the spatio-temporal variation of PV, the variability of the state of charge in coordinated ES, and the use of demand-manageable loads. In addition to using both system and customer-oriented indices, reliability assessment is presented for different load sectors (rural, suburban, urban) to demonstrate the range of variability and effectiveness of SGTs for different customer groups. Moreover, this chapter presents results using average values, probability distributions, and in some cases, analysis of the tail of these distributions to assess what impacts the proposed SGTs may have on high impact low probability events. Lastly, the work analyses the impact of undergrounding on reliability performance.

Given the complexity of modelling detailed networks, **Chapter 4** introduces a novel use of model order reduction techniques for the specific problem of network aggregation. The proposed methodology is used to derive reliability models of electricity networks, which exhibit a reduced number of equivalent components thereby simplifying the complexity for network re-

[3]The material presented varied significantly from Poster 1 due to the audience (researchers in risk analysis).

liability analysis. Using several case studies, the proposed method is shown to allow for faster reliability assessments while preserving high accuracy.

Chapter 5 explores how the accuracy of the proposed methodology in Chapter 4 may be increased especially for radial networks despite current method limitations. This is achieved using a novel application of state reduction or state pruning techniques, prior to performing model order reduction, that substantially increases the reliability assessment accuracy. Lastly, the capability of the developed procedure to include time-varying demand profiles as well as accommodate the impact of SGTs in the simplified/reduced system models is demonstrated.

Finally, **Chapter 6** reviews the main results of this research and presents the key limitations, some of which form the basis of the future research directions that are also discussed.

Chapter 2

Continuity of Electricity Supply in Modern Power Systems

This chapter examines the background, literature review, challenges and current solutions, related to the continuity of electricity supply in power networks, especially those endowed with SGTs and their effect on network functionality and specifically reliability. Initially, the context for the assessment of CoS (within the wider context of QoS) is presented using relevant interruption data from various European countries, highlighting also the various security and regulator-imposed requirements for supply restoration times. There is also a critical analysis of the perceived level of CoS from the customer perspective in addition to presenting the various customer compensation schemes already offered in different countries for unsatisfactory CoS. This is followed by an overview the most widely used metrics and CoS assessment methodologies. Then, an analysis of the SGTs integrated into power networks and used for this research is presented together with a review of their impact on network functionality. Finally, the chapter discusses the need to aggregate networks to provide more accurate SGT-impact assessments followed by the contributions of this PhD research to the state of the art in reliability assessment methodologies, SGT modelling and power network reduction methodologies.

2.1 Regulatory Framework for Continuity of Supply

Through periodic reports, the Council of European Energy Regulators (CEER) addresses 3 major aspects of the quality of electricity supply across its member countries in Europe [21]. These are continuity of supply (availability), voltage quality, and the commercial quality i.e. the speed and accuracy of dealing with customer requests. This thesis is concerned primar-

ily with the CoS which concerns supply interruptions and focuses on events during which the voltage at the supply terminals of a network user drops to zero or nearly (practically) zero. In deregulated markets especially, network users expect a high CoS at a competitive and affordable price. This includes even those networks with significant penetration of SGTs (which are described in Section 2.3). In distribution networks particularly, the DNOs are therefore tasked with the optimisation of the CoS performance of their networks. To ensure that this optimisation is done in an economically efficient way, considering the customers' expectations and willingness to pay (WTP), most countries have national regulatory authorities (NRAs). CoS may be described by various quality dimensions/indicators which are traditionally useful for making decisions on the planning and management of power networks. The most common ones are the number of interruptions per year, unavailability (interrupted minutes) and energy not supplied per year [21, 22]. Accordingly, NRAs utilise regulatory instruments based on accurate definition and assessment of these indicators to complement incentive regulation which may take the form of price or revenue-cap mechanisms, penalty/reward schemes, etc. All these aspects are discussed in this section mentioning also the new changes in system operation that necessitate studies such as those presented in this PhD research.

2.1.1 Unplanned Interruptions

To classify CoS, most countries differentiate between planned and unplanned interruptions. A planned interruption is defined as a prearranged interruption for which network users are informed in advance (e.g. at least 48 hours in the UK [21]) due to the execution of scheduled works on the electricity network. An unplanned interruption is one where there is an interruption of supply to customers for longer than 3 minutes[4] where notification has not been given to the customers during the prescribed notice period. It is important to note that there are significant differences in CoS monitoring across European countries regarding the type of interruptions monitored, the reported level of detail and even the interpretation of the different indicators [21]. Performance comparisons between different countries and even DNOs within the same country are important because they provide useful case studies that are needed for CoS improvement while raising benchmark performance in different networks.

It is important to appreciate that the aforementioned CoS indicators may be calculated with or without exceptional events. There is a general lack of harmonisation in what events may be classified as 'exceptional' across different countries. For example, some countries take a statistical approach while others base their definition on the causes of an event (e.g. natural causes). Exceptional events are hard to predict, occur with relatively very low probability and

[4]The definition of unplanned interruptions varies for different countries e.g. it is 1 minute in the USA.

usually lead to major system disruption depending on the severity and duration. These events are the focal point of system resilience studies but hardly inform reliability studies (or targets) because reliability is more concerned with the events that occur during normal operating conditions and thus have relatively higher probability i.e. not statistical outliers. Accordingly, this PhD research, which focuses mainly on reliability, considers unplanned system interruptions excluding exceptional events. Figure 2.1(a) presents the minutes lost per year for unplanned interruptions excluding exceptional events in various countries. The analysis focuses only on those countries where the minutes lost never exceeded 200 and shows a continuously decreasing trend in nearly all countries. Similarly, Figure 2.1(b) presents the interruptions per year for countries not exceeding 3.5 interruptions. This also demonstrates either constant continuity levels or a smooth general tendency for an increase in CoS for nearly all countries [23].

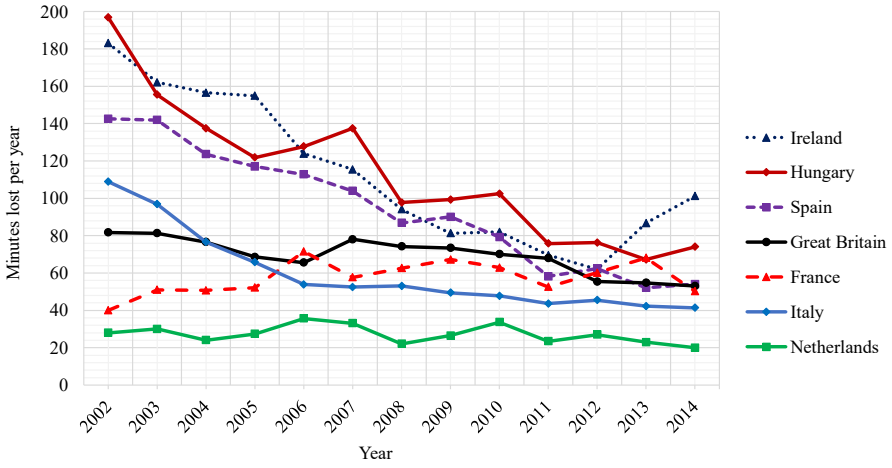

(a) Minutes Lost per year (not exceeding 200 minutes)

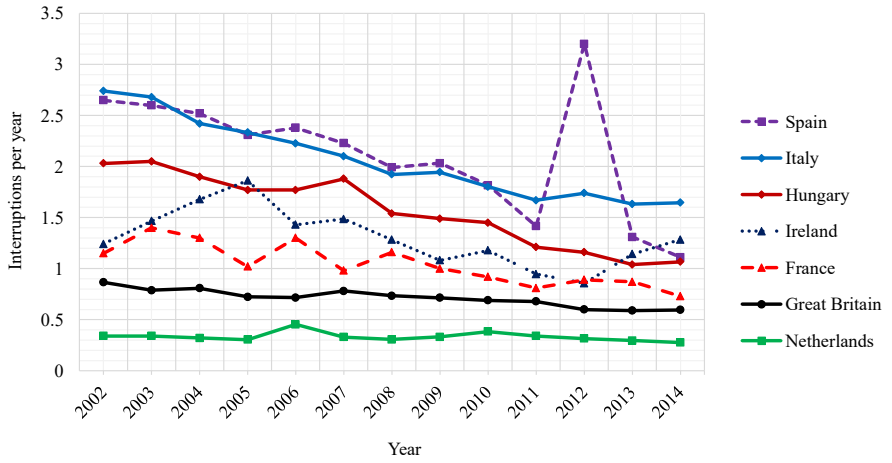

(b) Interruptions per year (not exceeding 3.5 interruptions)

Figure 2.1: Unplanned sustained interruptions excluding exceptional events [23].

On top of varying network operation ideologies, it is important to note that the differences in performance across different countries are also heavily dependent on the technical characteristics of the various networks. These are based on population density, network topology, climate, and even policy. One key CoS performance differentiator is the proportion of cable circuits used in each network. Table 2.1 presents the length of overhead lines (OHLs) and underground cables (UCs) at both LV and MV levels in 2014. When compared to Figure 2.1, it is evident that the countries with a higher percentage of UCs have lower values of the corresponding interruption indicators. For example, UCs made up over 84% and 48% of the total length of LV and MV circuits in Great Britain (GB), respectively, compared to only around 27% and 20% of the corresponding lengths in Hungary. Correspondingly, both the minutes lost and the number of interruptions suffered in GB were substantially less than those recorded in Hungary [21]. Additionally, the indicators in the Netherlands present the best CoS performance and this might be related, at least in part, to having a 100% use of UCs in both LV and MV networks.

Table 2.1: Length of circuits in European countries in 2014 [21].

	LV circuits (Length in km)				**MV circuits (Length in km)**			
Country	**OHLs**	**UCs**	**Total Length**	**Percentage of UCs**	**OHLs**	**UCs**	**Total Length**	**Percentage of UCs**
France	403550	302556	706106	42.85%	338628	288208	626836	45.98%
Great Britain	60813	328850	389663	84.39%	167951	158763	326714	48.59%
Hungary	64859	23841	88700	26.88%	53920	13480	67400	20.00%
Ireland	58098	12362	70460	17.54%	82800	9526	92326	10.32%
Italy	537399	320578	857977	37.36%	215102	173660	388762	44.67%
Netherlands	0	145712	145712	100.00%	0	105181	105181	100.00%
Spain	254491	189273	443764	42.65%	155901	92855	248756	37.33%

2.1.2 System-level Regulator Requirements for Quality of Supply

This section deals with existing quality regulation frameworks in a few European countries for electricity distribution networks. NRAs develop frameworks to ensure that the QoS is either maintained (if satisfactory[5]) or improved to socio-economically acceptable levels. Common actions taken by NRAs to achieve such goals take the form of publishing continuity data and implementing reward/penalty (financial incentive) schemes [21]. DNOs are henceforth tasked to implement investment, management and operational decisions to ensure high QoS levels based on regulator-set targets. Accordingly, measurement of CoS (a subset of QoS) is a prerequisite to set appropriate standards and penalty/reward regimes. Using robust and reliable data, it is possible to ascertain the actual continuity levels against which to set relevant targets. This subsection details the regulatory frameworks for CoS available in France, Germany and

[5]If the QoS level is already high, then a further improvement might be very costly for the customer.

the UK to illustrate not only their shared goals of achieving high CoS levels but also the slightly different approaches adopted to achieve these goals at the national level. The frameworks in the UK are further utilised in Chapter 3 of this thesis to demonstrate the risk of customer interruption times when different SGTs are deployed thereby proving informative of the potential benefits these technologies can have to CoS if deployed correctly.

2.1.2.1 Security of Supply Requirements in France

Like many countries, France uses a combination of rewards and penalties for CoS regulation in both its transmission and distribution networks. For the distribution networks specifically, the main indicator used is the system average duration of interruptions (SAIDI). The expected Cos level is estimated in line with the investment program of the distribution companies and past values of indicators considered in the incentive scheme. Even though no difference is made between rural and urban areas, this scheme requires a minimum CoS improvement for all distribution companies. For example, the expected CoS levels that corresponded to no penalty and no reward were 68, 67, 66 and 65 minutes for 2014, 2015, 2016 and 2017 respectively. The incentive rate for DNOs is given according to (2.1) where for example, the incentive of €4.3M/min corresponds to a value of lost load of about €6/kWh.

$$INC_N \;=\; -4.3 \times (SAIDI_{N\_ref}) \times \ln\left(\frac{SAIDI_N - 34}{SAIDI_{N\_ref} - 34}\right) \tag{2.1}$$

where INC_N is the incentive of the year N (reward if positive; penalty if negative), $SAIDI_N$ is the system average interruption duration index for the year N (including planned interruptions), and $SAIDI_{N\_ref}$ is the reference SAIDI for year N set at e.g. 65 minutes for 2017 [21].

2.1.2.2 Security of Supply Requirements in Germany

The quality regulation system in Germany aims to achieve a socio-economically acceptable CoS level which is not necessarily set by the NRA. DNOs get rewards or penalties based on overall CoS performance in comparison to the other DNOs. Overall performance is measured using SAIDI for LV and the average system duration of interruptions (ASIDI) for MV networks[6]. Each DNO is benchmarked against an individual reference level ($SAIDI_{i*}$). This reference value is load density-dependent (accounts for network structural differences) and is obtained using regression analysis. Proportionately, the difference between the CoS reference level and the DNO's current SAIDI level ($SAIDI_i$) is transformed into a monetary amount by

[6]Both SAIDI and ASIDI are explicitly defined in Section 2.2.2.

multiplication with a price of quality per unit and the number of customers served by that DNO. A fixed percentage of the allowed revenues is used to set the cap and floor for the rewards and penalties which are calculated using:

$$Reward/Penalty = (SAIDI_{i*} - SAIDI_i) \times Customers_i \times Price\ of\ Quality \tag{2.2}$$

Both the DNO's performance level and the CoS reference level are calculated as a mean of the continuity indicators for the past 3 years. This is done to cater for the stochastic influences in network reliability. The price of quality is based on the value of lost load and is estimated using a macroeconomic approach where data is obtained from national accounting. Given that there is no predetermined minimum improvement required, improving or worsening continuity is an optimisation decision taken by the DNO [21].

2.1.2.3 Security of Supply Requirements in the UK

In the UK, OFGEM considers the nature, frequency (CI), duration (CML) and consequences of supply outages to develop incentive scheme targets under the Guaranteed Standards (GS) [11] for the restoration of the interrupted supply. These schemes are developed as part of the Security and Quality of Supply (SQS) legislation for which OFGEM sets standards and performance levels for rectification of network faults to limit their impact on end-users. The incentives are intended to encourage DNOs to invest in operational tools and sometimes even infrastructure e.g. to the last mile of power supply, to ensure lower frequency and duration of supply interruptions. Conversely, the GS require DNOs to compensate end-users in all cases when network reliability performance is lower than the level of service required, considering also exceptional events e.g. severe weather conditions.

DNOs are rewarded/penalised according to the Interruption Incentive Scheme (IIS), based on their performance against agreed target reliability levels. The relevant cost estimations are conducted during the price control process and are valid for 8 years (the next price control will start in April 2023 [24]). Also, there is a limit to the penalties and rewards which is set to 2.5% of the return on regulatory equity (RoRE) [21]. RoRE is used to monitor the financial performance of DNOs under a given price control. Figure 2.2 shows DNO-group financial performance against cost allowances for the first and second years of the RIIO-ED1 price control period where a number of DNOs reached the cap on the rewards that can be earned under the IIS [11] and only Western Power Distribution (WPD) overspent on its allowances. Moreover, the supply to electricity customers must be restored within a specified period following an interruption. SQS legislation defines relevant time limits as maximum durations to restore at least

a minimum Group Demand (GD) of customers. Six classes of supply (A to F) are defined on GD ranges as shown in Table 2.2. which presents the minimum demand to be restored within a specified time [25].

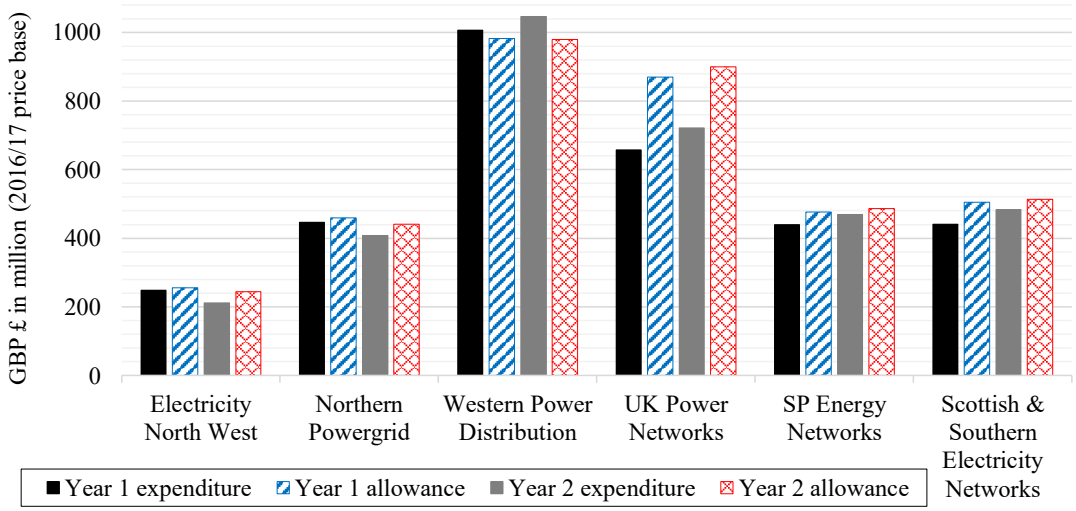

Figure 2.2: DNO financial performance against cost allowances for 2015-17 [11].

Table 2.2: UK security of supply requirements for interrupted customers [25].

Class of Supply	**Range of GD**	**Minimum demand to be met after first circuit outage**
A	GD $\leq$ 1 MW	In repair time: GD
B	1 MW < GD $\leq$ 12 MW	(a) Within 3 h: GD - 1 MW
		(b) In repair time: GD
C	12 MW < GD $\leq$ 60 MW	(a) Within 15 min: min GD - 12 MW; 2/3 GD
		(b) Within 3 h: GD
D	60 MW < GD $\leq$ 300 MW	(a) Immediately: GD - up to 20 MW
		(b) Within 3 h: GD
E	300 MW < GD $\leq$ 1500 MW	Immediately: GD
F	GD > 1500 MW	According to transmission license security standard

2.1.3 Regulations and Compensation for Single Users

In general, measurements of CoS are performed at both the system level (the focus of the previous section) and user-specific/customer level [21]. Usually, system-level measurements are done on an aggregate basis while user-level measurements are usually based on surveys asking customers about their satisfaction, expectations, and WTP (for high quality or to accept low-quality levels) [26, 27]. It is necessary to ascertain the CoS level as perceived by the network users because residential households will often have different usage patterns than business or

industrial consumers. This will result in diverging views about the CoS thereby requiring that appropriate standards and incentives are set for varying measurement (system/customer) levels as well as varying customer groups. Attention to this by DNOs results in increased profits through both rewards (or avoiding penalties) and avoidance of lost revenue due to customer interruptions.

Many countries specify minimum standards for QoS levels accompanied by associated payments to guarantee that single users are compensated for below-standard DNO performance. Mostly, economic compensation involves the individual duration of long unplanned interruptions. In these compensation schemes, the minimum duration of an interruption eligible for compensation varies between 1 hour (in the Netherlands) and 24 hours (in Ireland). These schemes are variant between countries for example, in Estonia and Romania, customers are eligible for compensation even for planned interruptions if they exceed certain thresholds. In Spain and Portugal, the compensation scheme considers the aggregated performance (total CI or CML) for a year. Poland offers compensation for the total duration of interruptions while in Italy, MV customers are compensated only in case of exceeding the maximum number of short and long interruptions in a year [21]. In the UK, OFGEM specifies requirements for the duration of customer interruptions to protect domestic and non-domestic customers from excessive long interruptions. These protect customers that have no special agreements with DNOs and are outlined in the Electricity Standard of Performance Regulations [28] which lists the maximum admissible durations of interruptions and corresponding penalties, as presented in Table 2.3.

Table 2.3: UK regulator-imposed requirements for supply restoration times [28].

No. of Interrupted Customers	**Maximum Duration to Restore Supply**	**Penalty paid to each (£)**	
		Domestic Customer	**Non-domestic Customer**
Less than 5,000	12 h	75	150
	After each succeeding 12h	35	35
5,000 or more	24 h	75	150
	After each succeeding 12h	35	35

The 12-hour standard applies under normal weather conditions. However, if the interruption is caused by an exceptional event, then the customer is only eligible for compensation after being without power for a minimum of 24 hours, or 48 hours for large events. These pay-outs are capped to £700 per customer per year. Also, specific compensation schemes are available for

the worst served customers (WSCs) in some countries e.g. the UK where funding is available[7] (£1000 per customer per scheme) for DNOs who demonstrate QoS service improvements for WSCs[8] [21, 29].

Compensation is not received automatically in every country. Out of the 17 European countries that compensate customers, only 11 offer automatic compensation: Estonia, Finland, France, Greece, Hungary, Italy, Netherlands, Portugal, Spain, Sweden and the UK. Even in these countries, automatic compensation will be case-specific. For example, in the UK only customers on the priority service register receive automatic compensation. In other countries, users are required to ask for compensation. For example, in Norway DNOs are only required to annually inform their customers on how to request compensation, as well as to make a standard request form available. Remarkably, customers in Slovenia are required to provide their own interruption recorded data to the DNO when they make a compensation claim for the calendar year [21].

2.1.4 Customer View of Network Reliability

In addition to the compensation schemes and regulatory frameworks introduced in the previous section, this section considers the capacity of the DNO meet users' expectations in ensuring continuous supply to their premises. This valuation is vitally important in determining the WTP for electricity and it establishes the market value and thus business case for the provision of electricity. A higher WTP is often ensured by confidence in the CoS [11, 30] which is characterised by the aforementioned quality dimensions. A key motivator for developing accurate methods to assess these quality dimensions is the strong correlation between a high level of CoS and the corresponding customer valuation of electricity as a commodity. Moreover, it is reported that nearly 80% of customer outages are caused by failures in the distribution network [31, 32]. Therefore, DNOs are keen on ensuring optimal network performance to result in higher levels of customer satisfaction. Evidence of DNOs exceeding their performance targets for 2016-17 is presented in Figure 2.3 [11]. Whereas system-wide indices such as those presented in earlier sections are typically used to assess network performance, there is a requirement to complement these with customer-based indices. This results not only in more accurate quantification of the risk of outages to affected customers but also in the accurate identification of worst-served customers.

[7] This is not considered strictly a specific regulation or standard in the UK. DNOs have a use-it-or-lose-it allowance to improve network reliability for qualifying customers with significantly poor service.

[8] A worst served customer is considered one who experiences a minimum of 12 unplanned higher voltage interruptions over a three-year period, with at least 3 higher voltage interruptions each year.

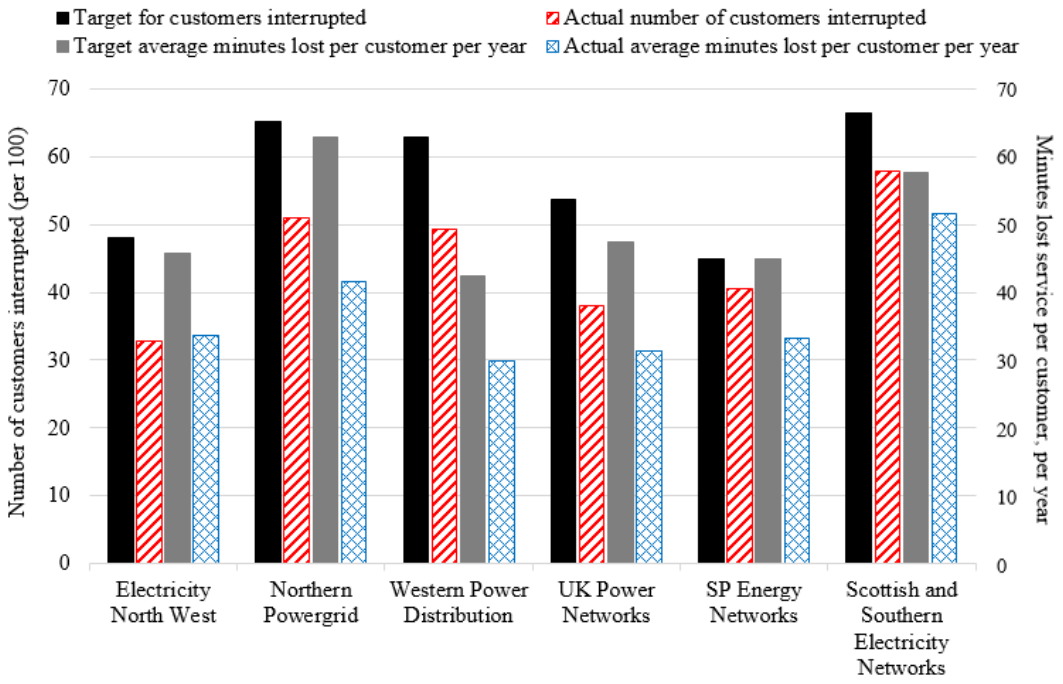

Figure 2.3: UK Customer interruptions and minutes lost 2016-17 [11].

Invariably, the reported CoS data depends on the population density, network topology and characteristics, types of power components (PCs) and the voltage level. Although CEER has continuously recommended that reporting of CoS indicators should be differentiated/disaggregated accordingly, there is slow uptake of this notion by various nations. For example, only 5 European countries provided CoS data in [33] which was disaggregated to different population densities i.e. urban, suburban, and rural areas. This is even though DNOs usually report fault events in their systems by distinguishing them based on types of PCs, network types, load sectors, voltage levels i.e. MV and LV etc.

In the UK, the current reliability-performance reporting structure only requires each DNO to provide the average CI and CML for their serviced areas. However, since each of the 14 UK DNOs delivers electricity to millions of customers spread across at least 10,000 km^2 in varying types of networks, i.e. rural areas to cities and towns, a single average value aggregating reliability performance over this spatial extent is insufficient to adequately describe the variation in network reliability performance [34]. While there might be some evidence to support the view that cities have fewer CI and CML than rural areas, it is necessary to quantify not only the extent of such variations but also identify the cases in which rural areas might have better performance [35]. When all UK DNOs exceed the regulator-imposed performance targets e.g.

in 2016-17 (Figure 2.3), there is a risk of under-evaluation of WTP, by especially the WSCs, because of the 'normalising' effect due to the other highly reliable areas served.

The use of disaggregated data will make it easier to identify priorities for regulation and network interventions [36]. This means that for example WPD, which overspent on its annual allowances as shown in Figure 2.2, can substantially reduce its expenses with targeted interventions in low-reliability areas as well as avoidance of mandatory payments to customers where necessary due to a failure to meet the regulator-set guaranteed standards of performance. Furthermore, through harmonisation of the definitions of the various QoS indicators as well as the relevant data collection procedures in different European countries, it will be possible to make performance comparisons that may result in drawing relevant lessons to improve the QoS for different customer groups. This will be especially useful for networks dominated by intermittent DERs such as PV. Chapter 3 of this thesis not only models these RES in typical MV networks but also provides a comprehensive reliability performance adequately characterising customers in different networks types (rural, suburban and urban). The results are bolstered by quantification of the impacts of DERs in these different network types.

2.2 Continuity of Supply Assessment

Having introduced the wider context of CoS in the previous section, this section defines all the relevant terms and metrics useful in a CoS assessment. SQS incorporates three main aspects - reliability, power quality (PQ) and quality of technical services. First, security is concerned with the system's ability to respond to transient events without becoming unstable or resulting in loss of load. PQ describes the changes in power (voltage, current or frequency) that interfere with the normal operation of electrical equipment [37]. Reliability, which is the focus of this thesis, is the continuity of power supply when expressed as the ability of the PCs to function as intended [38].

2.2.1 Network Reliability

Reliability analysis invariably involves probability theory due to the probabilistic behaviour of power systems. For example, random failures of system PCs are generally outside the control of power system personnel, loads have inherent uncertainties and it is nearly impossible to obtain an exact load forecast. Additionally, the integration of DERs and information-control technologies into power systems greatly increases the uncertainty in system operation and planning, as well as the sources of system failure. The task of increasing system reliability requires the identification of the necessary measures required to reduce system unreliability while pro-

viding means to justify acceptable reliability levels. It is important to note that reliability evaluation of power systems should recognise not only the likelihood of failure events but also the severity of their consequences. Furthermore, the practical operation of power systems requires an appreciation of the fact that zero-unreliability is impractical because random failure events are uncontrollable. Therefore, an acceptable level of reliability must be justified both financially and technically [39].

Reliability analysis is required in the deregulated era of the power industry because the level of competition forces utilities to plan and operate systems closer to their limits. Accordingly, continuously stressed operation conditions have led to a deterioration in system reliability to the tune of various power outage events all over the world in the past few years. On top of the subsequent economic loss, considerable outage lengths call into question the sufficiency of the commonly used N-1 contingency criterion to provide a reasonable reliability level. However, given that it is difficult to justify N-2 or N-3 principles, one of the alternatives to improve system reliability is to include reliability evaluation into the power system design, planning, operation, and maintenance. Alongside keeping system reliability within acceptable ranges, it is also important to continuously inform customers about the inevitable level of unreliability associated with the delivery of power in terms of outage frequency, duration and probability. Also, by alerting them to the use of various resources, customers can improve the reliability of their premises in response to market and environmental conditions [39].

Reliability may be defined as the ability of a system device to operate without interruptions for the manufacturer-specified period (usually equipment lifetime) under normal operating conditions. Reliability may be extended to the whole system, or parts of it, focusing on different aspects e.g. PC reliability and customer/end user's reliability. One of the integral parts of reliability is adequacy which is defined as "the ability of the system to supply aggregate electric power and energy requirements of the consumers at all the times" [40] and refers to static system conditions, e.g. for long-term planning and investment purposes. The literature also reveals that reliability is often mentioned in concert with the terms maintainability and availability. Maintainability is the probability that a repairable PC or system can be repaired/restored to operational effectiveness in a defined environment within a specified period and in accordance with prescribed procedures. Correspondingly, increased maintainability implies shorter repair times. Finally, availability is the probability that a repairable PC or system is operational/not failed under defined environmental conditions [37, 41].

PC Outage models

To adequately characterise system reliability, it is important to note firstly that PC outages are the root cause of system failure. Therefore, it is useful to determine the relevant outage models and subsequently calculate the relevant system states and their consequences, to result in the accurate calculation of reliability indices. PC outages are usually classified into two: independent and dependent. Independent outages are further classified into forced, semi-forced and planned outages, or as full and partial failures according to failure states. Forced failures are distinguished as repairable and non-repairable. Most failures in power systems are repairable but nonrepairable failures also occur in real life. Dependent outages usually take the form of cascade failures and common cause failures e.g. simultaneous failure of a double line circuit due to lightning. Notably, dependent outages produce much more severe consequences than independent ones i.e. major power outages and blackouts [39]. This thesis concerns itself with only forced failures of repairable PCs as well as nonrepairable failures, which require the inclusion of PC ageing (mandatory in reliability evaluation) models to provide more realistic analyses of power system asset utilisation.

To model repairable forced failures when considering large generating units, it is usually necessary to consider outage models with multiple derated or partial output states based on the power output e.g. adjustable turbine blades in hydropower production. Models may also be adjusted to include various failures such as partial and multiple failures, and even planned outages. However, in distribution network analysis, the most used outage model for repairable forced failures only has two states (operating and failed). This model is common due to its simplicity and effectiveness in the description of PC failure. Accordingly, it is utilised in thesis and illustrated using Figure 2.4(a) which shows an up-down-cycle process together with the associated state space diagram given in Figure 2.4(b). The average unavailability (U) is given by [39], [42]:

$$U = \frac{\lambda}{\lambda+\mu} = \frac{MTTR}{MTTF+MTTR} \tag{2.3}$$

where λ is the failure rate (failures/year), μ is the repair rate (repairs/year), MTTR is the mean time to repair (hours), MTTF is the mean time to failure (hours), $\lambda = \frac{1}{MTTF}$ and $\mu = \frac{1}{MTTR}$ and the availability, $Av = 1 - U$ [41].

It is widely accepted that faults occur anywhere in a power system, and therefore that the probability of failure of any system PC (following a relevant outage model) may be quantified through the corresponding PC failure rate. In the event of a system or PC fault that leads to the outage of some customers, reliability analysis must provide the (expected) number of

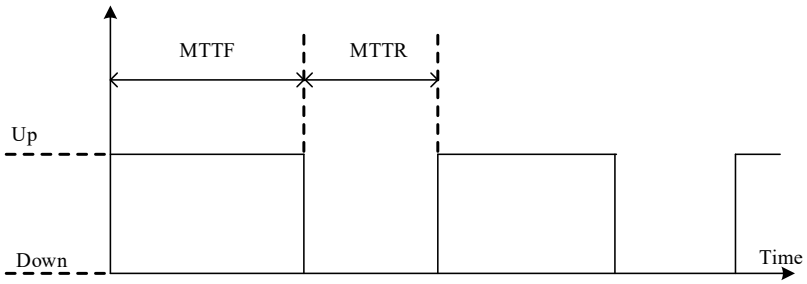

(a) Up-and-down cycle

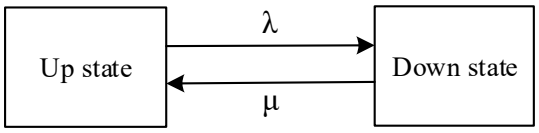

(b) State space diagram

Figure 2.4: Outage model for a repairable PC with 2 states [39].

disconnected customers, the (expected) duration of their outage and the (expected) amount of energy which is not supplied, using relevant indices.

2.2.2 Reliability Indices

Given the diversity of the incidents/faults that lead to interruptions to the supply of customers, types of interruptions must be classified. This is based mainly on the time period between the loss of supply and when it is finally restored. Long interruptions (LIs) are defined as loss of supply because of de-energisation in interconnecting system PCs. Short interruptions (SIs), usually resultant from switching operations, are classified as such, as long as supply is restored in less than 1 minute (in the USA) [43] or 3 minutes (in Europe) [21]. Some countries also classify interruptions lasting less than 1 second as transient interruptions. Others (e.g. UK, Norway, Sweden), however, classify these transients together with the short ones [21]. While most reliability studies provide LI-indicators, it is important to acknowledge that there are self-extinguishing faults (and other transient events) which are cleared by automatic reclosing. While these are usually the subject of PQ-related studies, there is a need to integrate such aspects into comprehensive reliability analyses [38] especially given the integration of SGTs that add to the complexity of network protection. Accordingly, this thesis provides reliability analyses that capture SI-events under normal operating conditions and even quantifies the impact that SGTs may have on SI-indicators. These are relevant results on the back of recom-

mendations from organisations such as CEER that continuously advocate for more widespread reporting on transient interruption indicators [21].

Reliability indices are either absolute or relative measures of system reliability [19]. Absolute indices are the values that a system is expected to exhibit based on past performance. These are considerably hard to predict given the uncertainties associated with predicting system requirements. This thesis uses relative reliability indices that are easier to interpret and assess because system behaviour is evaluated before and after the consideration of a design or operating change. This allows for the accurate quantification of SGT-impacts because there is reasonable confidence in the relative differences in the indices since uncertainties in data and system requirements are embedded in all network scenarios. Generally, there are several indices but some of the most used may be subdivided into sustained interruption, momentary and load-based indices [37]. The following system and customer-oriented indices are utilised in this thesis due to their widespread use in both research and industry, as well as their capability to adequately characterise different CoS levels as required by the goals set for this research. The corresponding mathematical definitions are provided as follows [44]:

2.2.2.1 Sustained Interruption Indices

The system average interruption frequency index (SAIFI) is the average number of sustained interruptions per customer recorded for a year. It is expressed in interruptions/customer/year.

$$SAIFI = \frac{\sum Customers\ Interruptions}{\sum Customers\ Served} \tag{2.4}$$

The corresponding customer index to SAIFI is the customer average interruption frequency index (CAIFI) which focuses only on the sustained interruptions for those customers experiencing interruptions whereby each customer is counted once. It is expressed in interruptions/affected customer/year and is particularly useful in recognising chronological trends in system reliability.

$$CAIFI = \frac{\sum Customers\ Interruptions}{\sum Distinct\ Customers\ Interrupted} \tag{2.5}$$

The system average interruption duration index (SAIDI) denotes the average duration of sustained interruptions in hours per customer for a year[9]. It is expressed in hours/customer/year.

$$SAIDI = \frac{\sum Duration\ of\ Customer\ Interruptions}{\sum Customers\ Served} \tag{2.6}$$

[9]The CI index (used in the UK) is equivalent to SAIFI but is calculated as the number of interruptions per 100 customers per year. Similarly, the CML index is equivalent to SAIDI.

Similarly, the corresponding customer index is given by the customer average interruption duration index (CAIDI) which deals with the average duration of interruptions per interrupted customer per year. It is expressed in hours/affected customer/year.

$$CAIDI = \frac{\sum Duration\ of\ Customer\ Interruptions}{\sum Customers\ Interrupted} = \frac{SAIDI}{SAIFI} \tag{2.7}$$

The average energy not supplied (ENS) during sustained interruptions is expressed using MWh/-customer/year. This is important for assessing the economic value of reliability, network planning decisions, and for future power networks, operational decisions.

$$ENS = \frac{\sum Energy\ not\ supplied}{\sum Customers\ Served} \tag{2.8}$$

Correspondingly, the average customer curtailment index (ACCI) is the equivalent customer index to ENS which only focuses on interrupted customers. It is useful for monitoring changes in ENS between calendar years and is expressed in MWh/affected customer/year.

$$ACCI = \frac{\sum Energy\ not\ supplied}{\sum Customers\ Interrupted} \tag{2.9}$$

2.2.2.2 Momentary Interruption Indices

SIs, voltage sags and swells can potentially damage sensitive equipment (e.g. power electronics). To evaluate system reliability, the momentary average interruption frequency index (MAIFI) considers momentary (short – 1min/3min) interruptions. It is expressed in (short) interruptions/customer/year. The time-aggregation rules are quite important when calculating MAIFI because multiple interruptions during a 1 or 3-minute period, due to automatic reclosing actions, may be counted as a singular event for MAIFI or as multiple events[10]. This will invariably have substantial effects on the index calculation.

$$MAIFI = \frac{\sum Momentary\ Customers\ Interruptions}{\sum Customers\ Served} \tag{2.10}$$

The corresponding customer index to MAIFI is, to the best of the author's knowledge, not provided for in reliability analysis literature. This is understandable given it is not a very commonly used index, with about half of the countries monitored by CEER not distinguishing between LIs and SIs. Accordingly, this research proposes a new index – customer average

[10]There also exists the Momentary Average Interruption Event Frequency Index ($MAIFI_E$) which indicates the average frequency of SI events but excludes those immediately preceding a LI.

momentary interruption frequency index (CAMIFI), described mathematically by (2.11), for quantification of SIs to customers affected only.

$$CAMIFI = \frac{\sum Customer\ Momentary\ Interruptions}{\sum Distinct\ Customers\ Affected} \tag{2.11}$$

2.2.2.3 Risk Assessment Indices

Although the main focus of reliability studies is on the high probability and low impact events [45], there are instances where the results in this thesis allow for brief analyses of heavy-tail distributions. The long tails of the resultant index probability density functions (PDFs) represent high impact low probability (HILP) events. One widely used metric for quantifying these worst cases is an α-percentile risk metric called the conditional value-at-risk (CVaR) [46]. CVaR quantifies the expected value of risk in the region beyond the usual confidence levels i.e. the value at risk (VaR) which is represented in the tail of the PDF curve for the chosen reliability index (e.g. SAIDI, SAIFI, ENS). Therefore, it defines the value of an index that is expected in the higher $(1-\alpha)\%$ of the cases [47] and is described mathematically using (2.12). More details on the application of this index for the reliability analyses in this thesis are presented in Sections 3.4 and 3.5.

$$CVaR_{\alpha}^{z} = \int_{VaR}^{+\infty} x f(x) dx \tag{2.12}$$

where $f(x)$ refers to the probability distribution function obtained from the annual reliability index results considering a time window of z years [48, 49].

2.2.2.4 Load Based Indices

Albeit not utilised in this thesis, this category of indices is worthy of mention. Load based indices focus on the amount of connected load (in kVA) rather than the number of customers served. They are especially useful when measuring system performance of areas serving relatively few customers that have relatively large concentrations of demand such as industrial/-commercial customers. The most common ones are the average system interruption frequency index (ASIFI) and the average system interruption duration index (ASIDI). As expected, in a system with homogeneous load distribution, ASIFI and ASIDI should be the same as SAIFI and SAIDI.

$$ASIFI = \frac{\sum Connected\ kVA\ of\ Interrupted\ Load}{\sum Connected\ kVA\ Served} \tag{2.13}$$

$$ASIDI = \frac{\sum Connected\ kVA\ Duration\ of\ Interrupted\ Load}{\sum Connected\ kVA\ Served} \tag{2.14}$$

2.2.3 Reliability Assessment Methodologies

To assess reliability indices, there are essentially two main approaches: analytical or stochastic simulation. Firstly, both approaches require the same system analysis methods and equations i.e. for load flow calculations and determining the adequacy of system states [19, 39]. However, analytical techniques represent the system using simplified mathematical models that require mathematical solutions for the evaluation of indices. Conversely, simulation techniques estimate the indices by simulating the "life" of the system and its stochastic behaviour in a chronological or non-chronological way. The differences between both techniques are summarised in Table 2.4 [37].

Table 2.4: Differences between analytical and simulation methods.

Analytical	**Simulation**
More effective for simple operating conditions and systems	Preferable for complex operation conditions and when high-impact events are significant
Usually an oversimplification of the system and may become unrealistic	Can capture all system processes and characteristics
Relatively short computational times	Considerable computational times
Same result for the same system, model and input data	Results depend on imposed precision and randomness
Results are limited to average values	Results comprise average values and probability distributions

Probabilistic simulation techniques are increasingly being preferred over analytical ones because of their capacity to provide more information about the randomness of network behaviour than point averages [37]. Together with the aforementioned requirements for more accurate risk management due to both technical and economic considerations, it is important now more than ever, to gain as much insight into network functionality with as much information as possible to aid both planning and operational decisions. The most common probabilistic simulation technique is the Monte Carlo Simulation (MCS) procedure for which there are two variants – random (non-sequential) and sequential simulations. The random (NMCS) approach simulates the basic intervals during system lifetime by choosing intervals randomly while the sequential (SMCS) approach simulates them in chronological order [19, 39].

Notably, MCS is a fluctuation process therefore resultant indices should have a confidence band. Although there is no guarantee that simulating more samples can result in less error, it is

undisputed that the confidence band decreases as the number of simulated samples increases. To that end, the coefficient of variation is a common convergence criterion often used to ensure MCS accuracy (provide a confidence band). Alternatively, a maximum number of samples may be stipulated as the stopping rule (both approaches are used in this thesis). Either NMCS or SMCS is more suited to different analyses based on system effects and general objectives. The key merits of SMCS are that there is an accurate evaluation of frequency and duration indices, flexibility in modelling any state duration distribution, and the capacity to calculate the statistical probability distribution of system indices – these are all reported weakness of NMCS. On the other hand, SMCS requires significantly more computational time and storage. On top of that, it requires all the parameters associated with component state duration distributions (and all transition rates between all possible states). For multiple state component representations (failure modes), all this input data might prove difficult to obtain [19, 39]. This PhD research utilises both variants of SMCS - state duration sampling (SDS) and system state transition sampling (STS) whereby any use of and reference to 'SMCS' methods is abbreviated to 'MCS' methods.

Failure rates (λ) and mean repair times (MTTR) are two basic inputs for both SDS and STS MCS methods. These parameters are allocated to all system PCs and then used to assess the whole or part of the system, individual bulk supply points (BSPs) or consumers. In SDS, the up and down cycles of all PCs are simulated first, and a system state operating cycle is then obtained by combining all the component cycles. The technique is widely used for distribution network reliability despite drawbacks such as large memory storage and computational requirements. In STS, a system state transition sequence is created and used to calculate indices without requiring the sampling of component up and down cycles and storing chronological information of the system state. However, it has a significant restriction that all state residence times must follow an exponential distribution [50] - this is not a restriction in SDS.

2.2.3.1 State Duration Sampling

The first step in SDS is to specify the initial state of all PCs – usually assumed to be in the up state. The next step is to generate uniformly distributed random variates[11] and convert them into system state durations i.e. time to fail (TTF) and time to repair (TTR). The conversion is done according to the relevant probability distributions for failure and repair of PCs. This is an advantage of SDS because operation and repair processes may assume varied probability distributions for state duration [37]. For example, considering failure times to follow an

[11] A random variate is a random number sequence following a given distribution.

exponential distribution, the cumulative distribution function (CDF), is given by:

$$F(t) = R_i = 1 - e^{-\lambda_i t} \tag{2.15}$$

where λ_i is the failure rate of the PC_i (frequency/year) and R_i is a uniformly distributed random number in the interval [0,1] for PC_i. The sampling value for the state duration (TTF) will then be obtained using the inverse transform method[12] [37, 39, 42]:

$$TTF_i = F^{-1}(R_i) = -\left(\frac{1}{\lambda_i}\right)\ln(1-R_i) \tag{2.16}$$

which is the equivalent to (2.17) because $(1-R_i)$ is distributed uniformly in the same way as R_i:

$$TTF_i = -\left(\frac{1}{\lambda_i}\right)\ln(R_i) \tag{2.17}$$

Similarly, TTR may be obtained if the PC repair is assumed to follow a Weibull distribution, whose CDF is given by:

$$F(t) = R_i = 1 - e^{\left[-\left(\frac{t}{\alpha}\right)^{\beta}\right]} \tag{2.18}$$

where α and β are the scale and shape parameters of a Weibull distribution. Equivalently, the state duration (TTR) will be given by:

$$TTR_i = F^{-1}(R_i) = \alpha\left[-ln\,(1-R_i)\right]^{1/\beta} \tag{2.19}$$

Again, because $(1-R_i)$ is distributed uniformly in the same way as R_i, then:

$$TTR_i = \alpha\left[-ln\,(R_i)\right]^{1/\beta} \tag{2.20}$$

With:

$$\alpha = \frac{MTTR}{\Gamma\left(1+\frac{1}{\beta}\right)} \tag{2.21}$$

where $\Gamma(\cdot)$ is the gamma function [37] and MTTR is equivalent to the repair rate (μ_i) of PC_i. Importantly, the special case of the Weibull distribution where $\beta = 2$, interpolates to a Rayleigh distribution. The chronological sequence of operating-cycles can be deduced by sampling TTF, then TTR, then TTF, and this creates the state transition process (artificial cycle of system

[12] Other methods such as the composition method and acceptance-rejection method may also be used.

operations and failures) [39]. For each discrete system timestep or event, the system will have a new topology depending on what equipment is faulty or operational. This new state is analysed using power flow computation with the application of corrective actions where necessary such that reliability indices may be obtained cumulatively for the simulation period. Simulations (random number generation and subsequent system assessment) are repeated until the imposed MCS stopping criterion [37].

2.2.3.2 State Transition Sampling

STS focuses on state transitions of the entire system rather than on PC states or PC state durations. Consider a system containing m PCs and that the state duration of each PC follows an exponential distribution. The system is in state S_k with the associated PC transition rates given by λ_i where $(i = 1,...,m)$. It is important to note that in this STS context, depending on the PC state in state S_k, λ_i may represent a failure rate or repair rate. It can be shown that the system will transit to system state S_{k+1} depending on the random state duration of the PC which departs earliest from its present state in system state S_k i.e.:

$$T = min_i(T_i) \tag{2.22}$$

where T is the duration of system state S_k and T_i is the state duration of the i$^{\text{th}}$ PC. Since T_i of each PC follows an exponential distribution with λ_i, then T also follows an exponential distribution with λ where $\lambda = \sum_{i=1}^{m} \lambda_i$. Using conditional probability theory, it is possible to determine if the transition from state S_k to S_{k+1} is caused by the departure of PC j from its present state in system state S_k. It can then be shown that the probability of PC j departing from its present state at time t_0 is given by [51]:

$$P_j = \frac{\lambda_j}{\sum_{i=1}^{m} \lambda_i} \tag{2.23}$$

where P_j is the probability of departure of the j$^{\text{th}}$ PC from its present state. Expression (2.23) means that the state transition of any PC (according to P_j) leads to a possible state transition and that for a system of m PCs, there can be m possible reached states. Using (2.23), the probability of each of the m system PCs transiting from their present state can be calculated. The probability of the m states that could possibly be reached can then be successively placed in the interval [0,1] as shown in Figure 2.5 (because $\sum_{j}^{m} P_j = 1$). As done in SDS, the next step is to generate a uniformly distributed random number R_i between 0 and 1. If R_i falls between the segment corresponding to P_i, then the transition of the i$^{\text{th}}$ PC leads to the next system state.The

consequences of each system state may then be analysed, and all relevant indices updated before generating a new random number R_i. The simulation is repeated until the stopping criterion is reached [50, 51]. The traditional STS MCS method is used in thesis Chapters 4 and 5 to calculate network reliability for different network scenarios. Given that these chapters discuss system reduction to a variable number of system states, STS is necessary as SDS is only applicable to systems with distinct PCs. A traditional STS MCS is adopted because it adequately demonstrates the required accuracy capability of the reduction methodologies proposed.

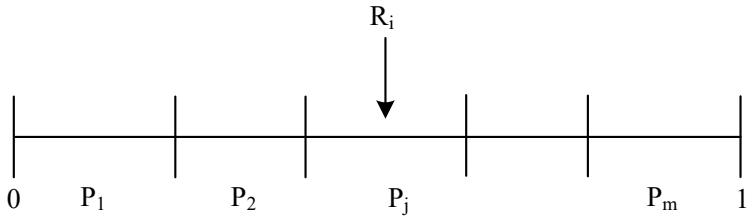

Figure 2.5: Explanation of state transition sampling [50].

2.3 Smart Grid Technologies

This PhD research seeks to ascertain how PV, DSR and ES integrated into power networks will influence the assessment of supply continuity (which is a constituent element of QoS). This subsection provides the state of the art with regards to their impacts in terms of network operation and specifically, reliability. It is worth reiterating that the smart grid concept has various components e.g. wide area measurement, condition monitoring, advanced asset management, smart metering, increased penetration of DERs, etc. This research focuses specifically on the integration of the above mentioned DERs into power systems using deployment techniques that constitute their functionality as smart interventions (SGTs) for CoS improvement through diversification of the energy portfolio and provision of backup supplies during system faults.

2.3.1 Impact on Network Operation

Most statistics show that failures in distribution systems account for an odd 80% of all interruptions that result in the unavailability of supply to loads [31]. Therefore, before looking at the current research gaps in the impact assessment of the considered SGTs from a reliability perspective, it is useful to review their impacts on network functionality/operation to provide a further understanding of their contribution to the overall QoS (which includes CoS). This

is beneficial as it identifies relevant phenomena in SGT operation that inform the deployment techniques proposed in this thesis to improve the overall network reliability.

Collectively, SGTs provide increased fuel saving with cogeneration, reduced demand charges for large customers, engineering cost savings from voltage and power factor correction, reduced risk of power outages, reduced carbon emissions, scalability, generation augmentation, and renewability, among others [52]. Moreover, through techniques such as active network management [53], it is possible to maximise the penetration of DG through coordinated voltage control using transformer on-load tap changers and voltage regulators, fault level studies, feasibility studies for the addition of power electronics, and network reconfiguration. Practically, DNOs often employ network reconfiguration (NR) to ensure CoS through alternative power supply routes and to improve reliability without additional cost [32], especially with the presence of shunt capacitors (SCs) and reactors. NR is a process of altering the open/close status of tie/sectionalising lines of distribution networks. Notably, SGT-integration increases the efficiency of NR schemes through better loading patterns by reduction of the load burden on centralised power supply utilities, improved voltage profiles and application of DG in the restoration process during contingencies. This also has the effect of reducing the required frequency of NR and thus extending PC lifetime. Moreover, research in [31] investigated the impact of NR on network reliability performance by using a chemical reaction optimisation algorithm which imitates molecular interactions to search for the optimal radial configuration. In this case, the molecules represented the set of links/tie lines of the distribution network. By using the IEEE 33 bus standard test network, the study found that NR is very effective in reliability enhancement in the presence of DGs more than with SCs.

Nonetheless, there are significant uncertainties about SGT impact on network operation and performance due to their temporal and spatial variability and the decentralised nature of their operation and control. Accordingly, grid integration of SGTs requires the suitable management of various balancing services markets such as frequency response, reserve services, and reactive power services. There must also be revised unit commitment and economic dispatch, improved DNO response to system outages [32] and adequate CoS impact assessments (the focus of this thesis). The following subsections provide relevant operational concerns about each of the considered SGTs focusing on their impact on network functionality while also discussing the current state of the art in terms of impact on network reliability. Later chapters provide more specific information about their detailed design and application in this research.

2.3.2 Photovoltaic Systems

The three most encountered configurations of PV systems are grid-connected systems, battery-charging stand-alone systems and load-connected systems [54]. Grid-connected systems typically have roof-installed PV units that deliver dc power to a power conditioning unit (PCU) which converts it to ac and supplies the building. The PCU ensures efficient PV operation in accordance with the appropriate current and voltage (I-V) curves during changing weather conditions. Also, the PCU allows for bidirectional power flow between the grid and the building depending on the level of PV supply. Battery storage may be included depending on the energy requirements. This PhD research mainly focuses on this PV configuration and its variants i.e. no grid connection, less complicated PCU, etc. This is because it is relatively simple, can often result in high reliability and may also have high PV-efficiency with the appropriate usage of a maximum power point tracking unit. Integrated with advanced energy management systems (EMSs), this configuration takes advantage of relatively low-cost power during periods (middle of the day) where utilities have relatively high electricity rates.

On the other hand, off-grid standalone systems usually have battery storage and/or a backup generator where an inverter converts battery dc voltage into ac for conventional electricity and its charging function allows the generator to top up the batteries when solar is insufficient [54]. The last category of PV systems is those where there is direct coupling with the load, without any battery storage e.g. most water-pumping systems. Both categories of PV configurations can be very cost-effective especially in remote areas where the only supply alternatives may be noisy high maintenance generators or extending the existing grid to the site at a high cost. However, they may suffer from inefficiencies without diversification of energy supply especially due to the dependence of PV supply ambient conditions (solar intensity, spectral variations in overcast conditions, temperature, and wind speed).

Grid-connected PV systems present several operational concerns such as voltage variations, harmonic distortions, reactive power requirements, flicker, voltage unbalance, grounding, lightning protection and the optimisation of system controls. Also, large scale PV integration increases the network short circuit capacity (fault current) and leads to voltage rise at the point of common coupling (PCC) which requires changes to the associated protection coordination. Harmonics, inherent in ac power, are increased by the addition of PV inverters in grid-connected systems. Due to the stochastic behaviour of PV, the times of the peak PV power generation might not, and typically do not coincide with the peak demands (depending on the category of end consumers) thereby resulting in a less than optimal utilisation of the generated power [55]. Moreover, the rise in voltage flicker due to rapid variations in cloud movements (clouding), has an effect of wearing out tap changers owing to the sensitivity to short-term voltage fluctuations, and thus a reduction in transformer lifetimes. Accordingly, solutions have

been suggested in the form of on load automatic tap changers and step voltage regulators at distribution level [56], ramp-rate control using ES [55, 57], use of inverters for power factor control by absorbing or injecting reactive power [58], overvoltage prevention at the PCC through coordinated active power curtailment, and overvoltage protection schemes [59], among others. Furthermore, the influence of PV on overall network performance for LV customers has also been quantified in [60] using active and reactive power flows, system losses, voltage profiles, and harmonic effects. The results provide a good basis upon which to consider MG using PV for CoS improvement.

Focusing on CoS, research in [61] discussed quantification of the effects of PV on power system reliability but mainly focused on finding the optimal placement of PV installations and employed a relatively low-resolution time-step (1 day) for the presented probabilistic models. Also, [62] focused on minimising lifetime, energy and load-loss costs. PVs were connected to a 22 kV distribution system to investigate the effects of multi-distributed generators through assessment of SAIFI, SAIDI and even the cost of outages [63]. The results focused on DG capacity and location. Similarly, due to the spatial variability of RES, the Roy Billinton test system was used a case study in [52] to quantify the possible level of reduction of distribution losses and chance of interruptions if DGs were placed closer to the customers. As expected, the DG was found to provide voltage support and relieve overloads in grid-connected operation. This is bolstered by another study in [64] which also emphasised the importance of optimally placing DG sources to obtain the largest potential benefits for grid reinforcement.

2.3.3 Demand-side Response

DSR constitutes various energy management programs designed to control energy consumption on the customer's side. By managing consumer demand during key periods, there is a substantially better use of existing resources resulting in wide-ranging benefits such as deferment of network investment costs. DSR may be categorised into the following programs: energy conservation i.e. reducing demand for most hours of the day, load management i.e. reducing peak demand (peak shaving) or shifting demand from peak to off-peak hours, and fuel substitution i.e. influencing the customer's choice between electric or natural gas services from a utility. These DSR programs are usually delivered using one of several strategies – energy information programs, rebates on energy-efficient appliances, incentives to help DNOs to reduce commercial and industrial demand, programs for remote control of customer appliances e.g. water heaters and air conditioners, and tariffs designed to shift or reduce loads (time-of-use rates, demand charges, real-time pricing) [54]. A common example of tariff programs is the Economy 7 tariff in the UK where customers benefit from cheap off-peak electricity for up to seven hours during the night depending on the electricity supplier. This encourages customers

to use appliances e.g. washing machines, dishwashers, etc. at night to reduce their energy bills. Figure 2.6 compares demand profile classes 1 and 2 which correspond to domestic users using an unrestricted (ordinary) tariff and those on the economy 7 tariff, respectively. For each class, the average half-hourly demand per customer for a winter weekday is presented [65].

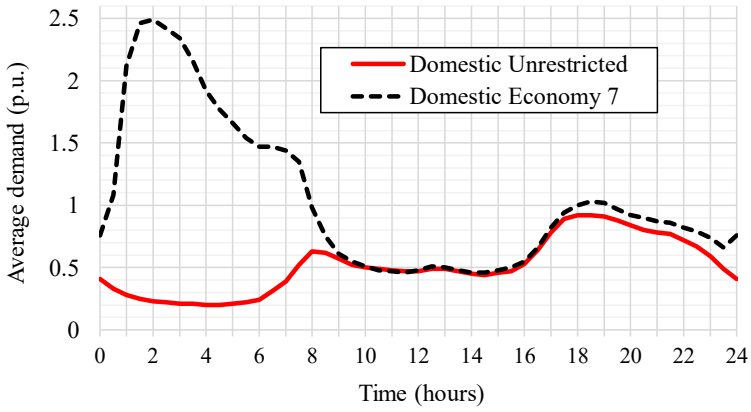

Figure 2.6: UK domestic profile classes 1 and 2 for a winter weekday [65].

The recent growth in RES provides for network flexibility by providing additional energy demands. It has been estimated that as much as 5% of the total winter peak demand in the UK may be deferrable through pertinent DSR strategies and incentives. On top of that, DSR can alleviate network contingencies and manage constraints. This can extend the useful lifetime of certain PCs and defer network investment costs [66]. Most DSR programs are implemented for large industrial customers because the load size is sufficient to make a substantial contribution to grid ancillary services. However, developments such as RES-integration, advances in digital information and user load control, are encouraging DSR programs among also the residential and commercial customer groups. Although, this justifies the use of DSR for residential dwellings, this thesis acknowledges that demand-side resources in residential and commercial load sectors are highly distributed and deeply embedded in the LV and MV networks. This makes it difficult to raise the necessary demand volumes required to participate in the balancing market despite allowing for improvements in individual customer CoS through the reduction in amounts of ENS. The current measure to solve this challenge is through the use of "aggregators" which may be defined as "demand service providers that combine multiple short-duration customer loads for sale or auction in organised energy markets" [67]. Accordingly, there are DSR programs that have been implemented with varying success e.g. by UK Power Networks (UKPN), a DNO, which run tenders for flexible DSR services from aggregators to reduce or shift peak demand in the winters of 2017/18 and 2018/19 [68].

In recent literature, the influence of DSR on overall network performance for LV customers has been investigated in [69] demonstrating the associated changes to aggregate load characteristics and system performance (active and reactive power flows). Notably, a shifting demand DSR program was used as opposed to the peak shaving strategy adopted in this thesis and in [66] where optimal power flow (OPF) was used to maximise benefits from DSR. These benefits were quantified using the ability of the modelled demand-responsive loads to relieve constraints in the upstream network and provide ancillary services like operating reserve. Moreover, the results highlighted the opportunity for DNOs to participate in DSR especially by implementation at optimum network locations. For the CoS specifically, [70] showed that flexible demand could enhance system reliability through reductions to expected ENS and loss of load probability (LOLP) by making the power demand responsive to nodal pricing and then communicating price signals to customers as soon as they were cleared on the market. As expected, the study found that the use of flexible demand can lead to a more efficient use of the network capacities while lowering overall energy bills. Finally, [71] incorporated DSR into a distribution network reliability assessment methodology considering the daily probability of LIs and SIs to provide a more realistic assessment of DSR impact on QoS.

2.3.4 Energy Storage

AC power production requires the instantaneous consumption of generated electricity to ensure system synchronism. However, the stochastic behaviour of both load demand patterns and RES availability due to ambient conditions presents significant challenges to system operation. Therefore, system operators procure ancillary services [7] to ensure SQS by balancing demand and supply. ES may provide one or more these services such as enhanced frequency response, reactive power services, etc. It is commonly used to level the load curve, develop islanded or grid-connected microgrids by promoting a greater utilisation of RES and provide corrective action (supply) during N-1 security operations. ES is also central to electricity arbitrage as it allows for the shifting of consumption from high to low tariff periods which also leads to energy savings and network congestion reduction. Not to mention, ES may also be used to compensate PV fluctuations to achieve flat feeder voltage profiles and thus reduce the number of voltage-regulation operations which leads to lower system operational costs [72]. Several studies have been performed e.g. [73, 74], which assess the benefits from ES for peak shaving, frequency regulation and operational optimisation.

Although ES is available at large and medium scales for connection to the transmission and distribution systems, respectively, this work models the use of small-scale ES that is connected to single end-use customers in a similar configuration to the previously presented grid-connected PV systems that can utilise batteries. Interestingly, [75] compares centralised configurations of

ES (normally preferred by DNOs) to distributed ones. The results show that both configurations mitigate network voltage and thermal issues. Furthermore, local ES installations are found to be able to support voltage regulation and power loss reduction but with expectedly limited effects. That research further recommends that ES should charge automatically based on ambient conditions for better overall performance. Accordingly, that recommendation forms one of the novelties of the ES application in this thesis as an EMS is modelled to manage the charging and discharging cycles of ES systems according to ambient conditions, electricity tariff during grid supply and connected demand. Therefore, more accurate modelling of ES is achieved which results in a more realistic evaluation of the proposed benefits to the improvement of CoS.

Additionally, the proposed model is an improvement to comparable studies where a fixed state of charge is modelled for ES operation [76] or where the variation of charge is dependent only on the local energy supply [77]. MCS was used in [76] to quantify impacts, using loss of load expectation (LOLE), when varying ES capacities were integrated to power systems utilising wind and/or solar energy. In [77], an optimal ES capacity and peak PV installation are designed and their impact is demonstrated using reductions in LOLE alongside energy cost savings. Lastly, research in [78] reviews the literature but focuses more on ES sizing, economic operation and optimisation. Less emphasis is given to the assessment methodologies that incorporate ES in order to quantify the impacts on CoS as well as the relevant modelling of the ES state of charge.

It is also important to classify the available storage technologies which may be categorised by type of technology: electrical (supercapacitors, superconducting magnetic energy storage), mechanical (flywheels, pumped storage, compressed air), electrochemical (batteries), and chemical (hydrogen) storage systems [79]. This thesis focuses only on battery systems that have the capability to recharge and which present relatively simple models with high efficiency for each cell. Furthermore, the research does not focus necessarily on the various existing types of batteries used (e.g. lithium-ion, redox flow, zinc-oxide, lead-acid, etc.) but rather their application as ES devices which can supply power during system interruptions to alleviate system faults and hence improve CoS.

2.4 The Need for Reduced-order Models

The previous section details relevant works where the various impacts of SGTs have been quantified. Nevertheless, due to system complexity and size, there remain significant challenges concerning the correct assessment of these technologies in terms of reliability performance. This section introduces the requirement to reduce the complexity of networks through aggregation to allow for the accurate evaluation of reliability metrics without the burden of very

detailed network models that require correspondingly large simulation times. This is especially important in the new paradigm of SGT-integration into power networks. SGTs increase the complexity of the network by changing network characteristics e.g. the short circuit level, reducing demand in unpredictable ways due to their inherent intermittence, and introducing non-traditional power flows i.e. from customer-to-customer and/or customer-to-grid. This added complexity requires the development of accurate aggregation techniques that account for not only the temporal but also the spatial variability of RES-based SGTs in approximate system reliability evaluation. The resultant simplified benchmark models can then be used to determine efficient future investments for a flexible and secure power grid with appropriate reliability standards.

2.4.1 Network Reduction in Reliability Analysis

Power systems are inherently complex and can often be accurately described only by using models with several variables, depending on the intended application. Since complex models are computationally expensive to simulate, it is common practice to use simplified representations of the power system for analysis and design purposes. Reduced models might also be necessary due to other practical reasons, for example when only a limited number of measurements are available for system monitoring, or in the case of interconnected power systems whose single areas (owned by different utilities) are reluctant to share complete and detailed system information [80]. Even with systematic problem decomposition, the pragmatic choice is often to use reduced versions of the original network to run system simulations, where the computational complexity depends at least polynomially on the size of the network [81].

It is common in network studies to simplify the utilised models to obtain a system description with the best trade-off between accuracy and complexity. The size of the network models is generally reduced by substituting sets of connected elements (buses, lines, transformers, etc.) and transforming them into smaller and numerically equivalent systems [82]. Typical applications of this approach include symmetrical or asymmetrical short circuit calculations and load flow calculations. In these cases, the performance of the reduced networks representations is evaluated in terms of accuracy of the power flow results with respect to the (more complex) initial model [83].

The typical approach for traditional network reduction (TNR) in a reliability context is to reduce the entire system to a single equivalent element by systematically combining appropriate series and parallel branches of the reliability network [39]. For example, series branches in a 2-PC network may be substituted using (2.24) while parallel branches may be substituted using

(2.25):

$$U_{se} = U_1 + U_2 - U_1 U_2 \tag{2.24a}$$

$$\lambda_{se} = \lambda_1 + \lambda_2 \tag{2.24b}$$

$$Av_{se} = Av_1 Av_2 \tag{2.24c}$$

where U denotes the unavailability and Av the availability. The subscripts $1,2$ and se represent PC $1,2$ and the equivalent series network respectively. Similarly, the subscript pe represents the equivalent parallel network.

$$U_{pe} = U_1 U_2 \tag{2.25a}$$

$$\mu_{pe} = \mu_1 + \mu_2 \tag{2.25b}$$

$$Av_{pe} = Av_1 + Av_2 - Av_1 Av_2 \tag{2.25c}$$

The main drawbacks of TNR are a) its limited applicability, i.e. only to networks with relatively simple topology [84]; b) it cannot be used to calculate customer-based reliability indices such as CAIDI and CAIFI [44] because it does not allow for an accurate aggregation of demand at different network nodes; c) the impact of critical or unreliable areas and components on the system reliability metrics becomes increasingly harder to distinguish; d) it is difficult to accommodate some relevant reliability features such as different modes of failure, maintenance and weather effects. Despite those drawbacks, this method is useful in practice particularly for simple analysis where analytical refinements are not desired [19]. Given these limitations, alternative approaches have been developed, such as the decomposition method, which is based on conditioning a complex system on the state of a key PC [84]. However, this method is not suitable for large systems because, as the number of key PCs increase, the model quickly becomes unmanageable. There also exist analysis algorithms based on testing minimal paths (or using the minimal cut set approach) [84] but their main drawback is that, for large systems, the increased number of paths and cut sets leads to a combinatorial explosion.

Another method for network reduction, termed alternative existing method (AEM) for this thesis, calculates the equivalent PC failure rate (of the reduced system) as the sum of all PC failure rates (2.26), while the equivalent PC repair rate is the reciprocal of the average of all PC repair rates (2.27):

$$\lambda_{eq} = \sum_{i=1}^{N} \lambda_i \tag{2.26}$$

$$d_{eq} = \frac{1}{N} \cdot \sum_{i=1}^{N} d_i \tag{2.27}$$

where N is the number of PCs, λ_i and d_i are individual PC failure rates and repair times, respectively, and λ_{eq} and d_{eq}, are the equivalent failure rates and repair times, respectively, for the entire aggregated network. AEM was used in [85, 86] to develop reliability equivalents of LV and MV networks to provide more realistic representations in reliability studies. However, AEM suffers from 2 critical drawbacks – it neither accounts for varying network topologies nor the spatial distribution of demand.

2.4.2 Model Order Reduction in Power Networks

This thesis explores a new approach to network reduction for reliability assessment purposes based on a robust mathematical approach called MOR. The chosen method relies on singular value decomposition (SVD) and balanced truncation (BT). Consider the following linear time-invariant system with input u and output y:

$$\begin{aligned} \dot{x}(t) &= Ax(t) + Bu(t), \\ y(t) &= Cx(t), \end{aligned} \tag{2.28}$$

The internal dynamics of the system are represented by the state vector $x(t) \in \mathbb{R}^n$, whose evolution over time is determined by the system matrix $A \in \mathbb{R}^{nxn}$ and by the input matrix $B \in \mathbb{R}^{nxm}$. In the formulation for this thesis, there is no direct input/output relationship and the system output $y(t)$ corresponds to a linear combination of the state $x(t)$, according to the output matrix $C \in \mathbb{R}^{qxn}$. Using BT, the dynamical system describing the reliability of the network is simplified by first calculating its Hankel singular values (HSVs) [87], which indicate the relevance of each system state in terms of reliability, and then the dynamics which have a smaller impact on the considered reliability indices are neglected. One of the key challenges in the application of MOR is ensuring the accurate calculation of empirical (controllability and observability) Gramians that are obtained by solving computationally expensive Lyapunov equations. These Gramians (2.29) allow for the computation of HSVs that quantify the contribution of different system modes to the considered dynamics thereby allowing for modal truncation. The controllability Gramian P determines how much the inputs u affect each component in the state x while the observability Gramian Q quantifies the impact of each state component in x on the system outputs y [88].

$$P = \int_0^\infty e^{At} B B^t e^{A^T t} dt, \qquad Q = \int_0^\infty e^{A^T t} C^T C e^{At} dt, \tag{2.29}$$

MOR aims at reducing the order n of the system while preserving the fundamental relationships between its inputs and outputs. Therefore, the state vector $x(t)$ is projected onto a low-dimensional subspace, neglecting the less relevant system dynamics. The MOR is performed to minimise, for any input $u(\cdot)$, the error between the output response of the reduced model $\hat{y}(\cdot)$ and the one of the original model $y(\cdot)$ [89]. The reduced-order system is constructed as:

$$\begin{aligned} \dot{\hat{x}}(t) &= \hat{A}\hat{x}(t) + \hat{B}u(t), \\ \hat{y}(t) &= \hat{C}\hat{x}(t), \end{aligned} \tag{2.30}$$

where $\hat{A} \in \mathbb{R}^{rxr}$, $\hat{B} \in \mathbb{R}^{rxm}$, $\hat{C} \in \mathbb{R}^{qxr}$, and $r < n$. Chapter 4 of this thesis provides the detailed mathematical formulation developed to demonstrate how BT is used to reduce the order of dynamical systems for reliability analyses.

2.4.2.1 Linear Systems

MOR has already been applied in various power system analyses: For linear systems, [90] developed a linear reduction procedure based on truncated balanced realisation which was efficient in the computation of system frequency response as well as control design. Given the aforementioned complexity of Gramian calculation, [90] introduced the use of modal information to approximate these Gramians and the method demonstrated simplicity. Nonetheless, it was limited to relatively small systems because not all modes are easily obtained in large systems. Linear systems were also investigated in [91] with an emphasis on the use of probabilistic laws to determine system parameters. Appropriately, a balanced form of a random linear time-invariant system was produced within the probabilistic range of its uncertain parameters thus ensuring that only the weakly controllable and observable states were truncated. However, application of this method to more complex systems was hindered by the computational cost which rises with the model dimension and the number of uncertain parameters. The simplification of a controller for a linear system was proposed in [92]. The main goals were to reduce the computational cost in the analysis of a large-scale dynamical plant by producing a reduced plant model that guaranteed stability while also retaining the fundamental characteristics of the original model. As expected, the compensator design of the reduced system was comparatively easier while giving approximately the same time domain specification. However, the error bound was not provided a priori as balanced realisation based on Gramians was not employed. This is one of the key benefits of balanced truncation which is accordingly used in this thesis.

2.4.2.2 Nonlinear Systems

For power system analysis and control, nonlinear models are often preferred because they offer a better description of dynamic behaviour. However, this increases the computational complexity and thus requires the development of reduced-order models especially given the increasing scale and complexity of power systems which correspondingly increases the order of the dynamic models and makes real-time analysis and control more difficult. Accordingly, [93] proposed a nonlinear model reduction approach based on balancing empirical Gramians with results showing that the order of the reduced model could be as low as 20% of a 15-generator original model under the condition of maintaining the stability and the input-output behaviour. A similar approach was utilised in [94] but focused on ensuring that the external system was also modelled as a nonlinear system rather than being linearised as is often done for simplicity. Therefore, the results demonstrated higher accuracy and calculation efficiency compared with balanced truncation based on a linear model. Balanced empirical Gramians were also studied in [95] to investigate how external excitations of a 4-generator nonlinear power system affected the Gramian reduction. The study achieved a reduction in the system order of one-third under stability constraints. Although previously mentioned studies were based on purely nonlinear systems, [96] devised two reduction strategies for piece-wise linear models based on output weighting. However, even though the reduced-order models obtained were robust and guaranteed stability under certain system conditions, there were also cases of instability. This made the process of finding an appropriate order (of the reduced model) difficult. Also, [97] developed a new approach which was a compromise between nonlinear model reduction for better accuracy and linear reduction for faster simulation. Based on the variations of the system state, the method adaptively switched between linearly reduced models (for small changes to the state) and nonlinearly reduced models (for fault periods).

2.4.2.3 Large Power Systems and Systems with SGTs

Given the requirement to reduce large power systems, [98] used a linear system reduction method and the work was successful for small-signal stability. Since the method operated using sparse descriptor matrices, it was more amenable to dynamic models of large-scale power systems. Moreover, one of the key computational requirements of MOR is computing and storing Gramians which was overcome by ensuring they were never explicitly formed or stored but only used in the implicit calculation of reduced-order models. The results showed a fast computation of reduced models while keeping the memory requirements relatively low. Similarly, [99] developed a MOR procedure for large-scale power system models that preserved the access to selected parameters just as achieved with the original model. These parameters were related to decentralised power system devices such as stabilisers that are used for damping con-

trol of electromechanical oscillations. The results were given for large practical power system models used in small-signal stability.

MOR has also been used to obtain reduced models of some of the SGTs earlier introduced in this chapter. Notably, [100] developed a procedure which allowed for the evaluation of PV-connected power systems effectively and quickly. The proposed approach developed non-aggregate Markov models of PV output that retained some time-sequential elements of the PV output. This was followed by intelligent state-space reduction that effectively increased the density of loss-of-load states and removed unnecessary samplings to optimise the adopted pseudo-sequential MCS technique. Although the results show a reduction in computational times, the use of a nonsequential MCS is usually accelerated as compared to SMCS which is more accurate when historical events affect present system conditions. Furthermore, the method has inconsistencies between the state pruning time and the simulation time. Likewise, [101] developed a reduced model for accurately predicting the PV system energy output for the specific use of reliability assessment. The main goal was to produce a reduced PV model to be integrated into reliability assessment tools and effectively replace the more accurate but complex PV models. The results concentrate more on accuracy and less so on the savings in computational time.

Using the singular perturbation theory, reduced models of battery ES systems were developed in [102] to address the problem of interfacing high-power electronics in large-scale system simulations. The key achievements were establishing a complete electromagnetic transient model and ensuring that the obtained reduced models were accurate for transient simulations while being computationally efficient. The singular perturbation theory was also used in [103] to develop a reduced-order small-signal model for a microgrid to cater for both islanded and grid-tied conditions. In that case, the reduction was achieved by preserving the “slow” states which dominate system dynamics while eliminating the so-called fast states which usually originate from intentionally added inductance and capacitance, and parasitic elements inherent to practical microgrids (with DER units). The reduced model successfully predicted the power injection at different buses although it was not very accurate for overshoots and undershoots due to the truncation of fast states.

2.4.2.4 Alternative MOR Methods

Albeit not explored in this research, another important class of MOR methods is based on Krylov subspaces (moment matching). These are efficient in circuit simulations and simulation of machine tools and may sometimes also involve the computation of Gramians [87] as is common in the SVD-based MOR methods already introduced. For example, reduction of a

large-scale multiport piezo energy harvester was achieved in [104] demonstrating a good match for harmonic simulations. In addition to the energy harvester, the proposed algorithms could be applied to other linear multi-physical devices and in the development of control circuits. The basic Krylov subspace method was extended in [105] to reduce large scale power systems and the key achievements included the development of efficient techniques for solving Lyapunov equations and the extension of the MOR to unstable systems. Lastly, the extended Krylov subspace method was also used to reduce interconnected systems in [106] focusing on low computational complexity and the added capability of enforcing constraints on the reduced model to ensure the preservation of slow and poorly damped system modes.

2.5 Contributions to the State of the Art

This section provides an overview of the contributions of this PhD research to the state of the art. These contributions are presented according to the literature reviewed in this Chapter on reliability assessment methodologies, the impact of SGTs on network reliability performance and finally, the techniques for network reduction in reliability analysis.

2.5.1 Reliability Assessment Methodologies

Section 2.2.3 presents the commonly used probabilistic MCS techniques for reliability assessment based on SDS and STS. Accordingly, Chapter 3 of this thesis utilises an enhanced SDS MCS method for reliability analyses by modelling PC repair times using a Rayleigh probability distribution because it more accurately captures the required input conditions as compared to exponential distributions which are often used in comparable studies e.g. [52, 107, 108]. It is also important to add that the enhanced procedure includes the use of time-varying PC failure rates considering the expected PC lifetime and even models the exact time of the day at which PC faults occur so that the correlation with the associated energy unserved is more accurate. Not to mention, the time-sequential analysis includes both the variation of demand and that from RES e.g. PV. These are all important improvements to comparable analyses such as [52, 63, 109] where these factors are not considered. Lastly, the method is also adapted to include the regulator-set requirements for CoS (Table 2.2) such that the resultant indices provide accurate quantification of the risk of customer interruption times with meaningful implications for stakeholders e.g. DNOs.

2.5.2 Impact of SGTs on Reliability Performance

Section 2.3 provides details of the prevalent modelling of the SGTs considered for this research i.e. PV, DSR and ES. To improve the modelling of PV, Chapter 3 designs a locally installed grid-connected PV system operated without any EMS to improve CoS by providing energy during periods of solar irradiation to alleviate the effects of grid faults. This is envisaged as a future smart grid scenario where it is expected that many energy consumers will diversify their energy portfolios with one or more DERs. Moreover, modelling PV units as local MG reduces the impact of the grid on the PV operation i.e. distribution losses, network faults such as accidents, etc. Not to mention, this work introduces a novel modelling of the stochastic behaviour of PV into reliability analyses to quantify the possible overestimation of CoS benefits if the effects of uncontrollable cloud movements are explicitly added. Lastly, this research uses a high-resolution timestep (30 minutes) to provide more realistic results in CoS improvement as compared to comparable studies in the literature previously provided (Section 2.3).

Focusing on DSR, this thesis investigates the use of load management DSR programs which aim to lower ENS during supply interruptions. As opposed to many comparable analyses, this research implements a novel application of DSR where demand is reduced during periods of high fault probability as opposed to those of peak demand. This ensures that the focus is kept on CoS improvement. Details on the application of DSR are provided in Chapter 3.

Finally, an EMS is modelled to manage the charging and discharging cycles of ES systems according to ambient conditions, electricity tariff during grid supply and connected demand. Therefore, more accurate modelling of ES is achieved which results in a more realistic evaluation of the proposed benefits to the improvement of CoS. Also, the proposed model is an improvement to comparable studies where a fixed state of charge is modelled for ES operation or where the variation of charge is dependent only on the local energy supply. This thesis builds on work in [110] where the UK SQS requirements (introduced in Section 2.1.2) were incorporated into smart grid reliability analysis and CI and CML indices then used to illustrate the risk of violating regulator requirements during power system operation. Accordingly, the deployed ES can reduce the average frequency and duration of interruptions and increase network reliability while providing suitable justification for investment using cost-benefit analyses.

2.5.3 Network Reduction Techniques in Reliability Analysis

Section 2.4 presents the commonly used methods for network reduction in reliability analysis and also provides a detailed review of the literature regarding the use of MOR in power networks. This PhD research recognises that MOR has demonstrated wide applicability in sim-

ulating large-scale mathematical models in the power engineering research domain for both steady-state and transient analyses. However, the extensive literature survey provided reveals that it has not been used for the specific problem of network aggregation for reliability studies. Accordingly, Chapter 4 addresses this research gap by developing a MOR network reduction procedure of SVD and BT that achieves fast computational times while preserving high index accuracy in reliability assessments. Additionally, Chapter 5 is used to demonstrate the advanced capability of the proposed MOR methodology to easily accommodate the inclusion of SGTs and accurately quantify their reliability impacts.

2.6 Chapter Summary

This chapter discusses the necessity to accurately quantify the impact that SGTs can have on continuity of electricity supply when integrated into power distribution networks. The research problem is first contextualised by defining relevant aspects concerning QoS (focusing on supply continuity) in power systems such as regulator requirements and customer compensation for poor network performance. Then, all relevant metrics and reliability assessment methodologies are presented to adequately classify the bases upon which SGT impact may be measured. Additionally, the chapter presents the most common SGTs alongside their various impacts on network operation (which include adding to network complexity). The chapter also reviews the most commonly used network aggregation methodologies which provide suitable means to more accurately quantify the impact of SGTs within the context of the aforementioned increase to network complexity. Finally, the chapter outlines how this PhD research contributes to the reviewed literature. This includes the advancement of a reliability assessment methodology based on MCS SDS, improved modelling of PV to capture the temporal variations, a novel application of DSR during the periods of highest fault probability, the inclusion of ES state-of-charge variation based on ambient conditions, electricity tariff and connected demand, and lastly, the novel use of MOR for reliability assessment of power networks.

Chapter 3

Reliability Enhancement using Smart Grid Technologies

This chapter presents an integrated approach for assessing the impact that different SGTs might have on the reliability performance of power networks. Various distribution systems, based on typical MV networks in the UK, are modelled. Moreover, analyses include the spatio-temporal variation of local renewable generation, the variability of the state of charge in coordinated energy storage, and the use of demand-manageable loads. Reliability assessment is made using both system and customer-oriented indices to provide a holistic representation of the potential benefits from SGTs, with special attention to frequency and duration of interruptions, and the energy not supplied to customers. Focusing on the customer perspective is a necessary attribute to reliability assessment which is often paid less attention since most regulatory operational guidelines and incentives are based on system indices. This chapter presents results using average values, probability distributions, and in some cases, analysis of the tail of these distributions to assess what impacts the proposed SGTs may have on high impact low probability events. Finally, this chapter introduces analyses concerning the need to disaggregate both system and customer-oriented performance indices into contributions from different types of modelled networks in the DNO serviced areas. These are practical considerations given that DNOs report fault events in their systems by distinguishing them based on types of components, network types, load sectors, voltage levels, etc. However, the same attention to classification is not paid when reporting reliability metrics. The comprehensive reliability assessment presented allows for a rigorous characterisation of the varying customer-groups.

3.1 Distribution Network Design

The first major analysis in this PhD research is to improve already existing techniques of reliability analysis to demonstrate the impact of SGTs on reliability performance. To provide a realistic analysis, this research utilises generic distribution networks which will invariably be dominated by SGTs in the future. These networks often differ in terms of characteristics and configuration based on geographical location and the load density served. They will often have varying network strengths, fault levels, transformer ratings, feeder types and lengths, and source impedances. Furthermore, the diurnal fluctuations during different seasons of the year (winter, autumn, spring, summer) influence the electrical characteristics of the network, associated operating levels and settings of protection devices. In addition, each network model should include an accurate identification of the associated load served through accurate load models. For steady-state analyses, static load models are sufficient to represent the changes in active and reactive power demands with respect to voltage and/or frequency. In reliability studies, accounting for these different variables is necessary to ensure that the models used can accurately emulate the network operating conditions and result in representative network performance. The next subsections provide detailed explanations of the network models used in this chapter.

3.1.1 Residential Load Modelling

Network load may generally be classified into different load sectors (residential, commercial and industrial) according the typical structure and composition of the electrical devices, equipment found in specific end-use applications where similar activities are performed, and patterns of active and reactive power demands. For the analysis in this chapter, the load is modelled to represent residential demand while later chapters will investigate the use of other load sectors. It is possible to decompose the residential demand into different end-use load (appliance) types based on energy consumption statistics [111]. For those loads that respond to changes in the ambient conditions, through for example user response or internal thermostatic controls, it is also possible to identify seasonal variation patterns. For example, lighting loading reduces during the summer while water heating demand increases in the winter. Figure 3.1 presents the electricity-use profiles from residential households, monitored over 12 months, for average loading conditions. Furthermore, the time-varying load curve is decomposed into contributions from different electrical appliances during different hours of the day.

The various electrical devices are divided into the following categories: Lighting, cold appliances, washing (drying, dishwashing), showers, water heating, heating, cooking, ICT, Audio-visual, and other appliances (e.g. doorbells, sewing machines, sunbeds, vacuum cleaners, paper

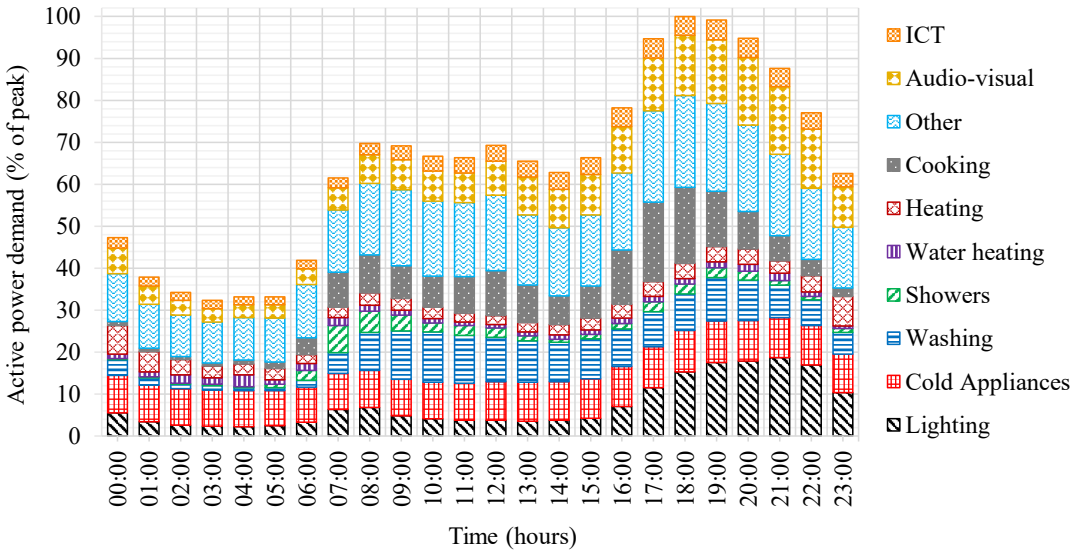

Figure 3.1: Decomposition of the daily average electrical use for typical UK households [111].

shredders, dehumidifiers, fans, hair dryers, etc.). Using this component-based load model allows for design flexibility because the contributions from different load types can be adjusted to suit expected changes in future loading conditions. Not to mention, this allows for accurate modelling of the proposed DSR techniques which are detailed later in this chapter. In addition to the active demand presented in Figure 3.1, reactive power demand is designed using a fixed power factor, typically varying around 0.95-0.98 [38].

As proposed in [112], the analysis in this chapter considers an average demand per customer of 0.375 kW under minimum and 2.27 kW under maximum loading conditions. Also, each customer distribution (11/0.4 kV) transformer is designed to consider the maximum number of customers to be supplied (obtained from equal contributions of each customer, based on their corresponding "after diversity demands") to avoid overloading the transformer rated capacity. This presents a 'worst case' scenario, enabling for a future upgrade of each network model, including new connections of DG and new customers.

Despite every residential dwelling being used for the same general purposes, it is possible to divide residential demand into three subsectors: urban (UR), suburban (SU) and rural (RU). The thresholds used to define these subsectors vary according to the country. They are usually made based on population or customers concentration e.g. Suburban ("Semi-urban") in Italy corresponds to "medium concentration" which is a territorial area of between 5,000 and 50,000 inhabitants while in Spain, it is between 2,000 and 20,000 customers. Similar distinctions are made in Portugal, Lithuania and France (number of inhabitants) [113]. However, some

countries such as Finland make subsector classifications based on the percentage of the network which is underground cable i.e. urban networks are supplied mainly by underground cables. Furthermore, in the case of Ireland, territories are split on an urban/rural divide only according to the length of the overhead lines [35]. In other areas [38], an additional subsector (highly urban) is also provided which is used to represent heavier loading conditions than in the urban areas as well as higher customer densities. The next subsection details how these subsectors are defined for this thesis.

3.1.2 LV Network Modelling

This research utilises developed generic network models (at LV and MV level) to represent the actual distribution systems connecting the several network GSPs with their secondary substations. In terms of network planning, the primary distribution system (11 kV or 6.6 kV in the UK) is typically a complex interconnected ring network containing many substations (indoor, outdoor or pole mounted), while the secondary distribution system (0.4 kV) is generally a radial network because of cost [114]. As discussed before, each network will have individual characteristics depending on location. For example, the high load densities in cities result in enclosed substations, shorter line lengths (typically less than 10 km), and thus underground cables (UCs) which are usually used to improve reliability of supply and aesthetics. Conversely, rural areas have their primary distribution by means of overhead lines (OHLs) while the substations are generally of the outdoor type, either pole mounted or switchgear type [115].

LV networks typically operate at around 415 V after the primary distribution voltage is stepped down by means of 11/0.4 kV distribution transformers. Generally, these networks are operated radially, with several LV feeders starting from the LV busbars of the infeeding substation. These are the main trunk feeders that may supply one or more lateral spurs and service connections, three-phase (3-ph) or single-phase (1-ph), which finally supply the customer's PCC and general protection panels. Table 3.1 provides detailed information about typical parameters of LV lines used for electricity distribution in the UK [38], [115]. Each LV line type is assigned an ID to ease the modelling of distribution feeders in the used LV network models.

The LV secondary substation typically comprises a single transformer with a rating of a few hundred kVA up to 1.5 MVA. Table 3.2 provides details of the 11/0.4 kV transformers operating in the UK, together with a direct correlation to the load subsector where each of them is typically used. All transformers listed have a $\pm 5\%$ tapping range and a basic load impulse level of 75 kV. Moreover, the windings are configured according to the Dyn11 vector group whereby the primary winding is connected in delta to isolate earth faults on the secondary side and to ensure transformer stability, while the secondary winding is normally connected in star with an

Table 3.1: Line parameters of LV networks in the UK [38, 115].

LV Line Type		**Cross-Sectional Area (CSA)**	**Positive seq.** Z_{ph}		**Neutral** Z_N	**Zero-phase seq.** Z_0		**Max Current**
			(Ω/km)					
ID	**Configuration**	(mm^2)	R_{ph}	X_{ph}	$R_{Neutral}$	R_0	X_0	**(Amps)**
A	Underground Line (Cable) EPR or XLPE 0.6/1 kV 4x(CSA) Al / Cu (earth) CNE	300	0.100	0.073	0.168	0.593	0.042	465
B		185	0.164	0.074	0.168	0.656	0.050	355
C		120	0.253	0.071	0.253	1.012	0.046	280
D		95	0.320	0.075	0.320	1.280	0.051	245
E		70	0.443	0.076	0.443	1.772	0.052	205
F		35	0.870	0.085	0.870	3.481	0.058	156
G	Overhead Line Aerial Bundled Conductor XLPE 4x(CSA) Al	120	0.284	0.083	-	1.136	0.417	261
H		95	0.320	0.085	-	-	-	228
I		70	0.497	0.086	0.630	2.387	0.447	195
J		50	0.397	0.279	-	-	-	168
K		35	0.574	0.294	-	-	-	148
L	Service Connection PVC or XLPE 0.6/1 kV 1x(CSA) Al / Cu (earth) CNE	35	0.851	0.041	0.900	3.404	0.030	120
M		25	1.191	0.043	1.260	4.766	0.030	100

earthed neutral to enable the supply of 1-ph loads operating at 230V [38, 115, 116]. Lastly, the impedance values provided in p.u. are given for the secondary side of the transformer. Tables 3.1 and 3.2 are used to provide design criteria for the network diagrams presented in Figures 3.2-3.4.

Table 3.2: Parameters of the 11/0.4 kV secondary distribution transformers [38, 115, 116].

Load Subsector	**Type**	**Rating (kVA)**	**Load Losses at 75 $^\circ C$ (W)**	**No-Load Losses (W)**	**Z (%)**	**Z (p.u.)**	
						R_{LV}	X_{LV}
Urban	Prefabricated Substation	1500	15810	1400	5	0.01054	0.04888
		1000	11000	1350	4.75	0.01100	0.04620
		800	7410	1000	4.75	0.00926	0.04658
Urban & Suburban	Ground / Pad mounted	500	5100	680	4.75	0.01020	0.04640
		315	3420	580	4.75	0.01085	0.04624
		200	2900	540	4.75	0.01500	0.04500
Rural	Pole mounted	100	1750	320	4.5	0.01750	0.04145
		50	1100	190	4.5	0.02186	0.03930

3.1.2.1 Urban Load Subsector

This subsector consists of house-type dwellings and low-rise buildings located in city urban areas and is characterised by medium to high concentration of customers. The subsector can also include flat-type dwellings, and multi-storey buildings depending on the level of development. Figure 3.2 provides the generic LV model which presents an underground arrangement operated radially. The 11/0.4 kV transformer used has a power rating of 500 kVA and supplies a total of 19 load clusters (or 190 1-ph customers). The network has four three-phase trunk feeders and is characterised by relatively short conductor lengths to ensure that the voltage regulation does not breach performance specifications, i.e. +10/-6%. During minimum and maximum loading conditions, the total average load is measured at 71 kW and 431 kW, respectively, with each load cluster having multiple customers [117].

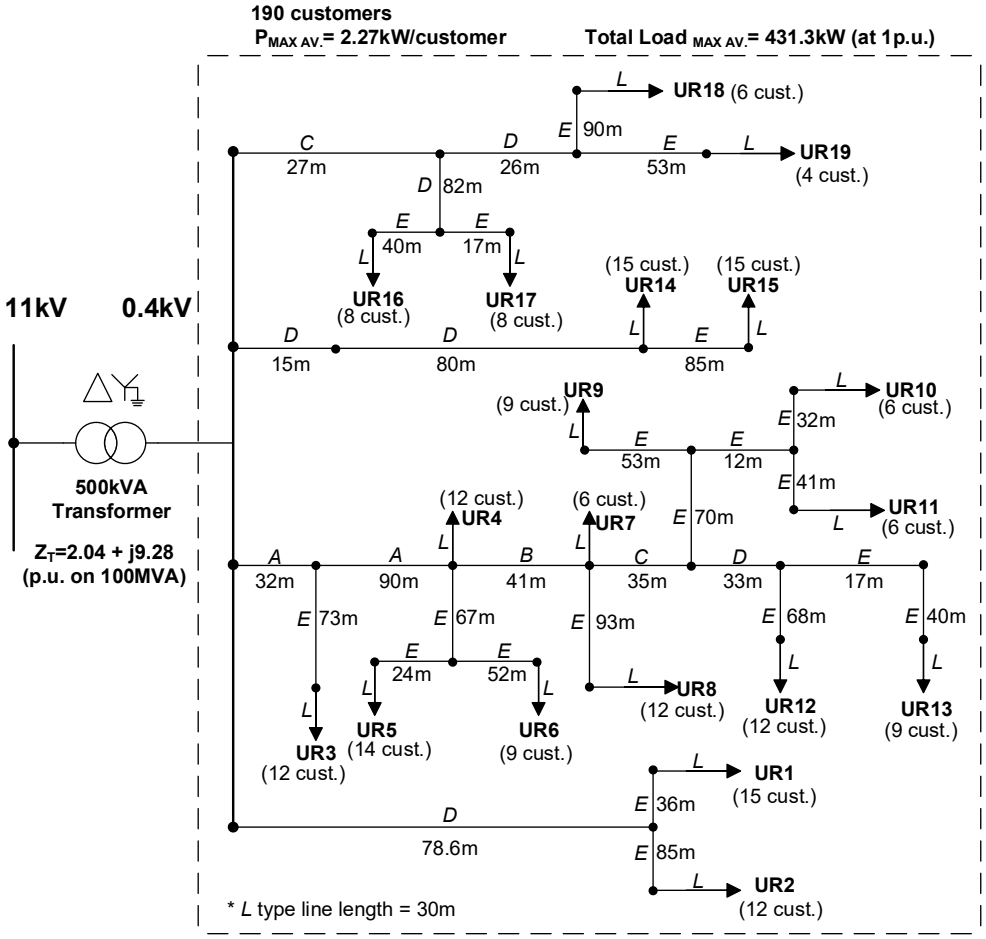

Figure 3.2: Urban generic LV distribution network model.

3.1.2.2 Suburban Load Subsector

This subsector represents individual house dwellings located in city suburban areas and towns near big cities. It is characterised by medium power density and often, a radial OHL distribution system is used because of the lower capital costs. The poles of these OHL distribution feeders are usually separated by 30m. The service connection can then be either an OHL or UC. Figure 3.3 provides the generic LV model where the 11/0.4 kV transformer has a 200 kVA rating and supplies a total of 9 LPs (or 76 1-ph customers). During minimum and maximum loading conditions, the total average load is measured at 29 kW and 173 kW, respectively [38].

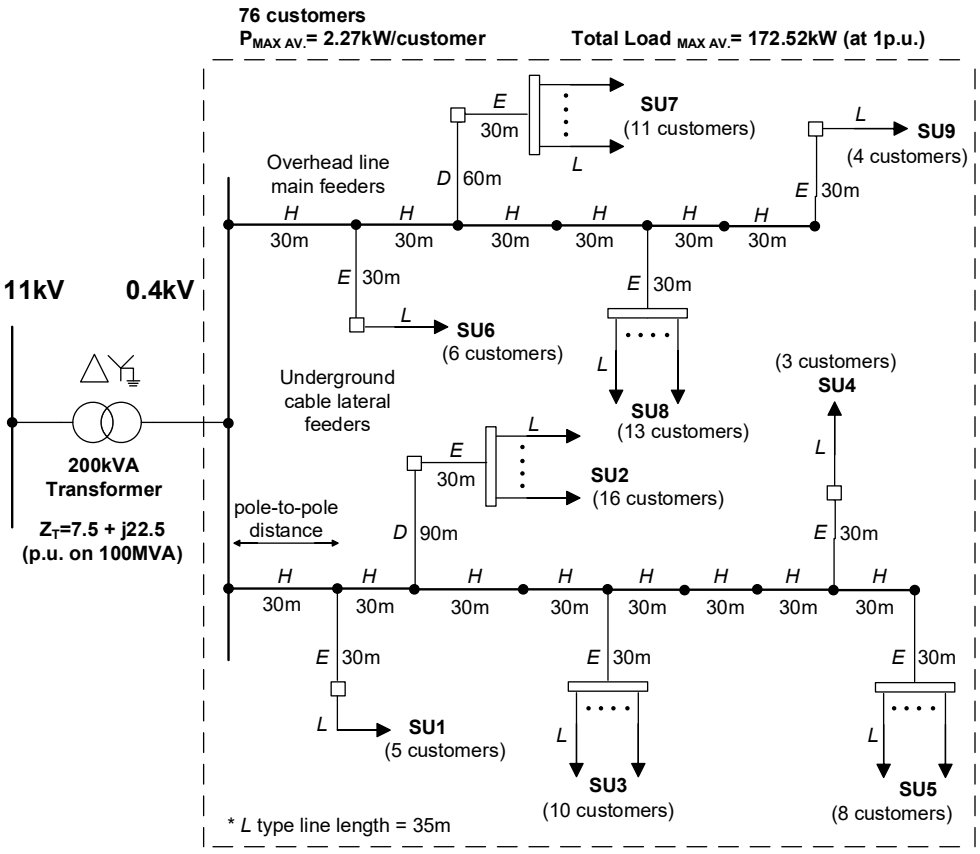

Figure 3.3: Suburban generic LV distribution network model.

3.1.2.3 Rural Load Subsector

This subsector represents house-type dwellings located in more remote areas. It is characterised by low power density and radial OHL distribution system configuration. The poles of the OHL distribution feeders are usually separated by 35m whereby each pole is used to protect (pole mounted fuses) and supply a single customer. Figure 3.4 provides the generic LV model

where the 11/0.4 kV pole mounted transformer has a 50 kVA rating and supplies a total of 19 1-ph customers. During minimum and maximum loading conditions, the total average load is measured at 7 kW and 43 kW, respectively [117].

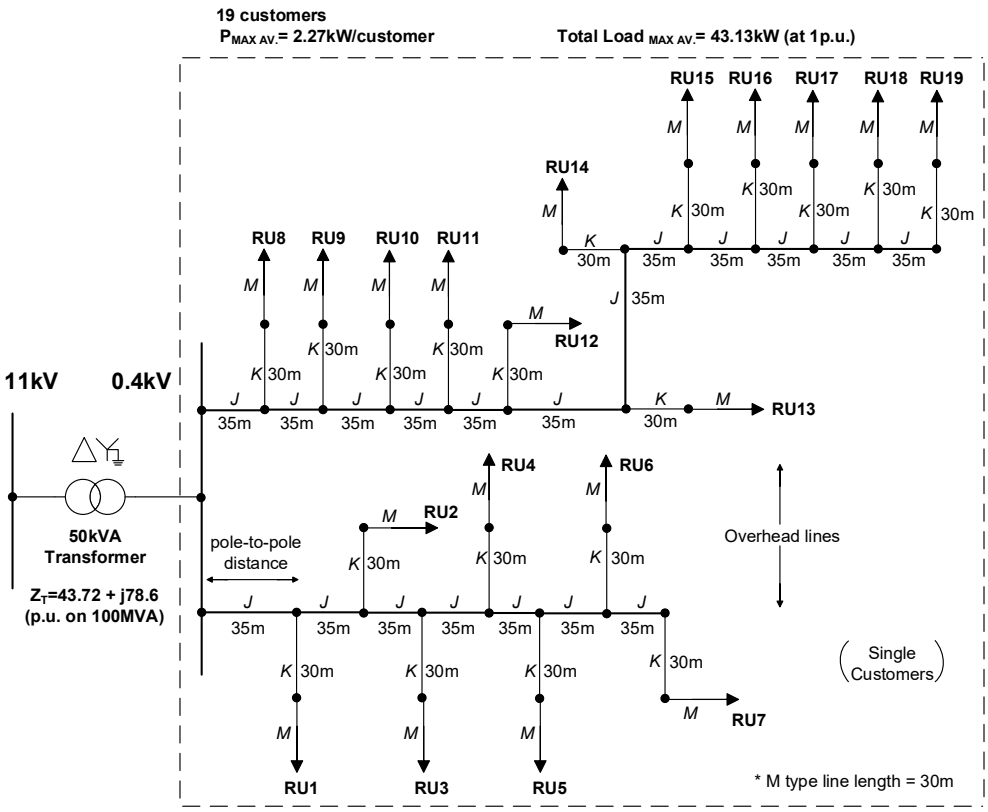

Figure 3.4: Rural generic LV distribution network model.

3.1.3 MV Network Modelling

This section presents generic MV distribution network models that have been developed with key considerations including appropriate selection of conductor sizes, choice of switchgear, fault ratings, transformer impedances and permissible voltage variations (according to SQS regulations in UK). These models also account for varying load density based on the network location (load subsector). The typical MV model includes a 33 kV 3-ph source (GSP) that is connected to a 33/11 kV substation. Depending on the type of network, the substation usually contains one or two transformers equipped with on load tap changing (OLTC) to control the secondary voltage at the prescribed range of $\pm 6\%$ [118]. The substation supplies several 11 kV outgoing feeders and each feeder supplies several 11/0.4 kV distribution substations. The network data used to build the MV generic models for each load subsector (UR, SU, RU)

using PSS®E are provided in Tables 3.3 and 3.4. Table 3.3 provides detailed information about configurations and parameters of 11 kV distribution feeders typically used in the UK while Table 3.4 provides details of the typical 33/11 kV transformers operating in the UK. Impedance values are given as p.u. on 100 MVA in both tables. Additionally, the vector group is Dyn11 for all listed transformers [38].

Table 3.3: Line parameters of MV networks in the UK [38, 116].

11 kV Line Type		**Cross Sectional Area**	**Positive seq.** Z_{ph} (Ω/km)		**Zero-phase seq.** Z_0 (Ω/km)		**Suscept. B/km**	**Max. current**
ID	**Configuration**	(mm^2)	R_{ph}	X_{ph}	R_0	X_0		**(Amps)**
O	Underground Cable - 3-core PICAS cable (screened, stranded Al) - 3-core XLPE stranded/ solid Al with 95mm^2 or 70mm^2 Cu wire screen	300	0.09917	0.06322	0.69422	0.22128	0.00027	525
P		185	0.12271	0.06575	0.85896	0.23011	0.00024	415
Q		95	0.1440	0.06662	1.00824	0.23318	0.00018	355
R	Overhead Line - AAAC (75°C) 150 or 100 mm^2 Oak AL4 - ACSR 54/9 mm^2 11 kV	150	0.11259	0.18363	0.39252	0.83701	0.00008	490
S		100	0.14658	0.26189	0.30166	1.31330	0.00001	395
T		50	0.21626	0.20694	0.74174	0.99861	0.00005	290

Table 3.4: Parameters of the 33/11 kV primary distribution transformers [38].

Load Subsector	**Rating (MVA)**	**Resistance R (Ω)**	**Reactance X (Ω)**	**Zero Seq. Reactance** X_0 (Ω)	**Tap range (p.u.)**		**Tap Step (p.u.)**	**Method of Earthing**
					Min	**Max**		
UR	30	0.030	0.780	4.00	0.80	1.04	0.0143	Resistance
	24	0.029	0.708	0.45	0.85	1.05		
	15	0.060	1.000	5.00	0.80	1.05		
UR & SU	10	0.069	1.000	0.50	0.85	1.05		
SU & RU	7.5	0.095	1.080	0.52	0.85	1.05		Solid/ Resistance
	5	0.140	1.300	0.80	0.85	1.05		
RU	2.5	0.361	2.800	1.77	0.81	1.04		

3.1.3.1 Generic Urban MV Network

MV networks in urban areas are characterised by relatively short cable lengths to ensure optimal voltage regulation due to the higher load density and proximity to the MV primary substation. Whereas underground MV networks usually present a meshed configuration, they are normally operated radially with the support of either another MV primary substation or a "reflection centre" in case of failure. This guarantees the supply of all connected feeders, from both ends of the network. In addition, the cable '0' (feeder with no load in normal operation)

connects both ends of the network and is used to enhance the system capability (capacity) to remain secure in case of a credible contingency event (N-1 security). In practice, DNOs plan these networks for a maximum of six 11 kV feeders from the 33/11 kV substation due to voltage regulation and power capacity criteria. Additionally, a maximum of ten 11/0.4 kV distribution transformers are supplied from each feeder with maximum supplied areas of 1200 Ha (low load density), 650 Ha (medium load density) and 480 Ha (high load density) [38].

Disconnection arrangements are present in MV networks to avoid supply interruption due to planned maintenance operations or unavoidable fault events. Therefore, DNOs follow specific criteria for the location of tele-controlled circuit breakers (TCBs) in the 11 kV feeders between both ends of the distribution network. Where the installed capacity is less than 3 MVA, there is no requirement to have any intermediate TCBs. However, for installed capacity between 3 MVA and 10 MVA, and feeder lengths less than 10 km, at least one TCB is necessary for the automated system protection. Furthermore, if the installed capacity is greater than 10 MVA, in addition to feeder lengths greater than 10 km, then two TCBs are considered optimal. Moreover, fault-detection mechanisms are usually installed between supply points or reflection centres and TCBs. Figure 3.5 presents a generic MV network model for an urban area, spanning a radius of approximately 3 km, considering all the described fundamentals of MV underground network planning and design. Accordingly, a 33 kV source strength of 543 MVA is designed which supplies a total of 9120 customers using 48 bulk supply points (BSPs) through two 15 MVA 33/11 kV transformers. The minimum and maximum loading conditions are approximately 3.4 MW and 20.7 MW, respectively [38].

Figure 3.5 also shows that the urban MV network consists of LV distribution networks connected to the 11/0.4 kV transformers. Due to the volume and complexity of MV networks, it would not be practical to represent all connected LV networks in the representative amount of detail, even for reliability studies. Therefore, the solution is to aggregate these downstream LV networks using aggregation techniques described in [117, 119] where the equivalent failure rate is the sum of all PC failure rates while the equivalent repair time is the mean of all PC repair times in the LV network. Therefore, each load supply point in the MV network presented in Figure 3.5 represents the aggregation of the urban generic LV network (Figure 3.2) – for which the power flows, voltage magnitude and power angle, for the MV network, remain unchanged from the detailed network models [120]. This aggregation is carried out for the SU and RU networks presented in the next subsections.

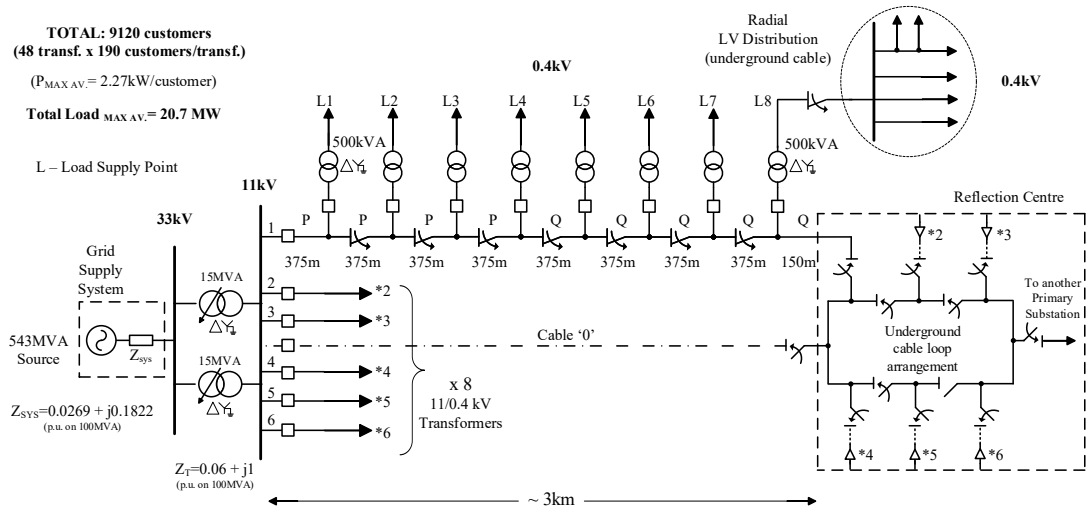

Figure 3.5: Urban generic MV distribution network model.

3.1.3.2 Generic Suburban MV Network

As previously mentioned, suburban and indeed rural areas are characterised by medium to low load density. Therefore, MV distribution systems are usually overhead (aerial) and radial as opposed to the meshed underground system presented for the urban network. Lower housing density and increased distance from the MV substation means that the feeder lengths are also increased which influences the voltage regulation, resulting in a lower reliability performance. These networks usually include automatic reclosing functionality in addition to the common overcurrent protection (phase, neutral, homopolar). The main distribution trunk feeder goes from the 33/11 kV substation to the boundary sectionaliser and presents a radial layout in normal operation. However, it is usually supported by another supply point (reflection centre), as in the urban MV case but with some key differences. While in urban networks, the reflection centre does not support any load in normal conditions, in aerial networks, it may supply some load as long as it is capable of providing enough capacity margin to supply any other lines in the event of a fault. Therefore, the reflection centre does not necessarily present a concentrated arrangement and thus TCBs can be installed in different locations. Moreover, the 11 kV lateral spur feeders (OHLs stemming off the trunk feeder), usually do not have any additional backup supply and each spur feeder supplies several groups of 11/0.4 kV distribution transformers, limited by voltage regulation and power capacity. DNOs typically group no more than eight LV transformers together within a maximum radius of 4 km (i.e. from the trunk 11 kV feeder to the furthest LV transformer). The aerial MV network also presents a coordinated protection arrangement enabled using TCBs, automatic sectionalisers, fixed disconnectors and auto-reclosing fitting [38].

Figure 3.6 presents a generic MV distribution network for a suburban area, spanning a 6 km radius, with a total of 3344 customers supplied through 44 BSPs. The network is designed with relevant network protection that is indicated in the model. Correspondingly, the 33 kV source strength is 423 MVA while the 33/11 kV transformers are 5 MVA. The minimum and maximum loading conditions are 1.3 MW and 7.6 MW, respectively [38].

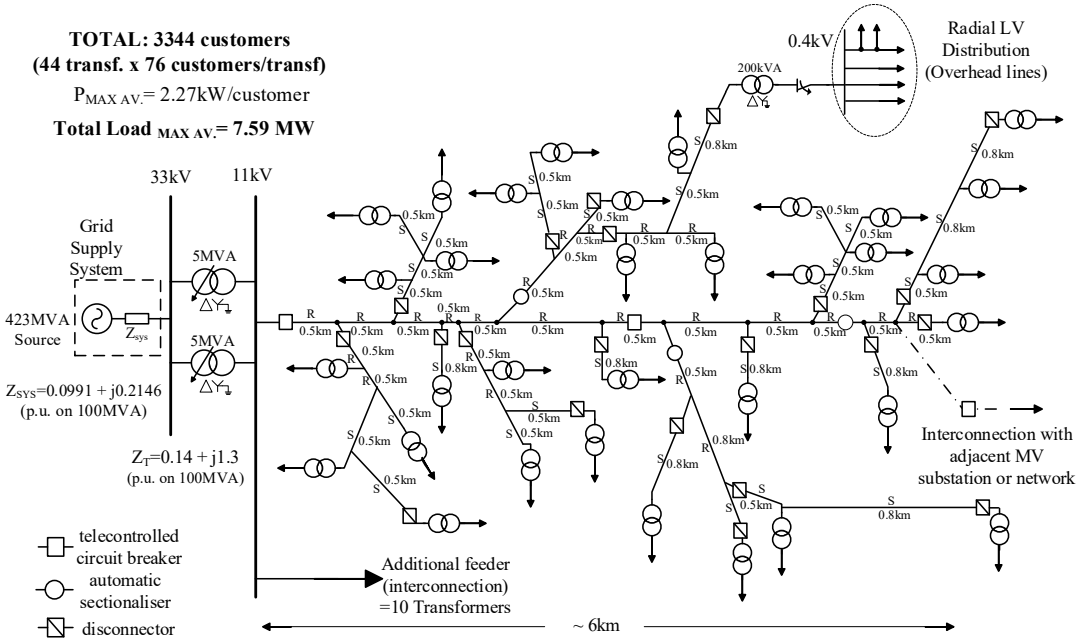

Figure 3.6: Suburban generic MV distribution network model.

3.1.3.3 Generic Rural MV Network

The generic MV network presented in Figure 3.7 for rural areas is also an aerial distribution system characterised by long overhead feeder lengths and a relatively low network strength. Accordingly, a 33 kV source strength of 136 MVA is designed in addition to only one 2.5 MVA 33/11 kV transformer that is used to supply the 646 customers through 34 BSPs, over a radius of 9 km. Finally, the minimum and maximum loading conditions are 0.25 MW and 1.5 MW, respectively [38].

3.2 Reliability Assessment Methodology

This section presents the methodology used for reliability assessment for the analyses presented in this chapter. As previously introduced, the major benefit obtained from using simulation-based reliability assessment is establishment of accurate representations of the deficiencies

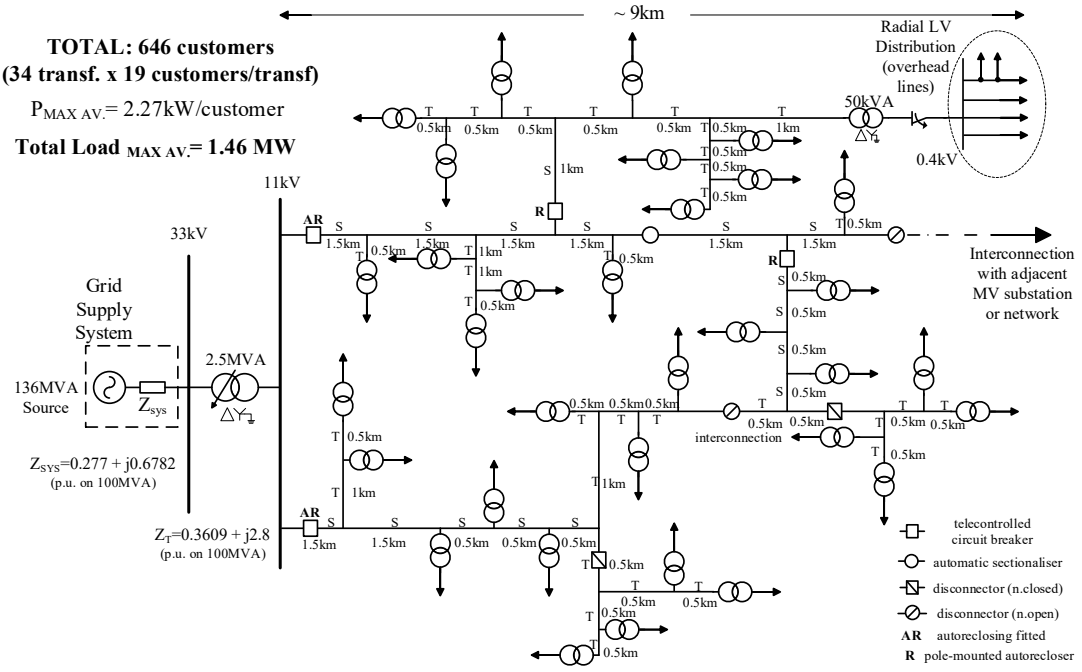

Figure 3.7: Rural generic MV distribution network model.

suffered by the system under test. Sequential simulation approaches make the assessment more realistic as historical events affect present conditions, especially considering the non-uniform ageing of PCs [37]. Accordingly, a time-sequential MCS methodology based on SDS is presented. This technique is enhanced from the traditional MCS by inclusion of time-varying PC failure rates and mean repair times, accounting for the changes in PC failure rates based on PC life time (40 years), inclusion of time-varying load profiles and a classification between short and long interruptions (SIs and LIs, respectively). Not to mention, the methodology can be adapted to include SQS regulations as explained in Section 2.1.2 by changing the mean repair times of any PC whose failure affects large sums of GD which are security constrained.

The main input parameters used for MCS are the failure rates and mean repair times, based on historical data. It is important to stress that the accuracy of the MCS method depends heavily on the accuracy of the input data used. Despite a wide variability in reported values of these input parameters, this thesis considers the database presented in Table 3.5 (extracted from [38]) which provides values used for different network components in this thesis.

These input parameters are allocated to each PC before system reliability is assessed. It has been previously shown in [107], that these are not static average values but are time-varying and are therefore more accurately represented using probability density functions (PDFs). Accordingly, the inverse (reverse) transform method described in Section 2.2.3 is used to generate

Table 3.5: Failure rates and repair times for network PCs [38].

Power Component	**Voltage** (kV)	**Failure rate** (λ) (failures/km/year) for feeders (failures/year) for other PCs	**MTTR** (hours)
Overhead Lines	0.4	0.168	5.7
	11	0.091	9.5
	33	0.034	20.5
Underground cables	0.4	0.159	6.9
	11	0.051	56.2
	33	0.034	201.6
Transformers	0.4/11	0.002	75.0
	11/33	0.010	205.5
	33/132	0.0392	250.1
Buses	0.4	0.005	24.0
	11	0.005	120.0
	33	0.080	120.0
Circuit Breakers	0.4	0.005	36.0
	11	0.0033	120.9
	33	0.0041	140.0
Fuses	0.4	0.0027	3.0
	11	0.0004	35.3

system state durations for SDS. As previously discussed, different PDFs e.g. Weibull, Gamma, Beta, etc. can be used to model the system states generated by PC failures and repair times i.e. TTF and TTR. However, the PDFs used i.e. exponential and Rayleigh, are used due to their suitability to the corresponding system state (TTF and TTR, respectively) as shown in [38]. Accordingly, (3.1) corresponds to (2.15) which is equivalent to (2.17) after inverse transformation while (3.2) corresponds to (2.18) which becomes (2.20).

$$TTF_{Exponential} = inv\left\{1 - e^{-\lambda_i t}\right\} \tag{3.1}$$

$$TTR_{Rayleigh} = inv\left\{1 - e^{\left[-\left(\frac{t}{\alpha}\right)^{\beta}\right]}\right\} \tag{3.2}$$

In addition, the time-varying PC failure rates are modelled based on a 'bathtub' distribution curve. This is done to model the higher likelihood of failure when the PC has just been installed and when it is near to the end of its service, within its expected lifetime [37]. Accordingly, the time-varying failure rate, $\lambda(t)$, is calculated using a time-varying scaling factor, $\alpha_{sf}(t)$, that follows a bathtub (Beta) distribution, and the constant failure rate (λ_c) given in statistics [107, 121]:

$$\lambda(t) = \alpha_{sf}(t) \cdot \lambda_c \tag{3.3}$$

To derive the bathtub distribution, the fundamental parameters of the beta distribution are set to $\alpha = \beta = 0.5$.The scaling factor is then calculated according to [122]:

$$\alpha_{sf}(t) = f(t;\alpha,\beta) = \frac{1}{\Pi\sqrt{t(1-t)}},\ for\ t \in [0,1] \tag{3.4}$$

where the scaling factor is restricted within the range [0,1] and thus it is extrapolated to the realistic lifespan of every PC in the network. This lifespan is modelled is 40 years for this analysis, but future work will provide more PC-specific lifespans to account for the different ageing patterns of different PC types. For example, transformers may function for 50 years where circuit breakers may only manage 30 years due to mechanical stresses caused by switching [107]. Figure 3.8 presents an example of a PC with a λ_c of 0.095 faults/year. Instead of using the λ_c (red dashed line) as the basic MCS input for PC failure, different time-varying λ values (black solid line) are utilised over the PC's lifespan.

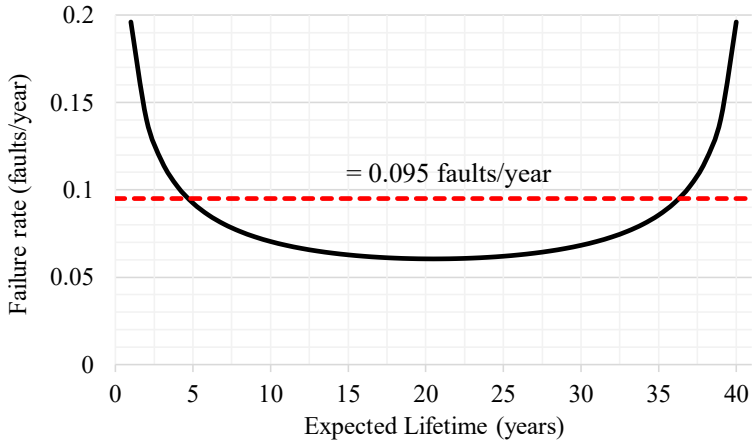

Figure 3.8: Bathtub distribution for a PC's time-varying failure rate over the expected lifetime.

It is important to note that $\alpha_{sf}(t)$ can be modelled using different PDFs to match the different stages of the bathtub curve such as the approaches used in [107] where the bathtub curve periods were divided into break-in, useful life, and wear-out periods, with each region being modelled with different distributions. Therefore, each simulation run is performed on a year-by-year time basis in 40-year cycles. At each time-step (30 minutes), a power flow calculation is run to evaluate the number of affected loads and the associated demand. Each simulation also includes a check to ensure that the simulated system conditions do not lead to overload of the transformers. Where operating limits are exceeded, the system protection devices are activated to protect network assets. The MCS algorithm is implemented using a combination of MATLAB code (presented in Appendix A) and PSS®E software, automated using Python

(presented in Appendix B). The main steps of the MCS approach used in this chapter are encapsulated in Figure 3.9 and are summarised as follows;

- assign failure rates and repair times/SQS time limits/protection settings to all PCs within the analysed system;
- establish probability distributions (e.g. exponential, Rayleigh) to model initial conditions;
- generate artificial cycle of system operations and failures using TTF (3.1) and TTR (3.2);
- run power-flow algorithm for each simulation time-step;
- check for system violations;
- run power-flow algorithm again;
- establish the number of interrupted customers and the duration of each interruption;
- compute frequency and duration indices, and ENS (using the trapezoid method [123]).

3.2.1 Theoretical Interruption Model

The methodology also includes a differentiation of system interruptions into SIs and LIs to recognise the different types of faults experienced. Accordingly, 54% of the faults are modelled as SIs while the rest are LIs [71]. Moreover, there is also a more accurate correlation between the moments when faults occur, and the actual load demand interrupted. This is achieved using the theoretical supply interruption model in Figure 3.10 [124] which is integrated into the MCS procedure. This is implemented by incorporating probability profiles of both SIs and LIs, giving "time of the day interruption probabilities" over the 24 hours of the day into the MCS algorithm, as presented in Figure 3.9. The theoretical model is constructed from previously recorded SIs and LIs statistics by two different European DNOs. These were particularly important for producing the empirical interruption probability models, which are applicable when specific SIs/LIs statistics are unavailable. Together with a comprehensive database of PCs from the UK DNOs, this model allows to reproduce more accurately the stochastic characteristics of the network reliability performance and hence more accurately assess the reliability indices, especially energy-related ones such as ENS [120].

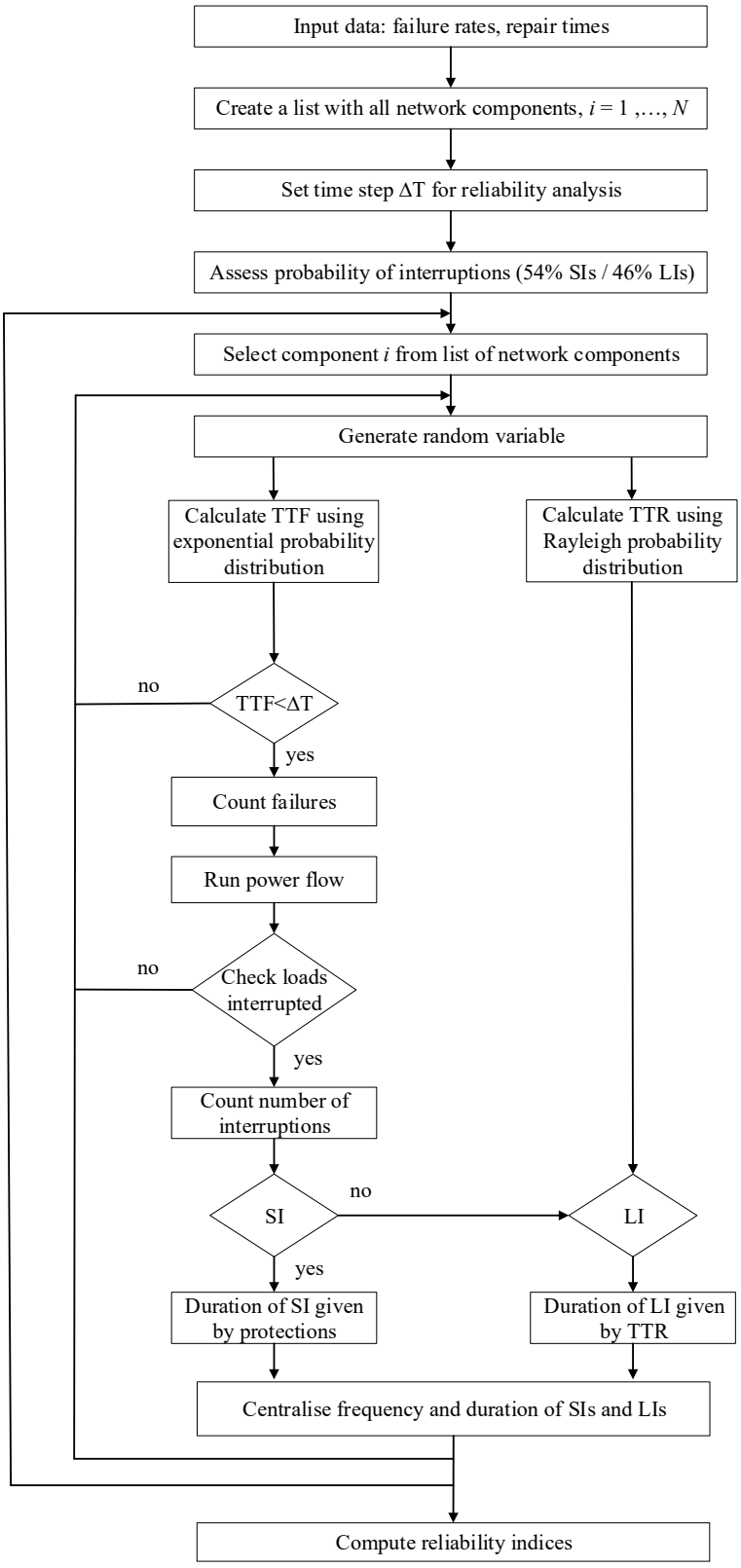

Figure 3.9: General algorithm for the MCS reliability assessment procedure [110].

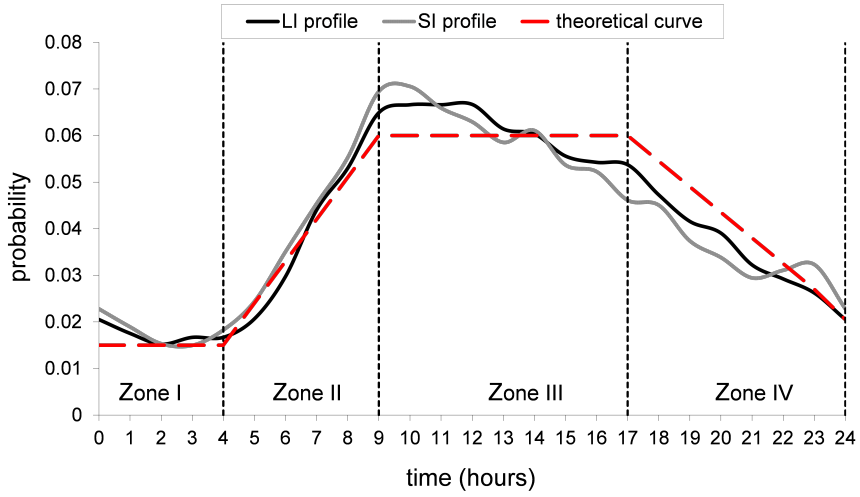

Figure 3.10: Daily probability of LIs and SIs and their approximation with a theoretical curve [124].

3.2.2 MCS Convergence Criteria

Precision is generally used as a criterion to stop the process of stochastic convergence in the MCS method. The coefficient of variation (CoV) of an estimator is a standardised measure of relative dispersion defined by the ratio between the standard deviation and the mean [125].

$$CoV = \frac{\sqrt{var(x)}}{\bar{x} \cdot \sqrt{N}} \times 100\ (\%) \tag{3.5}$$

where $var(x)$ is the variance, $\bar{x}$ is the mean and N is the number of samples. For prescribed accuracy, MCS steps must be repeated until the CoV of the selected reliability index becomes lower than the level of tolerance imposed. For example, a typical tolerance level imposed is 7% for the interruption frequency i.e. SAIFI and MAIFI, and 12% for the unavailability i.e. SAIDI, CAIDI and ENS [126]. It has been reported that the CoV of ENS has the lowest convergence rate and should thus be used as the convergence criterion when analysing multiple reliability indices [39]. Alternatively, a maximum number of samples N can be imposed as a criterion for stopping the convergence process of MCS. According to (3.5), N is proportional to the system variance, for a fixed CoV. Therefore, to accelerate MCS (i.e. by decreasing the number of samples), while keeping the same precision, variance reduction solutions must be investigated. These, albeit not investigated in this thesis, include common random numbers, antithetic and control variates, importance and stratified sampling, and moment matching, etc [125]. It is important to note that previous work in [38] validated that 1,000 years was a suffi-

cient simulation time length to maintain the accuracy of the MCS tool employed for reliability assessment. This was achieved by investigating different sets of simulations done using 1000 years as well as sets for significantly longer period i.e. 34000 years. Accordingly, all simulations in this chapter use the MCS stopping criterion of $N = 1000$ years with a simulation resolution (timestep) of 30 minutes. In the later chapters of this thesis, the stopping criteria used will differ based on the network characteristics and the type of analyses.

3.3 Modelling Network Scenarios Incorporating SGTs

The reliability assessment methodology described in Section 3.2 may be used with any test system whereby the network is modelled, scripted and simulated for different network scenarios and functionalities. Table 3.6 specifies the network scenarios used to evaluate possible improvement or deterioration of network reliability performance which is quantified through the calculated reliability indices. Accordingly, these scenarios, which are detailed in the further text, consider a number of functionalities and aspects of DERs relevant for reliability analysis.

Table 3.6: Summary of urban MV network scenarios.

ID	Network Scenario	Description
SC-1	Base case	Inclusion of backup capability and SQS regulations
SC-2	DSR	Demand-side response for reliability improvement
SC-3	PV	Uncontrolled MG using the most probable PV power output
SC-4	PV+DSR	Combination of PV and DSR
SC-5	ES	EMS-Controlled MG supplying energy per customer per fault
SC-6	ES+DSR	Application of ES after DSR

3.3.1 SC1: Base Case

The reliability performance of the urban MV network shown in Figure 3.5 is assessed to establish a base case that is used as a reference for assessing the benefits of other considered scenarios. This base case network is modelled to include backup capability through normally open switches at the end of each of 6 main trunk feeders. These are configured for reclosing after a fault or discontinuity of supply as this is necessary especially in the urban load sector networks due to the volume and density of customers. In some cases, automatic reclosing is the operational practice as it adequately clears self-extinguishing faults and other transient events that do not result in LIs. Previous work in [127] illustrated that automatic reclosing provides the most enhancement to reliability performance and is an expected feature of future distribution networks. However, the analysis in this chapter considers backup switch reclosure

according to the time limits presented in Table 2.2 for interruption of varying GD, as these are practical operational guidelines for maintenance of CoS as stipulated by (UK) SQS regulation.

These regulations ensure that the maximum duration of interruptions is kept within certain limits based on the GD and number of customers being served. For example, PCs contributing to a loss of supply less than 1 MW are repaired within only 12 hours despite their MTTR. Additionally, crew response times to faults affecting GD>1 MW are accelerated to ensure regulator-set limits for the risk of customer outages are not exceeded. These are all standard functionalities of MV distribution network operation [110]. It is important to note that the merit of the proposed methodology is that the relative reliability indices are calculated and compared with each other (and against the base case) to quantify the relative improvement. This ensures that uncertainties in data and system requirements are embedded in all the indices. It also ensures that reasonable confidence can be placed in the relative differences and potential benefits of considered scenarios [19].

3.3.2 SC-2: Demand-Side Response

DSR schemes have already been compounded by national interest in countries such as the UK where the transmission system operator, National Grid, is creating customer opportunities by encouraging DSR participation from aggregators, large industrial and commercial consumers, and small to medium-size enterprises [7]. This DSR participation is expected to reduce costs across the energy supply chain, improve CoS by enabling better use of alternative energy sources and give customers more insight and control of their energy use. As the transition is made from DNO to Distribution System Operator (DSO) [15], it will become increasingly important that DSOs can adequately structure their balancing services markets to ensure a profitable and energy efficient operation.

Using the theoretical interruption model presented in Figure 3.10, this chapter evaluates a novel DSR scheme. During the period with a high fault probability of 9:00–17:00 hours, which is before the evening ramp period, the “washing” loads (i.e. domestic washing machines, dishwashers, etc.) are disconnected. This scenario represents application of ‘DSR for reliability improvement’, as it should ensure an enhanced reliability performance, as opposed to the more commonly applied DSR techniques, aimed at reducing the evening peak demand [71]. The results from this scenario do not demonstrate a substantial reduction in the ENS since a relatively small percentage (10%) of the residential load is disconnected for 8 hours. However, it highlights the potential for reliability improvement and can support further assumptions that more sophisticated DSR schemes can result in significant reliability-performance improve-

ment, result in a better CoS, higher energy efficiency and commercial benefits especially for participating customers [120, 128].

It is important to note that the execution of DSR in this chapter does not get into a very detailed modelling. For example, the costs associated with shifting demand are not considered (although they form part of the further work). Moreover, certain operational challenges such as thermostatic load failure, customer reluctance, distribution network integrity, market uncertainty and the rebound effect i.e. where demand increases after the activation of DSR [129], are also not considered. The analysis in this thesis is limited to utilising changes to the temporal variation of network demand (as a result of DSR) to demonstrate the potential effects in terms of network reliability.

3.3.3 SC-3: Uncontrolled PV

For assessment of reliability benefits from connecting PV MG, the PV power output is modelled considering same output for each residential dwelling. Given that future networks will feature high levels of penetration of DERs [130, 131, 132], this scenario illustrates potential benefits of PV integration (with 50% penetration) and assesses the impact of the spatio-temporal variation of PV systems. Notably, [133] presents a similar study using different PV penetrations on each urban MV feeder (10-100%) to better illustrate the expectation that future networks will have varying levels of spatially distributed PV penetrations. The PV penetration is calculated as the ratio of the peak PV power to peak load apparent power. Furthermore, the use of a realistic, rather than an ideal PV profile also avoids overestimation of the benefits by accounting for the clouding effect [120], which is detailed in the next sub-subsection.

3.3.3.1 The Stochastic Behaviour of PV

Most DNOs are reluctant to depend on the PV generation for power delivery capacity because it does not directly reduce the peak demand. However, it shortens the duration of the peak load, which further benefits loading patterns of PCs [134]. It has also been reported that these load reductions may extend PC lifetimes by reducing the failure rates when PV generation helps to reduce the frequency at which PCs are operated closer to their limits/ratings [54]. However, unpredictable cloud movements affect the power fluctuations of PV installations and cause voltage fluctuations that often require implementing network controls, or even changing settings of associated protection systems [135, 136]. The ‘randomness’ of input solar irradiance is modelled using the raw measured hourly data from field recordings on a 110-kilowatt peak (kWp) rooftop PV system. Figure 3.11(a) shows the measured distribution of PV output power values for each hour of a ‘typical’ summer day. As expected, the probability of low PV output

values is high during morning and evening hours, e.g., 0.07 p.u. is the most probable PV power output (0.36 probability) at 07:00 hours. The use of the most probable values enables modelling of the hourly PV power output for a typical (realistic) day, which is used in this analysis. This is more accurate than using statistical averages, as it accounts for realistic changes in the solar irradiation patterns. The analysis is repeated for cloudless conditions (which are rarely occurring for the whole day), herein termed 'ideal'. Both power output profiles for the realistic and ideal PV generation over a day are compared in Figure 3.11(b), illustrating not only the associated energy loss, but also indicating possible variations in calculated reliability indicators when either PV profile is used for the analysis.

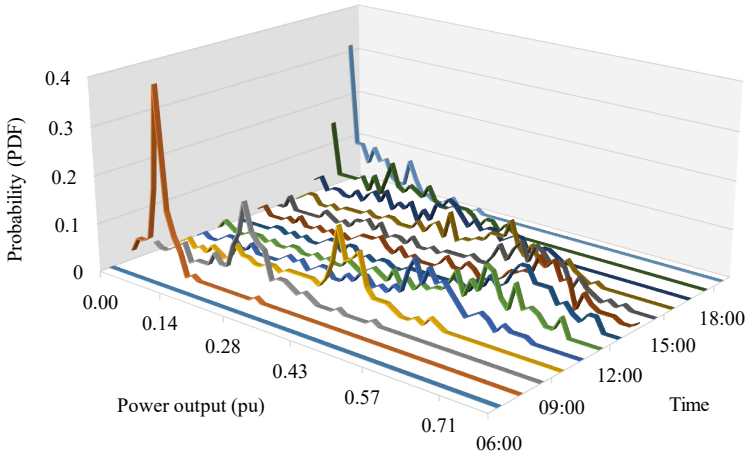

(a) Probabilistic variations of hourly output power

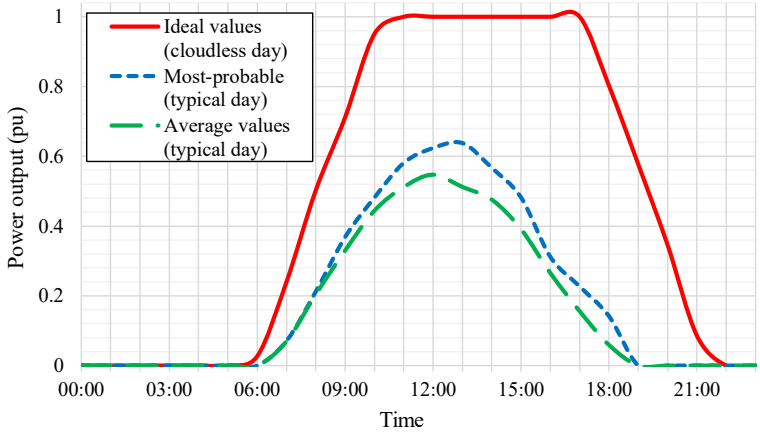

(b) Temporal power output variations for different power output models

Figure 3.11: PV power output modelling.

For the analysed PV penetration level of 50%, modelled as a uniform distribution of equal-size individual customer PV installations [132], the obtained results quantify the possible overesti-

mation of reliability-based benefits when the 'clouding' effect in PV outputs is not accounted for. Figure 3.11(b) also shows the average values for hourly PV output exemplifying the potential underestimation of reliability indices if average values are used.

3.3.3.2 Impact of Clouding Effect on Reliability Performance

Through comparative analysis, the reliability benefits of PV integration are assessed using both the realistic PV output profile and the ideal one (cloudless), to represent the full range of variation. The results in Table 3.7 indicate that when a realistic PV profile is used, the reduction in ENS from a base case (i.e., no PV integration) is 16.7%, while it is 38.9% when the ideal PV output profile is used. This represents a possible overestimation of the benefits of PV by 22.2%, when the variability of input solar irradiance and unpredictable cloud movements is neglected. It means that the projected increase in reliability from the use of ideal PV generation is more than double the expected increase from realistic PV generation. Similarly, there is an overestimation of the benefits of PV, by at least 22%, for each of the following indices: SAIDI, CAIDI and ACCI. Markedly, Table 3.7 does not present any indices measuring the frequency of interruptions as they indicate no over-estimation (0%). This is because the major causes of interruptions are system faults and PC failures, which do not affect the solar irradiance and associated PV energy availability, and therefore do not affect interruption frequency indices. PV alleviates the effects of LIs by providing energy thereby only lessening their duration, but not frequency, as perceived by the customer [120].

Table 3.7: Impact of the clouding effect on reliability indices.

Index	**Base case**	**PV**	*	**Ideal PV**	*	**Clouding Effect**
ENS (kWh/cust./y)	146.37	121.90	16.7%	89.42	38.9%	22.2%
ACCI (kWh/cust. int.)	1090.41	909.75	16.6%	664.17	39.1%	22.5%
SAIDI (hours/cust./y)	0.550	0.453	17.7%	0.332	39.6%	22.0%
CAIDI (hours/cust. int.)	3.678	3.043	17.3%	2.228	39.4%	22.2%

* Reduction from Base Case; cust. = customer; y = year; int. = interrupted.

Figure 3.12 illustrates the impact of clouding on ENS when PDFs are compared. It shows a reduction in the long tail of the PDF when either the realistic or ideal PV is deployed. This represents a reduction in the maximum value of the expected range of interruptions and is a major benefit as the probabilities of lower ENS values increase. As expected, there exists a clear overestimation, due to different PV operating conditions, as the maximum ENS values range from 1700 to 2100 kWh/customer/year. Given that these results are reliant on measured data from PV installations to deduce the most probable PV generation profile, there is

a strong correlation between the variation of realistic PV power output and its geographical (or meteorological) location [137], as well as its accuracy and resolution. Higher incidence of unpredictable cloud-movements would lower the overall energy availability, thereby lowering the PV's value in increasing reliability performance. Furthermore, the variability of wind (both stand-alone and in hybrid PV-wind systems) would result in similarly skewed reliability performance results, when the modelling accuracy is the same as in this analysis.

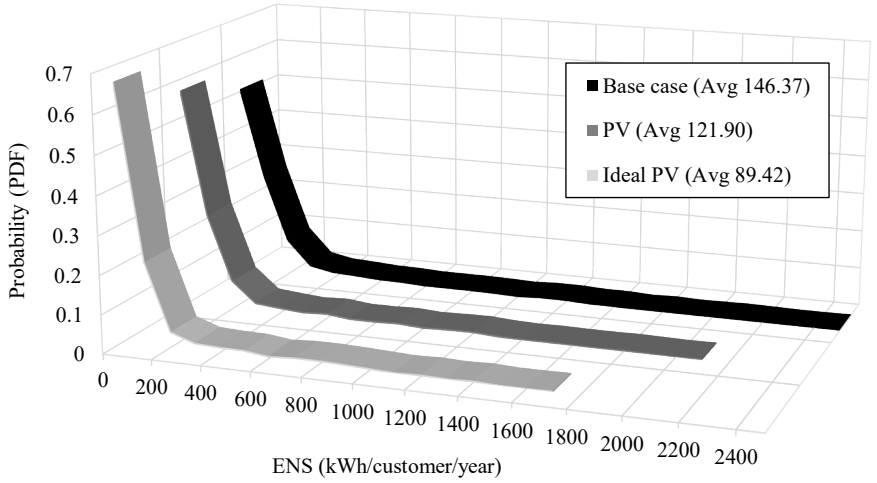

Figure 3.12: Impact of PV integration on the ENS to customers.

3.3.3.3 SC-4: PV+DSR

This scenario models a coordinated application of PV (with most probable outputs) and the DSR technique explained in SC-2. The additional effect of preventive DSR actions on top of the variable PV generation is expected to reduce uncertainty resultant from unpredictable PV power outputs and provide an improved level of supply continuity to customers by ensuring that upstream faults do not interrupt as much load [120].

3.3.4 SC-5: Energy Storage

While many control techniques for ES focus on peak shaving applications and energy cost reduction [55, 138], this chapter utilises a specific smart application of ES, which is designed to improve reliability performance by providing a backup capacity per customer, per fault, with the intention of reducing the ENS and duration of sustained interruptions. The selected backup capacity is 3.67 kWh, based on the energy networks association (ENA) G83 engineering recommendation in [139] for peak power that can be provided by a small-scale single-phase

rooftop PV. Although the ES capacity is modelled based on the single-phase rooftop PV, the ES device modelled can store energy from other forms of MG such as wind. ES operation is controlled by an EMS to provide seamless power switching capabilities and continuous supply to the end-customers. The energy is stored from PV MG operating in islanded mode and is expected to result in a better reliability performance than the uncontrolled PV (SC-3). While similar scenarios in previous work [71], [140] modelled ES systems with constant state of charge (SOC) characteristics, this research uses a realistic SOC-level variation and thus provides more realistic results. The SOC is modelled based on solar irradiation, demand, and electricity tariff during grid supply conditions [141]. Therefore, the EMS is modelled to capture more accurately the SOC and the available ES output power. The temporal variations of these quantities then determine SOC variations. To prevent overheating and ensure long battery lifetime, SOC limits are set to 40% and 100% as previously utilised in [141, 142]. The ES SOC capacity is modelled following equation (3.6) [143] which fully considers both charging and discharging efficiencies of the ES system; the latter being higher, as detailed in [144, 145]:

$$SOC(t) = SOC(t-1) + \eta_{ch}.(P_{ch}(t)\Delta t) - \frac{Pdis(t)\Delta t}{\eta_{dis}} \tag{3.6}$$

where $SOC(t)$ = SOC of the battery at time t (kWh), P_{ch} and P_{dis} are electrical power input and output at time t, while η_{ch} and η_{dis} are charging and discharging efficiencies respectively.

3.3.4.1 ES System Configuration

The EMS configuration shown in Figure 3.13 is based on a real microgrid system tested in the Smart Grid Laboratory at the University of Bath, UK. The designed 12-panel PV system has rated peak power of 3.67 kW and voltage of 444 V [146]. A 4 kW DC/DC buck converter steps down the voltage to a 24 V rated battery bank (made by series-parallel connection of four 12 V batteries), which can supply maximum current of 200 A (corresponding to maximum power of 4.8 kW). The converter, battery bank and 10 kVA inverter are linked with a common coupling 24 V DC bus. The inverter is also connected to the DC bus and allows for a bi-directional energy exchange (and energy trading) via one-phase of a three-phase mains supply [141]. The EMS controls power output from PV either directly, or through the ES, since a grid-connected mode is not designed for ES-charging in this analysis.

3.3.4.2 ES System Operation

Figure 3.14(a) presents the SOC for the ES system. For a typical day, system operation may be described as follows: the initial SOC may be assumed 40% at 00:30 hours. It essentially

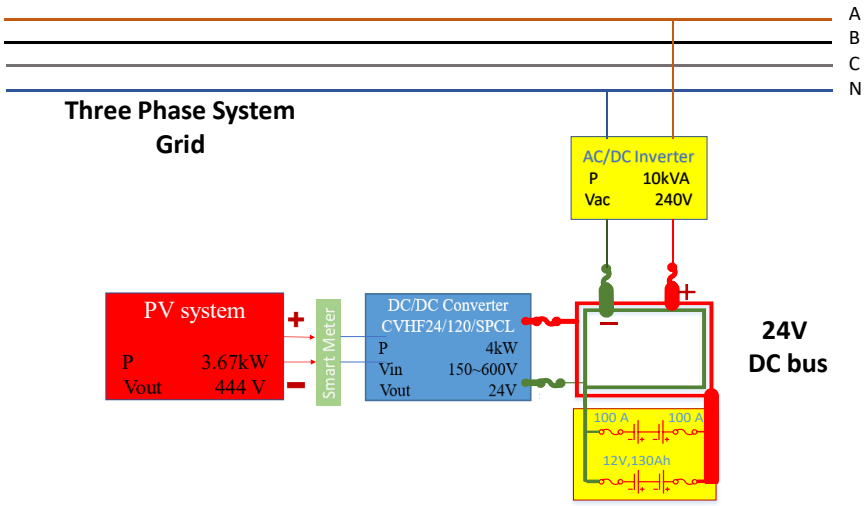

Figure 3.13: Single-phase EMS configuration.

remains at this level until 05:00, when PV starts to generate and charge the ES by 07:00. Between 07:00 and 11:00, ES remains at approximately 100% SOC. It then discharges due to increased demand (between 11:00–15:00) and charges up again during a relatively low tariff period (15:00–18:30). Evening peak demand is met in part, by discharging the ES system up to 22:00 where the EMS takes advantage of the low demand and low rate late-night tariffs to charge the ES. Figure 3.14(b) shows the power output: positive values indicate discharging while negative values correspond to charging. System operation assumptions include: no charge-discharge losses, no occurrence of unexpected failures (no failure rate), and the ES apparatus is not damaged by large upstream network faults [133].

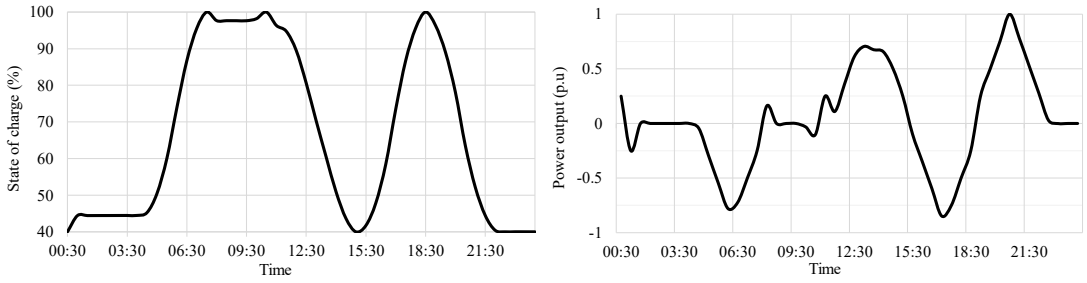

(a) State of charge

(b) Power output

Figure 3.14: Battery SOC and power output for a typical summer day.

3.3.4.3 SC-6: ES+DSR

In this scenario, the EMS-controlled ES is deployed as a well-designed corrective action on top of a preventive DSR application (SC-2). In case of an upstream fault (whose effect is reduced due to DSR action), the EMS will provide additional power, available from either PV system, or ES, or both, in order to supply all loads and thus significantly reduce the duration of supply interruptions, or even completely prevent them. Therefore, this combination of several SGTs for a localised and smart energy management ("smart interventions") is expected to result in the highest benefits for system and customer reliability performance [120].

3.4 System-Oriented Reliability Performance Assessment

The average values of system reliability indices are presented in this section. These include indices that measure the frequency of SI (MAIFI) and LI (SAIFI), the duration of LI (SAIDI) and energy not supplied (ENS). Additionally, PDFs and CDFs of these indices are also presented to illustrate the stochastic variability as well as the potential benefits that are not immediately obvious. Notably, the application of DSR on its own in SC-2 (Table 3.6) does not offer significant benefits, as only the washing loads are disconnected during a span of about 10 hours in the day. This results in a 7.7% reduction of ENS from the base case but offers no significant improvements in other reliability indices. This explains why SC-2 is not individually assessed in the reliability performance analyses that follow. The major benefits from this scenario are realised mainly through aggregation with other smart grid technologies, such as PV and ES, which are related to scenarios SC-4 and SC-6, respectively [120].

3.4.1 Frequency of Interruptions

Table 3.8 presents the results for the network reliability performance with integration of the considered smart interventions, where their benefits are quantified by the reductions of index values relative to the base case. Focusing on the frequency of sustained interruptions, the results from scenarios SC-5 and SC-6 show that the controllability of MG using ES is important for reduction of SAIFI by 71.5% and 75%, respectively. On the other hand, Table 3.8 highlights the advantages of PV - shown by no change in MAIFI, which is better than the 4.4% and 3.7% increases when ES scenarios are deployed. This can not only negatively affect the power quality, but also require changes to the settings of the main substation protection schemes [147]. This increase in MAIFI is due to the use of backup ES, which can alleviate faults in the upstream network, either by total removal of the outage or by converting LIs into SIs. However,

this is not an evident result from the PV scenarios (SC-3 and SC-4), as no intelligent control is designed [120].

Table 3.8: Frequency of long and short interruptions.

ID	Scenario	SAIFI (Ints/c/y)	*	MAIFI (Ints/c/y)	*
SC-1	Base case	0.157	_	0.208	_
SC-3	PV	0.157	0%	0.208	0%
SC-4	PV+DSR	0.157	0%	0.208	0%
SC-5	ES	0.045	71.5%	0.218	-4.4%
SC-6	ES+DSR	0.039	75.0%	0.216	-3.7%

* Reduction from Base Case; ints = interruptions; c/y = customer/year.

Figure 3.15 provides important additional information to the average values presented in Table 3.8 by showing the PDFs of both SAIFI and MAIFI for scenarios SC-1, SC-4 and SC-6. Figure 3.15(a) illustrates that SC-6 (ES+DSR) significantly increases the probability of 'zero' LIs, while SC-4 (PV+DSR) offers almost no improvement to the base case. This can be attributed to the fact that in SC-6, the energy stored is utilised as a corrective action when network faults occur, yet no control measures are implemented in SC-4. The PDFs for the frequency of SIs are plotted in Figure 3.15(b), showing that the little to no degradation from the base case MAIFI. As expected, both scenarios SC-4 and SC-6 do not significantly affect MAIFI values as discussed in Section 3.3.3. Furthermore, both graphs show a spiky increase in the probability value at 1 interruption/customer/year, which is due to system faults affecting all supplied customers, e.g., due to a fault at the primary substation (when both supplying 33/11 kV transformers fail) with no alternative (backup) supply to customers [120]. Therefore, this methodology is capable of accounting for both SIs and LIs; producing accurate results that correspond to the estimated reliability performance.

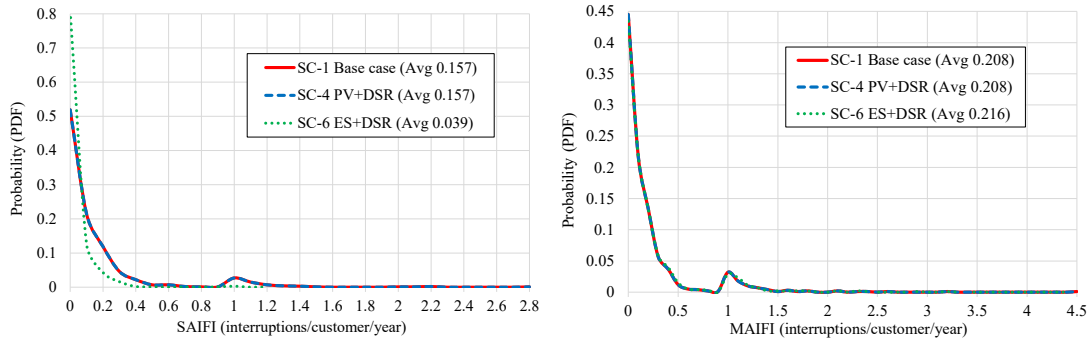

(a) LIs (b) SIs

Figure 3.15: Probability distribution of the frequency of interruptions.

When compared to SAIFI, the impact of the proposed SGTs on MAIFI is less substantial. However, the tail of the PDFs presented in Figure 3.15(a) can be further analysed using the CVaR risk metric introduced in Section 2.2.2.3. This research calculates the CVaR at a confidence level of 95% which is commonly used in the analysis of potential HILP events [46, 48]. The CVaR obtained for the base case means that the average SAIFI in the worst 5% of the cases would be 0.0028. As expected, the PV+DSR scenario does not reduce the CVaR due to the lack of control measures as discussed in the previous paragraph. However, scenario SC-6 leads to a 57% reduction in the CVaR of the SAIFI index which represents an important contribution as it means that the deployment of this smart scenario can also limit the impact of HILP events. The main reason for this is because the stored energy is used as a corrective action that reduces the total number of customer interruptions thereby reducing both the expected or mean value of SAIFI as well as the impact of the worst-case scenarios.

3.4.2 Duration of Interruptions

Deployment of PV+DSR in SC-4 results in a reduction of interruption duration times by 26% (Table 3.9). Moreover, using an EMS-controlled ES combined with DSR (SC-6) results in nearly a halving (48.7%) of the expected average interruption duration times. This is a significant result for DNOs, as they can use this smart intervention as a planning tool to take advantage of this improvement of reliability performance in both technical and commercial terms i.e. in avoiding regulator-imposed penalties for non-satisfactory performance [120].

Table 3.9: Duration of sustained interruptions.

ID	Scenario	SAIDI (hours/cust./y)	Reduction from Base case
SC-1	Base case	0.550	_
SC-3	PV	0.453	17.7%
SC-4	PV+DSR	0.407	26.0%
SC-5	ES	0.310	43.7%
SC-6	ES+DSR	0.282	48.7%

The resulting PDFs for SAIDI index in Figure 3.16 reveal that scenarios SC-5 (ES) and SC-6 (ES+DSR) have reduced tails, which translates to lower probabilities of long-duration interruptions, as compared to the base case. Both ES scenarios also increase the probabilities of the short-duration interruptions, increasing their probability from only 0.33 in the base case, to 0.54 and 0.56 in SC-5 and SC-6, respectively.

Similarly, PV scenarios (SC-3 and SC-4) reduce the duration of the longest interruptions, as well as marginally increase the probability of short-duration interruptions. This result is be-

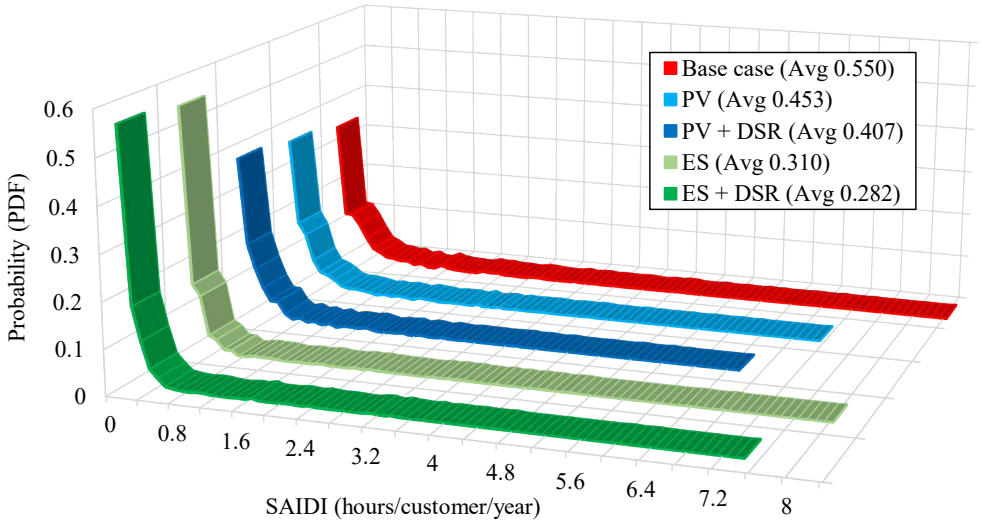

Figure 3.16: Comparison of the PDFs for the SAIDI index.

cause ES being applied as a corrective action after the faults, while PV is applied as a preventive measure. Therefore, ES does not offer as much reduction in the duration of the longest interruptions as PV, whose deployment offers available energy to alleviate effects from upstream network faults, even without intelligent control from EMS. This might place the use of standalone PV systems, without ES, as a more economical option. Moreover, the base case CVaR for SAIDI (0.0084 hours/cust./y), at the 95% confidence level, is reduced by 23% when PV+DSR is deployed as compared to only 12% by ES+DSR. However, when pros and cons of either technology are weighed, the impact of ES is controllable and therefore far more predictable than the uncontrolled PV. The larger benefits from ES+DSR are exemplified by nearly a halving of the maximum plausible duration of individual interruptions, which reduces from over 300 hours in the base case, to only 156 hours in the SC-6 scenario [120]. Finally, Figure 3.17 shows the resulting CDFs for the duration of interruptions from scenarios SC-1, SC-4 and SC-6. It illustrates that the probability of up to 1-hour supply interruptions increases from 54% in the base case to 81% when SC-4 is deployed, and finally to 91% for SC-6.

Therefore, the results quantify the risk of paying compensation to customers experiencing interruptions longer than the specified duration threshold (as in the UK SQS regulations given in Section 2.1.2). This can be associated with the considered scenarios and smart grid functionalities, which then can be used to evaluate potential cost-benefit effects at both the planning and operational stages. Furthermore, it can be analysed in terms of not only CoS improvements to customers, i.e. through the reductions of average duration of long interruptions, but also in terms of the higher probabilities of shorter-duration interruptions [120].

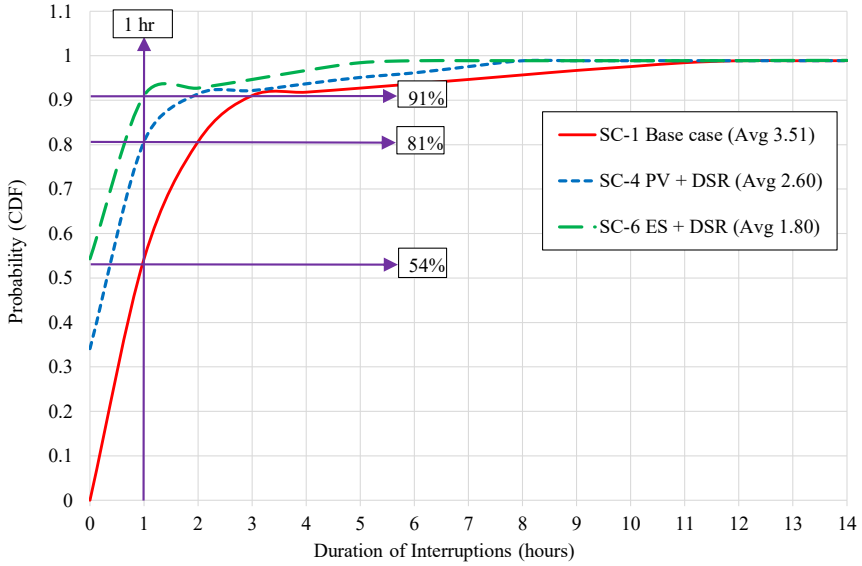

Figure 3.17: Comparison of CDFs illustrating the impact on the duration of interruptions.

3.4.3 Average Energy Not Supplied

Regarding the risk associated with the energy not supplied to customers, Table 3.10 presents the results for the ENS index. As expected, SC-6 results in the most significant reduction to ENS (41.8%), because ES is applied as a controlled reliability-corrective action, additionally enhanced by a reliability-oriented DSR scheme. In addition, uncontrolled PV in combination with DSR reduces the average ENS (by 24.4%).

Table 3.10: Assessment of the average energy not supplied.

ID	Scenario	ENS (kWh/cust./y)	Reduction from Base case
SC-1	Base case	146.37	-
SC-3	PV	121.90	16.7%
SC-4	PV+DSR	110.63	24.4%
SC-5	ES	93.03	36.4%
SC-6	ES+DSR	85.21	41.8%

Figure 3.18 further illustrates the improvement in average ENS values for different load supply points in the urban MV network when SC-6 is implemented. The resulting average ENS values exhibit a repetitive pattern from one MV feeder to the next (each with 8 load supply points) due to the symmetry of the network design (Figure 3.5). Furthermore, the use of time-varying failure rates and repair times for network PCs, incorporated in the PDFs used as inputs in the MCS algorithm, ensure that the 'randomness' of network behaviour is more accurately

modelled. For example, Figure 3.18 shows that ES has a higher impact on the ENS reduction at some load supply points, e.g., 27 and 41 on feeders 3 and 6, respectively (over 80% reduction), than it does at other load supply points, such as 37 and 38 on feeder 5 (approximately 20% reduction). Overall, ES contributes much more to ENS reduction than DSR, as it represents a post-fault corrective action, while DSR is deployed as a preventive measure to reduce the ENS during the high fault probability periods [120].

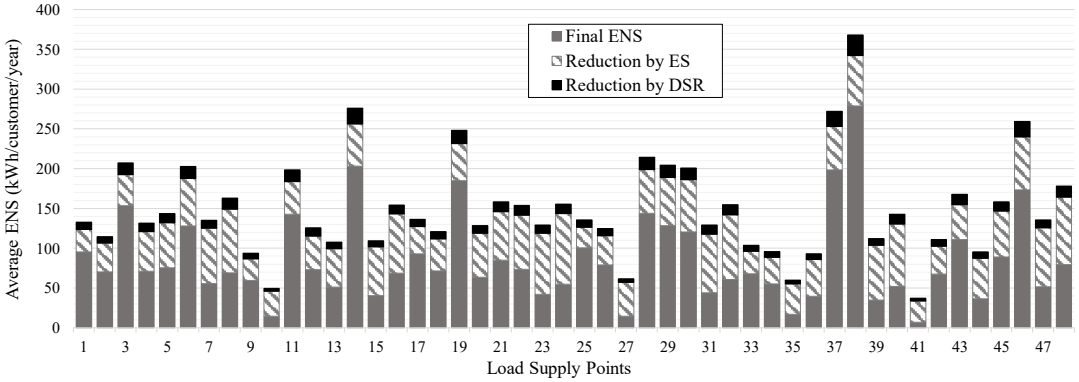

Figure 3.18: Average ENS for different load supply points.

3.5 Evaluation of Customer-Oriented Power Supply Risk

System-wide indices as calculated in the previous section, are periodically required from each DNO to assess network performance against relevant performance targets. However, one of their main drawbacks is that they include customers who enjoy uninterrupted power supply for substantially long periods, thereby concealing some of the shortcomings of network performance, especially to worst served customers. Moreover, it is financially important for DNOs to have a deeper understanding of the value attached to their service by customers. This information can help DNOs to develop targeted solutions to different customer groups and hence raising their WTP [148]. Therefore, this section analyses specifically the customer-based indices i.e. those measuring system reliability for only those customers who are affected by interruptions. These indices accurately represent the customer-view of network performance and are thus invariably useful in ascertaining their WTP [149]. For this customer-oriented analysis, only scenarios (SC-1, SC-4 and SC-6) will be analysed as the results for system indices already reveal expected improvements from the addition of DSR to SC-3 and SC-5 resulting in scenarios SC-4 and SC-6, respectively.

3.5.1 Frequency of Sustained Interruptions

Table 3.11 illustrates results for the frequency of sustained interruptions given the considered scenarios. For only those customers affected by interruptions, the average interruption frequency (CAIFI) is unchanged from the base case scenario when PV+DSR is deployed since no control technique is implemented; PV only provides additional energy during the occurrence of faults. Conversely, CAIFI is reduced significantly, i.e. 22.6% from the base case, when ES+DSR is deployed. The enhancement offered by ES is further highlighted when the number of customers affected is assessed before/after its application. The average number of LPs affected by interruptions reduces from nearly 7 in the base case, to roughly 2 when either ES scenario is deployed [120].

Table 3.11: Frequency of long interruptions to affected customers.

ID	Scenario	CAIFI (Ints/aff. cust.)	*	LPs Affected (avg)	*
SC-1	Base case	0.720	_	6.644	_
SC-4	PV+DSR	0.720	0%	6.644	0%
SC-6	ES+DSR	0.557	22.6%	1.643	75.3%

* Reduction from Base Case; ints = interruptions; cust. = customer; aff. = affected

The CAIFI PDFs presented in Figure 3.19 further confirm the benefits of the ES+DSR scenario. Notably, both displayed scenarios do not have any values occurring within the range 0-1, because CAIFI is only calculated for customers affected by interruptions, implying that the individual average CAIFI values can only be less than one if they are zero (when no LP is affected by interruption). As expected, the implementation of ES+DSR increases the probability of having 0 interruptions per affected customer from the base case scenario. However, it simultaneously increases the largest plausible number of interruptions that can be experienced at a single LP: from 2.8 (base case) to 4. In addition, the base case CVaR for CAIFI (0.0028 interruptions/affected customer), at the 95% confidence level, increases to 0.0078 when ES+DSR is implemented. This means that in the worst 5% of cases, the average interruption frequency to affected customers increases. However, this effect is best explained by the fact that the EMS-controlled ES is deployed as a corrective action when faults occur. While in most cases it can completely ensure supply continuity by alleviating the effects of upstream network faults, in the cases where it only lowers the interruption duration, the overall effect is to have fewer customers affected for the same number of interruptions, therefore resulting in a higher ratio of interruptions per affected customer, i.e. higher CAIFI. This is further discussed in Section 3.5.4, where results for the ACCI index are presented. In summary, ES+DSR reduces the number of customers affected significantly more than it reduces the total number of customer interruptions, thus resulting in a highly plausible CAIFI. Also, Figure 3.19 illustrates a 'peak'

around the value of CAIFI = 1 due to the coincidence of faults and number of affected customers, especially when system faults affect large parts of the network and lead directly to interruptions of loads [148], as highlighted in Figure 3.15.

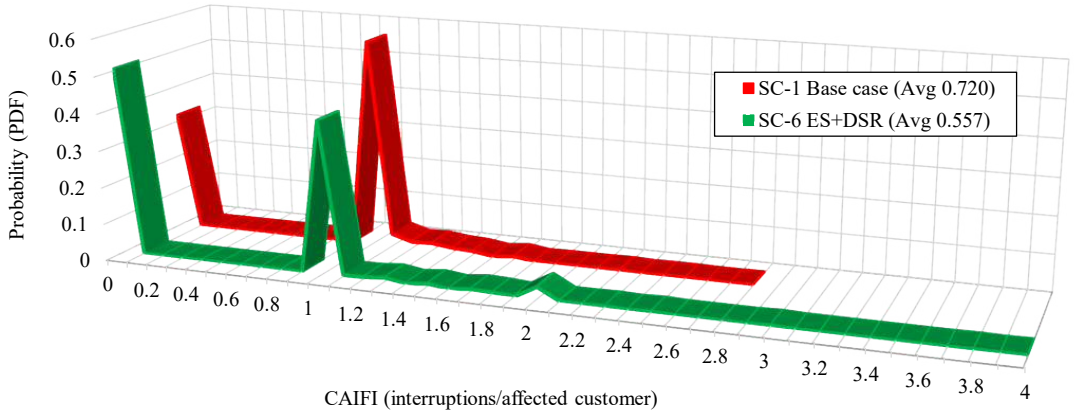

Figure 3.19: Comparison of PDFs for the CAIFI index.

CAIFI is particularly useful in recognising chronological trends in the reliability of a distribution network, highlighting the years when not all supplied customers are affected by interruptions, and many experience supply continuity [19]. Table 3.12 further analyses this phenomenon by focusing on the probability of supply interruptions to a particular number of LPs. ES+DSR increases the probability of not having any LP affected by interruptions by almost 60%. Furthermore, using ES+DSR increases the probability of having only one LP affected by 55%. As a direct consequence of those increments, the probability of LIs affecting anywhere between 2 and 47 LPs is nearly halved in this SC-6 scenario. Most importantly, the SC-6 smart intervention lowers the probability of having all LPs (48) affected by interruptions by 95%. Specifically, in 1000 years, all LPs are simultaneously affected by interruptions only 3 times when ES+DSR is used, as compared to 62 times when no smart interventions are deployed [120, 148].

Table 3.12: Probability of the number of LPs affected by supply interruptions.

Number of LPs Affected	**Probability**		**Reduction from SC-1**
	SC-1: Base case	**SC-6: ES+DSR**	
0	0.320	0.508	-58.8%
1	0.147	0.228	-55.1%
2-47	0.471	0.261	44.6%
48	0.062	0.003	95.2%

The results in Table 3.12 are further detailed in Figure 3.20. ES+DSR significantly increases the probability of having a lower number of LPs affected by interruptions, while substantially decreasing the probability of having a greater number of LPs affected. In some cases, the reduction is so great that it completely negates number of interruptions experienced by that number of LPs e.g. for LPs 17–24, 26, 30, 32 and 33 [148]. Moreover, the heavy tail distribution presented by Figure 3.20 can be further analysed by using a CVaR computation at a 95% confidence level. While the base case CVaR for the number of LPs affected by interruptions is 2.976, this value becomes 0.144 when ES+DSR is implemented. This means that this smart scenario can reduce the impact of HILP events by a 95% reduction in the average number of LPs affected in the worst 5% cases. On top of providing a further explanation for the unexpected increment in CVaR when analysing CAIFI, this result also promotes the use of risk-averse modelling in network planning by adequately quantifying the risk of HILP events [150]. Finally, the scatter plot in Figure 3.21 further demonstrates the capability of ES+DSR to 'confine' the effect of supply interruptions to much fewer LPs than in the base case scenario and also lower the total number of affected customers [148].

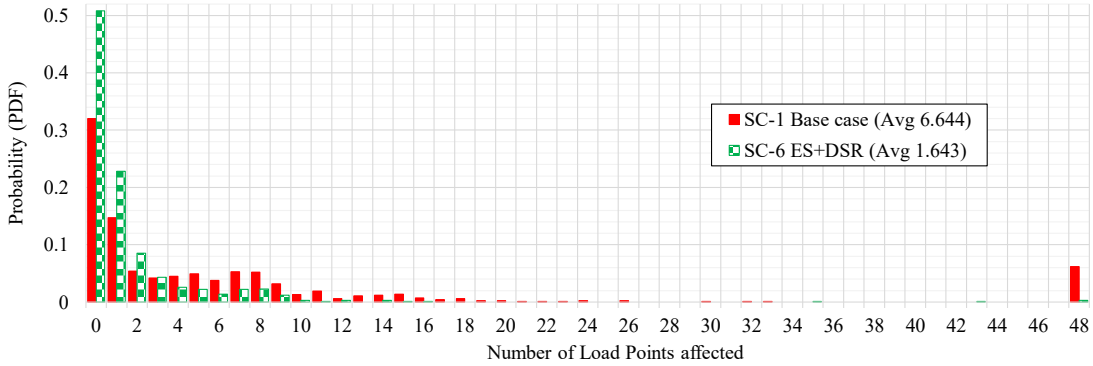

Figure 3.20: Probabilities of the number of LPs affected by supply interruptions.

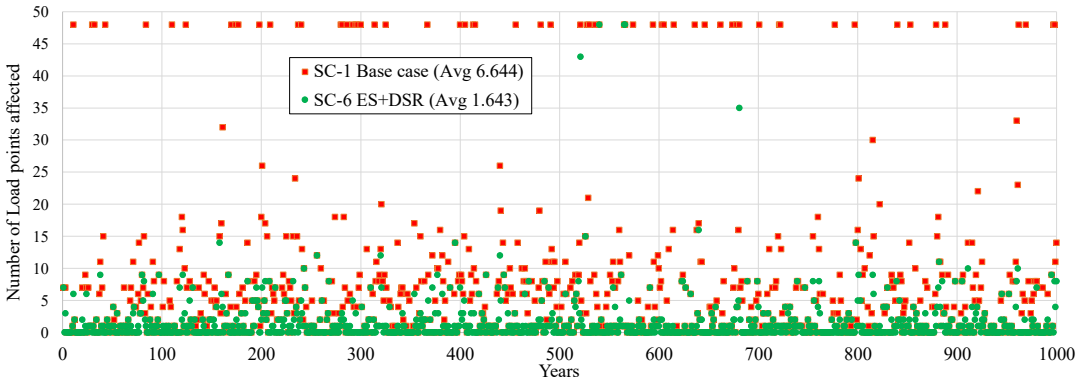

Figure 3.21: Number of LPs affected by supply interruptions.

3.5.2 Frequency of Momentary Interruptions

Short interruptions, voltage sags and swells can potentially damage sensitive equipment. To evaluate system reliability, MAIFI considers momentary interruptions that may affect several types of loads. Most studies assessing the frequency of SIs present average values of MAIFI [151, 152], which is a system-wide index that considers all customers including even those not subject to momentary loss of power supply. There is a reluctance to quantify the SI-frequency to only the affected customers [21, 153]. Accordingly, this research proposes a new index – customer average momentary interruption frequency index (CAMIFI), described mathematically by (2.11), for quantification of SIs to customers affected only [148]. Table 3.13 shows no discernible improvement in CAMIFI after application of PV+DSR. ES+DSR also provides only a 2.7% increase in average CAMIFI value from the base case. This is because, in the current design, ES+DSR is unable to ensure complete backup capability during a sustained fault, and only offers a high percentage alleviation of the upstream network fault i.e. it 'converts' some LIs to SIs thereby changing their classification. This insignificant impact on CAMIFI is also due to ES+DSR systems being locally installed, and, given the varying distances between LPs and fault locations, it is not feasible for different EMS systems to respond simultaneously to SIs [148]. A more significant impact would be expected from larger-capacity ES given the advanced technology and detection of momentary faults [153].

Table 3.13: Frequency of short interruptions to affected customers.

ID	Scenario	CAMIFI (Ints/aff. cust)	Reduction from Base case
SC-1	Base case	0.797	_
SC-4	PV+DSR	0.797	0%
SC-6	ES+DSR	0.819	-2.7%

3.5.3 Duration of Sustained Interruptions

The first thing to note about Table 3.14 is that the results suggest that coordinated operation of ES increases (worsens) CAIDI as shown by the 69.7% increase in SC-6. Conversely, a 25.2% reduction in this outage time is reported when SC-4 is deployed. Accordingly, if e.g. a customer experienced a 2-hour interruption previously, the outage duration would increase to 3.4 hours with the implementation of ES+DSR, yet it would decrease to 1.5 hours if PV+DSR were deployed [148]. However, this 'increase' is because CAIDI is directly calculated from the ratio of SAIDI to SAIFI, and thus it is dominated by the greater reduction of SAIFI i.e. 75% (Table 3.8) than the reduction of SAIDI i.e. 48.7% (Table 3.9).

Table 3.14: Duration of sustained interruptions for affected customers.

ID	Scenario	CAIDI (housr/cust. int)	Reduction from Base case
SC-1	Base case	3.678	_
SC-4	PV+DSR	2.751	25.2%
SC-6	ES+DSR	6.243	-69.7%

Figure 3.22 presents the CAIDI PDF plots where ES+DSR increases the CAIDI average, the duration of longest interruptions i.e. tails of the PDF, and the average CAIDI in the worst 5% cases (CVaR) by 282%. Conversely, PV+DSR contributes to a reduction in the average value of the CAIDI index with a corresponding reduction in the duration of the longest interruptions [148] and a 22% reduction in the average CAIDI in the worst 5% cases. This is explained by the fact that PV+DSR does not reduce SAIFI, yet it lowers SAIDI index by 26% in SC-4 (Table 3.9).

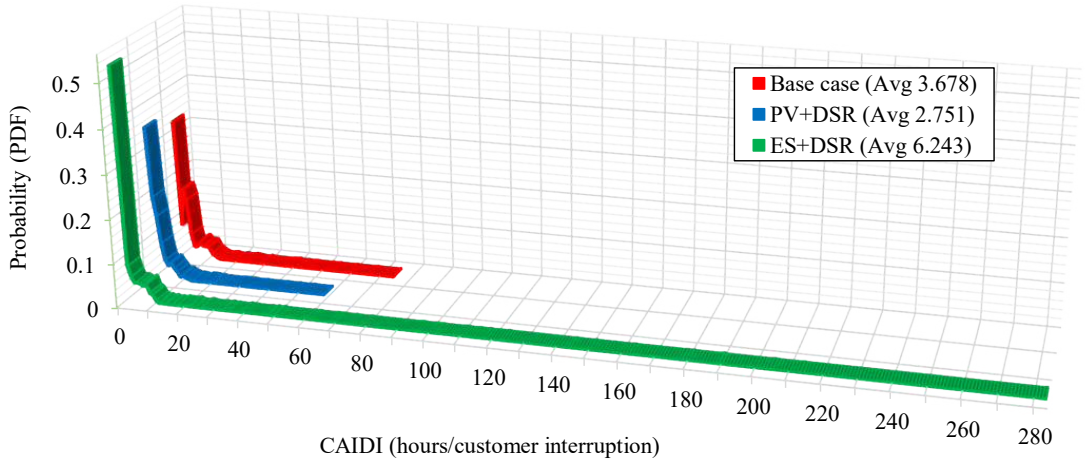

Figure 3.22: Comparison of PDFs for CAIDI index.

3.5.4 Average Customer Curtailment

Through the quantification of the ACCI, it is possible to establish not only the necessity of implementation of the proposed reliability improvement techniques but also the network infrastructure requiring most intervention. Regarding the risk associated with the energy not supplied to customers, Table 3.15 presents the reliability assessment results for ENS to only those customers affected by supply interruptions. Uncontrolled PV, in combination with DSR, positively affects ACCI by a 24% reduction. Again, the results showing LPs affected in each scenario are presented to further classify the reliability performance, especially for ENS. Ac-

cordingly, PV does not effect the average number of LPs affected by interruptions, as it is locally uncontrolled and therefore cannot prevent the occurrence of upstream network faults. It can only reduce the average ENS per affected customer. It is important to note that the percentage increase of ACCI, of 64.2% in SC-6, should not be interpreted as a weakness of the EMS-controlled ES technology. The reason for this 'increase' is that the overall effect of the ES technology is to significantly reduce the number of interruptions – in most cases, ensuring continuous supply. This means that the total number of affected customers reduces so greatly that the denominator for the calculation of ACCI renders the resulting value higher than in the base case. Implementation of ES is therefore effective in reducing the ACCI as it also lowers the number of affected customers (by over 75%) [120, 148]. This can be proven if the product of the ACCI and LPs affected is taken for all scenarios. This will reveal that affected customers enjoy less ENS when ES+DSR is deployed. This result is of great importance to stakeholders such as DNOs and especially customers who require highly reliable and continuous supply.

Table 3.15: Energy not supplied to affected customers.

ID	**Scenario**	**ACCI (kWh/aff. cust.)**	*	**LPs Affected (avg)**	*
SC-1	Base case	1090.41	-	6.644	-
SC-4	PV+DSR	828.99	24.0%	6.644	0%
SC-6	ES+DSR	1790.79	-64.2%	1.643	75.3%

* Reduction from Base Case; aff. = affected; cust. = customer.

Figure 3.23 illustrates the positive effects of ES+DSR by assessing the probability of different amounts of energy not supplied per interrupted customer (ACCI). SC-6 greatly improves the probability of having no energy curtailment to nearly 0.5, from 0.32 in the base case, which is directly related to the enhancement of reliability performance and CoS. However, an important feature in Figure 3.23 is the higher probability of larger values of ENS (>4000 kWh/customer interrupted) when ES+DSR is deployed, as compared to values from the uncontrolled PV case or the base case. Although it is seemingly a weakness, this is explained by the fact that ES effectively prevents occurrence of system interruptions by providing a back-up continuous microgrid-based supply to the customers. For the calculation of ACCI, this means relatively short sustained interruptions will be "converted" to continuous supply, based on the available SOC of the ES, rendering LPs with these DERs no longer affected by the upstream faults. However, this is not the case for the relatively longer sustained interruptions, resulting in a lower number of affected customers, but relatively unchanged individual interruption durations and energy unsupplied. This may be clarified by using an example from the presented results, where for one particular year (before any smart intervention-base case), there were eight affected LPs, with one relatively long LI and seven relatively short LIs. After the

application of ES, the seven relatively short LIs were converted to continuous supply, but the one relatively long LI was largely the same, thereby reducing only the ENS for that period. This results in a much higher ACCI for this particular year when ES is deployed, due to the modified (i.e. reduced) number of customers affected, as compared to the base case. Therefore, it is important to emphasise that ES is undoubtedly the most effective DER technology for improving reliability performance, even though this may not be apparent and immediately clear from the presented results for some indices [148].

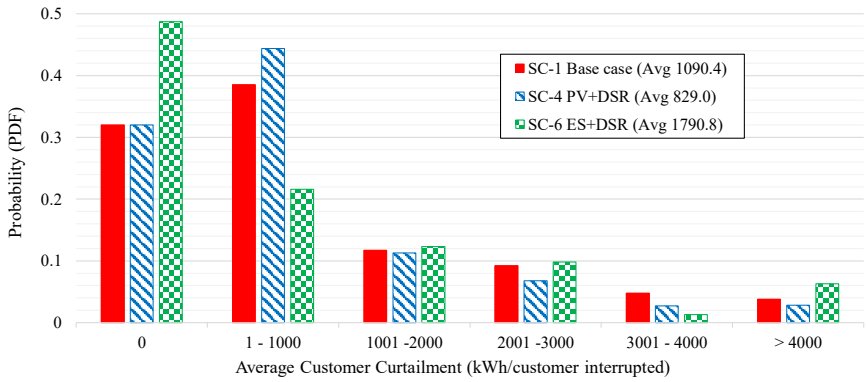

Figure 3.23: Comparison of PDFs for ACCI values for different scenarios.

3.5.5 Comparison with System-wide Reliability Evaluation

To demonstrate the variance between customer-oriented and system-wide reliability indices, Table 3.16 presents each index grouped by different reliability parameters i.e. frequency and duration of interruptions and ENS. Comparing each customer index with its system equivalent reveals a disproportionate gap between these indices. This is because customer-oriented indices consider only the customers affected by interruptions as compared to system-wide indices that account for all customers served. For example, system ENS is at least 7 times smaller than ENS to affected customers (ACCI) in SC-1 and SC-4, and over 21 times smaller in the case of SC-6. Similar differences are demonstrated in the other index categories and this emphasises the requirement to assess network reliability from the customer perspective in addition to the more system-centric evaluations [148].

3.6 Disaggregation of Reported Reliability Performance Metrics

There exists an overarching requirement for DNOs to report a more detailed evaluation of network performance due to the high variability in supplied networks. This is motivated by the recent drive in various countries to report disaggregated indices according to network type

Table 3.16: Customer-Based vs System-Wide Reliability Metrics.

Parameter	Index	SC-1 Base Case	SC-4 PV+DSR	SC-6 ES+DSR
Frequency of LIs	CAIFI (ints/aff. cust.)	0.720	0.720	0.557
	SAIFI (ints/cust./year)	0.157	0.157	0.039
Frequency of SIs	CAMIFI (ints/aff. cust.)	0.797	0.797	0.819
	MAIFI (ints/cust./year)	0.208	0.208	0.216
Duration of LIs	CAIDI (hours/aff. cust.)	3.678	2.751	6.243
	SAIDI (hours/cust./year)	0.550	0.407	0.282
Energy not supplied	ACCI (kWh/aff. cust.)	1090.41	828.99	1790.79
	ENS (kWh/cust./year)	146.37	110.63	85.21

aff. cust. = affected customer; int = interruption

(RU/SU/UR), as it provides essential information for decision-making on measures for CoS improvements [33]. Accordingly, this section introduces the critical need to report reliability performance metrics by distinguishing between different customer-groups, load demand and network types, within very large service areas managed by DNOs. These are practical considerations given that DNOs report fault events in their systems by distinguishing them based on types of components, network types, and voltage levels. As stated in Section 3.1.1, based on various factors, power distribution systems supplying residential demand may be categorised into rural, suburban and urban networks. While the first sections in this chapter dealt with analysis on the urban network, it is expected that analysis of the rural and suburban networks will result in different performance metrics because they represent the varying topographical layouts, demand densities, and network parameters. Notably, LPs in each presented MV network are 34, 44 and 48, while the total network components are 404, 520 and 592 for the RU, SU and UR networks, respectively. Accordingly, the contribution of this section is to demonstrate the range of reliability index variation, from both system and customer perspectives, in different networks. When added to the correspondingly different impacts of DERs, this analysis provides a rigorous characterisation of varying customer-groups.

3.6.1 Development of the Aggregate Network

Given that DNOs usually report aggregated values of the reliability indices describing the performance of their networks, this research presents reliability indices for a network (termed AGG) which is the equivalent of aggregating the 3 networks presented in this section (RU, SU and UR). This network, therefore, has 13110 customers served by 126 main LPs. To calculate what would be the equivalent reliability indices for this AGG network, a weighted mean of each index is calculated using the 3 subnetworks. System and customer-oriented indices of the AGG network are obtained from the 3 subnetworks using (3.7) and (3.8):

$$Index\_Sys_{AGG} = \frac{\sum_{i\in\Omega_L}^{N} LP_i index_i}{\sum_{i\in\Omega_L}^{N} LP_i} \tag{3.7}$$

$$Index\_Cus_{AGG} = \frac{\sum_{i\in\Omega_L}^{N} LP_i index_i}{\sum_{k\in\Omega_A}^{N} LP_k} \tag{3.8}$$

where $Index\_Sys_{AGG}$ and $Index\_Cus_{AGG}$ are the system and customer-oriented indices respectively, *index* is the reliability index under consideration, i and k represent each subnetwork, LP is the number of load points, set Ω_L contains all subnetworks and set Ω_A contains only the LPs affected by either LIs or SIs depending on the index considered for each network. This provides a basis upon which to compare the performance of what would be an entire network area served by a DNO, with the performance of its subnetworks that have varying characteristics, network configuration and customers served [154].

3.6.2 Comprehensive Reliability Assessment

The previously described MCS procedure (Section 3.2) is utilised to carry out reliability assessment for each subsector network, without integration of any smart interventions. MCS results exemplify the variation arising from the fact that the different networks are made up of a different mix of PCs, demand supplied, and network configuration. This variation is central to the contribution of the section as it emphasises the requirement to disaggregate network reliability performance based on network type [154]. To complete the base case performance for each subsector network, there is the inclusion of SQS regulations which stipulate maximum durations of supply restoration based on supplied GD. Additionally, the integration of DERs in each network is modelled considering SC-4 (PV+DSR) and SC-6 (ES+DSR) in Section 3.3. This further illustrates the varying impacts of these technologies in different network types.

3.6.2.1 Base Case Network Performance

Table 3.17 presents the reliability indices obtained for each network for the base case performance (i.e. without DERs). The indices provided are all standard indices aside from CAMIFI, which has been previously defined in Section 2.2.2 and represents a measure of the frequency of SIs to only affected customers. Indices for the AGG network are also presented, which effectively represent a weighted mean of the indices from all 3 networks (as usually presented by DNOs when reporting on their network reliability performance). Both system and customer-oriented indices are presented highlighting again the significant disproportionate gap between each index pair for the same parameter e.g. ACCI is at least 5 times greater than the corresponding ENS for all assessed networks. For especially WSCs, customer-oriented indices are necessary to reveal network shortcomings often concealed by system indices. This results in presenting a more accurate picture of the customer-view of network performance and in some cases aiding DNOs to manage customer expectations and thus WTP. The information on performance variability presented by these index sets is as valuable as that obtained from assessing different network types and therefore merits their inclusion in DNO-reported network performance.

Table 3.17: Base case performance for all load subsector networks.

Parameter	**Index**	**Reliability Performance**			
		RU	**SU**	**UR**	**AGG**
Frequency of LIs	CAIFI (ints/aff. cust.)	0.719	0.966	0.720	0.839
	SAIFI (ints/cust./year)	0.139	0.296	0.157	0.201
Frequency of SIs	CAMIFI (ints/aff. cust.)	0.804	1.023	0.797	0.906
	MAIFI (ints/cust./year)	0.188	0.368	0.208	0.259
Duration of LIs	CAIDI (hours/aff. cust.)	4.337	5.078	3.678	4.490
	SAIDI (hours/cust./year)	0.629	1.351	0.550	0.851
Energy not supplied	ACCI (kWh/aff. cust.)	135.38	653.95	1090.41	687.76
	ENS (kWh/cust./year)	17.85	150.70	146.37	113.20

aff. cust. = affected customer; int = interruption

Given the lower number of customers served by the RU network (646) as well as the lower number of PCs (404), it is generally expected that most of the RU system indices calculated will be the lowest of the 3 networks in Table 3.17. Accordingly, the UR network outperforms the RU network in indices such as SAIDI, CAIDI, and CAMIFI due to the evidence suggesting that denser networks (having a higher ratio of customer/km) have fewer minutes lost per customer per year than less dense networks [35]. There is also a strong correlation between the number of supply interruptions and which type of network serves customers [35]. Not to mention the commensurately higher number of backup supply alternatives. While it might be expected that UR customers experience higher levels of CoS (low number of interruptions, and

for short periods), the results reveal that this is not a straightforward case. This is because of the varying number and type of PCs, stochastic nature of network behaviour, number of, and spatial variability of customers served. It is also important to note that the AGG network is heavily influenced by the SU network which generally exhibits the worst reliability performance because of the high number of PCs (520), customers served (3344) and dominance of overhead lines for power distribution, which are generally more likely to fail than underground cables used in the UR network, for example [154].

3.6.2.2 Impact of ES+DSR on Frequency of Interruptions

While Table 3.17 presents only the base case results for each network performance, Figure 3.24 shows the corresponding impact from the designed ES+DSR smart intervention, in terms of frequency of interruptions. By providing the percentage reductions of each index from its value in the base case, it is possible to quantify the impact of these technologies on network performance. As previously explained, the effect of PV+DSR is not considered as its amount of penetration is not enough to influence the frequency of interruptions. The deployment of PV+DSR, at a 50% PV penetration and 10% demand for DSR, essentially lowers the period for which a customer experiences an interruption, thereby reducing only the ENS.

However, Figure 3.24 shows that the predominantly corrective application of ES+DSR reduces SAIFI by 75% in the UR network and by over 35% in the RU one. The impact of ES+DSR is less significant on CAIFI index, as previously explained (Table 3.11). For both indices measuring frequency of LIs, the UR network benefits most from the application of ES+DSR. Additionally, CAIFI shows a significantly higher reduction after the application of ES+DSR in the UR network than in the others. Notably, both indices measuring frequency of SIs experience an increase from the base case when ES+DSR is deployed. This is mainly due to those occasions when ES lowers the length of LIs to such an extent that they last for only short periods, i.e. long enough to be classified as SIs. Therefore, while ES+DSR does not directly affect frequency of SIs, it does convert some LIs to SIs. Again, this increase in the frequency of SIs indices should not be interpreted as a negative impact on the network transient behaviour but rather as an improvement in network capability to alleviate faults [154].

The comparative analysis is extended by considering Figure 3.25 which presents the CDFs of SAIFI for each network after ES+DSR deployment. As before, ES+DSR exhibits the highest impact on the UR network followed by the RU and SU networks. Notably, each customer in any of the 3 networks has a very high probability of experiencing no more than 1 LI per year. Additionally, customers in the UR network are more likely to experience shorter interruptions than customers in the RU and progressively, SU network [154]. Although it would be expected

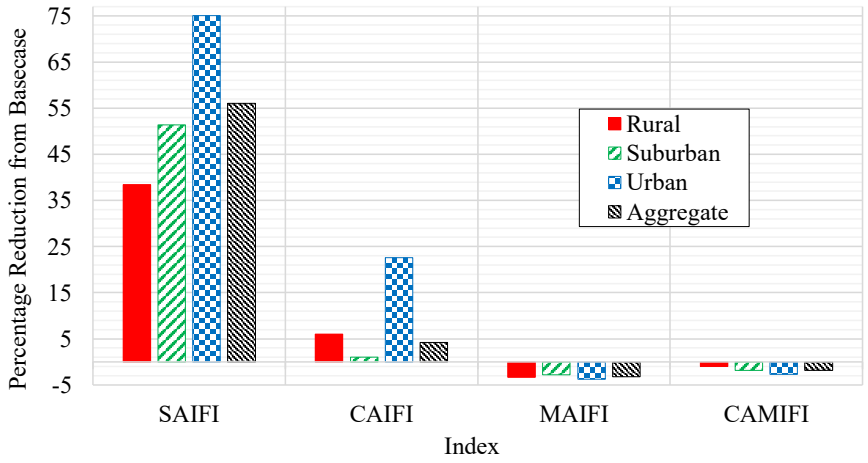

Figure 3.24: Impact of ES+DSR on the frequency of LI indices.

that customers in the SU network should experience better network reliability than those in the RU network, the results demonstrate that this is not the case due to the significantly higher number of PCs (more faults) and customers in the SU network.

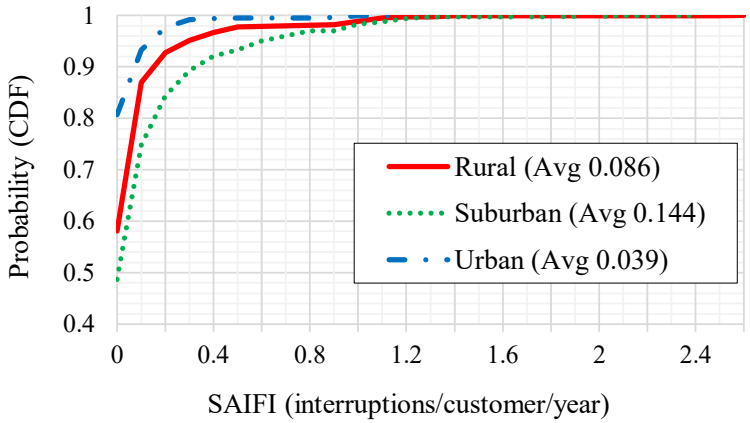

Figure 3.25: Impact of ES+DSR on SAIFI for all MV networks using PDFs.

3.6.2.3 Impact of DERs on Duration of Interruptions

Firstly, Figure 3.26 combines two reliability parameters i.e. energy not supplied and duration of LIs because of their strong correlation. Secondly, Figure 3.26(a) shows that PV+DSR generally has a substantial effect on these two reliability parameters reducing each related index by at least 23% from the base case value. On the other hand, ES+DSR (Figure 3.26(b)) presents a slightly different effect on network reliability performance. As expected, the level of reduction of both system-oriented indices (ENS and SAIDI) is much higher than that in the PV+DSR

case, as the EMS-controlled ES technology makes a more intelligent use of energy resources. Focusing on the load subsector, the impact of ES+DSR on the UR network is also communicated by the fact that corresponding ENS and SAIDI percentage reductions from the base case are marginally highest in this network than in the RU and SU networks.

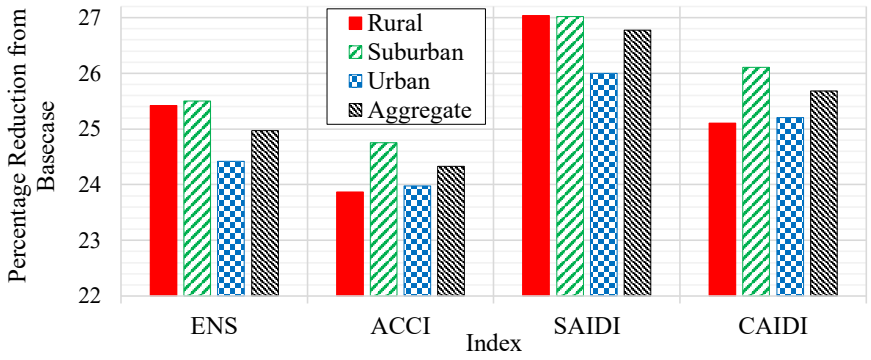

(a) PV+DSR

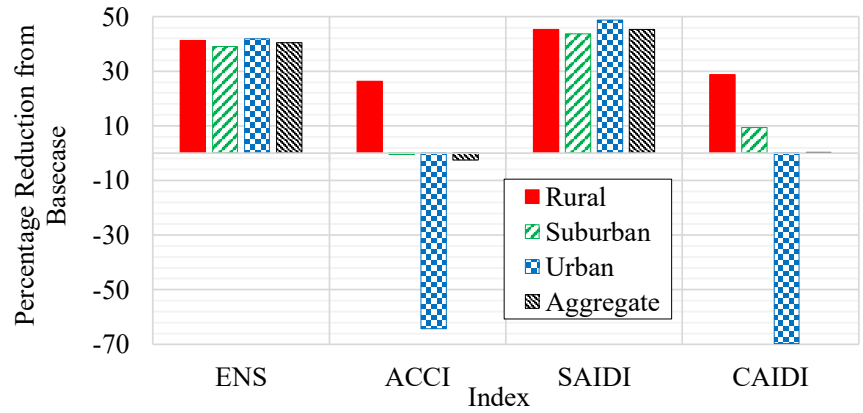

(b) ES+DSR

Figure 3.26: Impact of smart interventions on ENS and duration of LI indices.

Reporting disaggregated indices becomes especially important when customer-oriented indices (ACCI and CAIDI) for these same reliability parameters are assessed. ES+DSR has the effect of increasing (hence 'worsening') ACCI significantly for the UR network, less so for the SU network, and offering a reduction in the RU network. Similarly, ES+DSR only increases the value of CAIDI in the UR network. The performance of both indices in the UR network is due to its symmetric nature which allows for more 'balanced' occurrence of faults that are significantly alleviated by the action of ES+DSR, leading to not only continuous supply but also a significant reduction in the number of LPs affected. This has the effect of increasing these two customer-oriented indices and presenting the unexpected result of a worse reliability

performance. However, the increase in these indices is a sign that ES+DSR is most effective in the UR network, as explained in Section 3.5.4 (the product of ENS and LPs affected).

Also, the number of affected LPs is significantly reduced, thus presenting a higher ACCI or duration of LIs for only the affected customers. Table 3.18 illustrates this property whereby the percentage number of LPs affected by LIs reduces from 14% of the 48 LPs (6.64) in the base case to only 3% when ES+DSR is applied, for the UR network. Conversely, the reductions to the number of LPs affected by LIs are not as large when ES+DSR is deployed in the RU (12% to 8%) and SU (23% to 11%) networks. Table 3.18 also confirms the minor changes in the MAIFI and CAMIFI indices given the small changes to the number of LPs affected by SIs for each network when DERs are deployed [154]. Finally, the PV+DSR scenario is not included since it does not have a meaningful impact on the LPs affected by LIs or SIs for each network.

Table 3.18: Number of LPs affected by supply interruptions.

	Network Scenario	**Base case**			**ES+DSR**		
	MV Network	**RU**	**SU**	**UR**	**RU**	**SU**	**UR**
	Total Number of LPs	34	44	48	34	44	48
LIs	**Number of LPs Affected**	4.22	10.26	6.64	2.56	4.81	1.64
	Percentage of LPs affected	12%	23%	14%	8%	11%	3%
SIs	**Number of LPs Affected**	5.58	12.63	8.39	5.76	12.82	8.60
	Percentage of LPs affected	16%	29%	17%	17%	29%	18%

Figure 3.27 presents the CDF analysis of SAIDI when ES+DSR has been deployed. This graph confirms that there is better reliability performance improvement in the UR network through the effective use of ES+DSR. Moreover, there is a higher probability (0.833) of customers experiencing an interruption of 0.2 hours or 12 minutes in the UR network, than the same probability in the RU network (0.629) and the SU network (0.508). This result is significant as it highlights key planning and operational decisions for the focus and deployment of such technologies to these various types of distribution networks [154].

3.6.2.4 Impact of DERs on Average Energy Not Supplied

Despite currently not being widely reported by DNOs to regulators [11], the ENS index is central to a very useful understanding of the capability of a network to minimise the impact of supply interruptions to the customers served. By limiting ENS, it is possible to raise the WTP of customers who are then more tolerant about the occurrence of supply interruptions given their confidence in the ability to have alternative supply during these periods. In this way, upstream faults that affect the CoS are more tolerable given that customers continue to enjoy a high-quality continuous supply. However, even if DNOs reported this index, as they

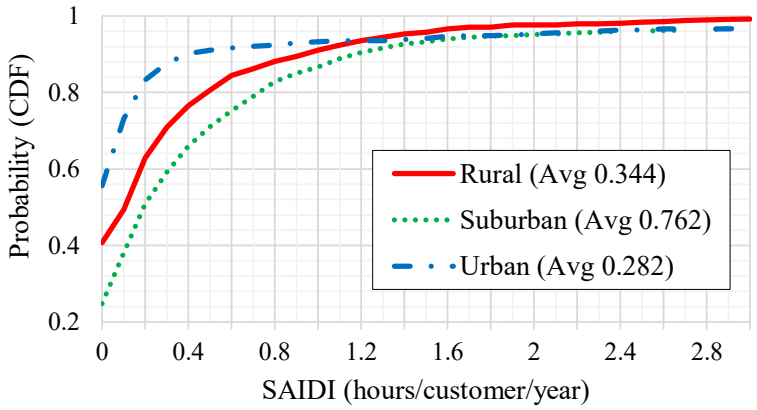

Figure 3.27: Impact of ES+DSR on SAIDI for all MV networks using PDFs.

currently do for SAIFI and SAIDI indices, they might do so by aggregating the total ENS in their served area. A PDF of the resultant ENS index might look like the one present in Figure 3.28, which shows the PDF for the AGG network earlier described. This once again compels the necessity for disaggregation of this ENS index because the main effect of having these networks aggregated is to significantly lower the collective probability of having no (or 0) ENS to the network. The network aggregation tends to 'confine' possible ENS values to the average value given various contributions from the constituent networks i.e. RU, SU and UR. This is also the case when DERs are applied to the so-called AGG network.

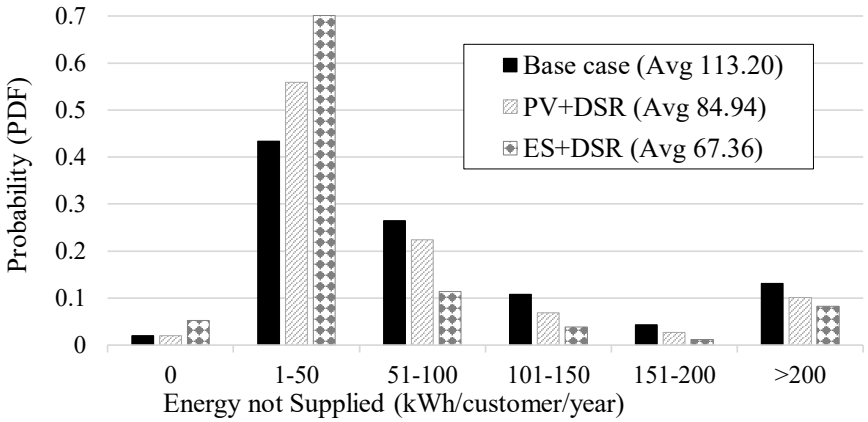

Figure 3.28: ENS per scenario for the AGG network.

Furthermore, even in this case, ES+DSR has the most significant impact of increasing the probability of ENS values within the range 1-50 kWh per customer per year, given the combined average reduction to the ENS offered by ES+DSR in all constituent networks [154]. Therefore, as part of the recommendation from this research, Figure 3.29 illustrates how much information

can be extracted from these networks if their reliability performance indices are disaggregated and reported as such. As can be seen, the values of ENS around 1-50 kWh mainly occur in the RU and SU networks i.e. have the highest probability of occurrence. Conversely, the UR network depicts a situation where most ENS values are likely to be 0 (for all network scenarios) as opposed to being in the region of 1-50 kWh/customer/year [154]. It is also evident that while the RU network will have a very low likelihood of having any of its customers suffer more than 100 kWh of ENS per year, different customers in the SU network will invariably have a much more variable spread of the possible ENS each year. In addition, as a direct comparison to the SU network, the UR network benefits significantly from ES+DSR, which raises the probability of 0 ENS from the base case. It is also notable that, despite the larger number of customers in the UR network (9120) as compared to 3344 customers in the SU network, the probability of ENS values higher than 200 kWh per customer per year are relatively similar regardless of the DERs deployed. This means that the UR network has got a significantly better overall performance than the SU network. It is thus clear that the possible amount of information lost is significantly higher if ENS index is reported with Figure 3.28 as opposed to Figure 3.29.

3.6.3 Impact of Undergrounding on Network Reliability Performance

The results presented in Section 3.6.2 contain an extra layer of information which concerns the impact of using underground cables in distribution networks in conjunction or in place of overhead lines. Different studies [33] on this topic tend to have the expectation that underground cables experience fewer incidents (i.e. less failure rates) but conversely longer interruption times because they take longer to be repaired than overhead lines. This is mainly because underground cables are protected from many common causes of failure e.g. storms, vehicular incidents, etc. although they may sometimes suffer damage by earthworks or specific rare natural events e.g., floods and will generally be more difficult (take longer) to repair. There is therefore a deduction that the positive effect of undergrounding (increasing the percentage of underground lines in the network) on SAIFI should be higher than the benefits on SAIDI. However, often, no such trend is observed in real world datasets [33]. The modelling and simulation results in this thesis may be used to reproduce and validate this unexpected observation.

Using Table 3.19 (obtained from Table 3.17), it is possible to quantify the positive effects of 'undergrounding' on SAIFI and SAIDI by comparing the improvement in each indicator between the RU (100% overhead lines) and UR MV networks (100% underground cables). The SAIDI reported in the UR network (without any DERs) is 12.56% lower than that in the RU network. Conversely, the SAIFI reported in the UR network is 12.95% higher than in the RU network. This confirms an unexpected result as it would be expected that SAIDI would be higher while SAIFI is lower in the UR network. However, due to the significantly

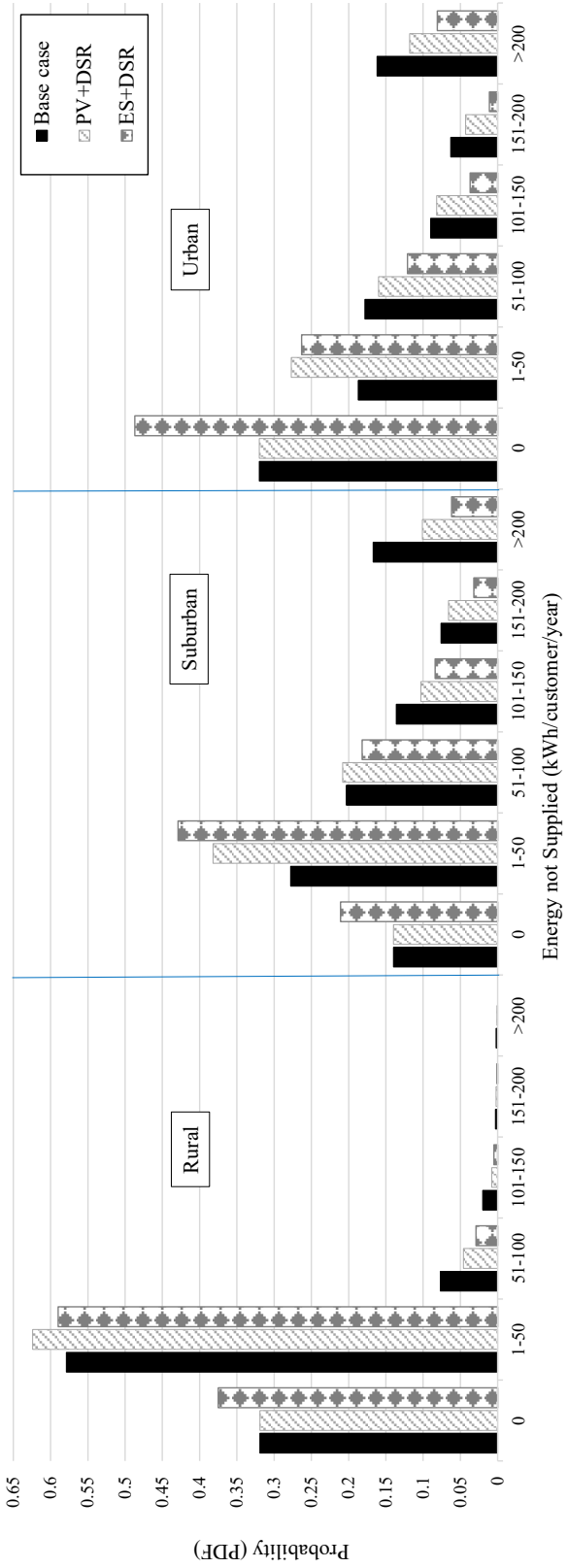

Figure 3.29: ENS per network per scenario for all MV networks.

higher number of customers and PCs in the UR network, there are more faults affecting more customers and thus the higher SAIFI (0.157). Also, the SAIDI is lower (0.550) in the UR network due to the symmetric nature of the network model used i.e. a repetitive pattern of identical feeders with the same number of customers. Future work will provide a more robust analysis by considering spatially disaggregated reliability data (failure rates and repair times) for the different load sectors to ensure that differences in network topologies are modelled more accurately. For example, usually crew response times in UR networks are higher than in RU areas. Therefore, the MTTR of the PCs in UR networks is lower and this often results in lower SAIDI. Moreover, the protection settings, and indeed the devices used, in RU and UR networks are usually different. Therefore, these must also be considered before a totally data-accurate modelling can be achieved.

Table 3.19: Impact of Undergrounding - Rural and Urban.

Index	**Rural (OHL)**	**Urban (UC)**	**Reduction from RU**
SAIDI (hours/cust./year)	0.629	0.550	12.56%
SAIFI (ints/cust./year)	0.139	0.157	-12.95%

In addition, Table 3.20 compares the SU network (both OHLs and UCs) to the UR network. These networks are represented by 44 LPs and 48 LPs, respectively. Results demonstrate that SAIDI improves (reduces) by 59.29% compared to a SAIFI reduction of only 46.96% as more undergrounding is added into the network (UR). It would be expected that the reduction in SAIFI would be greater than that in SAIDI because UCs generally have a lower number of failures but take longer to repair than OHLs. However, the symmetrical nature of the UR network results in a higher reduction in SAIDI than the reduction in SAIFI. For a fairer comparison, the future work will include the spatial disaggregation of failure rates and repair times as stated in the previous paragraph.

Table 3.20: Impact of Undergrounding - Suburban and Urban.

Index	**Suburban (OHL+UC)**	**Urban (UC)**	**Reduction from SU**
SAIDI (hours/cust./year)	1.351	0.550	59.29%
SAIFI (ints/cust./year)	0.296	0.157	46.96%

3.7 Conclusions

This chapter presents various analyses utilising an enhanced MCS methodology. Some of the key methodology benefits include its wider applicability to varying system configurations and load mixes, as well as its capability to demonstrate the relative reliability-performance benefits of different SGTs. Accordingly, the chapter presents an investigation of the potential reliability performance improvements from the implementation of three SGTs: PV, ES and DSR. The technology potential is assessed by percentage improvements in the calculated standard reliability indices over the base case (no SGTs). The analyses are illustrated for typical MV distribution systems. Additionally, the impact of cloud movements and transients on the PV power output is investigated alongside the associated energy loss and the effects of clouding on system reliability performance. Results show the possible overestimation of PV benefits if clouding effects are not accurately accounted for in PV models. ES presents the highest capability to reduce the number of interrupted customers, and more importantly, the ENS.

Furthermore, the chapter is also concerned with emphasising the need for the commonly used system-wide reliability indices to be complemented with customer-oriented indices to accurately assess power supply risk, especially to worst served customers. It is found that the benefits offered by DERs are even more pronounced when customer-oriented indices are utilised. Savings realised in reductions to ENS (to affected customers) have comparative financial implications and can form part of the justification for the installation of local ES systems, whose deployment is often cautioned by the attached costs. Finally, the chapter emphasises the necessity to distinguish between customer-groups in different types of distribution networks when reporting the associated periodic reliability performance. This leads to a disaggregation of the typically reported aggregate index values (which mask true location-specific system performance) thereby allowing for suitable identification of opportunities for targeted performance-enhancing solutions given the various strengths and weaknesses of the individual networks.

Chapter 4

Model Order Reduction for Reliability Assessment of Flexible Power Networks

Chapter Overview

When assessing the performance of large MV systems such as those presented in the Chapter 3, the core reliability assessment methodology used is limited in efficacy by the computational time and burden required, as well as the accuracy of the utilised aggregation techniques used to lower system complexity. For that purpose, specifically tailored aggregation techniques need to be integrated to this methodology that adequately represent the varying network topologies as well as the spatial distribution of the demand supply points. Model order reduction (MOR) has demonstrated its robustness and wide applicability in simulating large-scale mathematical models in the engineering research domain. Therefore, this chapter proposes a novel application of MOR techniques of balanced truncation to quantify relevant reliability metrics of power distribution systems. MOR is used to derive reliability models of electricity networks, which exhibit a reduced number of equivalent components and thus simplify the complexity for network analysis. The numerous case studies presented, based on both radial and meshed systems, demonstrate that the proposed method allows for a faster reliability assessment through MCS while preserving high accuracy. The proposed MOR-for-reliability methodology is compared against other reduction techniques introduced in Chapter 2 such as TNR and AEM.

It is important to highlight that the MCS analyses in this chapter are also time-sequential. However, while Chapter 3 used only SDS for MCS analyses, in this chapter, STS is utilised.

This is because MOR is used to reduce the number of system states and therefore MCS must be done while focusing on state transitions of the entire system rather than on PC states or PC state durations. The standard methodology used for STS is as described in Chapter 2 and is performed on both original and reduced order networks to provide a fair comparison.

Statement of Authorship

This declaration concerns the article entitled:

Title	Model Order Reduction for Reliability Assessment of Flexible Power Networks.
Publication Status	In review
Details	M. B. Ndawula, I. Hernando-Gil, R. Li, C. Gu and A. De Paola, "Model Order Reduction for Reliability Assessment of Flexible Power Networks," submitted to the International Journal of Electrical Power and Energy Systems (Elsevier).
Copyright Status	Copyright is retained by the publisher, but I have been given permission to replicate the material here
Candidate's contribution to the paper	The candidate proposed the idea of the paper, prepared the journal manuscript, predominantly executed the coding and the experimental analysis during methodology development. A. De Paola predominantly helped to implement the methodology, considerably contributed to conceptualisation, reviewing and editing the manuscript, and supervision. I. Hernando-Gil contributed to the conceptualisation and methodology validation. C. Gu and R. Li contributed to editing the manuscript. Candidate's percentage contributions to the paper: Formulation of ideas: 80% Design of methodology: 50% Experimental work: 95% Presentation of data in journal format: 80%
Statement from candidate	This paper reports on original research I conducted during the period of my Higher Degree by Research candidature.
Signature and Date	

Abstract

Model order reduction (MOR) has demonstrated its robustness and wide applicability in simulating large-scale mathematical models in the engineering research domain. In this paper, MOR techniques are applied to quantify relevant reliability metrics of power distribution systems and the impact associated with the integration of different smart grid technologies. To the best of the authors' knowledge, this is the first application of MOR techniques of balanced truncation to derive reliability models of electricity networks, which exhibit a reduced number of equivalent components and thus simplify the complexity for network analysis. The extensive case studies presented, based on both radial and meshed systems, demonstrate that the proposed technique allows for a faster reliability assessment through Monte Carlo simulation while preserving high accuracy. The proposed methodology can also be applied to systems endowed with photovoltaic and energy storage technologies, emphasising that this approach represents a promising starting point for reliability analysis of more complex systems, which are normally characterised by a large penetration of these distributed energy resources.

Keywords: balanced truncation, distributed energy resources, distribution networks, model order reduction, Monte Carlo simulation, system reliability

Acronyms

AEM	Alternative Existing Method
BT	Balanced Truncation
CAIDI	Customer Average Interruption Duration Index
CAIFI	Customer Average Interruption Frequency Index
CoV	Coefficient of Variation
CTMC	Continuous Time Markov Chain
DNO	Distribution Network Operator
ENS	Energy Not Supplied
ES	Energy Storage
HPC	High Performance Computing
HSV	Hankel Singular Value
LP	Load Point
MCS	Monte Carlo Simulation
MESS	Matrix Equation Sparse Solver
MOR	Model Order Reduction
OR	Order Reduction
PC	Power Component
PNS	Power Not Supplied

PSS®E	Power System Simulator for Engineering
PV	Photovoltaic
RBTS	Roy Billinton Test System
SAIDI	System Average Interruption Duration Index
SAIFI	System Average Interruption Frequency Index
TNR	Traditional Network Reduction

Nomenclature

A	system matrix or state transition matrix
B	control/input matrix
C	output matrix
$H(s)$	transfer function of the original system
$\hat{H}(s)$	transfer function of the reduced system
n	state space dimension of the original system
N	number of samples
P	controllability Gramian
Q	observability Gramian
r	state space dimension of the reduced system
T	transformation matrix
$u(\cdot)$	input
U	unavailability
$x(t)$	state vector
$y(\cdot)$	output of the original system
$\hat{y}(\cdot)$	output of the reduced system
σ	HSV of a system
λ	component failure rate
μ	component repair rate
$\|\cdot\|_\infty$	H_∞-norm of a rational transfer function

4.1 Introduction

Power systems are inherently complex and can often be accurately described only by using models with several variables, depending on the intended application. Since complex models are computationally expensive to simulate, it is common practice to use simplified representations of the power system for analysis and design purposes. Reduced models might also be necessary due to other practical reasons, for example when only a limited number of measurements are available for system monitoring, or in the case of interconnected power systems whose single areas (owned by different utilities) are reluctant to share complete and detailed system information [1]. Even with systematic problem decomposition, the pragmatic choice is often to use reduced versions of the original network to run system simulations, where the computational complexity depends at least polynomially on the size of the network [2].

The employment of simplified network models has always been very common in reliability analyses of distribution networks [3, 4] and it is becoming even more relevant as the level of complexity in power systems rapidly increases [5], following the integration of photovoltaic renewable generation (PV) and technologies such as energy storage (ES), electric vehicles and demand response actuators. In a context of growing complexity, it will be necessary to use simplified benchmark models to accurately assess network reliability and determine efficient future investments for a flexible and secure power grid with appropriate reliability standards [6].

This paper proposes the utilization of model order reduction (MOR) tools to develop accurate reduced models of distribution networks for reliability purposes. A rigorous analytical method is used to obtain simplified grid representations that minimise the estimation error of relevant reliability indexes while ensuring significantly shorter computational times. Furthermore, the proposed methodology can easily accommodate the inclusion of PV and ES technologies and quantify their impact in terms of reliability. The rest of the paper is organised as follows: the state of the art is reviewed in the next section, and the background theory of MOR is explored in Section 4.3. Section 4.4 details the development of the methodology using MOR for reliability assessment. Section 4.5 evaluates the performance of the proposed approach on different case studies and conclusive remarks are presented in Section 4.6.

4.2 Network Reduction in Power System Analysis – Related Works

It is common in network studies to simplify the utilised models to obtain a system description with the best trade-off between accuracy and complexity. In these cases, the size of the network models is generally reduced by substituting sets of connected elements (buses, lines,

transformers, etc.) and transforming them into smaller and numerically equivalent systems [7]. Typical applications of this approach include symmetrical or asymmetrical short circuit calculations and load flow calculations. The performance of the reduced networks representations is evaluated in terms of accuracy of the power flow results with respect to the (more complex) initial model [8].

The typical approach for network reduction in a reliability context is to simplify the system representation by systematically replacing certain connected elements of the chosen reliability model (e.g., series and parallel configurations in reliability block diagrams) with fewer equivalent components exhibiting the same reliability properties. The main drawbacks of this method of network reduction are a) its limited applicability, i.e. only to networks with relatively simple topology [9]; b) it cannot be used to calculate customer-based reliability indices such as customer average interruption duration and frequency indices (CAIDI and CAIFI) [10] because it does not allow for an accurate aggregation of demand at different network nodes; c) the impact of critical or unreliable areas and components on the system reliability metrics becomes increasingly harder to distinguish; d) it is difficult to accommodate some relevant reliability features such as different modes of failure, maintenance and weather effects. Despite those drawbacks, this method is useful in practice, particularly for simple analyses where analytical refinements are not desired [4]. Given these limitations, alternative approaches have been developed, such as the decomposition method, which is based on conditioning a complex system on the state of a key power component (PC) [9]. However, this method is not suitable for large systems because, as the number of key PCs increase, the model quickly becomes unmanageable. There also exist analysis algorithms based on testing minimal paths (or using the minimal cut set approach) [9] but their main drawback is that, for large systems, the increased number of paths and cut sets leads to a combinatorial explosion.

This research explores a new approach to network reduction for reliability assessment purposes based on MOR. The chosen method relies on singular value decomposition and balanced truncation. The dynamical system describing the reliability of the network is simplified by first calculating its Hankel singular values (HSVs) [11], which indicate the relevance of each system state in terms of reliability, and then the dynamics which have a smaller impact on the considered reliability indexes are neglected. Model Reduction has already been applied in various power system analyses: MOR using balanced empirical Gramians was investigated for linear systems in [12-14] and nonlinear systems in [15-19]. Given the need to reduce large power systems, [20] used a linear system reduction method and the work was successful for small-signal stability while [21] performed a parametric MOR aimed at preserving parameters related to decentralised power system devices such as stabilisers. Additionally, MOR has been used to obtain reduced models of PV systems [22, 23], battery energy storage systems [24] and

of microgrids [25], using the singular perturbation technique. Albeit not explored in this paper, another important class of MOR methods is based on Krylov subspaces (moment matching). It was used for reduction of a large-scale multiport piezo energy harvester in [26] while in [27] and [28], this technique was extended to reduce large scale power systems and interconnected systems, respectively.

4.2.1 Article Contributions

This work proposes a novel approach for the creation of simplified network models for reliability assessment purposes. To the best of our knowledge, this is the first attempt to apply model order reduction (MOR) in this context and analytically derive simplified grid representations that contain the most important system dynamics and, at the same time, minimise the error of the considered grid reliability metrics. Time-sequential Monte Carlo simulations (MCSs) are carried out on systems of varying complexity to verify that the resulting reduced models provide a reasonably accurate reliability assessment while being faster to simulate. It is also shown that the proposed technique is able to effectively quantify the impact of PV and ES on network reliability. The proposed methodology is presented in Figure 4.1.

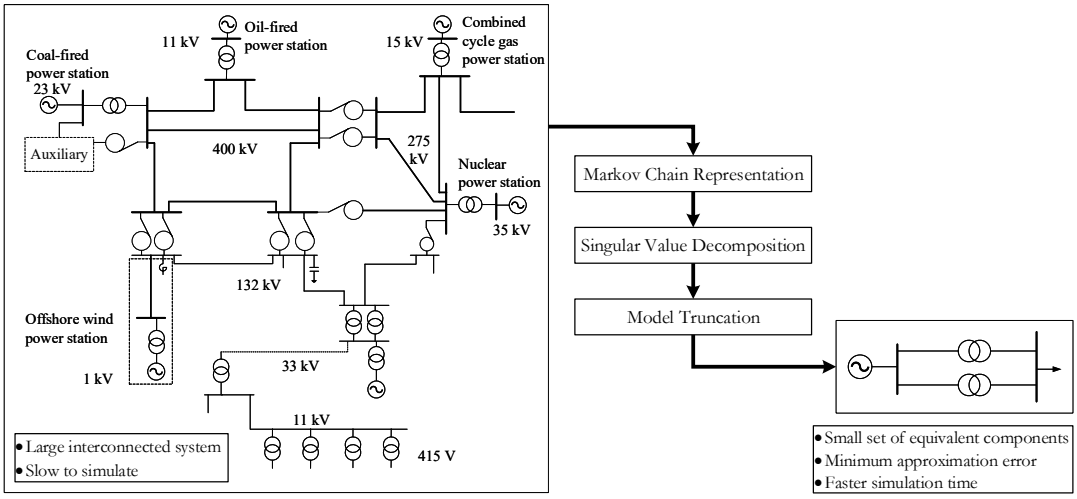

Figure 4.1: Representation of the proposed methodology.

4.3 MOR Theory

This section details the general theoretical framework of MOR and balanced truncation (BT) while the application of this technique to the specific problem of deriving simplified reliability models for distribution networks is presented in Section 4.4.

Let us consider the following linear time-invariant system with input u and output y:

$$\begin{aligned} \dot{x}(t) &= Ax(t) + Bu(t), \\ y(t) &= Cx(t), \end{aligned} \tag{4.1}$$

The internal dynamics of the system are represented by the state vector $x(t) \in \mathbb{R}^n$, whose evolution over time is determined by the system matrix $A \in \mathbb{R}^{nxn}$ and by the input matrix $B \in \mathbb{R}^{nxm}$. In the present formulation, there is no direct input/output relationship and the system output $y(t)$ corresponds to a linear combination of the state $x(t)$, according to the output matrix $C \in \mathbb{R}^{qxn}$.

Model order reduction (MOR) aims at reducing the order n of the system while preserving the fundamental relationships between its inputs and outputs. To this end, the state vector $x(t)$ is projected onto a low-dimensional subspace, neglecting the less relevant system dynamics. The MOR is performed to minimise, for any input $u(\cdot)$, the error between the output response of the reduced model $\hat{y}(\cdot)$ and the one of the original model $y(\cdot)$ [29].

We restrict our attention to stable systems, i.e. system which has a matrix A with all its eigenvalues in the open left half of the complex plane $\mathbb{C}^-$. We are interested in constructing a reduced-order system as in (4.2):

$$\begin{aligned} \dot{\hat{x}}(t) &= \hat{A}\hat{x}(t) + \hat{B}u(t), \\ \hat{y}(t) &= \hat{C}\hat{x}(t), \end{aligned} \tag{4.2}$$

where $\hat{A} \in \mathbb{R}^{rxr}$, $\hat{B} \in \mathbb{R}^{rxm}$, $\hat{C} \in \mathbb{R}^{qxr}$, and $r < n$. In the present context of linear systems, BT is one of the preferred methods for MOR since it preserves stability and provides a global computable error bound between the transfer functions of the original and the reduced-order system. This notion is expressed through the transfer functions $H(s), \hat{H}(s) \in \mathbb{C}^{qxm}$ of the original and reduced system, respectively, which denote the relationships between the input signal and the resulting output response in the frequency domain. An expression for the error between the original and the reduced system output, given by (4.3), is obtained by driving both systems with the same input $u(\cdot)$:

$$\|y - \hat{y}\|_2 \leq \|H - \hat{H}\|_\infty \|u\|_2 \tag{4.3}$$

where $\|\cdot\|_2$ is the Euclidean norm and $\|\cdot\|_\infty$ is the H_∞-norm of a rational transfer function [29].

4.3.1 Balanced Truncation

The fundamental principle of BT for MOR relies on the notions of controllability and observability matrices P and Q, as defined in (4.4) [30]:

$$P = \int_0^\infty e^{At} B B^t e^{A^T t} dt, \qquad Q = \int_0^\infty e^{A^T t} C^T C e^{At} dt, \tag{4.4}$$

In broad terms, the controllability Gramian P determines how much the inputs u affect each component in the state x. Similarly, the observability Gramian Q quantifies the impact of each state component in x on the system outputs y. The first step of the BT technique is a change of coordinates in the original system (4.1), according to the transformation matrix $T \in \mathbb{R}^{nxn}$:

$$\begin{aligned} \dot{\tilde{x}}(t) &= TAT^{-1}\tilde{x}(t) + TBu(t), \\ y(t) &= CT^{-1}\tilde{x}(t), \end{aligned} \tag{4.5}$$

It is possible to demonstrate that the matrix T can always be chosen to obtain new Gramians $\tilde{P}$ and $\tilde{Q}$ which are equal and diagonal:

$$\tilde{P} = TPT^T = \tilde{Q} = T^{-T} Q T^{-1} = \sum = diag(\sigma_1, \sigma_2, ..., \sigma_n), \tag{4.6}$$

In equation (4.6), the terms $\sigma_1, ..., \sigma_n$ denote (in non-increasing order) the Hankel Singular Values (HSVs) of system (4.1), which broadly speaking provide a measure of energy for each system state. The state vector $\tilde{x}$ in (4.5) can now be partitioned as $\tilde{x}(t) = \begin{bmatrix} \tilde{x}_1(t) \\ \tilde{x}_2(t) \end{bmatrix}$, where $\tilde{x}_1(t) \in \mathbb{R}^r$ contains the r state components associated to the highest HSVs of the system and indicates the dimension of the reduced system. The equations in (4.5) can be rewritten as:

$$\begin{aligned} \tilde{x}(t) &= \begin{bmatrix} \tilde{A}_{11} & \tilde{A}_{12} \\ \tilde{A}_{21} & \tilde{A}_{22} \end{bmatrix} \begin{bmatrix} \tilde{x}_1(t) \\ \tilde{x}_2(t) \end{bmatrix} + \begin{bmatrix} \tilde{B}_1 \\ \tilde{B}_2 \end{bmatrix} u(t), \\ \tilde{y}(t) &= \begin{bmatrix} \tilde{C}_1 & \tilde{C}_2 \end{bmatrix} \begin{bmatrix} \tilde{x}_1(t) \\ \tilde{x}_2(t) \end{bmatrix}, \end{aligned} \tag{4.7}$$

The reduced-order system (4.2) can then be obtained by simple truncation [29,31] from the balanced realisation (4.7) in partitioned form, with:

$$\hat{A} = \tilde{A}_{11} \in \mathbb{R}^{rxr}, \qquad \hat{B} = \tilde{B}_1 \in \mathbb{R}^{rxm}, \qquad \hat{C} = \tilde{C}_1 \in \mathbb{R}^{qxr}, \tag{4.8}$$

A key fundamental result of BT is that the global error between $H(\cdot)$ and $\hat{H}(\cdot)$, i.e. between the transfer functions of the original and reduced system, fulfils the following condition:

$$\|H - \hat{H}\|_\infty \leq 2(\sigma_{r+1} + \sigma_{r+2} + ... + \sigma_n) \tag{4.9}$$

where $\sigma_{r+1}, ..., \sigma_n$ are the neglected HSVs. This means that the dimension r of the reduced system can be selected to achieve the desired trade-off between system size and model accuracy.

4.3.2 Model Order Reduction of Systems without Inputs

As shown later on, the dynamical system considered in this work for grid reliability assessment does not have any input. This means that some minimal adjustments are required in the MOR technique presented in the previous subsection. In particular, the controllability Gramian P is not well defined and the matrix T for the change of coordinates in the original system is calculated to only diagonalize the observability Gramian Q:

$$\tilde{Q} = T^{-1}QT = \sum = diag(\sigma_1, \sigma_2, ..., \sigma_n), \tag{4.10}$$

The reduced-order system is then determined according to (4.5)-(4.8). In this specific case, the error bound of the model order reduction can be derived on the quadratic norm of the output. Recalling that the natural response of a linear system with initial state x_0 is equal to $y = Ce^{At}x_0$, in the changed coordinates we have:

$$\int_0^\infty \|\tilde{y}(t)\|_2^2 dt = \int_0^\infty \tilde{x}_0^T e^{\tilde{A}^T t} \tilde{C}^T \tilde{C} e^{\tilde{A}t} \tilde{x}_0 dt = \tilde{x}_0^T \tilde{Q} \tilde{x}_0 = \tilde{x}_0^T \cdot diag(\sigma_1, \sigma_2, ..., \sigma_n) \cdot \tilde{x}_0. \tag{4.11}$$

It follows that, if the reduced-order model is obtained according to the truncation presented in (4.8), we have the following error bound on the outputs $\tilde{y}$ and $\hat{y}$ of the original and reduced-order system:

$$\int_0^\infty \|\tilde{y}(t)\|_2^2 - \|\hat{y}(t)\|_2^2 dt \leq \sum_{i=r+1}^{n} \sigma_i \qquad \forall \tilde{x}_0 : \|\tilde{x}_0\|_1 = 1. \tag{4.12}$$

4.4 MOR for Reliability Assessment

The main aim of the proposed methodology is to develop a tool capable of creating simplified grid models that preserve the key features of the original network and allow for accurate and faster reliability analyses. This section presents the methodology for developing the system

model, performing the model order reduction, and finally carrying out time-sequential MCS analyses to quantify the reliability metrics of interest.

4.4.1 Modelling System Descriptor Matrices

This section describes how the MOR techniques discussed in Section 4.3 can be applied to the specific case of reliability assessment of distribution networks. As a first step, the working state of a generic grid is described as a continuous-time Markov chain (CTMC), under the common assumption of Poisson distributions for the fail/repair times of the system PCs. Each discrete state of the CTMC corresponds to a specific reliability state of the system components and the transitions between these states are associated with the failure or the repairing of a certain component. The discrete states and transitions of the CTMC, for the simple case of a system with two repairable components [3,32], are shown in Figure 4.2. In this example, each PC has two modes (UP/DOWN), and the failure and repair rates are denoted by λ and μ, respectively. Since we are considering 2 components, the resulting Markov chain will have 2^2 discrete states. The passage from state 1 (with both components UP) to state 2 (with component 1 DOWN and component 2 UP) will occur with rate λ_1, i.e. the failure rate of component 1. Conversely, the passage from state 2 to 1 will occur with rate μ_1, i.e. the repair rate of component 1.

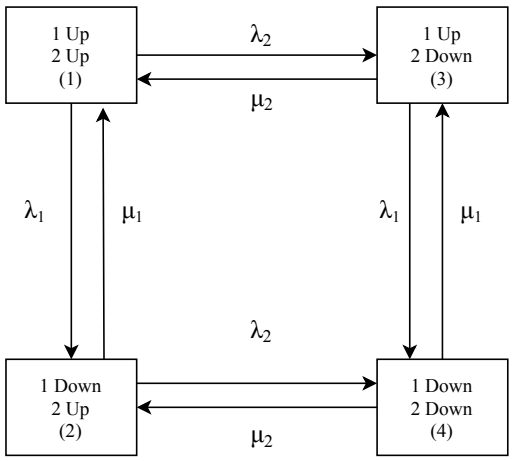

Figure 4.2: Markov chain representing a system with two repairable components [3].

On this basis, the proposed modelling approach uses a probabilistic description to characterise the state vector in the system (4.1): the dynamic state $x(t)$ will represent the probability of a specific reliability state of the system PCs (i.e. a specific discrete state of the CTMC) to occur at time t. The evolution of $x(t)$ follows the equations in (4.1) and the associated state matrix A

is given by (4.13).

$$A = \begin{bmatrix} -(\lambda_1+\lambda_2) & \mu_1 & \mu_2 & 0 \\ \lambda_1 & -(\lambda_2+\mu_1) & 0 & \mu_2 \\ \lambda_2 & 0 & -(\lambda_1+\mu_2) & \mu_1 \\ 0 & \lambda_2 & \lambda_1 & -(\mu_1+\mu_2) \end{bmatrix} \tag{4.13}$$

In the present case, the nondiagonal element a_{ij} of A equals to the transition rate from state i to j, whereas the diagonal elements a_{ii} are chosen to obtain zero-sum columns since the sums of the rates of all transitions leaving and entering the reliability state must be 0:

$$a_{ii} = -\sum_{j \neq i} a_{ij} \tag{4.14}$$

Note that the state matrix A corresponds to the transpose of the stochastic transitional probability matrix in [3] and, given its specific properties (zero-sum columns and non-negative off-diagonal elements), it is also a Metzler matrix [33].

We wish to emphasise that the proposed modelling approach can also accommodate common mode failures of system components, considering transitions to reliability states that have more than one additional component in DOWN mode. For example, in Figure 4.2, a common mode failure of the two system components would be modelled by a transition from state (1) to state (4), specifying its non-negative transition rate as the value of a_{41} in (4.13). Alternatively, cascaded failures can be modelled as events where the failure of a certain component leads to an increased failure rate of another component. For example, consider the possibility that a failure of PC1 increases the failure rate of PC2. This would imply that the transition rate from state (2) to state (4) in Figure 4.2 (i.e. the element a_{42} in (4.13)) would be higher than the transition rate λ_2 from state (1) to state (3), i.e. the element a_{31} in (4.13).

In the present case, we are not considering the terms $Bu(t)$ in (4.1), since the chosen reliability modelling approach does not entail any external input. As previously stated, the network reliability performance is based on uncontrollable fault occurrences and corresponding repairs to faulty PCs that allow for supply restoration and are performed with fixed rates.

The output $y(t)$ of system (4.1) has dimension 1 and corresponds to the expected value of the Power Not Supplied (PNS) at time t. This implies that each term c_j in the matrix C corresponds to the PNS associated to the k$^{\text{th}}$ reliability state of the system. For example, considering again that x_1 denotes the probability that all the system PCs are in the UP mode, we will have $c_1 = 0$.

With this approach, the Energy Not Supplied (ENS) in the system can be calculated by taking the integral of $y(t)$.

4.4.2 MOR Implementation

This subsection details the actual implementation of the proposed approach for network reliability assessment. The analysis will consider the ENS index as the reliability metric of interest. This is mostly used at transmission level and is usually less reported by distribution network operators (DNOs) but it is gradually being considered by regulators for an optimal system performance due to its value in the quantification of customer satisfaction. This can be seen in a few European countries where ENS is currently assessed at distribution level such as Norway and Romania [6]. ENS is also widely used in the literature for network reliability assessment e.g. [22,32]. As the power grid becomes more complex, this index will have to inevitably be considered as a benchmark for the performance assessment of DNOs.

Calculation of the Network Reliability Model

The first step in the implementation of the MOR procedure is the definition of x and y and the calculation of the matrices A and C in the dynamical system (4.1) describing the reliability of the network. From Section 4.4.1, $x(t)$ denotes the probability of each possible combination of reliability states of the system components at time t. The matrix A describes the evolution of x over time and is obtained from (4.13), where λ and μ denote respectively the failure and repair rates of the PCs and can be obtained from available published reliability data. The output $y(t)$ is assumed to be equal to the PNS of the system at time t, so that its integral over time returns the chosen reliability index, ENS. Since a single output is considered, the matrix C has dimensions $1 \times n$ and its k^{th} component corresponds to the power not supplied in the k^{th} reliability state of the system components considered in the state x. For example, $k = 1$ denotes the scenario with all system components in the UP state and therefore the associated value c_1 will be equal to 0. Conversely, since $k = n$ corresponds to the case with all components in the DOWN mode, the associated value c_n will be equal to the total power not supplied in this scenario. The calculation of C in networks with complex topology requires the use of power simulation software PSS®E (automated using Python), as power flow assessments must be used to determine the amount of power not supplied at each load point (LP), for each reliability state. Algorithm 1 summarises the steps used to construct matrix C in all the analyses presented.

Algorithm 1: Compute output matrix C

Input: Determine N power components of the test network

1: Assign 2 reliability states to each component – Up and Down
2: Create a list of all possible permutations of component states, indexed by $k = 1, 2, \ldots, n$ where $n = 2^N$
3: Initialise: $k = 1$
4: **while** $k \leq n$
5: Run power flow algorithm for system state k
6: Determine the total power not supplied c_k in system state k,
7: $k = k + 1$
8: **end while**
9: Compute C

Output: Matrix $C = \{c_1, c_2, \ldots, c_n\}$

Calculation of the Reduced-order Model

The MOR methodology is summarised as follows: develop a complete state-space representation (4.1) of a network reliability model; use system Gramians to determine which states contain the most useful 'information content' with respect to the selected reliability index (ENS); neglect the states with lower impact; finally, calculate a state-space representation of the reduced-order model that can adequately approximate the original system. The first step to perform the MOR on the original network model is to list the N repairable PCs that comprise the network and calculate the resulting failure and repair rates (λ and μ, respectively) from available reliability statistics. For simulation purposes, system (4.1) and all the associated systems are converted from continuous to discrete time, adequately rescaling the transition rates λ and μ according to the chosen simulation time-step, for example, $\Delta t = 1$ hour. Furthermore, matrix C is obtained using Algorithm 1.

It is important to appreciate that A in (4.13) has a rank of $n-1$, where n is the number of system states [3]. This follows from the chosen probabilistic description of the system, as the sum of probabilities for all the possible reliability states must always be equal to 1 i.e. the sum of columns in matrix A (i.e. the derivative of the total probability) must be equal to zero. This means that each column of A has zero sum (i.e. the sum over all the elements of each column is zero) and therefore one row can be written as the total sum (with changed sign) of the others. It follows that, a single state x_n can be neglected in the analysis and simply calculated ex-post as the sum of 1 minus the probability of the other states, modifying the A and C matrices accordingly. For this study, the removed system state is the one representing the probability of all PCs being in the UP state. The next step is to determine the transformation matrix T using (4.10) and then truncating (4.7) according to (4.8). This allows for a model reduction of the reduced form of the matrix A (which is full rank) from order $n-1$ to $r-1$. Finally,

the initially removed state is added back to the reduced model exploiting the aforementioned property of the sum of the derivatives $\dot{x}(t)$ and obtaining the new linear system as represented in (4.2). Notably, studies in [29] show that the calculation of the system observability Gramian Q in (4.4) using the new full rank state matrix A ensures that system stability is preserved when MOR is done using truncation.

4.4.3 Method Limitations

The proposed methodology represents a significant step towards a simplified and accurate analysis of complex networks. As demonstrated in the case studies of Section 4.5, the presented MOR approach allows for a faster reliability assessment with a minimum impact on accuracy. Nevertheless, the proposed approach still exhibits some limitations that will be tackled in future work. In particular, with the current formulation, the number of PCs of the original system that can be modelled is limited by hardware constraints. The two main computational-memory bottlenecks arise from building the state transition matrix A (4.13) and obtaining the system Gramians (4.4) by solving computationally expensive Lyapunov equations [29,31]. These issues were tackled by developing ad-hoc programming solutions and adopting the matrix equation sparse solver (MESS) toolbox [34] for a more efficient resolution of high-order Lyapunov equations. In future work, different techniques will be explored to obtain a faster computation of the relevant Gramian matrices, allowing for the simulation of larger systems. These techniques will exploit the low-rank property for solutions of large-scale, sparse Lyapunov equations [29] e.g. methods based on the Arnoldi process [35,36] and Krylov subspace methods [36,37]. A distributed system reduction will also be investigated, deriving the simplified grid model as a collection of interconnected smaller systems, each obtained with the MOR approach presented in this work.

Furthermore, peak demand profiles are utilised at network LPs in addition to the use of constant PC failure and repair rates used to calculate matrix A in (4.13). However, further work will integrate time-varying demand profiles as well as time-varying failure rates that account for the PC's lifecycle [38,39]. These model extensions will be implemented by utilising alternative MOR techniques presented in the literature for time-varying dynamical systems, such as the ones in [40,41]. These improvements will be accompanied by the incorporation of different load sectors (residential, industrial and commercial) into the network models to allow for a more accurate quantification of the impact of each system state based on the nature of the load supplied and the time during which network interruptions (leading to ENS) occur.

Also, for MCS analyses, the current methodology only returns models of order $r = 2$. Higher values of r result in system matrices A in (4.13) that are not in Metzler form. Therefore, the

associated system lacks the Markov property and cannot be simulated with MCS methods. Future research will test new methods for the approximation of Metzler matrices. Work in [42,43] investigated this aspect but the proposed methods were not directly applicable to reliability studies because they focused on the stability of the resultant Metzler matrix rather than its Markovian properties.

Finally, the frequency and duration of interruptions are not explicitly included in the chosen state-space representation (4.1) of the grid reliability. This means that reliability metrics - SAIFI and SAIDI can be calculated ex-post with MCSs but cannot be used as relevant metrics over which the approximation error of the proposed MOR procedure is minimized. However, SAIFI and SAIDI represent two fundamental indices in the evaluation of network reliability and therefore, in order to explicitly consider them in the MOR procedure, the current model will be expanded in future works, for example including additional states in (4.13) that keep track of the failure times of the different power components. Nonetheless, the analysis is still capable of demonstrating the effectiveness of the proposed MOR methodology, as the key aspect of its validation lies in comparing system outputs of the original vs. reduced-order system [29].

4.5 Results and Discussions

Relevant case studies are considered to evaluate the performance of the proposed MOR technique and its capability to generate accurate reduced models of system reliability. This work assumes an ideal operation of conventional generators in its network reliability assessment and focuses on the failure/repair behaviour of PCs at a transmission and distribution level. These include underground cables, overhead lines, transformers, protection devices, capacitor banks and busbars. Also, all analyses were carried out by using the high-performance computing (HPC) facilities at the University of Bath, UK. The particular hardware used has the following specifications: dual socket Intel Ivybridge nodes with E5-2650v2 processors, 2.6GHz with 8 cores, and 512GB of memory [44].

4.5.1 Illustration of MOR Functionality

An example of the proposed modelling approach and the associated MOR methodology is presented for the simple network in Figure 4.3. This network model is converted to state-space representation (4.1) by first defining the state vector x and output y. State x denotes the probability of each possible combination of reliability states of the system PCs (i.e. buses and lines) at time t. The associated state matrix A in (4.13) is calculated by using failure and repair rates of all system PCs and has a dimension of $n \times n$ where $n = 2^{|PCs|}$ is the order of the system.

The output y denotes the system output in terms of the total PNS to the two load points. It is a linear combination of entries in matrix C that correspond to the PNS associated to each system reliability state. For example, x_1 denotes the probability that all PCs are in the UP state and all the required power is being supplied, implying $c_1 = 0$. Conversely, since x_2 represents the probability that all PCs are in the UP state except bus B2, then the associated entry c_2 in matrix C will be equal to the power demand that is not being supplied in this case at bus B2, i.e. $c_2 = 10$.

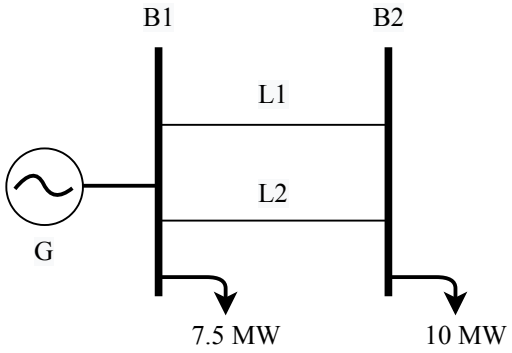

Figure 4.3: Test system with 4 components (system order $n = 2^4 = 16$).

Having asserted the meaning of $x(\cdot)$ and $y(\cdot)$ in the context of network reliability, as well as having calculated all system descriptor matrices, the system in Figure 4.3 is reduced using the MOR procedure presented. Recalling that this system has no input, the transformation matrix T for the change of coordinates in the original system is obtained using (4.10) instead of (4.6). The reduced-order system (4.2) is then determined by truncating system (4.5) according to (4.7)-(4.8). For a certain order r of the reduced model, the corresponding error bound on the output (i.e. on the chosen reliability index) is given by (4.12). As expected, larger values of r allow to include more information content and therefore achieve higher accuracy.

In Figure 4.4, we plot the output of the dynamical system, i.e. the power not supplied which, integrated over time, will equal the system energy not supplied. We recall that this is expressed as $Cx(t)$ in (4.1), where the single component $x_i(t)$ of the vector $x(t)$ indicates the probability of being in state i at time t. Note that the initial conditions of the system, denoted by $x(0) = x_0$, do not affect the steady-state behaviour of the system but only determine the starting point $y(0) = Cx(0)$ of the output response. For example, if it is known with probability 1 that all components are UP (working), then the initial PNS will be 0 MW and it will then increase to a steady state value $y_{ss} = Cx_{ss}$ over time. Zoomed-in values in Figure 4.4 show that the steady state value obtained for PNS (y_{ss}) is non-zero because the network contains uncontrollable PC failures that result in a small amount of unsupplied power in steady state conditions. Figure

4.4 also compares the output (i.e. the PNS index) of the original system with the output of a selection of reduced-order models with $r = 2$ and 4. As expected, the evolution of the PNS of the reduced-order models follows more closely the one of the original system when r is larger and more states are kept in the model. Indeed, the system behaviour for the reduced-order system with only 4 states (MOR-4 states) indicates no appreciable difference in the output of the reduced-order models and that of the original system.

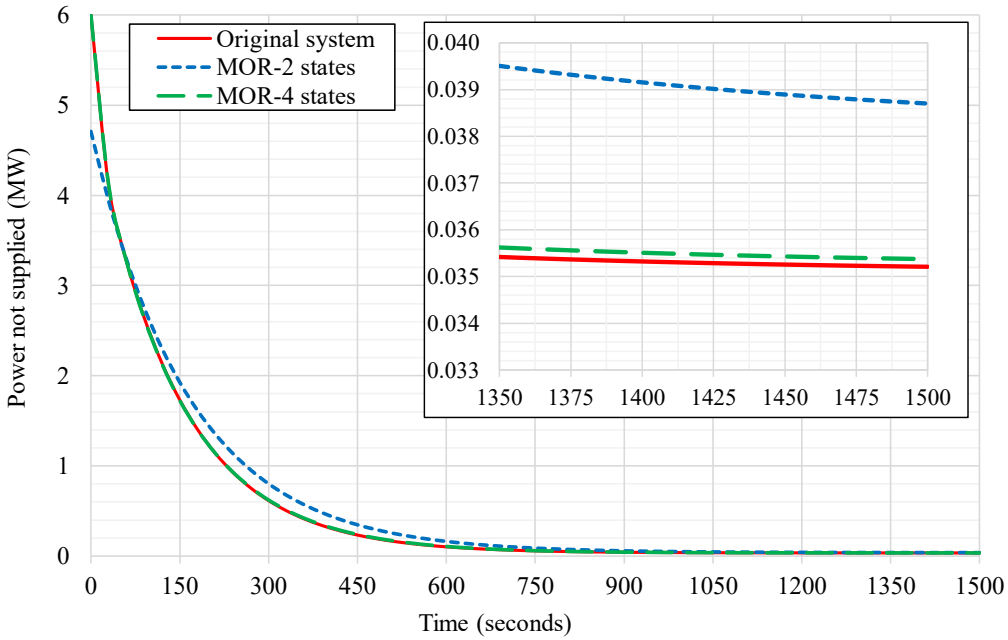

Figure 4.4: Evolution over time of PNS for the original system and reduced models with $r = 2$ and 4.

The analysis on this simple example is extended further by considering each possible order r for the MOR and quantifying the resulting reliability error as follows:

$$Error_r = \frac{\|\hat{y}_r - y\|_2}{\|y\|_2} \times 100 \tag{4.15}$$

where r is the order of the reduced system and $\hat{y}_r$ is the resulting output, $\|\cdot\|_2$ is the L_2 norm, and the error value is in per cent. In this case, y and $\hat{y}_r$ are vectors representing the outputs of the original and reduced-order system, evaluated at discretised time instants. Figure 4.5 compares the accuracy of the reduced model (i.e. percentage error in the evolution of the system's PNS) in Figure 4.5(a) with the system HSVs σ_i in Figure 4.5(b). Recall that the HSVs associated to the system states that are not included in the new reduced model quantify the upper bound on the approximation error of the analysis, according to (4.12). Using Figure

4.5(a) for comparison, there is a clear correlation between the system error attained with a reduced system of a certain order r and the HSVs associated to the number of system states considered in the reduced model.

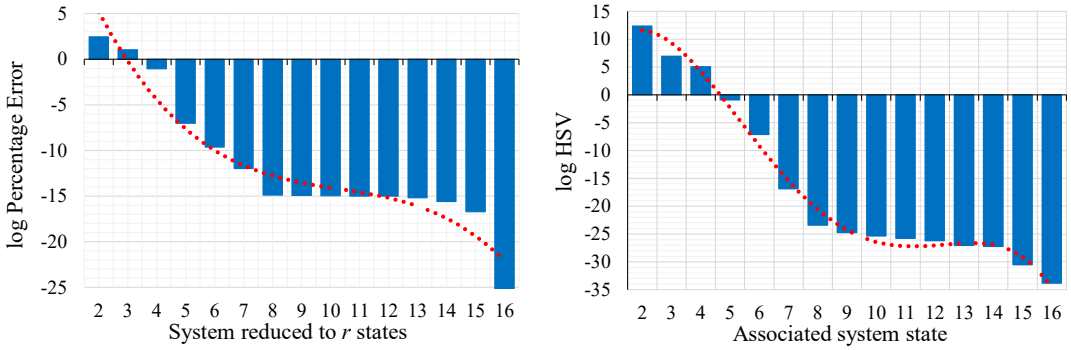

(a) Percentage Error (b) HSVs

Figure 4.5: Comparison between the accuracy of the reduced model and the HSVs of the original system.

4.5.2 MOR Reliability Performance Evaluation

To assess the performance of the proposed MOR technique, time-sequential MCSs are carried out on the original and reduced models to compare the required simulation time and quantify the accuracy of the reliability assessment. The MCS evaluates the annual ENS of the test systems by using a time step of 1 hour [45]. Moreover, to obtain acceptable index accuracy in all considered MCSs, and accurately compare the computational burden of both the original and reduced models, the total simulation period (or number of MCS samples) is based on achieving set thresholds for the coefficient of variation (CoV) [45,46]. The threshold value for the CoV is set to 0.2%, which is well below the typical tolerance level for ENS as given for example in [47] for different reliability indices.

Test System with 4 PCs

The test system in Figure 4.3 is composed of 4 PCs, each with only 2 possible reliability states (UP/DOWN), and its dimension is equal to 2^4. Following from the discussion in Section 4.4.2, this original system is reduced to 2 states using MOR and the ENS is evaluated in the two cases. Results are presented in Table 4.1 where the performance evaluation of MOR is compared with two other methods. As described in Section 4.2, using traditional network reduction (TNR) techniques, the original system is simplified to a single equivalent element by systematically combining appropriate series and parallel branches of the reliability network. Then,

the reliability of the remaining equivalent element equals the reliability of the original network [3] and will exhibit the same unavailability U (i.e. probability of being in DOWN mode). The relevant equations for reducing a network with 2 repairable PCs in series and parallel configurations are presented in [3]. The other existing method termed AEM [48] calculates the equivalent PC failure rate as the sum of all PC failure rates, while the equivalent PC repair rate is the reciprocal of the average of all PC repair rates. It is important to note that in order to fairly compare the performance of the proposed MOR technique with the two other techniques (TNR and AEM), all 3 reduction methods are used to reduce the original system of 16 states to 2 states (or one equivalent component). The ENS is then calculated in each case to determine the associated error. Moreover, given the fact that the original system is of a relatively small size, computational time reduction results are not presented as the reduction to 2 states in all cases does not offer any significant time saving from the original case. Instead, Table 4.1 focuses on the error obtained when assessing ENS for reduced order networks. Further analyses presented in the next subsections demonstrate the computational time saving achieved using the reduction methodology when applied to larger networks.

Table 4.1: Reliability performance for the 4PC test system.

Network	**System States**	**Average ENS (MWh/year)**	**ENS Error (%)**
Original	16	307.88	_
MOR	2	335.09	8.84 %
TNR	2	391.76	27.25%
AEM	2	504.32	63.81%

Table 4.1 illustrates the advantages of the MOR technique in terms of accuracy of network reliability assessment. The ENS value of the reduced network calculated with the new proposed approach exhibits the lowest error with respect to the original system (8.84%) when compared to both TNR and AEM techniques. It is important to note that this demonstrates the capability of the proposed MOR method in accounting for dispersed loads during network reduction unlike the case in both TNR and AEM techniques. This results in higher accuracy when using MOR for networks often characterised by highly dispersed loads as shown in the next subsection.

Roy Billinton Test System

The MOR approach for reliability analysis is applied to a relevant test case - the Roy Billinton Test System (RBTS) in Figure 4.6. This is a composite power system with 11 generator units, 2 generation buses, 4 load buses and 9 transmission lines. The transmission system voltage

level is 230 kV and the bus voltage limits are 1.05 p.u. and 0.97 p.u. The total generation capacity is 240 MW while the peak load is 185 MW. Bus 1 is assumed to be the slack bus under normal circumstances and the power factor at each bus is unity. The basic bus and transmission line reliability data i.e. failure rates and repair times are obtained from [49]. Based on the aforementioned assumptions, the original RBTS 'offers' a total of 15 PCs (6 buses + 9 lines) for this analysis each with only 2 possible reliability states, and its dimension is equal to 215. This original system is reduced to 2 states using MOR and the ENS is evaluated in the two cases. The complexity of this network configuration (meshed topology) means that TNR cannot be used to effect model reduction. Therefore, MOR is only compared with the AEM approach in the results presented in Table 4.2.

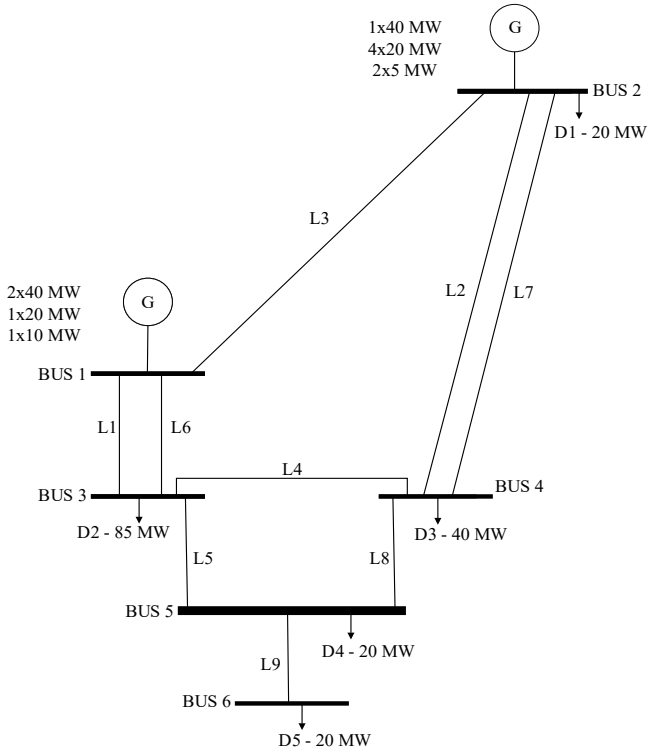

Figure 4.6: Single line diagram of the original RBTS with 15PCs [49].

Table 4.2 results illustrate that the reduced-order model obtained with the proposed MOR methodology estimates the ENS index of the RBTS with good accuracy while also providing a significant saving in the total computational time required to complete the reliability assessment. This shows that by constructing a reduced reliability model that only retains the most representative states with the highest 'information content', it is possible to trade much faster resolution times with a minimum impact on the accuracy of the reliability analysis. Table 4.2 also proves that the performance improvement of the proposed MOR method with respect

to the AEM approach is even more significant in meshed networks, which are often endowed with redundant components to facilitate provision of backup supply in case a PC with a parallel operation fails. In the AEM approach, these 'additional' PCs only serve to increase the total number of failures and thus result in a 6082.15% error in ENS calculation compared to only 6.28% in the MOR case. However, it is evident in Table 4.2 that there exists a slightly better time saving in computational time with AEM (96%) as compared to MOR (92.12%). This is because the time required to perform the order reduction (OR) of the original system to 2 states using MOR is significantly higher than with the AEM approach. Additionally, Table 4.2 also reveals that the relatively low CoV threshold (0.2%) accounts for the relatively large times required before MCS converges for each simulated network model.

Table 4.2: Reliability performance for the RBTS with 15PCs.

Network	**Average ENS (MWh/year)**	**ENS Error (%)**	**Computational Time (s)**			**Total Time Saving (%)**
			OR	**MCS**	**OR+MCS**	
Original	651.30	_	_	137089.0	137089.0	_
MOR	692.20	6.28%	5359.6	5443.4	10803.0	92.12%
AEM	40264.56	6082.15%	0.0	5484.2	5484.2	96.00%

Furthermore, to demonstrate the varying accuracy of the proposed MOR technique when applied to similar models of different size, a sensitivity analysis is performed by varying the size of the original system rather than the order of the reduced model. The original RBTS is simplified by applying standard techniques of reliability block diagrams [3]. This approach is used to obtain three different representations of the RBTS with 15, 12 and 9 PCs, respectively. As an example of the transformations that have been considered, lines 1 and 6 of the network, which connect bus 1 to bus 3 in Figure 4.6, are replaced by a unique equivalent line, whose fail/repair parameters have been obtained using the relevant equations in [3]. Each of the original RBTS models is reduced to $r = 2$ states using the proposed MOR technique, followed by time-sequential MCS analyses as described previously. The error in the estimation of the ENS and the computational time saving in the three representations of the RBTS are reported in Figure 4.7 as a function of the original system size. As expected, Figure 4.7(a) shows that a higher accuracy is achieved when the starting original system is less complex and has a lower number of PCs. Conversely, Figure 4.7(b) shows that there is a more consistent reduction of the computational time of the MCS when the 15PCs network is reduced to 2 states, as compared to an identical operation performed on the 9PC network.

Notably, the time saving (92.12%) achieved when the 15PCs network is reduced is only marginally higher than the saving (88.11%) when the 12PCs network is reduced. This is because while the reduced order systems in both cases have similar times for MCS convergence, the time required to perform MOR in the 15PC case is 5359.6s compared to only 35.8s in the

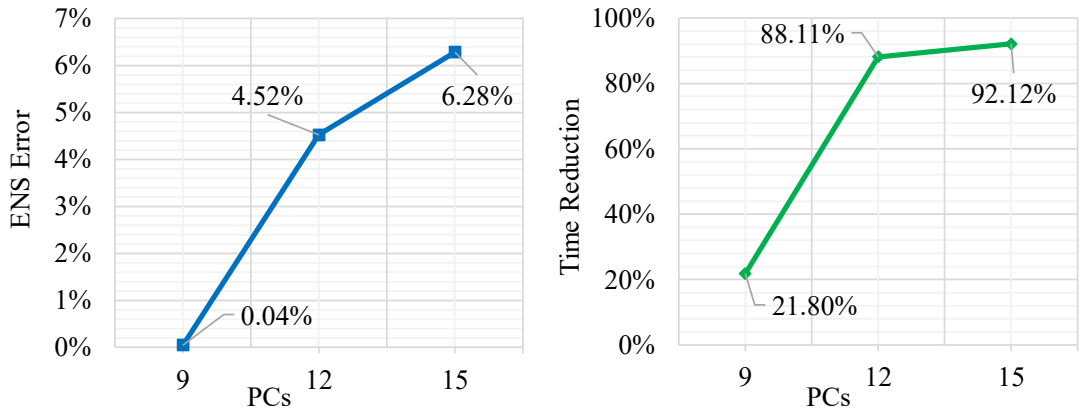

(a) ENS error

(b) MCS computational time reduction

Figure 4.7: Trends of MOR accuracy and MCS computational time with respect to network size.

12PC case (and 0.5s in the 9PC case). Nonetheless, the use of the proposed MOR technique results in a significant time saving in all cases and a validation of the expected trends for the sensitivity analysis.

Generic Medium Voltage Substation

To further demonstrate the performance of the proposed MOR methodology, it is tested on a generic medium voltage (MV) substation presented in Figure 4.8. With respect to the RBTS, which is a meshed network, this network exhibits a radial configuration. Moreover, it only has one aggregate load (and LP) as compared to 5 different LPs in the RBTS. This network, adapted from work in [50,51], consists of two 15 MVA 33/11 kV transformers supplying a mainly residential load of 9120 customers. The total average load is measured at 20.7 MW. Downstream the main 11 kV bus, only one equivalent feeder is used to represent the rest of the network, as well as the total aggregate load. The sensitivity analysis for this test case is also performed using the aggregation methods summarised in [3], resulting in 4 'versions' of this network (10, 9, 7 and 4 PCs respectively). Table 4.3 shows the varying number of types of components for each network. The reliability data used for these PCs are obtained from [51].

Figure 4.9 compares the results obtained when each of the networks (4PC-10PC) is reduced to $r = 2$ states. As shown in Figure 4.9(a), the ENS error increases when larger networks (i.e. more PCs) are considered. This represents an anticipated result since a reduction to only 2 states will be unable to capture the most relevant dynamics if the original system is too large and complex. Conversely, Figure 4.9(b) proves that the saving in the total computational time

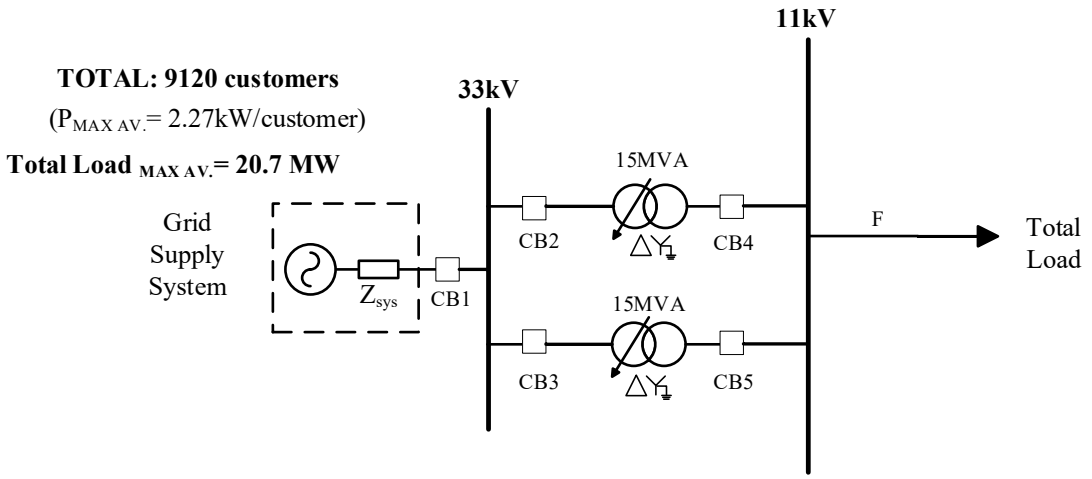

Figure 4.8: Generic MV substation model – 10PCs.

Table 4.3: Generic MV substation configurations.

Type of Component	**Original Network** No. of PCs			
	4	***7***	***9***	***10***
Buses	2	2	2	2
Transformers	2	2	2	2
Circuit breakers	0	3	5	5
Feeders	0	0	0	1

required for analyses is much larger when MOR is applied to a larger network (10PCs) as compared to a smaller one (4PCs). Notably, in all cases the computational time is mostly taken up by MCS, as the times required to perform MOR are only 0.05, 0.15, 0.39 and 1.44 seconds for the 4, 7, 9 and 10 PC systems respectively. This results in a negligible impact of MOR-time on the total computational time required to perform a reliability assessment for this network configuration.

Medium Voltage Distribution Network

The substation model presented in Figure 4.8 is expanded into a small-scale distribution network as shown in Figure 4.10 to further demonstrate the applicability of the proposed method. This network is adapted from a typical underground MV network for urban areas as presented in [51]. Accordingly, it presents a meshed configuration where normal network operation is supported with another supply point e.g., another primary substation or a “reflection centre”.

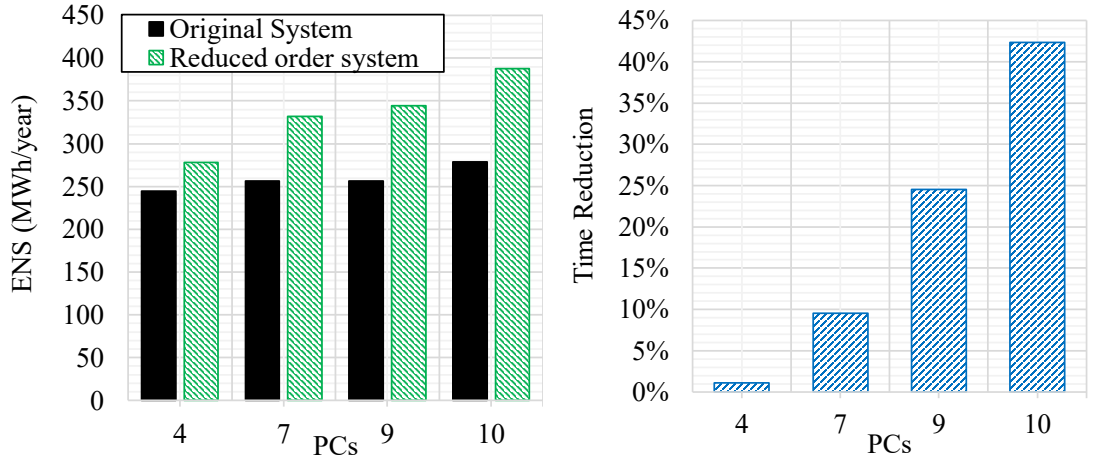

(a) ENS (b) Total Computational time

Figure 4.9: Trends of reliability accuracy and computational time of the MOR methodology with respect to the original size, for the generic MV substation presented in Figure 4.8.

The reflection centre guarantees the supply of all feeders connected from both ends of the network. It is important to note that Figure 4.10 is a scaled down version of the actual representation of an urban MV network due to the aforementioned hardware constraints in the implementation of MOR for large systems. The full network is typically designed for a maximum of six 11 kV feeders and ten 11/0.4 kV distribution transformers from each 11 kV feeder. This is in addition to the use of necessary protection devices such as fuses and circuit breakers. For this analysis, the distribution network in Figure 4.10 presents a total of 14 components (2 buses, 6 transformers, 4 underground cables and 2 switches). Furthermore, the network is modelled to have 4 LPs each supplying a total of 190 customers through a 500 kVA 11/0.4 kV distribution transformer. The basic reliability data used are obtained from [51]. For the results presented in Table 4.4, the original distribution network with 2^{14} states is reduced to 2 states using the proposed MOR approach. As seen with the RBTS network, it is not possible to reduce this distribution network using the TNR approach because of the network topology.

Table 4.4: Reliability performance for the distribution network.

Network	**Average ENS (kWh/year)**	**ENS Error (%)**	**Computational Time (s)**			**Total Time Saving (%)**
			OR	**MCS**	**OR+MCS**	
Original	263.68	_	_	76239.0	76239.0	_
MOR	274.62	4.15%	1611.6	4922.9	6534.5	91.43%

Table 4.4 demonstrates that the reduced order model obtained using the proposed MOR approach results in a good accuracy for the estimated ENS-index (4.15%) while providing a significant saving in the required computational time.

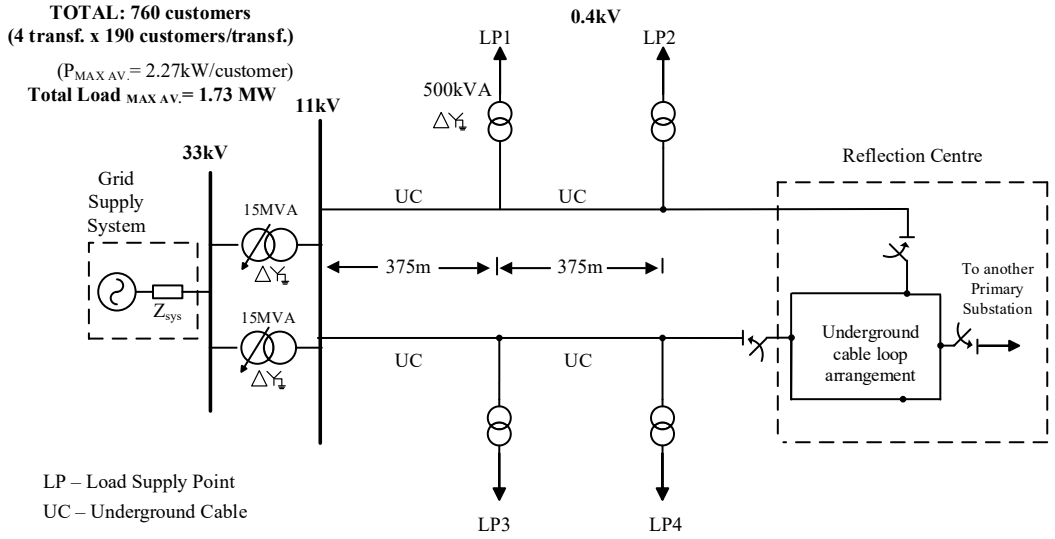

Figure 4.10: Small-scale distribution network model - 14PCs.

4.5.3 Integration of PV and Storage Technologies

The capability of the proposed MOR methodology to accommodate PV and ES in the simplified reliability models is now demonstrated. For this purpose, four distinct scenarios (presented in Table 4.5) are considered for the RBTS 12PC network. The SC1 (base case) scenario considers no PV or ES, while SC2A and SC2B scenarios represent the addition of PV to the network with different penetration levels. In this case, the PV generation is modelled as a constantly available power source whose power output is equal to the average of a typical PV generation profile. This is considered a good approximation of a realistic scenario if one assumes that the faults of PCs are uniformly distributed over time. Further work will ensure that the intermittent nature of the supply from PV, as well as the daily and seasonal cycles, can be added into the analysis.

Finally, SC3 includes ES resources, which are assumed to be locally available only to LPs D4 and D5 (combined 40 MW load). Given that these loads are the furthest from the main supply, it is expected that the use of ES will greatly enhance not only the ENS of the customers at LPs D4 and D5 but also the average system ENS. This ES configuration is designed to supply energy in the event of a fault occurrence that causes outage to either D4 or D5, and to completely alleviate the effect of faults at these loads. Based on previous work from the authors, further analyses will integrate other parameters such as energy price signals, state of battery charge, solar irradiance, or time-varying demand to the state and capacity of the ES system [50].

Table 4.5: Reliability performance with PV and ES.

ID	Scenario	Average ENS (MWh/year)		ENS Error
		Original system (12PCs)	Reduced-order system	
SC1	Base case	651.87	681.33	4.52%
SC2A	PV 25%	488.90	511.11	4.54%
SC2B	PV 50%	325.93	340.74	4.54%
SC3	ES	319.85	335.43	4.87%

As expected, results in Table 4.5 show that as PV penetration increases, the ENS to customers is progressively reduced. Furthermore, ES implementation almost halves the system ENS with respect to the base case, where the LPs D4 and D5 present poor reliability. Overall, the reduction of the system to 2 states in each scenario using MOR resulted in an error of only about 4.5% (Table 4.5). This demonstrates the capability of the MOR methodology to reduce the computational time of reliability analyses while accurately representing the impact of PV and ES on network reliability.

4.6 Conclusions and Further Work

This paper presents a novel application of MOR techniques for reliability analysis of distribution networks. The proposed analytical methodology, based on balanced truncation, allows to determine reduced network models with lower complexity and faster simulation times while minimising the resulting error on reliability metrics. The practical implementation of the algorithm has been described in detail and relevant case studies have been presented to demonstrate the capability of the proposed approach to capture the most important reliability dynamics of the original networks and provide simplified models that describe with good approximation the reliability of the original system. As expected, these simplified models guarantee an appreciable saving in the computational time required to perform reliability analyses. The case studies also demonstrate the capability of the proposed approach to assess the impact of PV and ES on the considered reliability metrics. The methodology developed in this paper is the first step towards a utilisation of MOR techniques for reliability assessment of power networks. The improvements suggested in the further work will allow for use of the proposed MOR technique in networks characterised by higher complexity and the substantial penetration of new technologies e.g. demand response, storage, electric vehicles.

Further work will enhance the proposed methodology by including dynamic PC failure rates and time-varying demand profiles. This will be in addition to the use of a minimum load

curtailment model in the computation of the output matrix C to ensure that network control actions for minimising the impact of outages to customers are included in the analysis. This inclusion will also be useful to further demonstrate the capability of PV and storage technologies to relieve network constraints and provide ancillary services. Moreover, the effect of cloud transients on PV generation and the evolution of the state of charge of the ES devices will be incorporated in future analyses for a more realistic modelling and analysis of the impact of these technologies on the network reliability. The dependence on computational requirements will also be addressed to enable the modelling of larger and more complex systems. This will include investigating new methods for the approximation of Metzler matrices that preserve their Markovian properties to allow for larger orders (r) of the reduced system. An alternative will also be to compare the proposed approach with other MOR approaches e.g. moment-matching. Finally, the methodology will be expanded to accommodate more reliability indices, such as those measuring frequency and duration of interruptions, as well as providing probability density functions to further describe the variation of these indices for given systems as these are key advantages in using MCS analysis for reliability analysis that the reduced system should be able to accurately illustrate. This will represent an important further step towards the application of this methodology in a practical context.

Declaration of Competing Interest

The authors declare no conflicts of interest.

Acknowledgements

This research made use of the Balena High Performance Computing (HPC) Service at the University of Bath.

References

[1] S. M. Ashraf, B. Rathore, S. Chakrabarti, Performance analysis of static network reduction methods commonly used in power systems, in: 2014 Eighteenth National Power Systems Conference (NPSC), IEEE, Guwahati, India, 2014, pp. 1_6. doi:10.1109/NPSC.2014.7103837.
URL http://ieeexplore.ieee.org/lpdocs/epic03/wrapper.htm?arnumber=7103837

[2] P. Fortenbacher, T. Demiray, C. Schaffner, Transmission Network Reduction Method Using Nonlinear Optimization, in: 2018 Power Systems Computation Confer-

ence (PSCC), IEEE, Dublin, Ireland, 2018, pp. 1_7. arXiv:1711.01079, doi:10.23919/PSCC.2018.8442974.
URL https://ieeexplore.ieee.org/document/8442974/

[3] W. Li, Risk Assessment of Power Systems: Models, Methods, and Applications: Second Edition, Vol. 9781118686, John Wiley & Sons, Inc., Hoboken, NJ, USA,2014. doi:10.1002/9781118849972.
URL http://doi.wiley.com/10.1002/9781118849972

[4] R. Billinton, R. N. Allan, Reliability Evaluation of Power Systems, 2nd Edition, Springer US, Boston, MA, 1996. doi:10.1007/978-1-4899-1860- 4.
URL http://link.springer.com/10.1007/978-1-4899-1860-4

[5] I. Hernando-Gil, B. Hayes, A. Collin, S. Djokic, Distribution network equivalents for reliability analysis. Part 1: Aggregation methodology, in: 2013 4th IEEE/PES Innovative Smart Grid Technologies Europe, ISGT Europe 2013, IEEE, Lyngby, Denmark,2013, pp. 1_5. doi:10.1109/ISGTEurope.2013.6695450.
URL http://ieeexplore.ieee.org/document/6695450/

[6] CEER, 6th CEER benchmarking report on the quality of electricity and gas supply, Tech. rep. (2016). URL https://www.ceer.eu/documents/104400/-/-/d064733a-9614-e320-a068-2086ed27be7f

[7] N. D. Tleis, Power Systems Modelling and Fault Analysis, 1st Edition, Elsevier, 2008. doi:10.1016/B978-0-7506-8074-5.X5001-2.
URL https://linkinghub.elsevier.com/retrieve/pii/B9780750680745X50012

[8] Y. Jiang, N. Acharya, Y. Pan, Model reduction for fast assessment of grid impact of high penetration PV, in: 2017 19th International Conference on Intelligent System Application to Power Systems, ISAP 2017, IEEE, 2017, pp. 1_6. doi:10.1109/ISAP.2017.8071384.
URL http://ieeexplore.ieee.org/document/8071384/

[9] M. Todinov, Methods for Analysis of Complex Reliability Networks, in: M. T. Todinov (Ed.), Risk-Based Reliability Analysis and Generic Principles for Risk Reduction, Elsevier, Oxford, 2007, pp. 31_58. doi:10.1016/b978-008044728-5/50003-2.
URL https://linkinghub.elsevier.com/retrieve/pii/B9780080447285500032

[10] IEEE Guide for Electric Power Distribution Reliability Indices (2012). doi:10.1109/IEEESTD.2012.6209381.
URL https://ieeexplore.ieee.org/document/6209381

[11] A. Antoulas, Approximation of Large-Scale Dynamical Systems: An Overview, IFAC Proceedings Volumes 37 (11) (2004) 19_28. doi:10.1016/S1474-6670(17)31584-7.
URL https://linkinghub.elsevier.com/retrieve/pii/S1474667017315847

[12] C. M. Rergis, R. J. Betancourt, A. R. Messina, Order Reduction of Power Systems by Modal Truncated Balanced Realization, Electric Power Components and Systems 45 (2) (2017) 147_158. doi:10.1080/15325008.2016.1248252.
URL https://www.tandfonline.com/doi/full/10.1080/15325008.2016.1248252

[13] L. Nechak, H. F. Raynaud, C. Kulcsár, Model order reduction of random parameter dependent linear systems, Automatica 55 (2015) 95_107. doi:10.1016/j.automatica.2015.02.027.
URL https://linkinghub.elsevier.com/retrieve/pii/S0005109815000898

[14] A. K. Prajapati, R. Prasad, A New Model Reduction Method for the Linear Dynamic Systems and Its Application for the Design of Compensator, Circuits, Systems, and Signal Processing 39 (5) (2020) 2328_2348. doi:10.1007/s00034-019-01264-1. URL http://link.springer.com/10.1007/s00034-019-01264-1

[15] X. Lan, H. Zhao, Y. Wang, Z. Mi, Nonlinear power system model reduction based on empirical gramians, in: 2016 IEEE International Conference on Power System Technology, POWERCON 2016, IEEE, Wollongong, NSW, Australia, 2016, pp. 1_6. doi:10.1109/POWERCON.2016.7754074.
URL http://ieeexplore.ieee.org/document/7754074/

[16] D. Osipov, K. Sun, Adaptive nonlinear model reduction for fast power system simulation, IEEE Transactions on Power Systems 33 (6) (2018) 6746_6754. doi:10.1109/TPWRS.2018.2835766.
URL https://ieeexplore.ieee.org/document/8357933/

[17] J. Qi, J. Wang, H. Liu, A. D. Dimitrovski, Nonlinear Model Reduction in Power Systems by Balancing of Empirical Controllability and Observability Covariances, IEEE Transactions on Power Systems 32 (1) (2017) 114_126. doi:10.1109/TPWRS.2016.2557760.
URL http://ieeexplore.ieee.org/document/7464373/

[18] H. S. Zhao, N. Xue, N. Shi, Nonlinear dynamic power system model reduction analysis using balanced empirical Gramian, in: Applied Mechanics and Materials, Vol. 448-453 of Applied Mechanics and Materials, Trans Tech Publications Ltd, 2014, pp. 2368_2374. doi:10.4028/www.scientific.net/AMM.448-453.2368.
URL https://www.scientific.net/AMM.448-453.2368

[19] S. S. Mohseni, M. J. Yazdanpanah, A. Ranjbar Noei, Model Reduction of Nonlinear Systems by Trajectory Piecewise Linear Based on Output-Weighting Models: A Balanced-Truncation Methodology, Iranian Journal of Science and Technology - Transactions of Electrical Engineering 42 (2) (2018) 195_206. doi:10.1007/s40998-018-0058-4.
URL http://link.springer.com/10.1007/s40998-018-0058-4

[20] F. D. Freitas, J. Rommes, N. Martins, Gramian-based reduction method applied to large sparse power system descriptor models, IEEE Transactions on Power Systems 23 (3) (2008) 1258_1270. doi:10.1109/TPWRS.2008.926693.
URL http://ieeexplore.ieee.org/document/4558425/

[21] Y. G. I. Acle, F. D. Freitas, N. Martins, J. Rommes, Parameter Preserving Model Order Reduction of Large Sparse Small-Signal Electromechanical Stability Power System Models, IEEE Transactions on Power Systems 34 (4) (2019) 2814_2824. doi:10.1109/TPWRS.2019.2898977.
URL https://ieeexplore.ieee.org/document/8640061/

[22] W. Liu, D. Guo, Y. Xu, R. Cheng, Z.Wang, Y. Li, Reliability assessment of power systems with photovoltaic power stations based on intelligent state space reduction and pseudo-sequential monte carlo simulation, Energies 11 (6) (2018) 1431. doi:10.3390/en11061431. URL http://www.mdpi.com/1996-1073/11/6/1431

[23] T. Gafurov, M. Prodanovic, J. Usaola, PV system model reduction for reliability assessment studies, in: 2013 4th IEEE/PES Innovative Smart Grid Technologies Europe, ISGT Europe 2013, IEEE, Lyngby, Denmark, 2013, pp. 1_5. doi:10.1109/ISGTEurope.2013.6695420.
URL http://ieeexplore.ieee.org/document/6695420/

[24] L. Wang, W. Long, Dynamic model reduction of power electronic interfaced generators based on singular perturbation, Electric Power Systems Research 178 (2020) 106030. doi:10.1016/j.epsr.2019.106030.
URL https://linkinghub.elsevier.com/retrieve/pii/S0378779619303499

[25] M. Rasheduzzaman, J. A. Mueller, J. W. Kimball, Reduced- Order Small-Signal Model of Microgrid Systems, IEEE Transactions on Sustainable Energy 6 (4) (2015) 1292_1305. doi:10.1109/TSTE.2015.2433177.
URL http://ieeexplore.ieee.org/document/7120179/

[26] M. Kudryavtsev, E. Rudnyi, J. Korvink, D. Hohlfeld, T. Bechtold, Computationally efficient and stable order reduction methods for a largescale model of MEMS piezoelectric energy harvester, Microelectronics Reliability 55 (5) (2015) 747_757.

doi:10.1016/j.microrel.2015.02.003.
URL https://linkinghub.elsevier.com/retrieve/pii/S0026271415000232

[27] Z. Zhu, G. Geng, Q. Jiang, Power System Dynamic Model Reduction Based on Extended Krylov Subspace Method, IEEE Transactions on Power Systems 31 (6) (2016) 4483_4494. doi:10.1109/TPWRS.2015.2509481.
URL http://ieeexplore.ieee.org/document/7381702/

[28] G. Scarciotti, Low Computational Complexity Model Reduction of Power Systems With Preservation of Physical Characteristics, IEEE Transactions on Power Systems 32 (1) (2017) 743_752. doi:10.1109/TPWRS.2016.2556747.
URL https://ieeexplore.ieee.org/document/7466074/

[29] U. Baur, P. Benner, L. Feng, Model Order Reduction for Linear and Nonlinear Systems: A System-Theoretic Perspective, Archives of Computational Methods in Engineering 21 (4) (2014) 331_358. doi:10.1007/s11831-014-9111-2.
URL http://link.springer.com/10.1007/s11831-014-9111-2

[30] K. J. K. J. Aström, Feedback systems : an introduction for scientists and engineers, Princeton University Press, Princeton, N.J. ; Woodstock, 2008.
URL https://www.cds.caltech.edu/~murray/books/AM05/pdf/am08-complete_22Feb09.pdf

[31] W. H. a. Schilders, H. a. V. D. Vorst, J. Rommes, Model Order Reduction: Theory, Research Aspects and Applications, 1st Edition, Vol. 13 of Mathematics in Industry, Springer Berlin Heidelberg, Berlin, Heidelberg, 2008. arXiv:arXiv:1011.1669v3, doi:10.1007/978-3-540-78841-6.
URL http://link.springer.com/10.1007/978-3-540-78841-6

[32] K. Hou, H. Jia, X. Xu, Z. Liu, Y. Jiang, A Continuous Time Markov Chain Based Sequential Analytical Approach for Composite Power System Reliability Assessment, IEEE Transactions on Power Systems 31 (1) (2016) 738_748. doi:10.1109/TPWRS.2015.2392103.
URL http://ieeexplore.ieee.org/document/7024191/

[33] T. Kaczorek, Positive 1D and 2D Systems, 1st Edition, Communications and Control Engineering, Springer London, London, 2002. doi:10.1007/978-1-4471-0221-2. URL http://link.springer.com/10.1007/978-1-4471-0221-2

[34] J. Saak, M. Köhler, P. Benner, Matrix Equation Sparse Solver (2019).
URL https://www.mpi-magdeburg.mpg.de/projects/mess

[35] K. Jbilou, A. Riquet, Projection methods for large Lyapunov matrix equations, Linear Algebra and its Applications 415 (2-3) (2006) 344_ 358. doi:10.1016/j.laa.2004.11.004.
URL https://linkinghub.elsevier.com/retrieve/pii/S0024379504004707

[36] M. Hached, K. Jbilou, Numerical solutions to large-scale differential Lyapunov matrix equations, Numerical Algorithms 79 (3) (2018) 741_ 757. arXiv:1705.09362, doi:10.1007/s11075-017-0458-y.
URL http://link.springer.com/10.1007/s11075-017-0458-y

[37] V. Simoncini, A New Iterative Method for Solving Large-Scale Lyapunov Matrix Equations, SIAM Journal on Scientific Computing 29 (3) (2007) 1268_1288. doi:10.1137/06066120X. URL http://epubs.siam.org/doi/10.1137/06066120X

[38] B. Retterath, S. Venkata, A. Chowdhury, Impact of time-varying failure rates on distribution reliability, International Journal of Electrical Power & Energy Systems 27 (9-10) (2005) 682_688. doi:10.1016/j.ijepes.2005.08.011.
URL https://linkinghub.elsevier.com/retrieve/pii/S0142061505000876

[39] Peng Wang, R. Billinton, Reliability cost/worth assessment of distribution systems incorporating time-varying weather conditions and restoration resources,IEEE Transactions on Power Delivery 17 (1) (2002) 260_ 265. doi:10.1109/61.974216. URL http://ieeexplore.ieee.org/document/974216/

[40] J. Roychowdhury, Reduced-order modelling of linear time-varying systems, in: IEEE/ACM International Conference on Computer-Aided Design, Digest of Technical Papers, ACM Press, New York, New York, USA, 1998, pp. 92_95. doi:10.1145/288548.288581.
URL http://portal.acm.org/citation.cfm?doid=288548.288581

[41] N. Lang, J. Saak, T. Stykel, Balanced truncation model reduction for linear time-varying systems, Mathematical and Computer Modelling of Dynamical Systems 22 (4) (2016) 267_281. doi:10.1080/13873954.2016.1198386.
URL http://www.tandfonline.com/doi/full/10.1080/13873954.2016.1198386

[42] J. Anderson, Distance to the nearest stable Metzler matrix, in: 2017 IEEE 56th Annual Conference on Decision and Control (CDC), Vol. 2018-January, IEEE, Melbourne, VIC, Australia, 2017, pp. 6567_6572. doi:10.1109/CDC.2017.8264649.
URL http://ieeexplore.ieee.org/document/8264649/

[43] T. Kaczorek, Positive stable realizations with system Metzler matrices, Archives of Control Sciences 21 (2) (2011) 167_188. doi:10.2478/v10170- 010-0038-z.
URL http://journals.pan.pl/dlibra/publication/97602/edition/84189/content

[44] University of Bath, Balena HPC cluster (2020).
URL https://www.bath.ac.uk/corporate-information/balena-hpc-cluster/

[45] N. Hadjsaïd, J. C. Sabonnadière, Electrical Distribution Networks, John Wiley & Sons, Inc., Hoboken, NJ, USA, 2013. doi:10.1002/9781118601280.
URL http://doi.wiley.com/10.1002/9781118601280

[46] R. Billinton, W. Li, Reliability Assessment of Electric Power Systems Using Monte Carlo Methods, Springer US, Boston, MA, 1994. doi:10.1007/978-1-4899-1346-3.
URL http://link.springer.com/10.1007/978-1-4899-1346-3

[47] A. B. Ocnasu, Y. Besanger, P. Carer, R. Edf, D. France, Distribution System Availability Assessment Monte Carlo and Antithetic Variates Method, 19 th International Conference on Electricity Distribution (0268) (2007) 21_24.
URL http://www.cired.net/publications/cired2007/search.html

[48] R. Billinton, P. Wang, Reliability-network-equivalent approach to distribution-system reliability evaluation, IEE Proceedings: Generation, Transmission and Distribution 145 (2) (1998) 149_153. doi:10.1049/ip-gtd:19981828.
URL https://digital-library.theiet.org/content/journals/10.1049/ip-gtd:19981828

[49] R. Billinton, S. Kumar, N. Chowdhury, K. Chu, K. Debnath, L. Goel, E. Khan, P. Kos, G. Nourbakhsh, J. Oteng-Adjei, A reliability test system for educational purposes - basic data, IEEE Transactions on Power Systems 4 (3) (1989) 1238_1244. doi:10.1109/59.32623. URL http://ieeexplore.ieee.org/document/32623/

[50] M. Ndawula, S. Djokic, I. Hernando-Gil, Reliability Enhancement in Power Networks under Uncertainty from Distributed Energy Resources, Energies 12 (3) (2019) 531. doi:10.3390/en12030531.
URL http://www.mdpi.com/1996-1073/12/3/531

[51] I. Hernando-Gil, I. S. Ilie, S. Z. Djokic, Reliability planning of active distribution systems incorporating regulator requirements and network reliability equivalents, IET Generation, Transmission and Distribution 10 (1) (2016) 93_106. doi:10.1049/iet-gtd.2015.0292. URL https://digital-library.theiet.org/content/journals/10.1049/ iet-gtd.2015.0292

4.7 Chapter Summary

This chapter presents a novel application of MOR techniques, based on balanced truncation, for reliability analysis of distribution networks. The practical implementation of the algorithm has been described in detail and relevant case studies, based on both meshed and radial systems, have been presented to demonstrate the capability of the proposed approach. Additionally, Appendix C presents a detailed example of the main MATLAB code used for its execution. As expected, the resultant simplified models adequately approximate the reliability of the original system while guaranteeing an appreciable saving in the computational time required to perform reliability analyses. Notwithstanding, the proposed method exhibits some limitations which are addressed in the next chapter. These are the use of peak demand profiles, modelling of SGTs and accuracy of the reduction procedure for radial systems with aggregate demand.

Chapter 5

Enhanced MOR with Time-varying Load Profiles and SGTs

The methodology developed in Chapter 4 is used to obtain simplified grid representations that minimise the estimation error of the ENS index while ensuring significantly shorter computational times. However, there are limitations to the applicability of the methodology as summarised in Section 4.4.3. One of the key limitations is that for MCS analyses, the current methodology only returns models of order $r = 2$. Higher values of r result in system matrices A in (4.13) that are not in Metzler form. Therefore, the associated system lacks the Markov property and cannot be simulated with MCS methods. The tentative approaches that are currently being envisaged to overcome this limitation are also presented. Nonetheless, the analysis is still capable of demonstrating the effectiveness of the proposed MOR methodology, as the key aspect of its validation lies in comparing system outputs of the original vs. reduced-order system. Notably, results in Section 4.5 reveal that the proposed methodology tends to perform better in networks presenting a meshed configuration as opposed to a radial one. This chapter explores how the developed MOR methodology may be enhanced to provide even higher accuracy despite the current limitations. This is achieved using a novel application of state reduction or state pruning techniques, prior to performing MOR, that partially addresses the computational-memory bottlenecks by reducing the initial system dimension before building the state transition matrix A and solving the expensive Lyapunov equations to obtain the system Gramians. Moreover, time-varying demand profiles are integrated into the methodology to enable more accurate analyses for ENS. Lastly, the capability of the developed MOR procedure to accommodate the impact of SGTs in the simplified/reduced system models is demonstrated better in this chapter with less simplifying assumptions for their modelling as were adapted in Chapter 4.

5.1 Introduction

One of the key drawbacks of current methods of reliability assessments of large (e.g. MV) networks is that GSPs representing the connection to various LV networks are often lumped together using simple load summation to reduce on computational times. These lumped LV networks usually represent several highly dispersed (spatially distributed) loads and this type of aggregation is inaccurate because it neglects the spatial variability of demand locations as well as the various equipment types located in these smaller (e.g. LV) networks. Therefore, the task of finding the single equivalent component which can adequately represent the LV network connected at the GSP of a MV network, meets the current capability of the MOR method. This means it is possible to investigate methods to ensure that the MOR-reduction results in more accurate results even for radial networks. Therefore, the main aspect covered in this chapter is developing state pruning (SP) techniques to reduce the size of the original system before performing order reduction using the proposed MOR procedure. The main aim is to increase the accuracy, reduce the computational burden, and hence extend the method applicability to larger systems (with more PCs).

5.2 MOR Enhancement using State Pruning

In the usual implementation of the developed MOR procedure (hereafter termed U-MOR), all possible system states of the original system are used to describe it in the state space representation (4.1) as described by the state space diagram (SSD) given in Figure 4.2. That SSD shows the discrete states and transitions of a CTMC for the simple case of a system with two repairable PCs. However, not all possible system states are required to adequately describe the original system. In practice, there will be a tolerance to the number of PCs that can be in the failed state simultaneously. For example, for a system with 15PCs, it is hardly likely that 7 PCs may all be in the failed state at the same time before the system is completely taken out of service. The result of which would mean that system transition rates to these low-probability states would become zero. These are states where the system would have already been completely shut down before they could be realised or transitioned to.

One advantage of using SSDs is that they can be modified by further (practical) knowledge of the systems they are meant to represent e.g. whether some states and transitions are inappropriate and even whether derated states are necessary [19, 42]. On top of that, various repair/fail processes can be represented, including common mode failures as explained in Section 4.4.1. Another quite useful result of this feature of SSDs is that certain state transitions may not be physically possible and can thus be removed, and perhaps others could be added. For example,

if we consider a 2PC-series system, it may be known that when one PC fails, the other PC is no longer operating and its failure rate in these circumstances becomes zero. In this case, state (4) (in Figure 4.2) does not exist, leaving only states 1-3 and the transition rates between these 3 states. This state removal or 'pruning' can then result in a simplified and reduced state space diagram [42].

In addition, one of the bottlenecks with U-MOR is the limitation on memory due to the size of the original system. This means that reducing the state space dimension using pruning techniques can increase the applicability of the method to larger systems. Notably, this application of state pruning is similar to techniques used in the state enumeration technique for power system risk evaluation [39]. Reducing the dimension of the state space before U-MOR is also beneficial in terms of lowering the computational burden of the procedure. This is because as the test systems become larger, the burden of solving the system Gramians grows rapidly and the complexity is usually $O(n^3)$ where n is the is the size of the original model [89].

It is important to point out that the term 'state pruning' has been used in reliability analyses in the literature for different purposes than that used in this chapter. Highly reliable power system networks hardly encounter many loss-of-load states. Therefore, when performing MCSs of these networks, convergence will generally be prohibitively computationally expensive if all system states are to be sampled. To make MCS converge faster, SP is implemented in studies such as [155, 156] to ensure that there as many loss-of-load states as possible in the state space without 'diluting' them with 'continuous-supply' states which are significantly more likely to be encountered. In this way, this implementation of SP-for-MCS-convergence will increase the probability of encountering loss-of-load states within that state space and lead to faster MCS convergence. However, the use of SP in this chapter is to remove/prune states from the original system which may be classified as 'non-practical' or 'very-low-likelihood' states. The theory of U-MOR is based on minimisation of the error between original and reduced order models. Accordingly, SP is applied to ensure that the original system model is described using only the states that 'offer' useful information for order reduction (for reliability purposes).

5.2.1 Developed Method for SP – Simple Network Topologies

To demonstrate the application of the SP application to U-MOR, consider the simple 4PC series network supplying a 10 MW load in Figure 5.1. Its configuration is such that there will be a supply outage if any of the 4 components is in the DOWN state. In the implementation of U-MOR, this network would have 2^4 (16) states where the only state of load supply would be the one where all components are UP. This means that the calculation the impact matrix C

using PNS would result in a C given by Table 5.1 for all different system states. Accordingly, the system matrix would be $A \in \mathbb{R}^{16x16}$ while output matrix would be $C \in \mathbb{R}^{1x16}$.

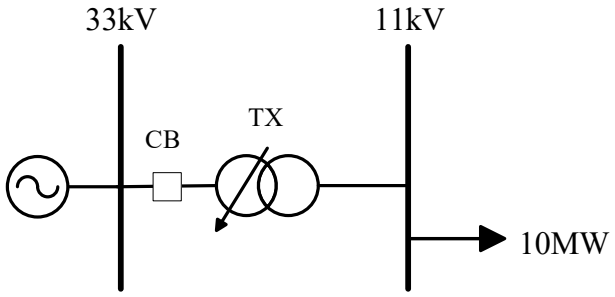

Figure 5.1: Series Network with 4 PCs.

Table 5.1: System states and corresponding impact in PNS.

System State	33 kV Bus	Circuit breaker	Transformer	11 kV Bus	PNS (MW)
S1	1	1	1	1	0
S2	1	1	1	0	10
S3	1	1	0	1	10
S4	1	1	0	0	10
S5	1	0	1	1	10
S6	1	0	1	0	10
S7	1	0	0	1	10
S8	1	0	0	0	10
S9	0	1	1	1	10
S10	0	1	1	0	10
S11	0	1	0	1	10
S12	0	1	0	0	10
S13	0	0	1	1	10
S14	0	0	1	0	10
S15	0	0	0	1	10
S16	0	0	0	0	10

Based on Table 5.1, it is possible to remove/prune all states where more than one PC fails because any instance of failure requires the system to return to system state S1. Therefore, the system states remaining are only S1, S2, S3, S5 and S9. Table 5.1 can then be transformed into Table 5.2 where it is evident that the remaining states correspond to the number of system states in the first enumeration depth of this system. The term enumeration depth is usually used in state enumeration (SE) method of power system risk and reliability assessment [39]. In the SE technique, it is required to enumerate (generate) all possible system states for the original system. However, it would not be computationally feasible to perform this enumeration for large systems since the number of system states increases exponentially with the number of components. Therefore, it is common to enumerate the system states until a given enumeration depth/failure level. The first failure level refers to the system states containing only one component failure while the second failure level refers to those containing two component failures, and so on. This approximation is acceptable with the SE method because the dominant (high

probability) modes of the system are usually described by the first few failure levels. The approximation is also generally acceptable since the transitions between system failure states are very rare whereas the transitions between normal and failure system states are dominant in real life [39].

This application of SP is clearly dependent on system topology as well as the consideration of the failure modes of the system. As previously explained, it is possible to model common mode failures using the proposed U-MOR technique. Similarly, when implementing SP, it is possible to include states that result from a common mode failure. Again, this design parameter is not in the scope of the thesis and is thus not considered. Furthermore, it is statistically possible for there to be a simultaneous occurrence of two independent failures. However, by using a sufficiently small-time step in the reliability assessment, it is possible to ignore also these types of failures because the failure of one component would have to precede another [42].

Table 5.2: Remaining system states after pruning and corresponding impact in PNS.

System State	33 kV Bus	Circuit breaker	Transformer	11 kV Bus	PNS (MW)
S1	1	1	1	1	0
S2	1	1	1	0	10
S3	1	1	0	1	10
S5	1	0	1	1	10
S9	0	1	1	1	10

Based on those assumptions allowing for SP, the SSD of the series network in Figure 5.1 will appear as illustrated in Figure 5.2. Accordingly, the system matrix would be $A \in \mathbb{R}^{5x5}$ while output matrix would be $C \in \mathbb{R}^{1x5}$. Therefore, the original 4PC series network is effectively reduced from 16 states to 5 states using SP.

5.2.1.1 Impact of SP on MOR

Without the proposition to use SP, the original 4PC (16 states) power network in Figure 5.1 would be directly reduced to 2 states using U-MOR. However, with the proposed application of SP, the original system can be reduced to its first failure level (5 states) and then reduced to 2 states using U-MOR. This order reduction procedure is hereafter termed SP1-U-MOR because SP is performed to the first failure level before using U-MOR to reduce the system. For this thesis, SP1-U-MOR is shortened to SP1-MOR. In this section, the impact of applying SP, on the performance of U-MOR, is assessed using the evolution over time of the PNS of each network. In addition, the singular values (SVs) in each case are compared.

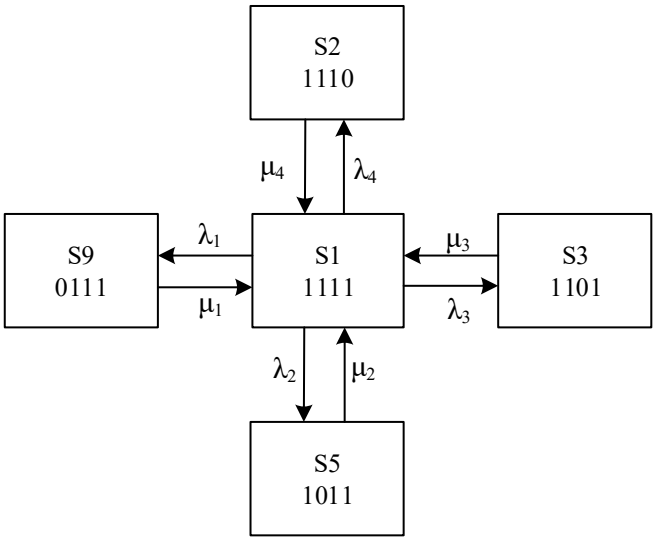

Figure 5.2: Markov chain representing the 4PC series system after SP.

5.2.1.2 Evolution of the System Output

Figure 5.3 presents the output of the dynamical system i.e. the PNS, of the simple 4PC system where we compare the output of the original system of 16 states to the output of the SP1-reduced system of only 5 states. As expected, the evolution of the PNS of the SP-reduced model follows very closely the one of the original system of 16 states because the pruned states have a very low probability of occurrence. This analysis is similar to that of Figure 4.4 which compared the evolution over time of PNS of the original and reduced order models.

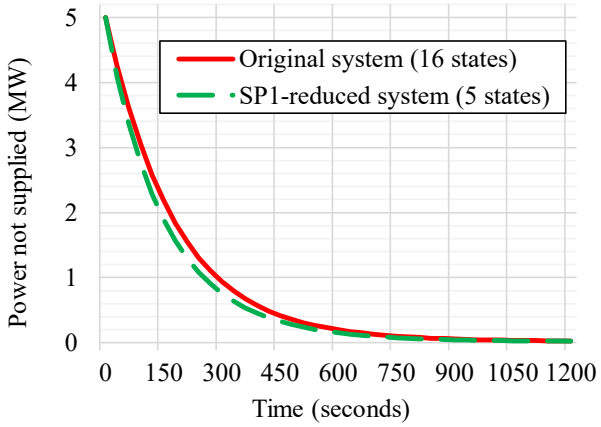

Figure 5.3: Evolution over time of PNS of the original and SP-reduced systems.

Recall that the initial conditions ($x(0) = x_0$) do not affect the steady-state behaviour of the system but only determine the starting point $y(0) = Cx(0)$ of the output response (5 MW in

Figure 5.3). Accordingly, if it was known with probability 1 that all components were UP (working) at time $t = 0$, then the initial PNS would be 0 MW and would increase to a non-zero steady state value $y_{ss} = Cx_{ss}$ over time. Section 4.5.1 showed that we can reduce the order of an original system to varying number of states and realise increasing accuracy as more states are included in the reduced order model. This is because more system dynamics are captured when more states are included. The SP1-reduced system can also be reduced to varying number of states with the same outcome. This makes it possible to compare 2 scenarios. The first is when the original system of 16 states is reduced to 2 states using U-MOR (as done in Section 4.5.1). In the second scenario, the SP1-reduced system of 5 states becomes the 'original' network which is reduced to 2 states using U-MOR. Again, this may alternatively be stated as: the original system of 16 states is reduced to 2 states using SP1-MOR. Figure 5.4 compares these two scenarios where the reduction to 2 states using SP1-MOR is more accurate in approximating the original system than U-MOR. This is expected because only 2 states are retained from a 'smaller' system when SP1-MOR is used as compared to the U-MOR case.

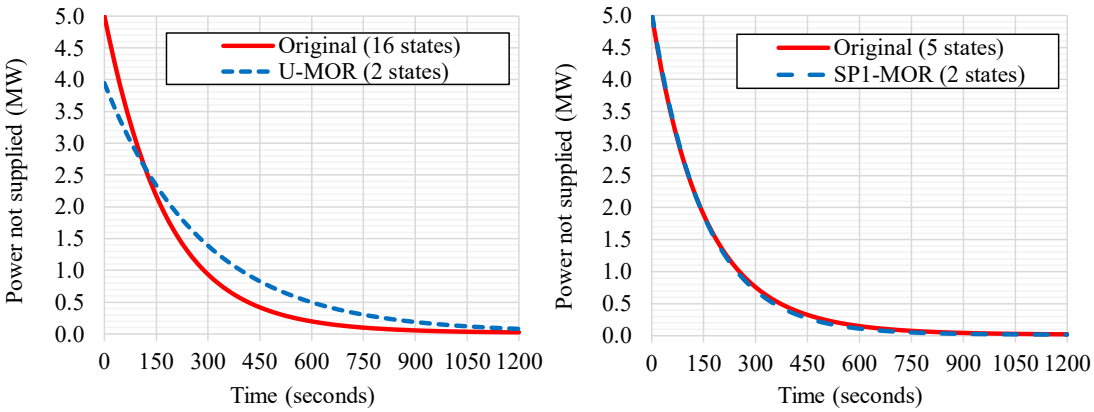

(a) U-MOR (b) SP1-MOR

Figure 5.4: Comparison between U-MOR and SP1-MOR using evolution over time of PNS.

5.2.1.3 System Singular Values

This comparison may be extended by comparing the SVD of both the original and SP-reduced networks. As previously introduced, the non-increasing SVs [87, 89] indicate the relevance (energy) of each system state in terms of reliability. Thus, the dynamics which have a smaller impact on the considered reliability indices can be neglected. Using Tables 5.3 and 5.4, we calculate the relative weight (RW) of each system state based on the system SVs. The impact of only retaining 2 states in the reduced order model is emphasised by comparing the RW of

2 states in the original system used for U-MOR (Table 5.3 [13]) with the RW of 2 states in the 'original' system used for SP1-MOR (Table 5.4). As expected, the 2 main states in the U-MOR method have 98.52% RW compared with 98.91% RW in the SP1-MOR method. This means there is more important 'information content' in the 2 states with SP1-MOR than in the 2 states with U-MOR. Subsequently, SP1-MOR is expected to perform better than U-MOR when MCS is done. The reliability performance results are shown in Section 5.3.

Table 5.3: SVs of the original system used for U-MOR.

System states	**2**	**3**	**4**	**5**	**6**		**15**	**16**
SVs	205681.35	2905.49	159.80	14.24	0.40		0.00	0.00
RW (%)	98.52%	1.39%	0.08%	0.01%	0.00%	...	0.00%	0.00%
Cumulative RW	0.985	0.999	1.000	1.000	1.000		1.000	1.000
ln SV	12.23	7.97	5.07	2.66	-0.92		-26.82	-28.64

Table 5.4: SVs of the original system used for SP1-MOR.

System states	**2**	**3**	**4**	**5**
SVs	29893.24	329.44	1.28	0.00
RW (%)	98.91%	1.09%	0.00%	0.00%
Cumulative RW	0.989	1.000	1.000	1.000
ln SV	10.31	5.80	0.25	-41.49

5.2.2 Developed Method for SP – Complex Network Topologies

In the current implementation of SP, only system states belonging to the first failure level are retained in the state space representation (4.1). The approximation resultant from this application of SP is therefore more accurate for systems with simple topologies, and with aggregated loads. More practical (and complex) networks have spatially distributed loads resulting in situations where there would be partial power supply even in the event of failure of 1 or more PCs i.e. tolerance to higher system failure levels. This tolerance is usually controlled by the relevant DNO and will be affected by several factors for example: system topology/configuration, operational limits' violations, economic value of lost load, system security (e.g. $N-1$ contingency), SQS regulations, etc. Indeed, the system must often be returned to normal operation quickly before further outages occur that might lead to system-wide outage. Also, the PC repair rate is usually higher than the PC failure rate which allows for the general premise of the SP application [19, 39, 42]. Therefore, for more complex systems, it is reasonable to improve the level of approximation used in the SP-reduction by including more states or raising the failure level used in the resultant SP-reduced model. This is especially necessary to retain

[13] For 2 or 3 significant decimal places, the values between system states 6 and 15 are indistinguishable.

those states which allow for partial power supply, subject to a tolerance level for the number of PCs that may be failed simultaneously (failure level/enumeration depth).

5.2.2.1 Method Adaptation for Complex Network Topologies

Let us consider the 14PC network diagram presented in Figure 5.5 which represents a modified suburban LV network containing one 315 kVA 11/0.4 kV transformer supplying 34 residential customers for a total load of 77.18 kW. For applicability to the developed MOR methodology, the network is reduced to an equivalent representation of 14 PCs i.e. 6 buses, 4 overhead lines, 2 circuit breakers, 1 fuse and 1 transformer. The line identifiers presented correspond to ID parameters given for LV networks in Table 3.1. For this network, it is possible for there to be partial power supply if only one PC goes DOWN. For example, if the bus supplying LP3 fails, LP1 and LP2 will still receive power supply. This system state may be maintained for a particular period depending on the requirements or tolerance of the system operator. Furthermore, the system could transition from a state where only LP1 & LP2 are supplied, to one where no LPs are supplied (a complete loss-of-load state). Therefore, the state space model will now include all such categories of states.

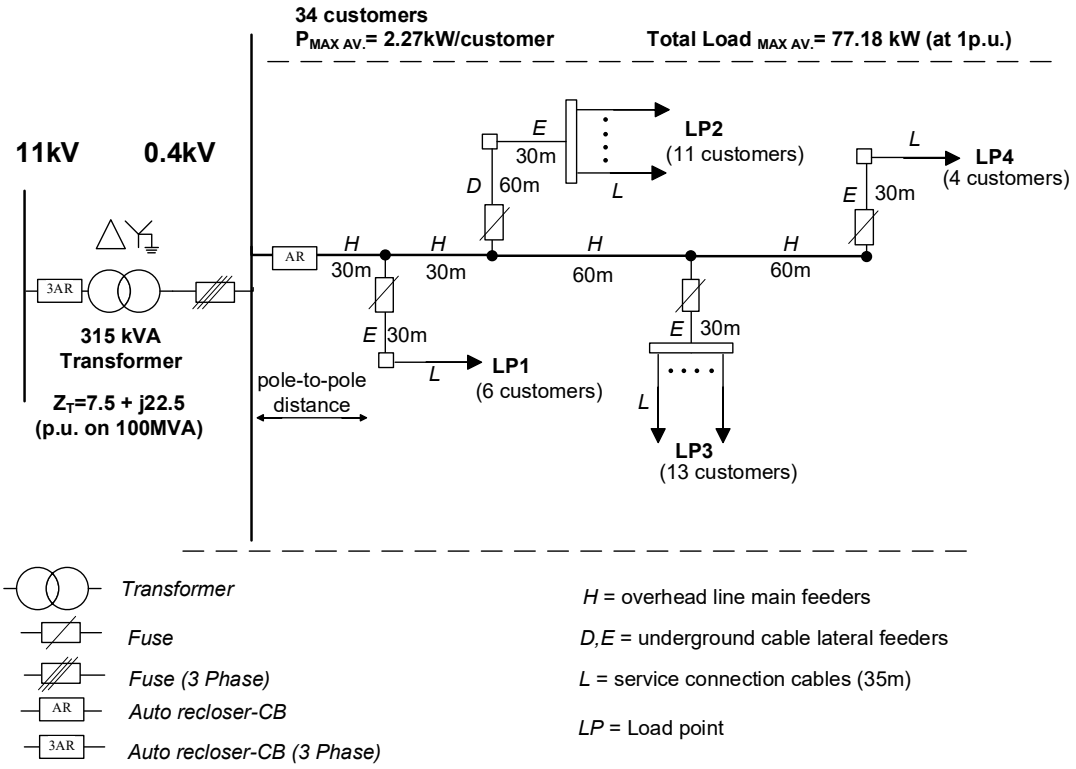

Figure 5.5: Modified suburban LV distribution network model – 14PCs.

5.2.2.2 Tolerance to the Number of Simultaneous PC Failures

This section analyses how the allowed/designed system failure level affects the accuracy of the SP-MOR process. To save time, only the analytical system unavailability [39] is used to obtain the ENS, without performing MCS comparative analyses which will be used in Section 5.3 when more comprehensive reliability analyses are presented. Table 5.5 presents the ENS obtained from the original network in Figure 5.5, compared with that of the different variants of MOR methods previously introduced. Another key benefit of Table 5.5 is that it can be adequately used to explain the key differences in the enhancements to MOR presented. The first row of Table 5.5 presents the ENS of the original network of 14 PCs (2^{14}=16384 states). Note that with the current formulation, the use of any MOR technique only results in a reduced system with 2 states. This explains the number of states for all MOR-reduced systems. It is also important to note that the 'failure levels' given in the table are not strictly based only on the number of simultaneous PC failures but also include the associated loss-of-load states that can be transitioned into. This approximation, based on limiting simultaneous PC failures is important because for large systems, it would certainly be very difficult to track all the state transitions using hand calculations.

The implementation of U-MOR is shown in the last row where the system failure level is 14 i.e. all 14 PCs may be allowed to be DOWN simultaneously, and all 16384 states of the original system are used to describe the original model (i.e. retained) before U-MOR is performed. The second row of Table 5.5 presents SP1-MOR i.e. where only 1 PC can fail before total system supply is restored. This results in only 15 states being used to describe the original system before U-MOR is performed. Correspondingly, 16369 states are not considered or are pruned.

Table 5.5: SP-MOR failure level analysis for the modified suburban LV network.

Network	**States**	**Failure level**	**ENS (kWh/year)**	**Abs Error (%)**	**States retained before U-MOR**
Original	16384	14	143.75	_	_
SP1-MOR	2	1	133.61	7.10%	15
SP2-MOR	2	2	143.18	0.40%	148
SP3-MOR	2	3	166.26	15.70%	492
SP4-MOR	2	4	179.24	24.70%	1478
SP5-MOR	2	5	188.64	31.20%	3474
U-MOR	2	14	209.51	45.70%	16384

To improve the approximation of SP1-MOR, SP2-MOR is presented, and it includes all partial or complete power supply states while also limiting the system failure level to only 2. This results in having 148 states kept before performing MOR while 16236 states are pruned. This implementation leads to a significantly low ENS approximation error of 0.4%. It is well known

that networks are sometimes operated closer to their limits so it is not inconceivable that this system may be operated for a higher failure level. To that end, SP-MOR is performed again but this time, increasing the failure level to 3, 4 and 5 with corresponding reductions to the states pruned. Finally, when failure level 14 is allowed for, then 'SP14-MOR' is equivalent to the U-MOR method.

For this network, 'SP2-MOR' results in the most accurate ENS index approximation. Table 5.5 shows that when more 'less-information' states are retained to describe the original system; the accuracy of the reduction procedure is lower. For this chapter, SP2-MOR will be used to compare order reduction accuracy in different networks. This is also because higher failure levels have already been reported to be rarely occurring and thus hardly having an impact on reliability performance, as published in [38] which looked at the probability of double and triple faults in normal network operation. To expound further on this, 'SP14-MOR' or the U-MOR method includes, in the original state space representation, a state where all PCs fail and of course, no power is supplied. Both theoretically and practically, such a state is hardly likely and might only occur if a very catastrophic low-probability high-impact event such as a massive lightning strike happens. Therefore, before doing MOR, we should already expect and roughly estimate the impact of this state and its value in informing the MOR-process. It is reasonable to assume that pruning such states before MOR is performed is only improving accuracy by removing the 'unnecessary information' used to describe the original network under test. In summary, the enhancement to the U-MOR procedure described in Chapter 4 is based on the initial system state selection used in the state space representation (4.1) to describe the original network. Use of SP-MOR introduces an approximation that provides a tolerance to the number of PCs that can be in the failed state simultaneously while ensuring that more partial load supply states are captured in the state space representation.

5.3 Test Cases and Results

This section presents all examined test cases. As in Chapter 4, for all analyses, the operation of conventional generators is assumed to be ideal and therefore when quantifying system sizes in terms of number of components, generators are not counted. To determine the performance of the reduction techniques discussed, time-sequential MCSs based on STS are carried out on the original and reduced models. Accordingly, the ENS approximation error and computational time required for MCS analyses are compared. For a fair comparison of the MCS time taken, the CoV threshold is set to 0.2% for all simulations. All analyses are designed to demonstrate the varying effectiveness of different network reduction methods, as the key aspect of their validation lies in comparing outputs of the original vs. reduced-order system in each case.

5.3.1 Simple 4PC Series Network

Consider the 4PC series network presented in Figure 5.1. Given its topology, it is possible to perform the following types of network reduction: TNR, U-MOR and SP1-MOR. It is unnecessary to use SP2-MOR and so on, as the topology and presence of only a single aggregated load, does not require it. Table 5.6 presents the results from the MCS analysis in terms of average ENS. The computational time taken is not reported because the associated savings due to order reduction are not significant given relatively small size of the original system. However, it highlights how much better SP1-MOR performs with an ENS error of only 0.65% compared to 36.57% using U-MOR. Moreover, SP1-MOR is significantly more comparable to TNR for which an ENS error of 0.33% is obtained. This result is significant as it makes the implementation of SP1-MOR very competitive with an already established method i.e. TNR, which provides sufficiently accurate reduced system models for this type of network configuration. Additionally, the ENS obtained in the original and SP1-reduced systems is compared. The 0.05% error demonstrates that the use of SP results in a highly accurate approximation of the original system and validates the use of the SP1-reduced system as the new 'original' system which is subsequently reduced using U-MOR in the SP1-MOR method.

Table 5.6: ENS index accuracy for the 4PC series network.

Network	States	ENS (MWh/year)	Absolute Error (%)
Original	16	144.13	–
U-MOR	2	196.84	36.57%
SP1-MOR	2	145.07	0.65%
TNR	2	143.66	0.33%
SP1-reduced	5	144.05	0.05%

5.3.2 Radial Network with Aggregate Load

The generic MV substation presented in Figure 4.8 presents a radial network configuration with aggregate load. Hence, it is possible to compare the performance of the following reduction methods – TNR, U-MOR, SP1-MOR and SP2-MOR. It would be possible to demonstrate the use of SP3-MOR and so on as well but given results presented in Section 5.2.2, it is not performed here. Table 5.7 presents the results from the MCS analysis and as envisaged, TNR exhibits the best performance while SP2-MOR performs progressively better than SP1-MOR. Noticeably, the error magnitude obtained using U-MOR is over 7 times larger than that by SP1-MOR.

Table 5.7: ENS index accuracy for the generic MV substation.

Network	States	ENS (MWh/year)	Absolute Error (%)	Total Time Taken (s)	Time Saving (%)
Original	1024	278.48	_	9433.43	_
U-MOR	2	387.06	38.99%	5423.27	42.51%
SP1-MOR	2	263.43	5.40%	5510.64	41.58%
SP2-MOR	2	270.21	2.97%	5438.30	42.35%
TNR	2	278.38	0.04%	5795.88	38.56%

5.3.3 Radial Network with Spatially Distributed Loads

The modified suburban LV network presented in Figure 5.5 presents a radial configuration with dispersed/non-aggregated loads. Given the topology, it is possible to compare the performance of the following reduction methods – TNR, U-MOR, SP1-MOR, and SP2-MOR. Table 5.8 presents the associated results where the main result is the fact that clearly the existence of spatially distributed loads makes TNR (13.41%) less effective than it was in the previous MV substation test case (0.03%) which had one aggregated bulk load. Furthermore, SP2-MOR performs much better than all other reduction techniques. It might therefore be argued that SP2-MOR (and therefore the proposed MOR methodology) is a superior approach to TNR when reducing networks with spatially distributed loads. As a matter of fact, this is one of TNR's most reported limitations [19, 157].

Table 5.8: ENS index accuracy for the suburban LV network.

Network	States	ENS (kWh/year)	Absolute Error (%)	Total Time Taken (s)	Time Saving (%)
Original	16384	143.75	_	64530.78	_
MOR	2	212.94	48.13%	4968.66	92.30%
SP1-MOR	2	133.79	6.93%	5639.64	91.26%
SP2-MOR	2	144.18	0.30%	5603.10	91.32%
TNR	2	163.03	13.41%	5216.34	91.92%

5.3.4 Meshed Network with Spatially Distributed Loads

In this test case, TNR is not used for network reduction because of the meshed configuration of the modified RBTS-12PC system (adapted from Figure 4.6). Therefore, it is possible to compare the performance of 3 reduction methods i.e. U-MOR, SP1-MOR, and SP2-MOR. Table 5.9 presents the relevant reliability assessment results. The key takeaway is that the performance of U-MOR for this meshed network topology is significantly better than the performance of U-MOR for the radial (parallel series) network topologies. Nonetheless, the results

demonstrate that the application of MOR-SP for network reduction to assess ENS is still more accurate than U-MOR.

Table 5.9: ENS index accuracy for the RBTS-12PC.

Network	States	ENS (MWh/year)	Absolute Error (%)	Total Time Taken (s)	Time Saving (%)
Original	4096	651.87	_	39958.42	_
U-MOR	2	681.31	4.52%	4727.39	88.17%
SP1-MOR	2	646.93	0.76%	3825.35	90.43%
SP2-MOR	2	654.45	0.40%	5334.79	86.65%

5.3.5 Results Comparison and Discussion

Figure 5.6 presents all the error values obtained when approximating ENS using each discussed method of network reduction for all the test cases presented. Firstly, Figure 5.6(a-c) show that the U-MOR performs significantly worse for radial networks than for meshed networks (Figure 5.6(d)). As discussed, there is significant improvement in the accuracy of the U-MOR method using SP enhancements while demonstrating that TNR is only a superior reduction approach when test networks present relatively simple and radial configurations with aggregated loads.

5.4 Time-varying Load Profiles

This section discusses the inclusion of time-varying load profiles into the developed MOR procedure as an added enhancement. This inclusion is vital to the accurate assessment of ENS in power networks and is a key feature of reliability analyses of real distribution systems as shown in earlier chapters of this thesis. To achieve this, the state space description in (4.1) is modified to include a time-varying output matrix C. This means that, for each system state, there is an associated impact in terms of PNS that is dependent on the modelled load profile. Recall that, the system output $y(t)$ corresponds to a linear combination of the state $x(t)$, according to the output matrix $C \in \mathbb{R}^{qxn}$ where q represents the considered output i.e. PNS. The PNS can thus be extended to become an array in each system state instead of a single output. This array includes varying load levels at different times of the day according to the designed time-varying load profile. For example, for a 10PC system, using peak demand profiles, the output matrix is $C \in \mathbb{R}^{1x1024}$. By including time-varying demand profiles, the matrix C is transformed to $C \in \mathbb{R}^{24x1024}$ if a 1-hour time-step is used to represent the load profile.

Figure 5.6: Comparing performance of different network reduction methods.

5.4.1 Generic MV Substation

To illustrate the use of MOR with time-varying load profiles, consider the MV substation presented in Figure 4.8. The aggregate load of 20.7 MW is considered to belong to a residential demand sector [158] whose demand profile is similar to that presented in Figure 3.1. Table 5.10 shows that there is a reduction in the ENS of each network model when time-varying load profiles are used. Importantly, the analysis shows the capability of the proposed reduction methods to accurately capture the same reduction in ENS, as is possible with original networks using conventional reliability assessment methods. Moreover, the fact that all the methods produce an ENS reduction of about 29.4% shows that the developed methods are consistent with already established techniques.

Table 5.10: Impact of time-varying load profiles in the MV substation reduced networks.

Network	States	ENS (MWh/year)		ENS Reduction
		Peak Load	Time-varying Load	
Original	1024	278.48	196.66	29.38%
U-MOR	2	387.06	273.19	29.42%
SP1-MOR	2	263.43	185.95	29.41%
SP2-MOR	2	270.21	190.72	29.42%
TNR	2	278.38	196.28	29.49%

5.4.2 Roy Billinton Test System

The analysis is extended to consider different types of load sectors as discussed in Section 3.1.1. The RBTS network presented in Figure 4.6 has 5 load buses each with a different type of demand sector represented. This is summarised in Table 5.11 where the designation of the load type (given in [159]) is translated into a demand sector type i.e. Residential (res), commercial (com) and industrial (ind) and the demand share at each bus is given. The demand share at bus 3 is selected based on [158] and is only intended to demonstrate varying load profiles for varying load subsectors for the purpose of this thesis. Figure 5.7 shows the different load profiles used at each bus as a result of the reported demand shares.

Table 5.11: Varying load profiles for different types of loads (res, com and ind).

RBTS Bus	Load (MW)	RBTS designation	Sector Type Used	Demand Share (%)
2	20	Small users, Gov't & institution	Res & Ind	50-50
3	85	Large Users, Small users, Office	Res, Com & Ind	45-31-24
4	40	Small Users	Res	100
5	20	Gov't & Institution, Office	Com	100
6	20	Small Users, Farms	Res & Com	50-50

Varying Impact of States

The introduction of different load subsectors increases the accuracy of the description of the system state space as given by (4.1) because it assigns more accurately the correct impact of a state based on the time at which an interruption occurs and the nature of the associated demand sector. For example, consider 2 system states of the RBTS 15PC network – 8497 and 17314. Using only peak demand to represent the load would result in the power supplied (PS) being given by Table 5.12 where the total PNS would be 20 MW in each state.

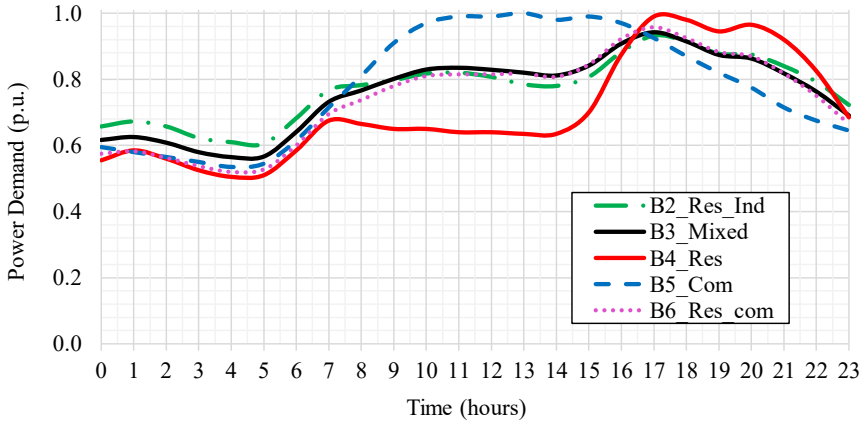

Figure 5.7: Load profiles at different demand buses in the RBTS.

Table 5.12: Varying impact of states in terms of PNS for different system states.

RBTS Bus	Rated Load (MW)	State 8497		State 17314	
		PS (MW)	PNS (MW)	PS (MW)	PNS (MW)
B2	20	0	20	20	0
B3	85	85	0	85	0
B4	40	40	0	40	0
B5	20	20	0	20	0
B6	20	20	0	0	20
Totals (MW)		165	20	165	20

However, using time-varying demand, each state exhibits a different maximum value for PNS while also following a different demand profile based on the nature of the demand served. This is shown in Figure 5.8(a) and is a more accurate modelling of the true impact of system states in terms of PNS. Analogously, 3 'similar-impact' states can be analysed as shown by Figure 5.8(b). The following buses are failed/DOWN in each state: bus B5 and B6 in state 232, bus B4 in state 2396, and bus B2 and B6 in state 8885. Using peak load, the total PNS in each state would be 40 MW. However, Figure 5.8(b) shows that these 3 states have substantially varying impact not only in terms of the maximum PNS but also the impact on the resultant ENS due to the incidence of fault occurrences with the load sector and time-dependent demand. Overall, this increases the accuracy of the minimisation error introduced by MOR when performing system reduction and extends the applicability of this system reduction method to more practical/larger power networks. As shown in Section 5.4.1, Table 5.13 shows a consistent reduction in the ENS when time-varying profiles are used as compared to peak demand profiles. The key, again, is the consistency of all developed MOR methods in accounting for a time-varying load profile by exhibiting reduced ENS.

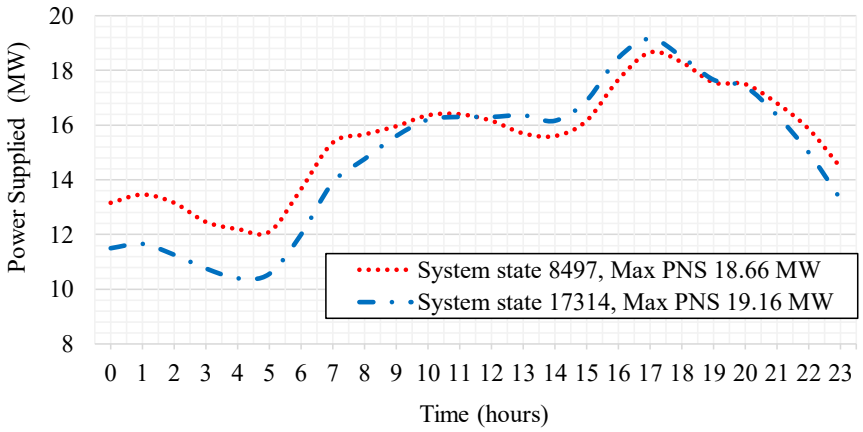

(a) Peak load PNS = 20 MW

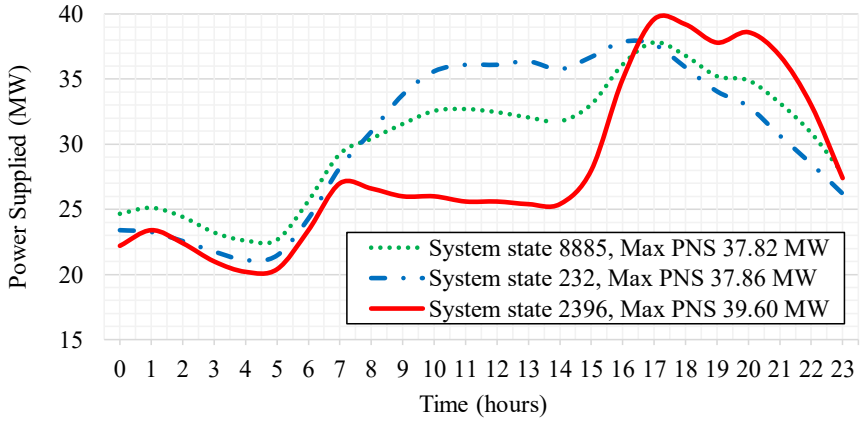

(b) Peak load PNS = 40 MW

Figure 5.8: Time-varying impact for different system states.

5.5 Integration of SGTs

As thoroughly discussed in Chapter 3, one of the key features of future power networks is the integration of SGTs and the associated network flexibility. These technologies significantly increase network complexity and require that more accurate reliability assessments are made to ascertain the benefits offered. Therefore, the capability of the proposed MOR methodology to accommodate SGTs in the simplified reliability models is demonstrated in this section. Having a reduced system that can demonstrate the effect of DERs is important to system planning as the key benefit in the use of system reduction methods is to reduce the time necessary for system studies and therefore the time taken to make decisions. This section considers the 3 main SGTs considered in this PhD research i.e. PV, DSR and ES. There is no combination of technologies as was shown in Chapter 3 because the major outcome intended from this analysis

Table 5.13: Impact of time-varying load profiles in RBTS reduced networks.

Network	States	ENS (MWh/year)		ENS Reduction
		Peak Load	Time-varying Load	
Original	32768	651.30	486.55	25.30%
U-MOR	2	692.20	524.11	24.28%
SP1-MOR	2	642.24	480.41	25.20%
SP2-MOR	2	664.73	502.60	24.39%

is to demonstrate the capability of the developed network reduction procedure in accurately showing the reliability impact of SGTs.

5.5.1 Network Scenarios incorporating SGTs

Table 5.14 presents 5 scenarios designed for the RBTS-15PC network. The SC1 (base case) scenario considers no SGT (but includes time-varying load profiles) while SC2A and SC2B scenarios represent the addition of PV to the network with different penetration levels. Moreover, this application of PV includes the effects of clouding as discussed in Section 3.3.3. This modelling also ensures that the intermittent nature of the supply from PV, as well as the daily and seasonal cycles, are added into the analysis. Unlike the DSR application presented in Section 3.3.2, the application of DSR in SC3 is done for peak shaving i.e. demand reduction during peak times to optimise the energy efficiency. Finally, SC4 includes ES resources, which are assumed to be locally available only to buses B5 and B6 (combined 40 MW load). Given that these loads are the furthest from the main supply, it is expected that the use of ES will greatly reduce not only the ENS of the customers at the associated LPs D4 and D5 but also the average system ENS. This ES configuration is designed to supply energy in the event of a fault occurrence that causes outage to either D4 or D5. Furthermore, it is modelled to account for the variation of its SOC based on solar irradiation, load demand, and electricity tariff during grid supply conditions, as discussed in Section 3.3.4.

Table 5.14: Network Scenarios for the RBTS-15PC with SGTs.

ID	Scenario	Description
SC1	Base case	Using time-varying load profiles, no SGTs
SC2A	PV 25%	25% PV penetration, accounts for PV clouding & stochasticity
SC2B	PV 50%	50% PV penetration, accounts for PV clouding & stochasticity
SC3	DSR	Peak shaving & better energy efficiency for demand reduction
SC4	ES	Applied at Buses 5&6, accounts for varying SOC of ES

5.5.2 Impact of SGTs & MOR Validation

This section presents the results in terms of ENS reductions from the base case that are realised when SGTs are integrated into the RBTS 15PC network. Additionally, the accuracy of the developed MOR methods is quantified. Table 5.15 presents the average ENS obtained in each scenario with the corresponding reduction in ENS when each SGT is integrated. As expected, the ENS to customers is progressively reduced as the PV penetration increases from 25% to 50% in scenarios SC2A and SC2B, respectively. Noticeably, the implementation of DSR for peak shaving leads to a slightly improved network performance as compared to a relatively low PV penetration (SC2A). Furthermore, ES implementation nearly halves the system ENS with respect to the base case, where the LPs D4 and D5 present poor reliability. It is important to note the consistency with which the developed MOR methods can demonstrate the same reduction in ENS as is obtained from the original network. This demonstrates the advanced capability of the MOR methodology to accommodate SGTs and enable accurate quantification of their impacts on network reliability, while invariably reducing the computational time required for MCS analyses. The average ENS in each network scenario (presented in Table 5.15) is presented graphically using Figure 5.9(a) while the percentage reduction of the ENS from the base case is presented in Figure 5.9(b).

Table 5.15: Reliability performance of the RBTS-15PC with SGTs.

Network	**SC1** [&]	**SC2A** [&]	***(%)**	**SC2B** [&]	***(%)**	**SC3** [&]	***(%)**	**SC4** [&]	***(%)**
Original	486.55	453.92	6.71	422.44	13.18	445.24	8.49	285.30	41.36
U-MOR	524.11	482.66	7.91	455.82	13.03	471.97	9.95	295.49	43.62
SP1-MOR	480.41	448.75	6.59	417.27	13.14	439.22	8.57	281.83	41.33
SP2-MOR	502.60	471.83	6.12	433.83	13.68	461.69	8.14	285.14	43.27

[&] ENS (MWh/year), *Reduction from base case (SC1)

5.6 Conclusions

Despite the current U-MOR methodology limitation of only reducing a system to 2 states, this chapter explores the use of SP techniques to enhance the accuracy of the proposed methodology especially for networks presenting radial configurations and with spatially distributed loads. The SP techniques are applied to reduce the system state space dimension, based on the designed failure levels, before applying the proposed U-MOR methodology to reduce the network to 2 states. SP is justified by considering that practical power systems are hardly likely to encounter system states with simultaneous failure of multiple PCs (high failure levels). The pruning of these low probability states before the application of U-MOR increases the accuracy of assessing ENS while extending the applicability of the aggregation method to incrementally

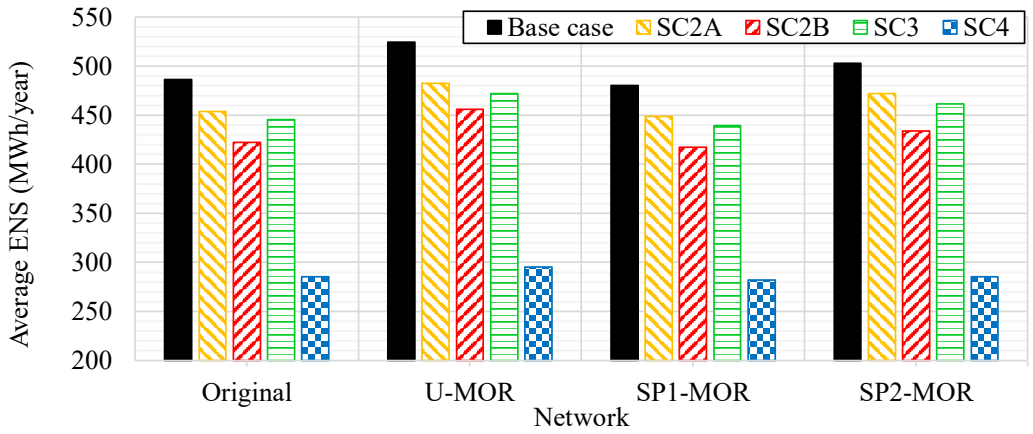

(a) Average ENS per network scenario

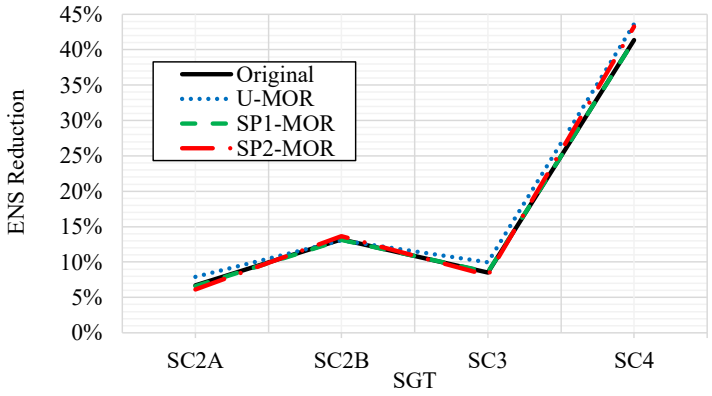

(b) ENS percentage reduction from the base case

Figure 5.9: Impact of SGTs on reliability performance of reduced order networks.

larger systems. Also, MOR is further enhanced by the inclusion of time-varying load profiles to provide a more realistic ENS assessment. Finally, through accurate impact assessments, the chapter demonstrates the advanced capability of the proposed MOR methodology to accommodate SGTs whose spatio-temporal variation adds substantially to network complexity.

Chapter 6

Conclusions and Future Research

This chapter summarises the main results of this research. This is followed by a detailed discussion of the key research limitations which are complemented by tentative approaches that are envisaged to overcome them in the future work. Finally, the chapter provides promising future research directions that can be followed to extend the main outcomes of this thesis.

6.1 Synopsis

This thesis presents probabilistic methodologies for distribution network reliability assessment that consider not only the variability of DERs (e.g. clouding effects in PV) but also the temporal variation of demand. Deployment techniques are proposed that combine the modelled SGTs to maximise their benefits in terms of CoS such as combining DSR and ES which proves most effective for reliability enhancement. Given that network aggregation is considered especially useful in simplifying systems endowed with SGTs, this research investigates novel techniques based on MOR to reduce the complexity of large networks and result in appreciable savings on the computational simulation time required for analyses. Collectively, these contributions are useful in an industry context as they motivate the use of reliability assessment methodologies for network planning as opposed to the statistical methods commonly used to assess reliability at the end of a reporting period merely to fulfil regulator-set obligations. The main reasons for the aversion to reliability assessment methodologies in industry are the high computational requirements and modelling complexity. Moreover, as some DNOs realise satisfactory performance using reactive maintenance and network investment, there is a reduced motivation to explore these techniques. However, this research develops methods and analyses that provide fast and accurate reliability results and quantify not only the effects of SGT integration

but also the associated risk in terms of customer supply outages which has correlated financial implications.

Chapter 2 examines the background, literature review, challenges and current solutions, related to the continuity of electricity supply (within the wider context of QoS) in power networks. It presents relevant interruption data highlighting also the different instruments used for regulation of CoS levels in different countries. The chapter consists of an overview of both the most widely used metrics and CoS assessment methodologies in power distribution networks followed by an analysis of the impact of the considered SGTs (PV, DSR and ES) on network functionality (and reliability). Given the added complexity to networks due to SGTs, the chapter also discusses the state of the art in power network aggregation/reduction methodologies. Finally, the chapter presents the proposed contributions of this research to the literature reviewed. Specifically, this includes the advancement of a reliability assessment methodology based on MCS SDS, improved modelling of PV to capture the temporal variations, a novel application of DSR during the periods of highest fault probability, the inclusion of ES state-of-charge variation based on ambient conditions, electricity tariff and connected demand, and lastly, the novel use of MOR for network aggregation in reliability assessment.

Using relevant models of MV distribution networks, Chapter 3 provides an integrated approach for assessing the impact of SGTs on reliability performance. The key contributions include an accurate demonstration of the spatio-temporal variation of PV, the variability of the state of charge in coordinated ES, and the use of demand-manageable loads. Using time-sequential MCS analyses based on SDS, special attention is given to the perceived level of CoS from the customer perspective by calculating average values and probability distributions of both the system- and customer-oriented indices. One of the main drawbacks in using only the system-oriented indices is that they include customers who enjoy uninterrupted power supply for substantially long periods, thereby concealing some of the shortcomings of network performance, especially to worst served customers. Accordingly, this research emphasises the use of customer-oriented indices which measure system reliability for only those customers who are affected by interruptions. Moreover, the chapter provides a rigorous characterisation of varying customer groups by presenting the reliability assessment for different load sectors (rural, suburban, urban) in addition to the use of risk metrics (CVaR) to define the expected values of the reliability indices in the worst-case (low probability) scenarios. Finally, the range of variability and effectiveness of SGTs in different spatial configurations is illustrated while also allowing for an analysis of the impact of undergrounding on reliability through load-sector performance comparisons.

Chapter 4 proposes a novel application of model order reduction techniques for the specific problem of network aggregation given the complexity of modelling detailed networks. Using

relevant case studies based on both meshed and radial configurations, the proposed MOR-for-reliability methodology is used to derive simplified reliability models of electricity networks that contain the most important system dynamics while minimising the error of the considered reliability metrics. Time-sequential MCS analyses based on STS are carried out on both original and reduced order systems to verify that the resulting reduced-order models provide a reasonably accurate reliability assessment while being significantly faster to simulate.

Chapter 5 explores enhancements to the MOR-for-reliability methodology proposed in Chapter 4. This is achieved using a novel application of state pruning techniques, prior to performing MOR, that substantially increases the reliability assessment accuracy, especially for radial networks. The state pruning is justified by considering the operation of practical power systems where it is hardly likely to encounter system states with simultaneous failure of multiple PCs. Therefore, such low probability states are pruned before MOR thereby extending the applicability of the MOR method to incrementally larger systems. Another key contribution of this chapter is that MOR is further enhanced by the inclusion of time-varying load profiles to provide a more accurate assessment of ENS. Finally, by combining the MOR improvements to the use of time-varying load profiles, this chapter demonstrates the advanced capability of the developed network aggregation procedure to accurately accommodate the impact of SGTs in simplified/reduced system models.

6.2 Research Limitations and Proposed Future Solutions

This section discusses the key research limitations which are each complemented by the tentative approaches that are envisaged to overcome them in the future work.

6.2.1 SGT Modelling

6.2.1.1 Failure of PV and ES Assets

The current research assumes an ideal operation of PV and ES assets such that their effectiveness is limited only by their power capacities and in the case of PV, coincidence with the demand peaks. Future analyses will provide for more realistic modelling by including the failures of this equipment, their associated repair times as well as the life-cycle of each asset. Although these statistical data are not easily/readily available, the inclusion of these failure parameters is vital to making the case of mass adoption of these technologies despite their already well-known benefits. Not to mention, this will be important to investigate how the usage of these assets can be mapped onto particular reliability levels. Therefore, the new reliability

assessment methodology will provide less optimistic results, recognising the fallibility of the deployed SGTs, as well as the system PCs.

6.2.1.2 Large-scale PV and ES

This research models the use of PV and ES as local MG units at customer premises. However, future distribution grids will also have PV farms and/or ES connected at the main substation and even higher voltage levels. This will be to emulate large-scale ES typically owned, controlled and managed by DNOs. Currently, the emphasis in this type of ES-configuration is to improve energy efficiency and provide balancing services such as frequency response and reserve services. However, future research will quantify plausible reliability enhancements from this ES-configuration. Moreover, analyses will include assessment of network hosting capacity for the proposed large-scale PV-based DG, as performed in [160] for wind-based DG, to ensure that relevant DG sizes are modelled while accounting for relevant operational network constraints. For completeness at an advanced stage, the analysis will also require integration with current use-of-system charges methodologies as well as evaluation of the contribution to the generation capacity margin.

6.2.2 Reliability Assessment Methodology

6.2.2.1 Expected PC Lifetimes

This thesis makes a substantial attempt to reduce the simplifying assumptions required for modelling. However, each PC is modelled to have the same expected lifetime (40 years) yet different PCs have different ageing patterns due to location, operating characteristics, etc. Similarly, PCs located near the coasts might deteriorate faster due to salt and storms whereas inland equipment may have longer lifetimes punctuated with different types of climate stresses. Also, the manufacturer of a PC will certainly have a significant impact on its useful life. Therefore, future work will include the provision of variable PC replacement periods based on the nature of the PC, number and duration of failures, and socio-economic factors that may prompt or delay PC replacement. This will involve the application of variants of the 'bathtub' distribution curve e.g. the 'saw tooth bathtub', to capture PC replacement after different periods. Simplifying assumptions will be made e.g. categorising excessively long interruptions (>MTTR) as direct requirements for early PC replacement.

6.2.2.2 Network and Load Modelling

It is also true that the generic LV and MV network models can be more representative of the actual distribution networks by updating them with location-optimised MG, shunt capacitors, isolators, etc. This can also look at possible microgrid applications for improvement of the local CoS by including e.g. peer-to-peer trading, and energy arbitrage i.e. taking advantage of time-varying electricity prices by selling/reducing demand at appropriate times. Not to mention, the load models used in the future work will consider both the seasonal variations of the demand profile as well as the daily temporal variation that is currently considered. In addition, dynamic modelling will be used to develop accurate coefficients for polynomial or exponential load models that will adequately categorise different load types (e.g. constant impedance, current and power used in static models), especially for transient studies.

6.2.2.3 MCS Resolution

The current time-sequential MCS methodology based on SDS has got a significant limitation of the resolution. For more accurate reliability assessments, it is necessary to model the minimum length of a time step to be at least the length of a SI (3 min in the UK, 1 min in the USA). Invariably, the higher resolution (i.e. smaller timesteps) increases the computational burden and requires more advanced methods for faster MCS convergence. Therefore, on top of investigating variance reduction/MCS acceleration techniques such as control and antithetic variates [125], the future work will also assess how Multilevel MCS [161, 162] methods may be used to enable time-step reduction. This MCS resolution enhancement will have the added advantage of allowing for an integrated reliability and power quality analysis as these smaller timesteps will make it possible to perform transient studies.

6.2.2.4 Range of Reliability Indices

The range of the reliability performance results should be extended by disaggregating the standard reliability indices into component-based contributions, to further propose reliability enhancement solutions such as targeted asset replacement or preventive maintenance, which are cognisant of pre-existing network infrastructure. This should be accompanied by disaggregation of fault statistics and reported reliability metrics by load-sector (rural, suburban, urban) as recommended by CEER [21]. Furthermore, probability boxes [163], which are often used in risk analysis or quantitative uncertainty modelling, will also be used to illustrate results due to the variability of DERs, the empirical distributions of PC reliability data (failure rates and repair times), and realised reliability indices. This uncertainty about the probability distribution shapes of both inputs (PC reliability data) and outputs (indices) can be better characterised

using techniques e.g. confidence bands, which are distribution-free i.e. making no assumption about the shape of the underlying distribution.

6.2.3 Model Order Reduction

6.2.3.1 Computation of System Gramians

The proposed MOR-for-reliability methodology represents a significant step towards a simplified and accurate analysis of aggregating complex networks. Nevertheless, the proposed approach exhibits a few limitations. With the current formulation, the number of PCs of the original system that can be modelled is limited by hardware constraints. The two main computational-memory bottlenecks arise from building the state transition matrix A (4.13) and obtaining the system Gramians (4.4) by solving computationally expensive Lyapunov equations [89, 164]. In this thesis, these issues were tackled by developing ad-hoc programming solutions and adopting the matrix equation sparse solver (MESS) toolbox [165] for a more efficient resolution of high-order Lyapunov equations. In future work, different techniques will be explored to obtain a faster computation of the relevant Gramian matrices, allowing for the simulation of larger systems. These techniques will exploit the low-rank property for solutions of large-scale, sparse Lyapunov equations [89] e.g. methods based on the Arnoldi process [166, 167] and Krylov subspace methods [167, 168]. A distributed system reduction will also be investigated, deriving the simplified grid model as a collection of smaller interconnected systems, each obtained with the proposed MOR approach.

6.2.3.2 Time-varying Failure Rates and PC Ageing

The current MOR methodology only utilises constant PC failure and repair rates to construct the state space representation as given by (4.1). This means that unlike the analyses presented in Chapter 3, the proposed methodology in Chapter 4 cannot adequately account for PC ageing (using the expected lifetime bathtub for example) which is important for accurate reliability analyses. Moreover, the use of spatially disaggregated PC failure rates is important to ensure that the effects of varying network topologies and load sectors (urban, suburban and rural) are accurately modelled in reduced-order networks. Future work will implement these enhancements by utilising alternative MOR techniques presented in the literature for time-varying dynamical systems, such as the ones in [169, 170] which are also reliant on balanced truncation, as utilised in this thesis.

6.2.3.3 Markov Property of Reduced Order Models

For MCS analyses, the current methodology only returns models of order $r = 2$. Higher values of r result in system matrices A in (4.13) that are not in Metzler form. Therefore, the associated system lacks the Markov property and cannot be simulated with MCS methods. Future research will test new methods for the approximation of Metzler matrices. Work in [171, 172] investigated this aspect but the proposed methods were not directly applicable to reliability studies because they focused on the stability of the resultant Metzler matrix rather than its Markovian properties. Another alternative will also be to compare the proposed approach with other MOR approaches e.g. moment-matching.

6.2.3.4 Reliability Metrics for Frequency and Duration of Interruptions

The frequency and duration of interruptions are not explicitly included in the chosen state-space representation (4.1) of the system reliability. This means that reliability metrics - SAIFI and SAIDI can be calculated ex-post with the time-sequential MCSs but cannot be used as relevant metrics over which the approximation error of the proposed MOR procedure is minimised. However, SAIFI and SAIDI represent two fundamental indices in the evaluation of network reliability and therefore, to explicitly consider them in the MOR procedure, the current model will be expanded in future works, for example including additional states in (4.13) that keep track of the failure times of the different power components.

6.3 Future Research Directions

Further to the aspects of future research already described, the most promising alternative to the current aggregation methodology limitations is to use machine learning for network aggregation. Like MOR, this technique has already demonstrated wide applicability in power engineering research problems as well as for reliability assessment [173, 174]. However, machine learning has not yet been used for the specific purpose of network aggregation for reliability. Studies such as [175] represent a good starting point for its application as an extension of the results presented in this thesis. Therefore, future research will aim to develop a network aggregation methodology that utilises traditional machine learning algorithms or artificial neural networks for state-space classification. This will then be integrated into the already developed time-sequential MCS methods to produce a reliability assessment approach that will overcome network complexity in terms of system topology, the stochastic distribution of faults, and the demand usage patterns. The major contribution will be the provision of reliability equivalent models that represent the most important system states while providing substantial savings in

the computational time required for reliability analyses. Moreover, the use of machine learning will introduce a 'dynamic' reliability assessment that will take advantage of new system conditions to produce "on-line" updates of reduced-order models. This will be integrated into the general theme of this research which is to assess SGT impacts in more accurate ways. It is also important to mention that techniques based on artificial neural networks have been used to monitor distribution systems where the emphasis is on overcoming the complexity added by DG installations [176].

Future research will also explore the quantification of the financial impact of the reliability-improvement solutions proposed by the deployment of smart grid functionalities through known/estimated cost implications. It will invariably include the development of new customer and system based economic-reliability indices. The resultant economically integrated reliability assessment methodology will provide economic justifications from a reliability perspective, in addition to the enhancements (justifications) in terms of improved network performance through implementation of SGTs. Hopefully, this will not only serve as an impetus for DNOs to consider SGT applications for network performance improvements but also encourage the use of fully integrated fast reliability methods in core planning processes and maintenance procedures for distribution networks.

References

[1] IEA, "European Union 2020: Energy Policy Review," *IEA*, 2020.

[2] European Parliament, "Directive (EU) 2018/2001 of the European Parliament and of the Council of 11 December 2018 on the promotion of the use of energy from renewable sources (Text with EEA relevance.)," tech. rep., European Parliament, 2018.

[3] BEIS, "The UK National Energy and Climate Plan (NECP)," Tech. Rep. January, BEIS, 2019.

[4] UK Parliament, "The Climate Change Act 2008 (2050 Target Amendment) Order 2019," *Statutory Instruments*, vol. 1056, 2019.

[5] M. AlMuhaini, "Impact of Distributed Generation Integration on the Reliability of Power Distribution Systems," in *Distributed Generation Systems*, pp. 453–508, London, England: Elsevier, first edit ed., 2017.

[6] National Grid ESO, "Future Energy Scenarios," tech. rep., National Grid ESO, 2020.

[7] National Grid, "Balancing services | National Grid," 2017.

[8] FERC, "U.S. Energy Independence and Security Act of 2007," tech. rep., FERC, Washington, DC, 2007.

[9] J. L. Acosta, K. Combe, S. Z. Djokic, and I. Hernando-Gil, "Performance Assessment of Micro and Small-Scale Wind Turbines in Urban Areas," *IEEE Systems Journal*, vol. 6, pp. 152–163, Mar 2012.

[10] G. Strbac, C. Ramsay, and D. Pudjianto, "Integration of distributed generation into the UK power system," tech. rep., OFGEM, 2007.

[11] OFGEM, "RIIO-ED1 Annual Report," tech. rep., OFGEM, London, UK, 2016.

[12] K. Alvehag and K. Awodele, "Impact of Reward and Penalty Scheme on the Incentives for Distribution System Reliability," *IEEE Transactions on Power Systems*, vol. 29, pp. 386–394, Jan 2014.

[13] SP Energy Networks, "SP Energy Networks Distribution Annual Report 2017/18," Tech. Rep. December, SP Energy Networks, 2018.

[14] Western Power Distribution, "RIIO-ED1 Business Plan Commitments Summary report Year four 2018/2019," tech. rep., Western Power Distribution, 2019.

[15] Energy Networks Association, "TSO-DSO Project-Forward Plan for Work," tech. rep., Energy Networks Association (ENA), 2017.

[16] R. Ghorani, M. Fotuhi-Firuzabad, P. Dehghanian, and W. Li, "Identifying critical components for reliability centred maintenance management of deregulated power systems," *IET Generation, Transmission & Distribution*, vol. 9, pp. 828–837, Mar 2015.

[17] L. Bertling, R. Allan, and R. Eriksson, "A Reliability-Centered Asset Maintenance Method for Assessing the Impact of Maintenance in Power Distribution Systems," *IEEE Transactions on Power Systems*, vol. 20, pp. 75–82, Feb 2005.

[18] The Institution of Engineering and Technology, "Modelling Requirements for GB Power System Resilience during the transition to Low Carbon Energy," tech. rep., The Institution of Engineering and Technology, 2015.

[19] R. Billinton and R. N. Allan, *Reliability Evaluation of Power Systems*. Boston, MA: Springer US, 2nd ed. ed., 1996.

[20] S. Djokic, I. Irinel-Sorin, and I. Hernando-Gil, "Integrated assessment of quality of supply in future electricity networks," Tech. Rep. Closed, University of Edinburgh, Edinburgh, 2013.

[21] CEER, "6th CEER benchmarking report on the quality of electricity and gas supply," tech. rep., Council of European Energy Regulators, Brussels, Belgium, 2016.

[22] OFGEM, "Reliability Incentive Methodology Statement," tech. rep., OFGEM, London, UK,, 2016.

[23] CEER, "Annex A Electricity – Continuity of supply," tech. rep., Council of European Energy Regulators, Brussels, Belgium, 2016.

[24] Ofgem, "RIIO-ED2 Framework Decision," tech. rep., OFGEM, London, UK, 2020.

[25] Energy Networks Association, "Engineering Recommendation P2 Issue 7 2019," Tech. Rep. 7, Energy Networks Association (ENA),, London, UK, 2019.

[26] Accent, "Expectations of DNOs & Willingness to Pay for Improvements in Service," Tech. Rep. July, Accent, London, UK, 2008.

[27] Accent, "Willingness to Pay Market Research SPN," tech. rep., Accent, London, UK, 2013.

[28] Statutory Instruments, "The Electricity (Connection Standards of Performance) Regulations 2015," 2015.

[29] OFGEM, "Report-RIIO-ED1 Annual Report," tech. rep., OFGEM, London, UK, 2018.

[30] G. Kjolle and K. Sand, "RELRAD–An analytical approach for distribution system reliability assessment," in *Proceedings of the 1991 IEEE Power Engineering Society Transmission and Distribution Conference*, pp. 729–734, IEEE, 1992.

[31] P. Sharma, N. Gupta, K. R. Niazi, and A. Swarnkar, "Investigation of network reconfiguration on the reliability and performance of distribution systems using CRO," in *2017 6th International Conference on Computer Applications In Electrical Engineering-Recent Advances (CERA)*, vol. 2018-Janua, pp. 80–85, IEEE, Oct 2017.

[32] N. Gupta, A. Swarnkar, and K. Niazi, "Distribution network reconfiguration for power quality and reliability improvement using Genetic Algorithms," *International Journal of Electrical Power & Energy Systems*, vol. 54, pp. 664–671, Jan 2014.

[33] CEER, "5th CEER Benchmarking Report on Quality of Electricity Supply 2011," tech. rep., Council of European Energy Regulators, Brussels, Belgium, 2011.

[34] Kunaifi and A. Reinders, "Perceived and Reported Reliability of the Electricity Supply at Three Urban Locations in Indonesia," *Energies*, vol. 11, p. 140, Jan 2018.

[35] CEER, "Third Benchmarking Report on Quality of Electricity Supply 2005," Tech. Rep. DECEMBER, Council of European Energy Regulators, Brussels, Belgium, 2005.

[36] S. C. Vegunta, C. F. A. Watts, S. Z. Djokic, J. V. Milanović, and M. J. Higginson, "Review of GB electricity distribution system's electricity security of supply, reliability and power quality in meeting UK industrial strategy requirements," *IET Generation, Transmission and Distribution*, vol. 13, pp. 3513–3523, Aug 2019.

[37] N. Hadjsaïd and J. C. Sabonnadière, *Electrical Distribution Networks*. Hoboken, NJ, USA: John Wiley & Sons, Inc., Jan 2013.

[38] I. Hernando Gil, *Integrated assessment of quality of supply in future electricity networks*. PhD thesis, The University of Edinburgh, 2014.

[39] W. Li, *Risk Assessment of Power Systems: Models, Methods, and Applications: Second Edition*, vol. 9781118686. Hoboken, NJ, USA: John Wiley & Sons, Inc., Mar 2014.

[40] NERC, "Glossary of terms used in research," in *Research Methods*, pp. 575–587, Elsevier, 2018.

[41] D. J. Smith, *Reliability, Maintainability and Risk 8e*. GB: Elsevier, ninth edit ed., 2011.

[42] R. Billinton and R. N. Allan, *Reliability Evaluation of Engineering Systems*. Boston, MA: Springer US, 1992.

[43] Institute of Electrical and Electronics Engineers, "IEEE Std 1159 - IEEE Recommended Practice for Monitoring Electric Power Quality.," *IEEE Std 1159-2009 (Revision of IEEE Std 1159-1995)*, vol. 2009, no. June, pp. 1–81, 2009.

[44] Institute of Electrical and Electronics Engineers, "IEEE Guide for Electric Power Distribution Reliability Indices," 2012.

[45] G. Strbac, D. Kirschen, and R. Moreno, "Reliability Standards for the Operation and Planning of Future Electricity Networks," *Foundations and Trends® in Electric Energy Systems*, vol. 1, no. 1, pp. 143–219, 2016.

[46] A. Moreira, B. Fanzeres, and G. Strbac, "Energy and reserve scheduling under ambiguity on renewable probability distribution," *Electric Power Systems Research*, vol. 160, pp. 205–218, Jul 2018.

[47] R. Moreno and G. Strbac, "Integrating high impact low probability events in smart distribution network security standards through cvar optimisation," in *IET Conference Publications*, vol. 2015, pp. 9 (6 .)–9 (6 .), Institution of Engineering and Technology, 2015.

[48] G. De Vanna, M. Longo, F. Foiadelli, M. Panteli, and M. Galeela, "Reliability and Resilience Analysis and Comparison of Off-Grid Microgrids," in *2020 55th International Universities Power Engineering Conference (UPEC)*, pp. 1–6, IEEE, Sep 2020.

[49] S. Espinoza, A. Poulos, H. Rudnick, J. C. de la Llera, M. Panteli, and P. Mancarella, "Risk and Resilience Assessment With Component Criticality Ranking of Electric Power Systems Subject to Earthquakes," *IEEE Systems Journal*, vol. 14, pp. 2837–2848, Jun 2020.

[50] R. Billinton and W. Li, "A system state transition sampling method for composite system reliability evaluation," *IEEE Transactions on Power Systems*, vol. 8, no. 3, pp. 761–770, 1993.

[51] R. Billinton and A. Jonnavithula, "Application of the state transition sampling technique to system reliability evaluation," *Quality and Reliability Engineering International*, vol. 13, pp. 311–315, Sep 1997.

[52] M. Hlatshwayo, S. Chowdhury, S. Chowdhury, and K. Awodele, "Impacts of DG penetration in the reliability of Distribution Systems," in *2010 International Conference on Power System Technology*, pp. 1–8, IEEE, Oct 2010.

[53] L. Ochoa, C. Dent, and G. Harrison, "Maximisation of intermittent distributed generation in active networks," in *CIRED Seminar 2008: SmartGrids for Distribution*, pp. 6–6, IEE, 2008.

[54] G. M. Masters, *Renewable and Efficient Electric Power Systems*. Hoboken, NJ, USA: John Wiley & Sons, Inc., Jul 2004.

[55] Y. Wang, X. Lin, and M. Pedram, "Adaptive Control for Energy Storage Systems in Households With Photovoltaic Modules," *IEEE Transactions on Smart Grid*, vol. 5, pp. 992–1001, Mar 2014.

[56] X. Liu, A. Aichhorn, L. Liu, and H. Li, "Coordinated Control of Distributed Energy Storage System With Tap Changer Transformers for Voltage Rise Mitigation Under High Photovoltaic Penetration," *IEEE Transactions on Smart Grid*, vol. 3, pp. 897–906, Jun 2012.

[57] M. J. Alam, K. M. Muttaqi, and D. Sutanto, "A novel approach for ramp-rate control of solar PV using energy storage to mitigate output fluctuations caused by cloud passing," *IEEE Transactions on Energy Conversion*, vol. 29, pp. 507–518, Jun 2014.

[58] D. Cheng, B. A. Mather, R. Seguin, J. Hambrick, and R. P. Broadwater, "Photovoltaic (PV) impact assessment for very high penetration levels," *IEEE Journal of Photovoltaics*, vol. 6, pp. 295–300, Jan 2016.

[59] R. Tonkoski, L. A. C. Lopes, and T. H. M. El-Fouly, "Coordinated Active Power Curtailment of Grid Connected PV Inverters for Overvoltage Prevention," *IEEE Transactions on Sustainable Energy*, vol. 2, pp. 139–147, Apr 2011.

[60] A. J. Collin, I. Hernando-Gil, J. L. Acosta, I. S. Ilie, and S. Z. Djokic, "Realising the potential of smart grids in LV networks. Part 2: Microgeneration," in *IEEE PES Innovative Smart Grid Technologies Conference Europe*, pp. 1–8, IEEE, Dec 2011.

[61] A. Faza, "A probabilistic model for estimating the effects of photovoltaic sources on the power systems reliability," *Reliability Engineering & System Safety*, vol. 171, pp. 67–77, Mar 2018.

[62] T. Adefarati and R. C. Bansal, "Reliability, economic and environmental analysis of a microgrid system in the presence of renewable energy resources," *Applied Energy*, vol. 236, pp. 1089–1114, Feb 2019.

[63] A. Ngaopitakkul and C. Jettanasen, "The effects of multi-distributed generator on distribution system reliability," in *2017 IEEE Innovative Smart Grid Technologies - Asia: Smart Grid for Smart Community, ISGT-Asia 2017*, pp. 1–6, IEEE, Dec 2018.

[64] M. R. Siddappaji and K. Thippeswamy, "Reliability indices evaluation and optimal placement of distributed generation for loss reduction in distribution system by using fast decoupled method," in *2017 International Conference on Energy, Communication, Data Analytics and Soft Computing, ICECDS 2017*, pp. 3171–3174, IEEE, Aug 2018.

[65] Elexon, "Guidance Load Profiles and their use in Electricity Settlement," tech. rep., Elexon, London, UK, 2018.

[66] B. Hayes, I. Hernando-Gil, A. Collin, G. Harrison, and S. Djokic, "Optimal Power Flow for Maximizing Network Benefits From Demand-Side Management," *IEEE Transactions on Power Systems*, vol. 29, pp. 1739–1747, Jul 2014.

[67] European Parliament, "Directive 2012/27/EU of the European Parliament and of the Council of 25 October 2012 on energy efficiency, amending Directives 2009/125/EC and 2010/30/EU and repealing Directives 2004/8/EC and 2006/32/EC," Tech. Rep. October 2012, European Parliament, 2012.

[68] E. Proffitt, "Profiting from Demand Side Response The Major Energy Users' Council in association with National Grid," tech. rep., Major Energy Users' Council, Britain, 2017.

[69] A. J. Collin, I. Hernando-Gil, J. L. Acosta, I.-S. Ilie, and S. Z. Djokic, "Realising the potential of smart grids in LV networks. Part 1: Demand-side management," in *2011 2nd IEEE PES International Conference and Exhibition on Innovative Smart Grid Technologies*, pp. 1–7, IEEE, Dec 2011.

[70] M. Song, M. Amelin, E. Shayesteh, and P. Hilber, "Impacts of flexible demand on the reliability of power systems," in *2018 IEEE Power & Energy Society Innovative Smart Grid Technologies Conference (ISGT)*, pp. 1–5, IEEE, Feb 2018.

[71] I. Hernando-Gil, B. Hayes, A. Collin, and S. Djokic, "Distribution network equivalents for reliability analysis. Part 2: Storage and demand-side resources," in *IEEE PES ISGT Europe 2013*, pp. 1–5, IEEE, Oct 2013.

[72] R. B. Bass, J. Carr, J. Aguilar, and K. Whitener, "Determining the Power and Energy Capacities of a Battery Energy Storage System to Accommodate High Photovoltaic Penetration on a Distribution Feeder," *IEEE Power and Energy Technology Systems Journal*, vol. 3, pp. 119–127, Sep 2016.

[73] J. Sa'ed, S. Favuzza, F. Massaro, and E. Telaretti, "Optimization of BESS Capacity Under a Peak Load Shaving Strategy," in *2018 IEEE International Conference on Environment and Electrical Engineering and 2018 IEEE Industrial and Commercial Power Systems Europe (EEEIC / I&CPS Europe)*, pp. 1–4, IEEE, Jun 2018.

[74] Y. Zheng, K. Meng, F. Luo, J. Qiu, and J. Zhao, "Optimal integration of MBESSs/S-BESSs in distribution systems with renewables," *IET Renewable Power Generation*, vol. 12, pp. 1172–1179, Jul 2018.

[75] Z. Qiao and J. Yang, "Comparison of centralised and distributed battery energy storage systems in LV distribution networks on operational optimisation and financial benefits," *The Journal of Engineering*, vol. 2017, pp. 1671–1675, Jan 2017.

[76] Bagen and R. Billinton, "Impacts of energy storage on power system reliability performance," in *Canadian Conference on Electrical and Computer Engineering, 2005.*, vol. 2005, pp. 494–497, IEEE, 2005.

[77] L. Koh, G. Z. Yong, W. Peng, and K. Tseng, "Impact of Energy Storage and Variability of PV on Power System Reliability," *Energy Procedia*, vol. 33, pp. 302–310, 2013.

[78] F. Mohamad and J. Teh, "Impacts of Energy Storage System on Power System Reliability: A Systematic Review," *Energies*, vol. 11, p. 1749, Jul 2018.

[79] D. Mohler and D. Sowder, "Energy Storage and the Need for Flexibility on the Grid," in *Renewable Energy Integration* (L. E. B. T. R. E. I. S. E. Jones, ed.), pp. 309–316, Boston: Elsevier, 2017.

[80] S. M. Ashraf, B. Rathore, and S. Chakrabarti, "Performance analysis of static network reduction methods commonly used in power systems," in *2014 Eighteenth National Power Systems Conference (NPSC)*, (Guwahati, India), pp. 1–6, IEEE, Dec 2014.

[81] P. Fortenbacher, T. Demiray, and C. Schaffner, "Transmission Network Reduction Method Using Nonlinear Optimization," in *2018 Power Systems Computation Conference (PSCC)*, (Dublin, Ireland), pp. 1–7, IEEE, Jun 2018.

[82] N. D. Tleis, *Power Systems Modelling and Fault Analysis*. Elsevier, 1st editio ed., 2008.

[83] Y. Jiang, N. Acharya, and Y. Pan, "Model reduction for fast assessment of grid impact of high penetration PV," in *2017 19th International Conference on Intelligent System Application to Power Systems, ISAP 2017*, pp. 1–6, IEEE, Sep 2017.

[84] M. Todinov, "Methods for Analysis of Complex Reliability Networks," in *Risk-Based Reliability Analysis and Generic Principles for Risk Reduction* (M. T. Todinov, ed.), pp. 31–58, Oxford: Elsevier, 2007.

[85] R. Billinton and P. Wang, "Reliability-network-equivalent approach to distribution-system-reliability evaluation," *IEE Proceedings: Generation, Transmission and Distribution*, vol. 145, no. 2, pp. 149–153, 1998.

[86] I.-S. Ilie, I. Hernando-Gil, and S. Z. Djokic, "Reliability equivalents of LV and MV distribution networks," in *2012 IEEE International Energy Conference and Exhibition (ENERGYCON)*, pp. 343–348, IEEE, Sep 2012.

[87] A. Antoulas, "Approximation of Large-Scale Dynamical Systems: An Overview," *IFAC Proceedings Volumes*, vol. 37, pp. 19–28, Jul 2004.

[88] K. J. K. J. Astrom, *Feedback systems : an introduction for scientists and engineers*. Princeton, N.J. ; Woodstock: Princeton University Press, 2008.

[89] U. Baur, P. Benner, and L. Feng, "Model Order Reduction for Linear and Nonlinear Systems: A System-Theoretic Perspective," *Archives of Computational Methods in Engineering*, vol. 21, pp. 331–358, Dec 2014.

[90] C. M. Rergis, R. J. Betancourt, and A. R. Messina, "Order Reduction of Power Systems by Modal Truncated Balanced Realization," *Electric Power Components and Systems*, vol. 45, pp. 147–158, Jan 2017.

[91] L. Nechak, H. F. Raynaud, and C. Kulcsár, "Model order reduction of random parameter-dependent linear systems," *Automatica*, vol. 55, pp. 95–107, May 2015.

[92] A. K. Prajapati and R. Prasad, "A New Model Reduction Method for the Linear Dynamic Systems and Its Application for the Design of Compensator," *Circuits, Systems, and Signal Processing*, vol. 39, pp. 2328–2348, May 2020.

[93] X. Lan, H. Zhao, Y. Wang, and Z. Mi, "Nonlinear power system model reduction based on empirical gramians," in *2016 IEEE International Conference on Power System Technology, POWERCON 2016*, (Wollongong, NSW, Australia), pp. 1–6, IEEE, Sep 2016.

[94] J. Qi, J. Wang, H. Liu, and A. D. Dimitrovski, "Nonlinear Model Reduction in Power Systems by Balancing of Empirical Controllability and Observability Covariances," *IEEE Transactions on Power Systems*, vol. 32, pp. 114–126, Jan 2017.

[95] H. S. Zhao, N. Xue, and N. Shi, "Nonlinear dynamic power system model reduction analysis using balanced empirical Gramian," in *Applied Mechanics and Materials*, vol. 448-453 of *Applied Mechanics and Materials*, pp. 2368–2374, Trans Tech Publications Ltd, Oct 2014.

[96] S. S. Mohseni, M. J. Yazdanpanah, and A. Ranjbar Noei, "Model Reduction of Nonlinear Systems by Trajectory Piecewise Linear Based on Output-Weighting Models: A Balanced-Truncation Methodology," *Iranian Journal of Science and Technology - Transactions of Electrical Engineering*, vol. 42, pp. 195–206, Jun 2018.

[97] D. Osipov and K. Sun, "Adaptive nonlinear model reduction for fast power system simulation," *IEEE Transactions on Power Systems*, vol. 33, pp. 6746–6754, Nov 2018.

[98] F. D. Freitas, J. Rommes, and N. Martins, "Gramian-based reduction method applied to large sparse power system descriptor models," *IEEE Transactions on Power Systems*, vol. 23, pp. 1258–1270, Aug 2008.

[99] Y. G. I. Acle, F. D. Freitas, N. Martins, and J. Rommes, "Parameter Preserving Model Order Reduction of Large Sparse Small-Signal Electromechanical Stability Power System Models," *IEEE Transactions on Power Systems*, vol. 34, pp. 2814–2824, Jul 2019.

[100] W. Liu, D. Guo, Y. Xu, R. Cheng, Z. Wang, and Y. Li, "Reliability assessment of power systems with photovoltaic power stations based on intelligent state space reduction and pseudo-sequential monte carlo simulation," *Energies*, vol. 11, p. 1431, Jun 2018.

[101] T. Gafurov, M. Prodanovic, and J. Usaola, "PV system model reduction for reliability assessment studies," in *2013 4th IEEE/PES Innovative Smart Grid Technologies Europe, ISGT Europe 2013*, (Lyngby, Denmark), pp. 1–5, IEEE, Oct 2013.

[102] L. Wang and W. Long, "Dynamic model reduction of power electronic interfaced generators based on singular perturbation," *Electric Power Systems Research*, vol. 178, p. 106030, Jan 2020.

[103] M. Rasheduzzaman, J. A. Mueller, and J. W. Kimball, "Reduced-Order Small-Signal Model of Microgrid Systems," *IEEE Transactions on Sustainable Energy*, vol. 6, pp. 1292–1305, Oct 2015.

[104] M. Kudryavtsev, E. Rudnyi, J. Korvink, D. Hohlfeld, and T. Bechtold, "Computationally efficient and stable order reduction methods for a large-scale model of MEMS piezoelectric energy harvester," *Microelectronics Reliability*, vol. 55, pp. 747–757, Apr 2015.

[105] Z. Zhu, G. Geng, and Q. Jiang, "Power System Dynamic Model Reduction Based on Extended Krylov Subspace Method," *IEEE Transactions on Power Systems*, vol. 31, pp. 4483–4494, Nov 2016.

[106] G. Scarciotti, "Low Computational Complexity Model Reduction of Power Systems With Preservation of Physical Characteristics," *IEEE Transactions on Power Systems*, vol. 32, pp. 743–752, Jan 2017.

[107] B. Retterath, S. Venkata, and A. Chowdhury, "Impact of time-varying failure rates on distribution reliability," *International Journal of Electrical Power & Energy Systems*, vol. 27, pp. 682–688, Nov 2005.

[108] S. Wang, Z. Li, L. Wu, M. Shahidehpour, and Z. Li, "New Metrics for Assessing the Reliability and Economics of Microgrids in Distribution System," *IEEE Transactions on Power Systems*, vol. 28, pp. 2852–2861, Aug 2013.

[109] H. Suyono, Wijono, R. N. Hasanah, and S. Dhuha, "Power distribution system reliability improvement due to injection of distributed generation," in *2017 10th International Conference on Electrical and Electronics Engineering, ELECO 2017*, vol. 2018-Janua, pp. 1485–1490, 2018.

[110] I.-S. Ilie, I. Hernando-Gil, and S. Z. Djokic, "Risk assessment of interruption times affecting domestic and non-domestic electricity customers," *International Journal of Electrical Power & Energy Systems*, vol. 55, pp. 59–65, Feb 2014.

[111] J.-P. Zimmermann, M. Evans, T. Lineham, J. Griggs, G. Surveys, L. Harding, N. King, and P. Roberts, "Household Electricity Survey: A study of domestic electrical product usage," tech. rep., Intertek, Milton Keynes, UK, 2012.

[112] P. Lyons, P. Trichakis, R. Hair, and P. Taylor, "Predicting the technical impacts of high levels of small-scale embedded generators on low-voltage networks," *IET Renewable Power Generation*, vol. 2, pp. 249–262, Dec 2008.

[113] CEER, "4th Benchmarking Report on the Quality of Electricity Supply," tech. rep., Council of European Energy Regulators, Brussels, Belgium, 2008.

[114] T. Haggis, "Network Design Manual," Tech. Rep. December, E-ON Central Networks, UK, 2006.

[115] E. Lakervi and E. J. Holmes, *Electricity Distribution Network Design*. Stevenage: Institution of Engineering and Technology, 2nd ed. ed., Jan 2003.

[116] SSE, "Information to assist third parties in the design and installation of secondary substations," tech. rep., SSE, Scotland, 2012.

[117] I. Hernando-Gil, B. Hayes, A. Collin, and S. Djokić, "Distribution network equivalents for reliability analysis. Part 1: Aggregation methodology," in *2013 4th IEEE/PES Innovative Smart Grid Technologies Europe, ISGT Europe 2013*, (Lyngby, Denmark), pp. 1–5, IEEE, Oct 2013.

[118] BSI, "BS EN 50160:2010 Voltage characteristics of electricity supplied by public electricity networks," 2011.

[119] I. Hernando-Gil, I. S. Ilie, and S. Z. Djokic, "Reliability planning of active distribution systems incorporating regulator requirements and network-reliability equivalents," *IET Generation, Transmission and Distribution*, vol. 10, pp. 93–106, Jan 2016.

[120] M. B. Ndawula, S. Z. Djokic, and I. Hernando-Gil, "Reliability enhancement in power networks under uncertainty from distributed energy resources †," *Energies*, vol. 12, p. 531, Feb 2019.

[121] Peng Wang and R. Billinton, "Reliability cost/worth assessment of distribution systems incorporating time-varying weather conditions and restoration resources," *IEEE Transactions on Power Delivery*, vol. 17, no. 1, pp. 260–265, 2002.

[122] D. C. Montgomery and G. C. Runger, *Applied Statistics and Probability for Engineers, 5th Edition*. Wiley, 5th ed. ed., 2010.

[123] Univesity of Utah, "Numerical Integration," tech. rep., Univesity of Utah, Utah, USA, 2014.

[124] S. Z. Djokic, I.-S. Ilie, and I. Hernando-Gil, "Theoretical interruption model for reliability assessment of power supply systems," *IET Generation, Transmission & Distribution*, vol. 8, pp. 670–681, Apr 2014.

[125] R. Billinton and W. Li, *Reliability Assessment of Electric Power Systems Using Monte Carlo Methods*. Boston, MA: Springer US, 1994.

[126] A. B. Ocnasu, Y. Besanger, P. Carer, R. Edf, and D. France, "Distribution System Availability Assessment Monte Carlo and Antithetic Variates Method," *19 th International Conference on Electricity Distribution*, no. 0268, pp. 21–24, 2007.

[127] M. B. Ndawula, *Reliability Modelling with Stochastic Behaviour of Intermittent Renewable Resources*. Master's thesis, University of Bath, 2017.

[128] M. L. Ellery, M. B. Ndawula, and I. Hernando-Gil, "Reliability Enhancement of LV Rural Networks using Smart Grid Technologies," in *2019 International Conference on Smart Energy Systems and Technologies (SEST)*, pp. 1–5, IEEE, Sep 2019.

[129] S. Halbe, B. Chowdhury, and A. Abbas, "Mitigating Rebound Effect of Demand Response using Battery Energy Storage and Electric Water Heaters," in *2019 IEEE 16th International Conference on Smart Cities: Improving Quality of Life Using ICT & IoT and AI (HONET-ICT)*, pp. 095–099, IEEE, Oct 2019.

[130] I. Hernando-Gil, Z. Zhang, M. B. Ndawula, and S. Djokic, "DG Locational Incremental Contribution to Grid Supply Level," *2020 IEEE International Conference on Environment and Electrical Engineering and 2020 IEEE Industrial and Commercial Power Systems Europe (EEEIC / I&CPS Europe)*, pp. 1–6, Jun 2020.

[131] U.S. Department of Energy, "High Penetration of Photovoltaic (PV) Systems into the Distribution Grid," Tech. Rep. June, U.S. Department of Energy, Ontario, CA, 2009.

[132] B. Mather and R. Neal, "Integrating high penetrations of PV into Southern California: Year 2 project update," in *2012 38th IEEE Photovoltaic Specialists Conference*, pp. 000737–000741, IEEE, Jun 2012.

[133] M. B. Ndawula, P. Zhao, and I. Hernando-Gil, "Smart Application of Energy Management Systems for Distribution Network Reliability Enhancement," in *Proceedings - 2018 IEEE International Conference on Environment and Electrical Engineering and 2018 IEEE Industrial and Commercial Power Systems Europe, EEEIC/I and CPS Europe 2018*, (Palermo, Italy), pp. 1–5, IEEE, Jun 2018.

[134] J. W. Smith, R. Dugan, and W. Sunderman, "Distribution modeling and analysis of high penetration PV," in *2011 IEEE Power and Energy Society General Meeting*, pp. 1–7, IEEE, Jul 2011.

[135] J. W. Smith, R. Dugan, M. Rylander, and T. Key, "Advanced distribution planning tools for high penetration PV deployment," in *IEEE Power and Energy Society General Meeting*, pp. 1–7, IEEE, Jul 2012.

[136] G. W. Chang, Y. H. Chen, L. Y. Hsu, Y. Y. Chen, Y. R. Chang, and Y. D. Lee, "Study of impact on high PV-penetrated feeder voltage due to moving cloud shadows," in *Proceedings - 2016 IEEE International Symposium on Computer, Consumer and Control, IS3C 2016*, pp. 1067–1070, IEEE, Jul 2016.

[137] I. Graabak and M. Korpås, "Variability Characteristics of European Wind and Solar Power Resources—A Review," *Energies*, vol. 9, p. 449, Jun 2016.

[138] D. Zhang, J. Guo, and J. Li, "Coordinated control strategy of hybrid energy storage to improve accommodating ability of PV," *The Journal of Engineering*, vol. 2017, pp. 1555–1559, Jan 2017.

[139] Energy Network Association, "Engineering Recommendation G83 Issue 2," Tech. Rep. 2, Energy Networks Association, London, UK, 2018.

[140] M. B. Ndawula, I. Hernando-Gil, and S. Djokic, "Impact of the Stochastic Behaviour of Distributed Energy Resources on MV/LV Network Reliability," in *2018 IEEE International Conference on Environment and Electrical Engineering and 2018 IEEE Industrial and Commercial Power Systems Europe (EEEIC / I&CPS Europe)*, pp. 1–6, IEEE, Jun 2018.

[141] P. Zhao, I. Hernando-Gil, and H. Wu, "Optimal Energy Operation and Scalability Assessment of Microgrids for Residential Services," in *2018 IEEE International Conference on Environment and Electrical Engineering and 2018 IEEE Industrial and Commercial Power Systems Europe (EEEIC / I&CPS Europe)*, (Palermo, Italy), pp. 1–6, IEEE, Jun 2018.

[142] C. Lili, M. U. Longhua, and L. I. U. Zhong, "Analysis of the operating characteristics of a PV-Diesel-BESS microgrid system," *Power System Protection and Control*, vol. 43, no. 12, pp. 86–91, 2015.

[143] F. Wang, L. Zhou, H. Ren, X. Liu, S. Talari, M. Shafie-khah, and J. P. S. Catalao, "Multi-Objective Optimization Model of Source–Load–Storage Synergetic Dispatch for

a Building Energy Management System Based on TOU Price Demand Response," *IEEE Transactions on Industry Applications*, vol. 54, pp. 1017–1028, Mar 2018.

[144] P. Zhao, H. Wu, C. Gu, and I. Hernando-Gil, "Optimal home energy management under hybrid photovoltaic-storage uncertainty: A distributionally robust chance-constrained approach," *IET Renewable Power Generation*, vol. 13, pp. 1911–1919, Aug 2019.

[145] C. Zhao, S. Dong, C. Gu, F. Li, Y. Song, and N. P. Padhy, "New Problem Formulation for Optimal Demand Side Response in Hybrid AC/DC Systems," *IEEE Transactions on Smart Grid*, vol. 9, pp. 3154–3165, Jul 2018.

[146] TrinaSolar, "TSM_PD14 Datasheet B," tech. rep., TrinaSolar, San Jose, CA, USA, 2017.

[147] T. McDermott and R. Dugan, "Distributed generation impact on reliability and power quality indices," in *2002 Rural Electric Power Conference. Papers Presented at the 46th Annual Conference (Cat. No. 02CH37360)*, (Colorado Springs, CO, USA), pp. D3–1–7, IEEE, 2002.

[148] M. B. Ndawula, A. D. Paola, and I. Hernando-Gil, "Evaluation of Customer-oriented Power Supply Risk with Distributed PV-Storage Energy Systems," in *2019 IEEE Milan PowerTech*, pp. 1–6, IEEE, Jun 2019.

[149] X. Xu, E. Makram, T. Wang, and R. Medeiros, "Customer-oriented planning of distributed generations in an active distribution system," in *IEEE Power and Energy Society General Meeting*, vol. 2015-Septe, pp. 1–5, IEEE, Jul 2015.

[150] R. Moreno, M. Panteli, P. Mancarella, H. Rudnick, T. Lagos, A. Navarro, F. Ordonez, and J. C. Araneda, "From Reliability to Resilience: Planning the Grid Against the Extremes," *IEEE Power and Energy Magazine*, vol. 18, pp. 41–53, Jul 2020.

[151] F. Soudi and K. Tomsovic, "Optimal trade-offs in distribution protection design," *IEEE Transactions on Power Delivery*, vol. 16, pp. 292–296, Apr 2001.

[152] R. Herman, C. Gaunt, and L. Tait, "On the adequacy of electricity reliability indices in South Africa," in *Proceedings of the South African Universities Power Engineering Conference, Johannesburg, 28-30 January 2015*, vol. 1, (Johannesburg), pp. 1–12, 2015.

[153] J. H. Eto and K. H. LaCommare, "Tracking the reliability of the U.S. electric power system: An assessment of publicly available information reported to state public utility commissions," tech. rep., Berkeley Lab, Berkeley CA,, 2013.

[154] M. B. Ndawula, A. De Paola, and I. Hernando-Gil, "Disaggregation of Reported Reliability Performance Metrics in Power Distribution Networks," in *2019 International Con-*

ference on Smart Energy Systems and Technologies (SEST), (Porto, Portugal), pp. 1–6, IEEE, Sep 2019.

[155] C. Singh and J. Mitra, "Composite system reliability evaluation using state space pruning," *IEEE Transactions on Power Systems*, vol. 12, no. 1, pp. 471–479, 1997.

[156] J. He, Y. Sun, D. Kirschen, C. Singh, and L. Cheng, "State-space partitioning method for composite power system reliability assessment," *IET Generation, Transmission & Distribution*, vol. 4, no. 7, p. 780, 2010.

[157] M. Todinov, *Risk-Based Reliability Analysis and Generic Principles for Risk Reduction*. Elsevier, 2007.

[158] B. P. Hayes, *Distributed generation and demand side management: Applications to transmission system operation*. PhD thesis, 2013.

[159] R. Billinton, S. Kumar, N. Chowdhury, K. Chu, K. Debnath, L. Goel, E. Khan, P. Kos, G. Nourbakhsh, and J. Oteng-Adjei, "A reliability test system for educational purposes - basic data," *IEEE Transactions on Power Systems*, vol. 4, no. 3, pp. 1238–1244, 1989.

[160] D. Fang, M. Zou, G. P. Harrison, S. Djokic, M. B. Ndawula, X. Xiao, I. Hernando-Gil, and J. Gunda, "Deterministic and Probabilistic Assessment of Distribution Network Hosting Capacity for Wind-Based Renewable Generation," in *2020 IEEE International Conference on Probabilistic Methods Applied to Power Systems (PMAPS)*, pp. 1–6, IEEE, 2020.

[161] L. J. Aslett, T. Nagapetyan, and S. J. Vollmer, "Multilevel Monte Carlo for Reliability Theory," *Reliability Engineering & System Safety*, vol. 165, pp. 188–196, Sep 2017.

[162] A. N. Huda and R. Živanović, "Accelerated distribution systems reliability evaluation by multilevel Monte Carlo simulation: implementation of two discretisation schemes," *IET Generation, Transmission & Distribution*, vol. 11, pp. 3397–3405, Sep 2017.

[163] S. Ferson, M. Balch, K. Sentz, and J. Siegrist, "Computing with confidence," in *ISIPTA 2013 - Proceedings of the 8th International Symposium on Imprecise Probability: Theories and Applications*, pp. 129–138, 2013.

[164] W. H. a. Schilders, H. a. V. D. Vorst, and J. Rommes, *Model Order Reduction: Theory, Research Aspects and Applications*, vol. 13 of *Mathematics in Industry*. Berlin, Heidelberg: Springer Berlin Heidelberg, 1st ed. 20 ed., 2008.

[165] J. Saak, M. Köhler, and P. Benner, "Matrix Equation Sparse Solver," 2019.

[166] K. Jbilou and A. Riquet, "Projection methods for large Lyapunov matrix equations," *Linear Algebra and its Applications*, vol. 415, pp. 344–358, Jun 2006.

[167] M. Hached and K. Jbilou, "Numerical solutions to large-scale differential Lyapunov matrix equations," *Numerical Algorithms*, vol. 79, pp. 741–757, Nov 2018.

[168] V. Simoncini, "A New Iterative Method for Solving Large-Scale Lyapunov Matrix Equations," *SIAM Journal on Scientific Computing*, vol. 29, pp. 1268–1288, Jan 2007.

[169] J. Roychowdhury, "Reduced-order modelling of linear time-varying systems," in *IEEE/ACM International Conference on Computer-Aided Design, Digest of Technical Papers*, (New York, New York, USA), pp. 92–95, ACM Press, 1998.

[170] N. Lang, J. Saak, and T. Stykel, "Balanced truncation model reduction for linear time-varying systems," *Mathematical and Computer Modelling of Dynamical Systems*, vol. 22, pp. 267–281, Jul 2016.

[171] J. Anderson, "Distance to the nearest stable Metzler matrix," in *2017 IEEE 56th Annual Conference on Decision and Control (CDC)*, vol. 2018-Janua, (Melbourne, VIC, Australia), pp. 6567–6572, IEEE, Dec 2017.

[172] T. Kaczorek, "Positive stable realizations with system Metzler matrices," *Archives of Control Sciences*, vol. 21, pp. 167–188, Jan 2011.

[173] N. Amjady and M. Ehsan, "Evaluation of power systems reliability by an artificial neural network," *IEEE Transactions on Power Systems*, vol. 14, no. 1, pp. 287–292, 1999.

[174] A. M. Leite da Silva, L. C. de Resende, L. A. da Fonseca Manso, and V. Miranda, "Composite reliability assessment based on Monte Carlo simulation and artificial neural networks," *IEEE Transactions on Power Systems*, vol. 22, pp. 1202–1209, Aug 2007.

[175] G. Li, Y. Huang, Z. Bie, and T. Ding, "Machine-learning-based reliability evaluation framework for power distribution networks," *IET Generation, Transmission and Distribution*, vol. 14, pp. 2282–2291, Jun 2020.

[176] J. H. Menke, N. Bornhorst, and M. Braun, "Distribution system monitoring for smart power grids with distributed generation using artificial neural networks," *International Journal of Electrical Power and Energy Systems*, vol. 113, pp. 472–480, Dec 2019.

Appendix A

MATLAB Model for MCS based on SDS

This thesis utilises the MATLAB code provided in this appendix to implement the time-sequential MCS methodology provided by Figure 3.9. The code includes use of time-varying PC failure rates and demand profiles (Section 3.2), application of backup action (Section 3.3.1) to alleviate network faults subject to SQS regulations regarding supply loss to GD, and differentiation of system interruptions into SIs and LIs (Section 3.2.1). Also, the code configures the correlation between the moments when faults occur, and the actual load demand interrupted using the theoretical supply interruption model in Figure 3.10. Modifications of this code have been used for the reliability analyses presented in Sections 3.3-3.6.

Input Data and MCS Code

```
%Time-sequential MCS based on SDS for the Suburban MV network%
%Time step = 30 mins%

clear
clc

tic;
%-------------------------------------------
% Input Reliability Data - Failure rates(Lambda) and
% mean repair times (mttr)

%number of Power Components
buses33=4;
```

```
buses11=168;
busesLV=88;
busesLV_1=44;
busesLV_2=44;
lines11=66;
lines11_1=52;
lines11_2=14;
CBs33=3;
CBs11=101;
fuses=44;
trafos3311=2;
trafos1104=44;  %520 PCs

% Length of lines/cables: (km)
length_lines_1=0.5; %(km)  % define length for
% each particular line/cable
length_lines_2=0.8; %(km)

%Definition of lambdas
lambda_bus_33=0.08;
lambda_bus_11=0.005;
lambda_bus_LV_1=0.005;
lambda_bus_LV_2=0.005;

lambda_line_11=0.091;  % This is per km;

lambda_CB_33=0.0041;
lambda_CB_11=0.0033;

lambda_fuse=0.0004;

lambda_trafo_3311=0.01;
lambda_trafo_1104=0.002;
%-----------------------------------------

%Definition of MTTRs
mttr_bus_33=140;
mttr_bus_11=120;
mttr_bus_LV_1=24;
mttr_bus_LV_2=24;

mttr_line_11=9.5;

mttr_CB_33=140;
mttr_CB_11=120.9;
```

```
mttr_fuse=35.3;

mttr_trafo_3311=205.5;
mttr_trafo_1104=75;

%Lambda input arrays
l_bus_33=lambda_bus_33*ones(1,buses33);
l_bus_11=lambda_bus_11*ones(1,buses11);
l_bus_LV_1=lambda_bus_LV_1*ones(1,busesLV_1);
l_bus_LV_2=lambda_bus_LV_2*ones(1,busesLV_2);
l_bus=[l_bus_33 l_bus_11 l_bus_LV_1 l_bus_LV_2];

l_line1=lambda_line_11*length_lines_1*ones(1,lines11_1);
l_line2=lambda_line_11*length_lines_2*ones(1,lines11_2);
l_line=[l_line1 l_line2];

l_CB_33=lambda_CB_33*ones(1,CBs33);
l_CB_11=lambda_CB_11*ones(1,CBs11);
l_CB=[l_CB_33 l_CB_11];

l_fuse=lambda_fuse*ones(1,fuses);

l_trafo_3311=lambda_trafo_3311*ones(1,trafos3311);
l_trafo_1104=lambda_trafo_1104*ones(1,trafos1104);
l_trafo=[l_trafo_3311 l_trafo_1104];

%MTTR input arrays
m_bus_33=mttr_bus_33*ones(1,buses33);
m_bus_11=mttr_bus_11*ones(1,buses11);
m_bus_LV_1=mttr_bus_LV_1*ones(1,busesLV_1);
m_bus_LV_2=mttr_bus_LV_2*ones(1,busesLV_2);
m_bus=[m_bus_33 m_bus_11 m_bus_LV_1 m_bus_LV_2];

m_line=mttr_line_11*ones(1,lines11);

m_CB_33=mttr_CB_33*ones(1,CBs33);
m_CB_11=mttr_CB_11*ones(1,CBs11);
m_CB=[m_CB_33 m_CB_11];

m_fuse=mttr_fuse*ones(1,fuses);

m_trafo_3311=mttr_trafo_3311*ones(1,trafos3311);
m_trafo_1104=mttr_trafo_1104*ones(1,trafos1104);
m_trafo=[m_trafo_3311 m_trafo_1104];
```

```
% Simulation input variables
years=1000;
multiplier=365; % down to days scale
days=years*multiplier;

lambda1=[l_bus l_line l_CB l_fuse l_trafo];
mttr=[m_bus m_line m_CB m_fuse m_trafo];
lambda=lambda1/multiplier;   %failure/day

% Variation of PC failure rates according to the Bathtub distribution
% Section 3.2, Expected lifetime = 40 years
bathtub = 40 * multiplier;  % 40 years in days
step = bathtub + 1;
% Different steps of the bathtub over 14600 days (40 years)
x = 1/step : 1/step : 1-1/step ;
y = zeros(bathtub,length(lambda));

for n = 1:length(lambda)
    y(:,n) = (lambda(n))./(pi*sqrt(x.*(1-x))); % Beta PDF with
    % mean value = lambda(n)
end

dim = size(y);
a = 1;
b = dim(1);

for m = 1:25  % (40 years * 25 times = 1000 years of simulation)
    LAMBDA(a:b,:)=y;
    a=a+dim(1);
    b=b+dim(1);
end

% Weibull parameters Short Interruptions (SIs):
G1=14.25;
b1=1.95;
% Weibull parameters Long Interruptions (LIs):
G2=14.35;
b2=2.35;

%-------------------------------------------
%Main SDS Code:

U1=rand(days,length(lambda));
U2=rand(days,length(mttr));

TTF=zeros(days,length(lambda));
```

```
TTR=zeros(days,length(lambda));

b3=2;   % RAYLEIGH Distribution: beta=2
G3=mttr/(gamma(1+(1/b3)));

for k=1:days
    for i=1:length(lambda)
        % Inverse Exponential CDF for Fault Rates
        TTF(k,i)=-1/LAMBDA(k,i)*log(U1(k,i));

        % Inverse Rayleigh CDF for TTR
        TTR(k,i)=G3(i)*(-log(U2(k,i)))^(1/b3); %given in hours
    end

end

f=find(TTF<1);

SI_LI=randsrc(length(f),1,[0 2;0.54 0.46]); % 0='SIs' 54%prob ,
% 2='LIs' 46%prob
LI=find(SI_LI);
SI=find(SI_LI<2);

f1=TTR(f);  % duration of interr. in hours
f1(SI)=0;   % vector divided in SIs and LIs (in hours)
f0=f1*2;   % (in 30min divisions) (i.e. adjustable accuracy)
f0(f0<2 & f0>0)=2;  % The minimum duration (max.accuracy) for LIs is
% 1h (2x30min) This is because the time-step is 30min (1 time-step = SI)
f2=round(f0);

Act_of_SIs = 100*length(find(f2==0))/length(f2); % Actual %age number of SIs

%-----------------
% Weibull (Random Variates) for SI and LI Distributions (over the day)
% This defines the exact time (in hours) at which SI-LI happen in day

U3=rand(length(SI),1);
T_SI=zeros(length(SI),1);
for j=1:length(SI)
    T_SI(j)=G1*(-log(U3(j)))^(1/b1);  % Times SIs
    while T_SI(j)>24
       U4=rand;
       T_SI(j)=G1*(-log(U4))^(1/b1);
    end
end
```

```
U5=rand(length(LI),1);
T_LI=zeros(length(LI),1);
for l=1:length(LI)
    T_LI(l)=G2*(-log(U5(l)))^(1/b2);  % Times LIs
    while T_LI(l)>24
       U6=rand;
       T_LI(l)=G2*(-log(U6))^(1/b2);
    end
end

% Time (in 30min divisions) at which SI-LI happen in day
T_SI_2=T_SI*2;
T_LI_2=T_LI*2;
T_SI_30min=round(T_SI_2); %rounded values (30min) of occurrence (SIs)
T_LI_30min=round(T_LI_2); % " (LIs)

T_SI_30min(T_SI_30min<1)=1; % This is to make sure that the rounded value
T_LI_30min(T_LI_30min<1)=1; % doesn't give a failure in time '0'

%-----------------
% Output Matrix 'B' for PSS®E (iterations=days):
B=ones(days,length(lambda));
B(f)=f1;  % 0='SIs' , 1=Normal Operation , 'duration of 'LIs' (value in h)

%------------------
% 'C', same Matrix 'B', but with time of occurrence of faults
B_SIs=find(B==0);
B_LIs=find(B~=0 & B~=1);

C=zeros(days,length(lambda));  % it must be a 'zeros' matrix to avoid
% confusion with other values (ones)

C(B_SIs)=T_SI_30min;  %(in rounded 30min over the day)
C(B_LIs)=T_LI_30min;
%----------------------------------------

tElapsed=toc;
save MCS_SDS_SU B C f2 Act_of_SIs tElapsed % saved variables
```

MCS Resolution – 30 minutes time-step

```
% ADJUSTMENT OF MCS Resolution to 30-mins timesteps to implement a time
% sequential analysis with correlated demand profiles.
```

```
clear
clc

load MCS_SEST_SU C

tic;
dim = size(C);
exp_n = 48;     % Determines the desired step size - 48 = 24h * 2 (30 min)

for k = 1:dim(1,2)
    p = 1;

    for n = 5000:5000:365000        % Iteration steps of 5000 days
        m = n-4999;
        a = C(m:n,k);         % works on column(PC) by Column(PC)

        for i = 1:length(a)

            a0 = i;
            if a(i)==0
                S(a0,:) = ones(exp_n,1);
            else
                b = ones(exp_n,1);
                b(a(i)) = 0;      % a(i) has to be an integer. This is
                S(a0,:) = b;     % ensuredby matrix C having only integers.
            end
        end

        P = zeros(exp_n*i,1);
        startpoint1 = 1;
        endpoint1 = 1;

        for j = 1:i
            endpoint1 = startpoint1 + (exp_n-1);
            P(startpoint1:endpoint1,1) = S(j,:);
            startpoint1 = endpoint1 + 1;
        end

        SP(:,p) = P;
        p = p+1;
    end

    p = p-1;
    A = zeros(length(P)*p,1);
    startpoint2 = 1;
    endpoint2 = 1;
```

```
    for q = 1:p
        endpoint2 = startpoint2 + (length(P)-1);
        A(startpoint2:endpoint2,1) = SP(:,q);
        startpoint2 = endpoint2 + 1;
    end

    S1(:,k) = A;
    clear S SP
end

for z = 1:dim(1,2)
    miniD(:,z) = S1(:,z);
end

% miniD is the output matrix with mostly ones and zeros situated
% at the exact time when SIs and LIs occur.

%-------------------------------------------------------
%-------------------------------------------------------
```

Classification between SIs and LIs

```
f0 = miniD==0;  % find interruptions in Matrix D
miniD(f0) = f2;   % allocate interruption durations from vector f2

% Extend those durations for LIs only to the corresponding timesteps:
f1 = find(miniD>1);

for m = 1:length(f1)

    for t = 0:(miniD(f1(m))-1)
        miniD(f1(m)+t) = 0;
    end

end

% The new mini matrix D is the output matrix for export to PSS®E to carry
% out risk and power flow analysis in 30min time steps.
% Because miniD is just 1s and 0s (PC states), we can afford to convert it
% to uint8 (using 1 byte) instead of leaving D as a double (8 bytes).

d = uint8(miniD);
TE = toc;
```

```
save D d TE
```

Application of Backup Action

```
% Application of Backup action through normally open switches at the end of
% each feeder.

% Step 1 - Create a submatrix 'Dnew' from 'd', with only those PCs that are
% affected by the backup action in the network (i.e. SQS legislation: 3h,
% 15 min, etc., depending on interrupted GD).

% For the Suburban MV network, the code applies backup action according to a
% time limit of maximum 3h (6X30min time steps) and generates a matrix
% 'Dnew_BV' with the required backup action for each PC (in each column).

clear
clc

load D d
Dnew = d(:,PCs_A);
dim = size(Dnew);
B = zeros(dim);

for j = 1:dim(1,2)

    A = Dnew(:,j);
    n = diff([3; A; 3]==0);           % '3' can be any integer
    f1 = find(n==1);
    dur = (find(n==-1)-find(n==1));

    for m = 1:length(f1)

        if dur(m) > limitvalue
            % For each LI, this is the limit value to track (backup
            % time=3h) (6x30min steps) If we want to set backup to
            % a fixed value of 3h, then: set q=6!!!
            q = randsrc(1,1,[2 3 4 5 6]); % If the interruption
            % is >6(3h), then q is the random (uniform) time limit
            % for backup:either 2(1h), 3(1.5h), 4(2h), 5(2.5h) or
            % 6(3h) time steps

            for p = q:(dur(m)-1)
                B(f1(m)+p,j) = 1;

            end
```

```
        end
    end
end

Dnew_BV = B;

Backup_Vector = sum(Dnew_BV,2); % Sums along the rows to ensure
% a column vector with on/off status for the backup switch
Backup_Vector(Backup_Vector~=0) = 1;

saveStructBV.(['Backup_Vector' num2str(ij)]) = Backup_Vector;
save (['Backup_Vector' int2str(ij)], '-struct', 'saveStructBV',...
['Backup_Vector' num2str(ij)]);

% Backup_Vector is the input for the backup switch N in PSS®E.
```

Appendix B

Python Model for Automation of PSS®E

After generating the state duration of each PC for each simulation timestep, the next step is to run power flow analyses to determine the impact of each state in terms of the total number of customers experiencing supply interruption and the corresponding energy not supplied. Given the length of simulation, the use of PSS®E can be automated using application program interface (API) routines. These routines are defined for PSS®E using various syntaxes namely batch commands, Fortran and Python. This thesis uses the Python code in this appendix which corresponds to the analysis for the suburban MV network. Accordingly, different code modifications have been used for the reliability analyses presented in Sections 3.3-3.6.

```
# Time-sequential MCS for the suburban Network (44 LPs, 520 PCs,
# 1000 years, 30-mins timestep)
# The code also considers the variation of load profile and power factor
# (PF).
#-----------------------------------------------------------
# Read Load Profile Data (Residential max demand) (17520 x 30min steps)
#Residential loads
LOAD=[]
h=open(r"""C:\Brian\PhD\MBN\Events_Conferences\SEST_2019\MBN\SEST\SU\
Base_case\Demand_Data\Residential\lp.txt""", 'r')
i = 0
while i < 17520:
  temp=float(h.readline())
  LOAD.extend([temp])
  i = i + 1
h.close()
```

```
# read PF data
PF=[]
h=open(r"""C:\Brian\PhD\MBN\Events_Conferences\SEST_2019\MBN\SEST\SU\
Base_case\Demand_Data\Residential\pf.txt""", 'r')
i = 0
while i < 17520:
  temp = float(h.readline())
  PF.extend([temp])
  i = i + 1
h.close()
#------------------------------------------------------------
import os,sys

p=1
while p < 1001:
  path1="C:\Brian\PhD\MBN\Events_Conferences\SEST_2019\MBN\SEST\SU\
  Base_case\Text_Files_MCS_to_PSSE\%d" %(p)
  os.chdir(path1)
  psspy.case(r"""C:\Brian\PhD\MBN\Events_Conferences\SEST_2019\MBN\
  SEST\SU\Base_case\PSSE_model\SEST_Suburban_Backup.sav""")

  # suppress outputs in the PSSE display
  psspy.report_output(6,"",[0,0])
  psspy.progress_output(6,"",[0,0])
  psspy.alert_output(6,"",[0,0])

  #initialise load status arrays (0=interrupted/not 0 = normal operation)
  l_1=[]
  l_2=[]
  l_3=[]
  # insert all load arrays until:
  l_44=[]

  # read 17520 x 30min status (0-open or 1-closed) coefficients
  NPCs=522 # declare number of power components     (+ 2 Backups =522 PCs)
  PC=[0]*NPCs #declare empty array of loads
  npc=0

  while npc<NPCs:
    PCtemp=[]
    exec "f=open('PC%d.txt', "r")" % (npc+1)
    i = 0
    while i < 17520:                    ### 17520 steps (1year in 30min)
      temp=float(f.readline())
      PCtemp.extend([temp])
```

```
    i = i + 1
  f.close()
  PC[npc]=PCtemp
  npc=npc+1

N=0
while N<17520:
  psspy.case(r"""C:\Brian\PhD\MBN\Events_Conferences\SEST_2019\MBN\SEST\
  SU\Base_case\PSSE_model\SEST_Suburban_Backup.sav""")
  #------------------------------------------------------------
  # Create subsystem with 44 loads (Residential)
  psspy.bsys(2,0,[0.0,0.0],0,[],44,[1017,10113,10119,10122,1027,10212,
  10216,10220,1036,1047,10413,10417,1059,10513,10519,10524,10530,10535,
  10539,1066,1078,10714,10719,10723,1086,1097,10912,10916,10920,1106,
  1117,11112,11116,11119,2016,2027,20212,20216,20220,2036,2047,20412,
  20416,20419],0,[],0,[]) #buses IDs

  # Change Load Profile (All residential customers)
  psspy.scal(2,0,1,[0,0,0,0],[0.0,0.0,0.0,0.0,0.0,0.0,0.0])
  psspy.scal(2,0,2,[2,0,1,0],[LOAD[N],0.0,0.0,0.0,0.0,0.0,0.0])

  # change PF
  psspy.scal(2,0,1,[0,0,0,0],[0.0,0.0,0.0,0.0,0.0,0.0,0.0])
  psspy.scal(2,0,2,[2,0,4,0],[ 0.0,0.0,0.0,0.0,0.0,0.0,PF[N]])
  #------------------------------------------------------------

  # Change status (on/off) for all Power Components (520 + 2Backup PCs):

  # Buses 33kV
  if PC[0][N]==0: psspy.dscn(1)
  if PC[1][N]==0: psspy.dscn(2)
  if PC[2][N]==0: psspy.dscn(11)
  if PC[3][N]==0: psspy.dscn(21)

  # Buses 11kV
  if PC[4][N]==0: psspy.dscn(12)
  if PC[5][N]==0: psspy.dscn(13)
  if PC[6][N]==0: psspy.dscn(22)
  # insert all buses until:
  if PC[171][N]==0: psspy.dscn(20417)

  # Buses 0.4kV
  if PC[172][N]==0: psspy.dscn(1016)
  if PC[173][N]==0: psspy.dscn(1026)
  # insert all buses until:
  if PC[259][N]==0: psspy.dscn(20419)
```

```
# lines (0.5km)
if PC[260][N]==0: psspy.branch_chng_3(100,1011,r"""1""",[0,_i,_i,_i,
_i,_i],[_f,_f,_f,_f,_f,_f,_f,_f,_f,_f,_f,_f],[_f,_f,_f,_f,_f,_f,_f,
_f,_f,_f,_f,_f],_s)
if PC[261][N]==0: psspy.branch_chng_3(1012,1021,r"""2""",[0,_i,_i,
_i,_i,_i],[_f,_f,_f,_f,_f,_f,_f,_f,_f,_f,_f,_f],[_f,_f,_f,_f,_f,_f,
_f,_f,_f,_f,_f,_f],_s)
# insert all lines until:
if PC[311][N]==0: psspy.branch_chng_3(2042,20417,r"""66""",[0,_i,
_i,_i,_i,_i],[_f,_f,_f,_f,_f,_f,_f,_f,_f,_f,_f,_f],[_f,_f,_f,_f,
_f,_f,_f,_f,_f,_f,_f,_f],_s)

# lines (0.8km)
if PC[312][N]==0: psspy.branch_chng_3(1033,1034,r"""21""",[0,_i,_i,
_i,_i,_i],[_f,_f,_f,_f,_f,_f,_f,_f,_f,_f,_f,_f],[_f,_f,_f,_f,_f,_f,
_f,_f,_f,_f,_f,_f],_s)
# insert all lines until:
if PC[325][N]==0: psspy.branch_chng_3(20413,20414,r"""65""",[0,_i,
_i,_i,_i,_i],[_f,_f,_f,_f,_f,_f,_f,_f,_f,_f,_f,_f],[_f,_f,_f,_f,_f,
_f,_f,_f,_f,_f,_f,_f],_s)

# 33kV breakers
if PC[326][N]==0: psspy.system_swd_chng(1,2,r"""1""",[0,_i,_i,_i],
_f,[_f,_f,_f,_f,_f,_f,_f,_f,_f,_f,_f,_f],_s)
if PC[327][N]==0: psspy.system_swd_chng(2,11,r"""1""",[0,_i,_i,_i],
_f,[_f,_f,_f,_f,_f,_f,_f,_f,_f,_f,_f,_f],_s)
if PC[328][N]==0: psspy.system_swd_chng(2,21,r"""1""",[0,_i,_i,_i],
_f,[_f,_f,_f,_f,_f,_f,_f,_f,_f,_f,_f,_f],_s)

# 11kV breakers
if PC[329][N]==0: psspy.system_swd_chng(12,13,r"""1""",[0,_i,_i,_i],
_f,[_f,_f,_f,_f,_f,_f,_f,_f,_f,_f,_f,_f],_s)
if PC[330][N]==0: psspy.system_swd_chng(13,23,r"""1""",[0,_i,_i,_i],
_f,[_f,_f,_f,_f,_f,_f,_f,_f,_f,_f,_f,_f],_s)
# insert all breakers until:
if PC[429][N]==0: psspy.system_swd_chng(10716,10720,r"""1""",[0,_i,
_i,_i],_f,[_f,_f,_f,_f,_f,_f,_f,_f,_f,_f,_f,_f],_s)

#switch fuses:
if PC[430][N]==0: psspy.system_swd_chng(1016,1017,r"""1""",[0,_i,_i,
_i],_f,[_f,_f,_f,_f,_f,_f,_f,_f,_f,_f,_f,_f],_s)
# insert all fuses until:
if PC[473][N]==0: psspy.system_swd_chng(20418,20419,r"""1""",[0,_i,
_i,_i],_f,[_f,_f,_f,_f,_f,_f,_f,_f,_f,_f,_f,_f],_s)
```

```
# 33_11 kV Transformers
if PC[474][N]==0: psspy.two_winding_chng_5(11,12,r"""45""",[0,_i,_i,
_i,_i,_i,_i,_i,_i,_i,_i,_i,_i,_i,_i,_i,_i],[_f,_f,_f,_f,_f,_f,_f,_f,_f,_f,
_f,_f,_f,_f,_f,_f,_f,_f,_f,_f,_f,_f,_f,_f],[_f,_f,_f,_f,_f,_f,_f,_f,_f,_f,_f,
_f],_s,_s)
if PC[475][N]==0: psspy.two_winding_chng_5(21,22,r"""46""",[0,_i,_i,
_i,_i,_i,_i,_i,_i,_i,_i,_i,_i,_i,_i,_i,_i],[_f,_f,_f,_f,_f,_f,_f,_f,_f,_f,
_f,_f,_f,_f,_f,_f,_f,_f,_f,_f,_f,_f,_f,_f],[_f,_f,_f,_f,_f,_f,_f,_f,_f,_f,_f,
_f],_s,_s)

# 11_04 kV Transformers
if PC[476][N]==0: psspy.two_winding_chng_5(1015,1016,r"""1""",[0,_i,
_i,_i,_i,_i,_i,_i,_i,_i,_i,_i,_i,_i,_i,_i,_i],[_f,_f,_f,_f,_f,_f,_f,_f,_f,
_f,_f,_f,_f,_f,_f,_f,_f,_f,_f,_f,_f,_f,_f],[_f,_f,_f,_f,_f,_f,_f,_f,_f,_f,_f,
_f,_f],_s,_s)
# insert all transformers until:
if PC[519][N]==0: psspy.two_winding_chng_5(20417,20418,r"""44""",[0,
_i,_i,_i,_i,_i,_i,_i,_i,_i,_i,_i,_i,_i,_i,_i,_i,_i],[_f,_f,_f,_f,_f,_f,_f,_f,
_f,_f,_f,_f,_f,_f,_f,_f,_f,_f,_f,_f,_f,_f,_f,_f],[_f,_f,_f,_f,_f,_f,_f,_f,_f,
_f,_f,_f],_s,_s)

# BACKUP SUPPLIES  (PC521/PC522 text files)
if PC[520][N]==1: psspy.system_swd_chng(3,111,r"""1""",[1,_i,_i,_i],
_f,[_f,_f,_f,_f,_f,_f,_f,_f,_f,_f,_f,_f,_f],_s)
if PC[521][N]==1: psspy.system_swd_chng(3,204,r"""1""",[1,_i,_i,_i],
_f,[_f,_f,_f,_f,_f,_f,_f,_f,_f,_f,_f,_f,_f],_s)

# Check for Bus Islands (Tree Option)
psspy.tree(1,0)
psspy.tree(2,1)
psspy.tree(2,1)
psspy.tree(2,1)
psspy.tree(2,1)
psspy.tree(2,1)

# Solve Newton-Raphson
psspy.fdns([2,0,0,1,1,0,99,0])

#### 'if' loops for substation (2 trafos in //)
### If Trafo 'GSP1' Fails (or PCs associated):
if PC[474][N]==0 or PC[2][N]==0 or PC[4][N]==0 or PC[327][N]==0
or PC[329][N]==0:
  ierr,tload2=psspy.brnmsc(21,22,'46','PCTMVA')
  if tload2 > 100:
    psspy.two_winding_chng_5(21,22,r"""46""",[0,_i,_i,_i,_i,_i,
    _i,_i,_i,_i,_i,_i,_i,_i,_i],[_f,_f,_f,_f,_f,_f,_f,_f,_f,_f,_f,
```

```
      _f,_f,_f,_f,_f,_f,_f,_f,_f,_f,_f],[_f,_f,_f,_f,_f,_f,_f,_f,
      _f,_f,_f,_f],_s,_s)

      # switch on backups should both transformers be out of service
      psspy.system_swd_chng(3,111,r"""1""",[1,_i,_i,_i],_f,[_f,_f,
      _f,_f,_f,_f,_f,_f,_f,_f,_f,_f],_s)
      psspy.system_swd_chng(3,204,r"""1""",[1,_i,_i,_i],_f,[_f,_f,
      _f,_f,_f,_f,_f,_f,_f,_f,_f,_f],_s)

    # Re-check for Bus Islands (Tree Option)
    psspy.tree(1,0)
    psspy.tree(2,1)
    psspy.tree(2,1)
    psspy.tree(2,1)
    psspy.tree(2,1)
    psspy.tree(2,1)

    # Solve Newton-Raphson again
    psspy.fdns([2,0,0,1,1,0,99,0])

    ### Repeat for Trafo 'GSP2'

  ### Get Output Files (44 Loads)
  ierr,l1=psspy.brnmsc(1016,1017,'1','PCTCPA')
  l_1.extend([l1])
  ierr,l2=psspy.brnmsc(10112,10113,'1','PCTCPA')
  l_2.extend([l2])
  ierr,l3=psspy.brnmsc(10118,10119,'1','PCTCPA')
  l_3.extend([l3])
  # obtain load output files until:
  ierr,l44=psspy.brnmsc(20418,20419,'1','PCTCPA')
  l_44.extend([l44])

  N=N+1

path2="C:\Brian\PhD\MBN\Events_Conferences\SEST_2019\MBN\SEST\SU\
Base_case\Results_Text_Files_PSSE_to_Matlab\%d" %(p)

os.chdir(path2)

l_1 = str(l_1)[1 : -1];
sys.stdout=open('Results\L1.txt','a')
print l_1
l_2 = str(l_2)[1 : -1];
sys.stdout=open('Results\L2.txt','a')
print l_2
```

```
l_3 = str(l_3)[1 : -1];
sys.stdout=open('Results\L3.txt','a')
print l_3
# print load text files until:
l_44 = str(l_44)[1 : -1];
sys.stdout=open('Results\L44.txt','a')
print l_44
sys.stdout.close()

p+=1
```

Appendix C

MATLAB Model for MOR

This appendix provides the MATLAB code developed for the MOR procedure discussed in Section 4.4.2 and summarised using Algorithm 1. The initial state space representation is generated before computing the relevant system Gramians that allow for a truncation of less important system states based on their HSVs. The reliability of the resultant reduced order is then assessed using a time-sequential MCS based on STS. Modifications of this code have been used for the reliability analyses presented in Section 4.5 as well as the enhancements discussed in Chapter 5.

Generating the State Space Representation

```
%MOR for a simple 4PC system.

clear
close all
clc

tic
%--------------------------------------------------%
Days = 365;
H = 24;
dt = 1; % Timestep in hours
tsperyear = Days*(H/dt); %8760

PCs = 4; % Number of Power components
N = 2^PCs; % Number of states

n = 1; % states of the reduced order system minus 1.
```

```
%Edit n to change the size of the reduced system%

lambda1 = [0.08 0.1 0.1 0.08]; % PC failure rates per year - Bus,line
lambda = lambda1/tsperyear; % Failure rate per timestep.

MTTR = [140 20.5 20.5 140];
MTTR = MTTR/dt; % Because MTTR is given in hours.
mu  = 1./MTTR; % Repair rate.

%-----------------------------------------------------%
%[AA] = f_Dynamics_matrix(N,lambda,mu); % Dynamics matrix ==
% State transition matrix Build the system matrix A by checking
% for associated PC transitions

Bin_states=dec2bin(flipud((0:N-1)'));
dim=size(Bin_states);
SM=zeros(dim); % State Matrix
for i = 1:dim(2)
    SM(:,i) = str2num(Bin_states(:,i));  % State 1 is when all PCs are in
    % service and state N is when all PCs are down.
end

AA = zeros(dim(1));

for k=1:length(SM)
    difr=zeros(dim);
    statechng=zeros(length(SM),1);

    for i=1:length(SM)
        difr(i,:)= SM(k,:) - SM(i,:);  % State_transitions
        statechng(i,:)=sum(abs(difr(i,:)));  % State_change_possibility
    end

    truepos = find(statechng==1); % Only_possible_jumps_are_to_state xyz
    TLmu = zeros(1,length(truepos));   % Associated_jump_prob_values

    for j=1:length(truepos)
        temp=find(difr(truepos(j),:)~=0);

        if difr(truepos(j),temp)<0
            TLmu(j)=mu(temp);
        else
            TLmu(j)=lambda(temp);
        end

    end
```

```
    AA(k,truepos) = TLmu;
    AA(k,k)= -(sum(AA(k,:)));
    clearvars truepos;
end

AA=AA'; %This is the algebraic (dynamics) matrix equation

BB = zeros(N,1); % original B

D1 = 7.5; % Demand at bus 1 in MW.
D2 = 10; % Bus 2 for 3PC system.
TD = D1+D2;
CC = [TD D1 TD D1 TD D1 D1 D1 0 0 0 0 0 0 0 0];
CC = TD-CC; % CC == original C
DD = 0 ; % original D
ini = zeros(N-8,1);
xx0 = [0.3;0.2;0.05;0;0.05;0.2;0.1;0.1;ini]; % Original Initial conditions
syss = ss(AA,BB,CC,DD); % Original system!
```

Order Truncation

```
Astar = AA(2:end,2:end);
B = AA(2:end,1); % control matrix
A = bsxfun(@minus,Astar,B);
D = CC(:,1); % direct term / feedforward/ feedthrough matrix
C = CC(:,2:end) - D; %Output Matrix == sensor matrix
x0 = xx0(2:end);
sys = ss(A,B,C,D); % Generate state space representation.

W = gram(sys,'o'); % observability gramian

[V,dia]=eig(W);       % V and dia are the Eigenvectors and Eigenvalues
% respectively for observability gramian matrix, W.
V = flipud(rot90(V,2));  % V and dia must be in a non-increasing order.

%-------------------------------------------------------------%
% New system----------------------------------------------%
A_new = V\A*V; % This is the equivalent of inv(V)*A*V
B_new = V\B;   % == inv(V)*B
C_new = C*V;
D_new = D;
x0_new = V\x0;  % inv(V)*x0;
sys_new=ss(A_new,B_new,C_new,D_new);
```

```
%Reducing it to n orders:
%--------------------------------------------------------------------%
A_red = A_new(1:n,1:n);
B_red = B_new(1:n,1);
C_red = C_new(:,1:n);
D_red = D_new;
x0_red = x0_new(1:n);
sys_red = ss(A_red,B_red,C_red,D_red);
%--------------------------------------------------------------------%

A_temp = bsxfun(@plus,A_red,B_red); %Major timesaver
Z1 = zeros(1,1+n);
A_ra = [Z1;B_red A_temp];  %A_ra - A matrix for the reduced augmented system
for k=1:length(A_ra)
    A_ra(1,k) = -sum(A_ra(:,k));
end
B_ra = zeros(n+1,1);
C_ra = C_red + D_red;
C_ra = [D_red C_ra];
D_ra = zeros(size(C_ra,1),1);
x0temp = 1-sum(x0_red);
x0_ra = [x0temp;x0_red];
sys_ra = ss(A_ra,B_ra,C_ra,D_ra);
%--------------------------------------------------------------------%
%--------------------------------------------------------------------%

TE=toc;
save(['MOR_n' int2str(n+1)],'sys_ra','x0_ra','TE') %Reduced order system
```